Title
Lineage-Specific Hijacking of Non-Canonical Cofactors In the Evolution of Lentiviral Vif Anti-APOBEC3 Activity

Author
Kane, Joshua Randall

Publication Date
2015

Peer reviewed|Thesis/dissertation

Lineage-Specific Hijacking of Non-Canonical Cofactors In the Evolution of Lentiviral Vif Anti-APOBEC3 Activity

by

Joshua R. Kane

DISSERTATION

Submitted in partial satisfaction of the requirements for the degree of

DOCTOR OF PHILOSOPHY

in

Biochemistry and Molecular Biology

in the

GRADUATE DIVISION

of the

UNIVERSITY OF CALIFORNIA, SAN FRANCISCO

Acknowledgements

I would first like to thank my thesis advisor, Nevan Krogan. Without a doubt this project would not have been possible under a different advisor, both due to the technology available within Nevan's group, and allowing me to explore in my research more independently than most graduate students experience. The large number of collaborations that made my thesis work possible were the bread and butter of the Krogan model of science, and it was a privilege to experience science as a multi-group effort rather than as a private affair. Under Nevan's tutelage, I not only learned how to be a productive, independent researcher, but also how to organize a scientific research effort. I am grateful for having had this experience.

There are many people within the Krogan group to whom I owe my success. Stef Jäger laid the fundamental groundwork for this project with her heroic effort that is the original HIV-1 AP-MS project. When I first rotated my knowledge of molecular biology was theoretical and of cell culture non-existent, but she provided me with the initial training that resulted in this successful work. You have my deepest thanks for this. I also need to thank Paul Hartley, whom when I was a bit lost in the woods during the early stages of my thesis work, took me under his wing and trained me how to be a much more competent and professional scientist and how to work closely with another researcher, something that is not always easy to do. I would like to thank Gwen Jang for being a good lab neighbor and helping each other out troubleshooting affinity purifications; Manon Eckhardt for always being not only a great scientist to whom I can always go to for advice, but also a great positive spirit and encouraging me to not let the gloom of graduate school get to me; and Billy Newton for not only taking the time to teach me idiosyncratic biochemistry, but for being a down-to-earth fun guy whom I could always enjoy a great conversation with, whether it be about science or the illiterati. I need to acknowledge our

lab manager Kathy Franks-Skiba for herding all the cats and making sure the lab didn't collapse into a anarchaic state of maximum entropy, and Linda Reilly for being an awesome lab assistant who always seemed to have time to help me out, especially when I waited until the last minute to do something important and esoteric, like mailing reagent to Iceland. I want to lastly thank all the numerous lab members not explicitly mentioned here whom were a big part of my graduate experience and instrumental to my success.

This project depended on a number of collaborations across a large group of disciplines. In particular, I need to acknowledge David Stanley from John Gross's group, who performed much of the incredible biochemistry that allowed this project to be so successful, especially during an early phase of very reasonable skepticism about the project's initial findings. I would also like to thank Jen Binning, who took over the biochemistry side of the project after David graduated, for demonstrating again the high quality of biochemists in John's group. I would also like to acknowledge Judd Hultquist, who started on this project as a student in Reuben Harris's group and ended it as a postdoc in Nevan's group. His voraciousness as a scientist is admirable, and his depth of knowledge of Vif and APOBEC3 was invaluable. I would also like to thank Rebecca LaRue from Reuben's group for providing reagents and advice in the early stages of this project. Her work with these different Vif and APOBEC3 proteins provided a strong framework for this project to build upon. I thank Sarah Barelier not only for her contributions to the project, but for showing me just how small a world it really is. I need to thank Jeff Johnson, Tasha Johnson (no relation), Billy Newton, and Edward Tang for being the awesome mass spec core of the Krogan lab, especially for the times when I asked every so nicely to have a couple samples bumped up in the queue and fulfilling my request. I want to also acknowledge and thank the Icelandic MVV team; although we have not met, you have my gratitude for the great virology data and I hope one day we can meet.

I have numerous PIs to acknowledge both for their contributions to this project and my graduate experience in general. John Gross is a phenomenal scientist and the most important PI that I interacted with during my time at UCSF other than Nevan. Simultaneously imposing and very approachable, he would always find time to offer mentorship and advice, for both the project we were collaborating on and for my graduate experience in general even though I was not in his group. I would like to acknowledge the contributions of Reuben Harris, whose lab provided not only many reagents and data, but for encouraging the project and helping to shape it, particularly in its early days. I thank James Fraser for very helpful discussions about CYPA, being generally enthusiastic about science, collaborations, and experiments, and for teaching me about shibboleth and the proper pronounciation of “Toronto”. I also thank Vala Andrésdóttir whom is the one member of the Icelandic team I had the pleasure of meeting in person. Her telling of the 1933 invasion of Iceland by MVV-ridden German sheep is one of my favorite science-related memories of graduate school.

I would like to acknowledge Jeff Cox who, along with John Gross and Nevan, is part of my thesis committee. Thank you for your advice and support.

I must acknowledge my undergraduate research experience as a large influence on my going to graduate school. I thank Mike Freeling for providing me with the opportunity to work in his group. I also thank Damon Lisch for allowing me to be a bit of a lab rat on the bench while I was supposed to be a code monkey. I am enormously indebted to Eric Lyons, who was my undergraduate research mentor. Not only was he singly the most important influence on my going to graduate school, he took me in when I had very little applicable skills to the posted position and not only trained me in bioinformatics, but gave invaluable advice about science, scientific careers, and life that I only truly appreciated after I made the mistakes he tried so hard to have me avoid. Thanks Eric, I’ve come a long way since SeqView, I owe you big-time.

I could not have finished graduate school without all the love and support from my friends. I want to particularly acknowledge four of my classmates that had a huge influence during my time in graduate school. Kelly Nissen came to UCSF with me from the Freeling lab, so the entire experience has felt very shared between us. Thanks for always being someone I could talk to without pretense. Dustin “Dusty” Dovala, tuberculosis biochemist, ill-timed chess player, outdoorsman extraordinaire. I thank Dustin for numerous unforgettable experiences, including trekking through snow in the high Serrias in July. I want to thank the only man perhaps more cynical than myself, Robert Stanley, for being someone who could look at the world as I do and laugh about it over a beer.

I cannot leave out my partner in crime and all other things, Betty Nascimento. Without a double the most unforeseen aspect of my life so far, the serendipitous nature of our relationship will forever be something in the back of my mind. Thank you for showing me how to be the best aspects of myself, for pulling me back up everytime I get knocked down, and for expanding my universe. You have truly made me a richer and better person and I cannot thank you enough.

Lastly, I must acknowledge and thank my family for the unconditional love and support that not only carried me through graduate school, but also got me there in the first place. To my parents, Glenn and Debra Kane, thank you for being great parents that were always supportive of me, of acknowledging my fledgling interest in science and nurturing it. I cannot thank you enough. I thank my brother Alex and my sister Kelly for helping to ground me while I was getting lost in the black hole that graduate school can be. I also wish acknowledge and thank my Uncle Rick for being an incredibly loving person even in spite of personal hardships. You were always there for me when I reached out, I won’t ever forget that.

Chapters 2, 3, and 4 largely contain previously published material.

Kane J.R., Stanley D.J., Hultquist J.F., Johnson J.R., Mietrach N., Binning J.M., Jónsson S.R., Barelier S., Newton B.W., Johnson T.L., Franks-Skiba K. E., Li M., Brown W. L., Gunnarsson H. I., Adalbjornsdóttir A., Fraser J. S., Harris R. S., Andrésdóttir V., Gross J. D., and Krogan N. J. (2015). Lineage-Specific Viral Hijacking of Non-canonical E3 Ubiquitin Ligase Cofactors in the Evolution of Vif Anti-APOBEC3 Activity. Cell Rep. 11, 1236–1250.

Contributions

Chapters 2 - 4

J.R.K. performed affinity purifications, scored mass spectrometry data, performed protein sequence analyses, created stable cell lines, and performed site-directed mutagenesis cloning, CsA assays, knockdown assays, and Jurkat nucleofection experiments. D.J.S. performed *in vitro* reconstitution of Vif-CRL complexes and ubiquitylation assays. J.F.H. performed single-cycle HIV-1 infectivity assays and assisted with Jurkat nucleofection experiment optimization. J.R.J., B.W.N., T.L.J., and K.E.F.-S. performed MS sample preparation, machine runs, and data searching. N.M., S.R.J., H.I.G., and A.A. performed MVV virology assays. J.M.B. generated SAXS envelopes of Vif-CRL5 complexes. S.B. performed NMR experiments. M.L. purified APOBEC3 proteins for *in vitro* ubiquitylation assays. W.L.B. sequenced MVV proviral sequences for hypermutation assays.

Chapter 5

J.R.K. and B.W.N. performed Ubiscan sample preparation, immunoprecipitation, and desalting with protocol generated by B.W.N. J.R.K. grew cells for Ubiscan, performed data analysis, performed SDS-PAGE, immunoblots, and affinity purifications, and cloned FKBP5 from cDNA.

Edward Tang performed AP-MS sample preparation. B.W.N. ran LC-MS/MS machine runs. J.R.J. performed data searching. Paul Hartley and J.R.K. performed T-bet assays. Erik Verschueren created RMSQ wrapper for MSstats package.

Lineage-Specific Hijacking of Non-Canonical Cofactors In the Evolution of Lentiviral Vif Anti-APOBEC3 Activity

Joshua R. Kane

Abstract

The retrovirus genus *Lentivirus*, which includes the human pandemic virus human immunodeficiency virus 1 (HIV-1), infect a wide range of mammals and are characterized by slow infections of host immune systems. HIV-1 encodes the accessory protein Vif, which hijacks a host Cullin-RING ubiquitin ligase (CRL) complex as well as the non-canonical cofactor CBFβ, to antagonize host APOBEC3 anti-viral proteins. To date, non-canonical cofactor recruitment to CRL complexes by viral factors has only been attributed to HIV-1 Vif. To further study this phenomenon, we employed a comparative approach combining proteomic, biochemical, structural, and virological techniques to investigate Vif complexes across representative clades within the *Lentivirus* genus, including primate (HIV-1, SIVmac) and non-primate (FIV, BIV, and MVV) viruses. We find that CBFβ is completely dispensable for the activity of non-primate lentiviral Vif proteins. Furthermore, we find that BIV Vif does not require any non-canonical cofactor MVV Vif requires a novel cofactor, Cyclophilin A (CYPA), for stable CRL complex formation and anti-APOBEC3 activity. Lastly, we present evidence testing the idea of novel Vif functions associated with non-canonical cofactor use. We propose a model of modular conservation of Vif complexes that allows for exaptation of novel functions through the acquisition of non-CRL associated host cofactors while preserving anti-APOBEC3 activity.

TABLE OF CONTENTS

LIST OF TABLES

LIST OF FIGURES

Chapter 1

Chapter 2

Chapter 3

Chapter 4

Chapter 5

Chapter 1: Viral Infectivity Factor (VIF) and APOBEC3 Antagonism in the *Lentivirus* Genus

INTRODUCTION

The viral family Retroviridae is characterized by reverse transcription (RT) of viral RNA genome to DNA followed by integration into the host cell genome. Once integrated, the provirus is expressed by host transcription machinery, leading to viral protein translation and eventually production of infectious virions budding off from the infected host cell (**Figure 1.1A**). The most well-known and well-studied retrovirus is human immunodeficiency virus 1 (HIV-1), which is found in the genus *Lentivirus*. Lentiviruses are characterized by their immune cell tropism, ability to infect non-dividing cells, eliciting slowly progressing, often chronic infections, and encoding numerous "accessory factors" evolved to modulate host cell environments to promote virus infectivity (Katzourakis et al., 2007). The HIV-1 genome can generally be categorized into three categories: (1) the structural / viral lifecycle genes of *gag*, *pol*, and *env*, which are absolutely required for the viral lifecycle and are found in all retroviruses; (2) regulatory genes of *tat* and *rev*, which regulate transcription of the integrated provirus, control viral transcript splicing, and ultimately export of genomic viral RNA for packaging in virions; and (3) accessory factors *vif*, *vpr*, *vpu*, and *nef* (Frankel and Young, 1998; **Figure 1.1B**). HIV-1 accessory factors act to rewire the infected cell to promote virus production by hijacking cellular machinery, redirecting host factors away from their normal sites of activity, and blocking innate immune signaling (Malim and Emerman, 2008).

HIV-1 viral infectivity factor (Vif) is a 23 kDa protein that acts as a potent viral countermeasure to host anti-viral defense. Early in HIV-1 research, Vif was established as required for viral infectivity, but a mechanism for its role in the viral lifecycle remained elusive

for nearly twenty years after the virus's discovery. In 2002-2003, multiple groups identified a host factor that greatly restricted HIV-1 infectivity in viruses that lacked Vif: apolipoprotein B mRNA editing enzyme, catalytic polypeptide-like 3G, or APOBEC3G. In the absence of Vif, APOBEC3G in infected cells binds to viral genetic material and is packaged into budding virions (**Figure 1.2A**). At the onset of the next cycle of viral infection, APOBEC3G initiates two mechanisms of anti-viral action. First, APOBEC3G reduces the processivity of viral reverse transcriptase (Gillick et al., 2013). Second, APOBEC3G exhibits DNA cytosine deaminase activity, targeting negative-strand cDNA generated during RT to deaminate cytosine bases to uracil, leading to rampant G-to-A mutants in the reading frame upon completion of RT, a process known as APOBEC3-mediated hypermutation (Harris et al., 2003; Iwatani et al., 2007; Mangeat et al., 2003; Zhang et al., 2003; **Figure 1.2B**). Hypermutation leads to either degradation of viral DNA due to uracil incorporation, or if integrated, prevents viral protein translation due to lethal nonsense mutations. Vif counteracts this viral antagonism by hijacking an endogenous Cullin-RING ubiquitin ligase (CRL) complex to target APOBEC3G for proteasomal degradation (Sheehy et al., 2002, 2003; Yu et al., 2003; **Figure 1.2C**).

CRL complexes are modular platforms for post-translationally modifying host proteins, catalyzing the conjugation of ubiquitin via its terminal carboxyl group to a substrate primary amine, either the protein amino (N) terminus or the ε-amine of lysine residues (Berndsen and Wolberger, 2014). This initial modification, known as mono-ubiquitylation, can have additional ubiquitin proteins conjugated to it to form a ubiquitin chain, known as poly-ubiquitylation. The architecture of the chain, determined by the lysine residue in ubiquitin used to form the ubiquitin-ubiquitin peptide bond, determines the cellular fate of the modified substrate (Ye and Rape, 2009). The best-characterized chain is the K48 chain, which is recognized by the 26S proteasome lid and leads to substrate proteolysis (Xu et al., 2009). Substrate specificity of the

CRL machinery is determined by a variable E3 substrate adapter; while the human genome encodes only seven Cullin scaffolds, they are engaged by hundreds of E3 proteins servicing thousands of protein substrates in cells (Clague et al., 2015); up to 20% of ubiquitylated proteins in cells are thought to be from CRL complexes (Mahon et al., 2014). Endogenous E3 proteins generally consist of two domains: a substrate-recognition motif from which E3 substrate specificity is determined, and a CRL-binding motif, which is shared among all E3 proteins that interact with a given CRL complex. The modularity of the CRL system, through the use of short linear motifs that allow multiple E3's to utilize a conserved CRL complex, is frequent target of viral molecular mimicry, allowing viral proteins to displace endogenous E3 proteins and re-purpose the ubiquitylation machinery to promote viral infection (Davey et al., 2011; Mahon et al., 2014).

HIV-1 encodes three accessory factors, Vif, Vpr, and Vpu, which hijack host Cullin-5, Cullin-4A, and Cullin-1 ubiquitin ligase complexes, respectively. Vif hijacks the Cullin-5 CRL complex (CRL5) containing Elongin B (ELOB), Elongin C (ELOC), and RING-Box protein 2 (RBX2) through molecular mimicry of a SOCS, or BC, box motif that allows Vif to bind ELOC (Stanley et al., 2008; Yu et al., 2004). Once hijacked, Vif acts as a substrate adapter for the CRL5 complex to target APOBEC3G for K48-chain poly-ubiquitylation (Mehle et al., 2004), resulting in the proteasomal degradation of APOBEC3G, depleting it from HIV-1 infected cells and preventing its packaging into virions, negating its anti-viral effect.

In the Lentivirus genus, Vif is the most conserved accessory factor, found in all extant lentiviruses except for the horse-infecting equine infectious anemia virus (EIAV) (Katzourakis et al., 2007; Kawakami et al., 1987). These Vif proteins share two notable features: they all contain SOCS-box motifs, meaning they all likely hijack an ELOC-containing CRL complex, and all Vif proteins examined so far maintain a conserved anti-APOBEC3 antagonism through

its degradation (LaRue et al., 2010). APOBEC3G is a member of a family of APOBEC3 proteins in the human genome, forming a tandem locus of seven APOBEC3 paralogs (A-H) (Jarmuz et al., 2002); at least five of these (C-H) can be antagonized by HIV-1 Vif (Hultquist et al., 2011). APOBEC3 paralog copy-numbers vary widely across mammalian genomes, with seven members observed in primate genomes, three in bovine and ovine genomes, four in feline genomes, and only one in murine genomes (Bogerd et al., 2008; Jarmuz et al., 2002; LaRue et al., 2008; Münk et al., 2008). The variability in APOBEC3 paralog numbers are thought to occur in a lineage-specific manner due to ongoing genetic conflict with pathogens like lentiviruses. APOBEC3 proteins exhibit positive selection in their amino acid sequences, a classic sign of genetic conflict with a pathogen (Daugherty and Malik, 2012).

While the role of HIV-1 Vif in APOBEC3 antagonism through its interaction with host CRL5 complex has been known for over a decade, only recently has a fundamental aspect of its biology been uncovered – the recruitment of the transcription co-activator core binding factor, beta subunit (CBFβ) to the CRL5 complex by Vif. The interaction between Vif and CBFβ was identified using affinity purification followed by LC-MS/MS mass spectrometry (AP-MS) of affinity-tagged HIV-1 Vif protein in HEK293 and Jurkat cell lines (Jäger et al., 2012a) as well as in H9 cells (Zhang et al., 2012). This interaction was found to be essential for Vif stability and expression, formation of a stable Vif-associated CRL5 complex both in vitro and in vivo, and to exhibit APOBEC3 antagonism (Hultquist et al., 2012; Jäger et al., 2012b; Kim et al., 2013; Miyagi et al., 2014; Zhang et al., 2012).. Curiously, CBFβ association with CRL5 complex was determined to be Vif dependent; CBFβ endogenous function is to form a heterodimer with RUNX transcription factors, stabilizing them and allosterically enhancing their DNA-binding activity (Huang et al., 2001; Tahirov et al., 2001). This lead to an intriguing hypothesis – that Vif recruits CBFβ to a hijacked CRL5 complex in order to disrupt RUNX-mediated gene expression

via a sequestration mechanism; a “dual-hijack” in that Vif hijacks a single CRL5 complex containing CBFβ in order to antagonize APOBEC3 and RUNX proteins simultaneously (**Figure 1.3**). Follow-up research showed Vif expression affected RUNX target genes and relieved RUNX interference of HIV-1 LTR promoter activity (Kim et al., 2013; Klase et al., 2014), consistent with the CBFβ sequestration model.

An outstanding question in recent Vif biology has been to what extent in the *Lentivirus* genus is the Vif-CBFβ interaction conserved, and if it is not, are there other CBFβ-like Vif interactors. An investigation of Vif proteins across all major representative clades of the *Lentivirus* genus as a whole is required to properly characterize Vif evolution. Specifically, a characterization of Vif interactors to determine molecular requirements for anti-APOBEC3 activity, and whether these interactors can enable Vif multi-functionality through “dual-hijack” mechanisms.

Figure 1.1

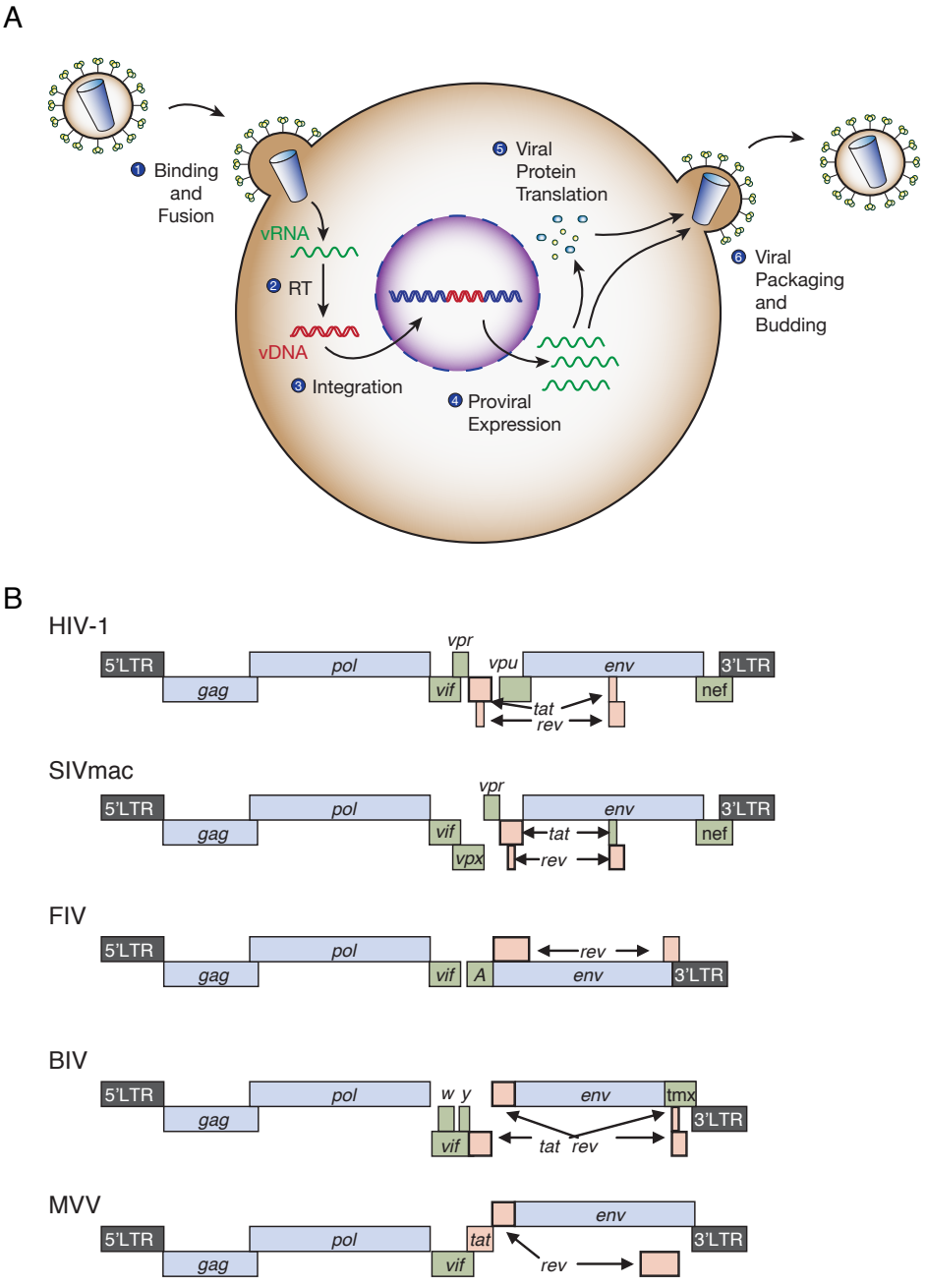
A
1 Binding and Fusion
2 RT
vRNA
vDNA
3 Integration
4 Proviral Expression
5 Viral Protein Translation
6 Viral Packaging and Budding
B
HIV-1
5'LTR
gag
pol
vif
vpr
vpu
env
3'LTR
nef
tat
rev
SIVmac
vpx
FIV
A
BIV
w
y
tmx
MVV

FIGURE 1.1: Overview of the HIV-1 Lifecycle

(A) A basic schema of the HIV-1 lifecycle. (1) After fusing with a CD4+ T-lymphocyte, HIV-1 releases the viral core containing enzymes and viral genomic RNA into the host cell. (2) Viral genomic RNA is reverse transcribed (RT) by the viral reverse transcriptase in to double-stranded DNA. (3) Viral DNA is integrated into the host genome by viral integrase. (4) The integrated provirus is expressed by recruited cellular transcriptional machinery. (5) Viral transcripts are translated by cellular ribosomes to synthesize new viral proteins. (6) Viral proteins and full-length viral genome RNAs assemble at the cell membrane, are packaged into virions, and a new virus buds from the infected cell.

(B) Cartoon of lentiviral genomes. Structural and enzymatic protein-coding genes are highlighted in blue (*gag*, *pol*, *env*); regulatory proteins are highlighted in red (*tat*, *rev*); all other genes (accessory factors) are highlighted in green. Adapted from St-Louis et al., 2004.

Figure 1.2

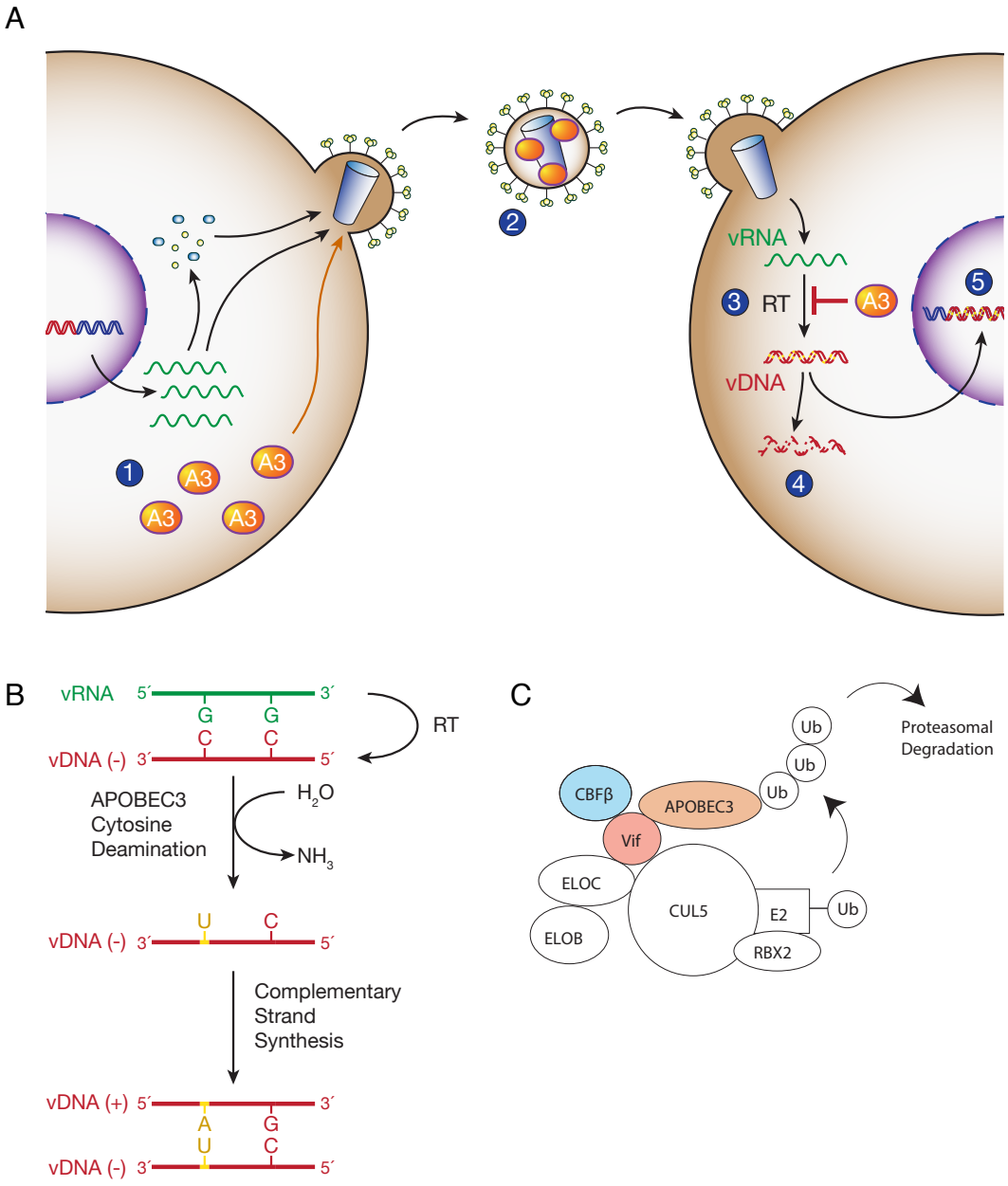
A
1
A3
A3
A3
A3
2
vRNA
3
RT
A3
vDNA
4
5
B
vRNA 5´ 3´
G G
C C
vDNA (-) 3´ 5´
RT
APOBEC3
Cytosine
Deamination
H2O
NH3
vDNA (-) 3´ U C 5´
Complementary
Strand
Synthesis
vDNA (+) 5´ 3´
A G
U C
vDNA (-) 3´ 5´
C
Ub
Ub
Ub
Proteasomal
Degradation
CBFβ
APOBEC3
Vif
ELOC
ELOB
CUL5
E2
Ub
RBX2

FIGURE 1.2: APOBEC3 Antagonism of HIV-1 Infection

(A) A basic schema of APOBEC3 antagonism of HIV-1 infection. (1) Members of the APOBEC3 family, including APOBEC3DE, F, G, and H, expressed in infected cells are packaged into budding virions in the absence of Vif protein. (2) Packaged APOBEC3 proteins are then carried to the next cell the virus infects. (3) During reverse transcription (RT) in the next round of infection, APOBEC3 proteins disrupt the processivity of reverse transcriptase and introduce G-to-A mutations in the viral reading frame through deamination of cDNA cytosines bases generated during RT. (4) Deaminated cytosines are uracil bases, which can lead to degradation of the viral DNA. (5) If the G-to-A mutated viral DNA is integrated, the provirus is rendered uninfectious due to deleterious mutations in viral genes. Adapted from Hultquist et al., 2011.

(B) Schema of APOBEC3-mediated cytosine deamination. The viral RNA genome is used as a template to generate a complementary DNA strand. The RNA strand is then digested by cellular RNAses. APOBEC3 proteins deaminate cytosine bases in the viral cDNA, which creates uracil bases in the cDNA. A complementary strand is then synthesized to create double stranded viral DNA, however uracil bases base-pair with adenine not guanine, leading to G-to-A mutations in the viral reading frame.

(C) APOBEC3 is neutralized by HIV-1 Vif. HIV-1 counteracts APOBEC3 antagonism with the accessory factor Vif, which recruits a Cullin-RING ubiquitin ligase (CRL) complex containing CUL5, ELOB, ELOC, RBX2, and CBFβ to target APOBEC3 proteins for poly-ubiquitylation, resulting in their degradation via the 26S proteasome.

Figure 1.3

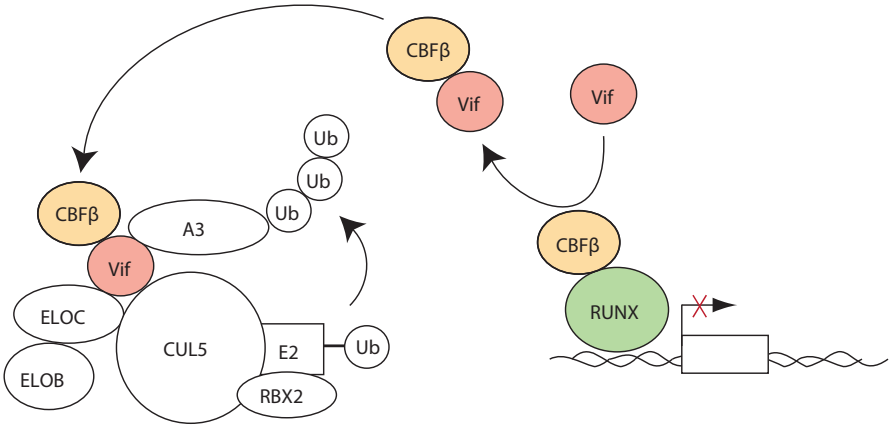
CBFβ
Vif
Vif
Ub
Ub
Ub
CBFβ
A3
Vif
CBFβ
RUNX
ELOC
CUL5
E2
Ub
ELOB
RBX2

Figure 1.3: HIV-1 Vif Dual Hijack Model

HIV-1 Vif hijacks CBFβ for dual function. Expression of Vif by HIV-1 results in sequestration of CBFβ in Vif-CBFβ-CRL5 complexes, preventing heterodimer formation of CBFβ with RUNX transcription factors. Sequestration blocks RUNX-mediated gene expression, and enables stable Vif assembly with CRL complexes to antagonize APOBEC3 proteins.

Chapter 2: Proteomic Analysis Reveals CBFβ is a Primate-Lentivirus Specific Vif Interactor

SUMMARY

Lentiviruses are a genus of retroviruses associated with slow, chronic infections of the immune system, with the human-infecting HIV-1 the most well-known and well-studied member. Lentiviral Vif is a viral accessory factor protein that nullifies host anti-viral APOBEC3 proteins by targeting them for poly-ubiquitylation and subsequent proteasomal degradation. Recently, a novel cofactor, CBFβ, was found to be required for HIV-1 Vif stability, assembly of CRL5 complexes, and anti-APOBEC3 activity, as well as potential other activities by antagonizing endogenous CBFβ function. We asked if this interaction with CBFβ is conserved amongst the *Lentivirus* genus, or if the interaction is specific to HIV-1. To this end, we carried out an affinity purification-mass spectrometry experiment in two human cell lines with five Vif proteins from representative clades in the genus – human infecting HIV-1, rhesus macaque-infecting SIVmac, cat-infecting FIV, cow-infecting BIV, and sheep-infecting MVV. We find that while all Vif proteins studied associate with a conserved CRL complex, only primate-infecting lentiviral Vif proteins, HIV-1 and SIVmac, associate with CBFβ. Furthermore, we show with functional assays that CBFβ is dispensable for Vif proteins that do not physically interact with CBFβ, MVV, BIV, and FIV. Lastly, we show through *in vitro* reconstitution assay that BIV Vif requires no CBFβ-like cofactor to assemble CRL5 complexes or to elicit ubiquitylation activity against purified cow APOBEC3 protein.

INTRODUCTION

Restriction Factors as a Barrier To Zoonosis

Lentiviruses are a genus within the retrovirus family characterized by slow, often chronic infections of the hosts' immune system that, depending on the species, may lead to immune deficiency. Unlike other viruses that can infect disparate hosts, such as Influenza, West-Nile Virus, or Dengue Virus, lentiviruses show much more limited host tropism, and are only known to infect mammals with some major clades, such as rodents, not known to have an associated lentivirus (Gifford, 2012). This is in part due to host restriction factors that limit viral host range (Sharp and Hahn, 2011). A restriction factor is a host factor, often interferon-stimulated, that reduces viral infectivity (Douville and Hiscott, 2010). This can be accomplished indirectly; for example, the restriction factor SAMHD1 acts to reduce viral reverse transcription efficiency by reducing cellular dNTP pools (Goldstone et al., 2011; Laguette et al., 2011). Others directly antagonize the virus. The membrane-anchored Tetherin (also known as BST2) acts to "tether" budding virions to the cell surface, reducing transmission of the virus within an infected host, and induces an interferon response after binding to virions (Neil et al., 2008). TRIM5 recognizes motifs in the virus core, stimulating anti-viral pathways and disrupting proper disassembly of the viral core (Fletcher and Towers, 2013). APOBEC3 proteins are packaged into budding virions, and inhibit reverse transcription processivity, and introduce mutations into viral reading frames, greatly reducing viral infectivity (Harris and Dudley, 2015). While each of these mechanisms are quite potent inhibitors of viral replication, the virus has evolved counteraction mechanisms to maintain infectivity even while the host cell can produce restriction factors. In HIV-1, Tetherin is counteracted by the accessory factor Vpu, which hijacks a CUL1-Skp1-βTRCP complex to target Tetherin for poly-ubiquitylation, causing its endocytosis from the cell surface so it can no longer block viral budding (Sauter, 2014). HIV-1 capsid proteins have evolved so that they are no longer recognized by human TRIM5 through interactions with various host factors (Rasaiyaah et al., 2013). Human APOBEC3 proteins are targeted by Vif for

poly-ubiquitylation and subsequent proteasomal degradation through hijacking of a CUL5-ELOB-ELOC-CBFβ CRL complex (Malim and Emerman, 2008).

These counteractions by the virus represent an ongoing genetic conflict between pathogens and their hosts, whereby an equilibrium condition is never reached as selective pressure constantly pushes the host factor to escape recognition by a viral antagonist, and the virus quickly evolves to adapt to this change and regain recognition (Daugherty and Malik, 2012). This diversifying, or positive, selection on host factors that interface with viral proteins leads to the creation of barrier to zoonosis, the spread of a virus from one host to another, as the restriction factors in a new host are diverged enough from the current host that viral counteracting proteins cannot neutralize them. Indeed, experiments using non-human primate restriction factors show potent inhibition of HIV-1 infection even with wild-type viruses (Chan et al., 2014; Hultquist et al., 2011).

Vif Displays High Sequence Diversity Despite Playing a Conserved Role in Apobec3 Antagonism

Lentiviruses infect most major clades of mammals, including primates, felines, and ungulates such as cows, sheep, and horses (Gifford, 2012). As APOBEC3 proteins can be found across these lineages (Bogerd et al., 2008; Jarmuz et al., 2002; LaRue et al., 2008; Münk et al., 2008)., lentiviruses must have a mechanism to overcome the barrier to infection they represent. Virtually all of them except for the horse-infecting EIAV encode a Vif protein that recognizes their natural host APOBEC3 proteins (Katzourakis et al., 2007; Kawakami et al., 1987), leading to their poly-ubiquitylation and subsequent proteasomal degradation to promote viral infectivity (Hultquist et al., 2011; LaRue et al., 2010; Sheehy et al., 2003; Yu et al., 2003). However, the mechanism by which this occurs, and particularly if these Vif proteins require CBFβ as a

requirement for Vif activity, was unclear. Viruses, particularly retroviruses, have high rates of sequence divergence due in part to lack of fidelity in RT, and this combined with genetic conflict may result in neutral Vif sequence divergence; however, an alternative explanation would be that other, functional changes in Vif are responsible for sequence divergence observations.

Interaction Discovery by AP-MS

HIV-1 encodes four accessory factors (Vif, Vpr, Vpu, and Nef) that can be characterized by their small molecular weight and their lack of enzymatic activity. Their functionality is determined by their interactions with host factors during infection leading to their repurposing, or hijacking, towards promoting viral infection (Malim and Emerman, 2008). A corollary to this phenomenon is that information about viral protein mechanism and activities can be ascertained by determining what host factors it physically interacts with. This involves two steps: first, isolating viral proteins with interacting host proteins still associated; and second, detecting these host factors. Affinity purification followed by mass spectrometry (AP-MS) is a common method used to accomplish this task. A given viral protein is fused to an affinity tag and then expressed in a host cell either on its own or from the viral genome during infection, then the viral protein is purified using the affinity tag in gentle conditions to prevent disruption of host factors bound to it. Once purified, the sample is subjected to liquid chromatography followed by two rounds of mass spectrometry (LC-MS/MS) that identifies the sequences of peptides in the sample, and these sequences are then used to identify which host proteins are present in the sample (Jäger et al., 2011). This type of experiment may be performed in any cell line that (1) can express a tagged viral protein and (2) has a sequenced genome, thus making it a powerful technique to map interactions over evolutionary time. AP-MS allows for the

investigation of what interactions are conserved across Vif proteins over the course of Lentivirus evolution, potentially revealing conserved or novel mechanisms across the genus.

RESULTS

Lentiviruses Show Strong Conservation of Vif Presence and Function Despite Highly Divergent Primary Sequences

This study examines Vif proteins from five major lentiviral lineages: the human pandemic virus HIV-1, the rhesus macaque-infecting simian immunodeficiency virus macaque (SIVmac), the cat-infecting feline immunodeficiency virus (FIV), the cow-infecting bovine immunodeficiency virus (BIV), and the sheep-infecting maedi-visna virus (MVV) (**Table 1**). Importantly, all of these Vif proteins from aforementioned lentiviruses have been previously demonstrated to mediate the degradation of natural host APOBEC3 proteins in human HEK293 cells (LaRue et al., 2010). This is critical for two reasons: (i) all of these Vif proteins can show anti-APOBEC3 activity in an experimental setting outside the context of infection, and (ii) all can perform this function against exogenously-expressed natural host APOBEC3 protein in human cells, without regard to the natural host tropism of the virus. Thus, all the non-human lentiviral Vif proteins used in this study are capable of mediating all host-pathogen interactions with the human orthologues of their natural host proteins required for mediating the degradation of their natural host APOBEC3 substrates.

Conservation of Vif within these viral genomes is assessed by two criteria: the ability to antagonize host APOBEC3 proteins, and the presence of an ELOC-binding BC-box motif, strongly suggestive of a conserved mechanism across Vif proteins of mediating APOBEC3 degradation via poly-ubiquitylation using a hijacked CRL complex (**Figure 2.1**). Despite this observed conservation of function and probable conservation of mechanism, Vif protein

primary sequences are highly divergent, sharing no more than 25% identity of between any pair of the five Vif proteins in this study (**Figure 2.2A**); even this number belies the true divergence of these proteins, as roughly half of the residues in each pair are unalignable (residue versus gap) and therefore are not used to calculate the identity or similarity scores. As the mechanism is largely inferred for all but the primate-infecting lentiviral Vif proteins, we sought to identify host factors required for Vif anti-APOBEC3 activity across the lentivirus genus.

AP-MS Reveals Conserved CRL Module Across Vif Evolution

To determine the evolution of Vif proteins through their interactions with host factors, we cloned five divergent Vif sequences from representative clades across the *Lentivirus* genus, from HIV-1^{NL4-3}, SIV_{mac239}, FIV, BIV, and MVV. 2xStrep or 3xFlag affinity tags were fused to either the amino (N-) or carboxy (C-) terminus of Vif proteins in pcDNA4/TO vectors for affinity purification – mass spectrometry (AP-MS) experiments, allowing for the unbiased detection of host proteins physically interacting with Vif baits. Previous literature demonstrated that all of these Vif proteins are able to induce the proteasomal degradation of natural host APOBEC3 proteins in human cell culture (LaRue et al., 2010); i.e., that human orthologs can substitute for all natural host factors required for Vif anti-APOBEC3 activity. We reasoned that as part of an initial screen, we could perform AP-MS experiments in human cell lines to determine interactions with Vif proteins required for anti-APOBEC3 activity. Affinity-tagged Vif proteins were either transiently transfected into HEK293T cells, or stably transfected into Jurkat TRex cells under a doxycycline-inducible promoter. Vif proteins were expressed for approximately 40 hours in 293T cells, or 18 hours in Jurkat T-cells, then cells were lysed and Vif proteins purified using affinity beads under conditions that would leave in vivo complexes intact. Purified eluates were subjected to SDS-PAGE followed by silver stain for quality control, then analyzed by

liquid chromatography followed by tandem mass spectrometry (LC-MS/MS) to identify co-purifying host factors (**Figure 2.2B-C**). 20 replicates in HEK293T cells and 2-3 replicates in Jurkat T-cells were run in this initial dataset. Interactions putatively identified by AP-MS were scored using the probability-based significance analysis of interactome (SAINT) algorithm (Choi et al., 2011). SAINT was selected out of three algorithms commonly used in the Krogan lab; the other two being mass spectrometry interaction statistics (MiST), developed to analyze the Jager HIV-1 global interaction dataset (Jäger et al., 2011), and the Comparative Proteomics Analysis Software Suite (CompPASS) developed to analyze overlapping host-host interactions in a deubiquitination enzyme dataset (Sowa et al., 2009). SAINT was selected due to the most consistent results in identifying known true positives without inclusion of known AP-MS non-specific interactors (host factors commonly observed in AP-MS data regardless of experiment bait protein). Interactions with a SAINT probability score ≥ 0.9 in at least one Vif dataset were included in the final datasets (Table 4**, Table 5**). Scored data was then organized by cell line and hierarchically clustered by Pearson correlation using SAINT scores **(Figure 2.3A)**.

The dataset immediately revealed a conserved module of CRL complex proteins, strongly suggestive of a conserved Vif mechanism for anti-APOBEC3 activity (**Figure 2.2D**). These data were verified by immunoblot (**Figure 2.2E**; **Figure 2.3B**). All Vif proteins showed strong binding to ELOB and ELOC in both cell lines tested. Interestingly, we observed what initially appeared to be a Cullin bias amongst the Vif proteins tested. CUL2 and CUL5 both use ELOB and ELOC as adapter proteins to bridge the interactions of the Cullin and the E3 substrate adapter (Sarikas et al., 2011); additional residues on the E3 protein discriminate between CUL2 and CUL5 binding (Kamura et al., 2004; Mahrour et al., 2008). However, additional experiments showed that the bias appeared to be strongly influenced by the terminus of affinity tags used, particularly with non-primate lentiviruses (**Figure 2.3C-D**). We

were unable to conclude whether or not the Cullin associations observed with different Vif proteins were representative of *in vivo* interactions, or artifacts from the use of affinity tags to purify and detect samples. Consistent with previous literature, detection of RBX1 or RBX2 in the Vif datasets correlated strongly with CUL2 and CUL5 abundance, respectively (Huang et al., 2009; Sarikas et al., 2011). Looking at conservation data, this core CRL module targeted by Vif is highly conserved across mammals; this is likely the reason for Vif functionality in human cell lines despite disparate natural host ranges (**Figure 2.4**).

CBFβ is a Primate-Specific Non-Canonical Cofactor

While the AP-MS Vif dataset confirmed a conserved mechanism of APOBEC3 antagonism through a hijacked CRL complex, CBFβ was only detected in purifications performed with primate-infecting lentiviral Vif proteins, from HIV-1 and SIVmac in either HEK293T cells or Jurkat T-cells (**Figure 2.2D**). Results were confirmed by immunoblot (**Figure 2.2E**; **Figure 2.3B**), and did not depend on affinity tag type or terminus (**Figure 2.3B-D**). A multiple sequence alignment of CBFβ shows that it is a highly conserved protein, making it unlikely that species-specific differences in CBFβ orthologs are responsible for the lacking of binding to FIV, BIV, or MVV Vif proteins (**Figure 2.4D**), and a recent study has shown that CBFβ proteins from multiple mammals can substitute for the human CBFβ in regulating HIV-1 Vif activity (Han et al., 2014). The possibility remained however that the interaction between CBFβ and these non-primate Vif proteins exists in vivo and regulates Vif anti-APOBEC3 activity, but is not strong enough to survive the conditions of affinity purification. To test this, we collaborated with Reuben Harris's group at the University of Minnesota to perform a single-cycle HIV-1 infectivity assay to test Vif dependence on CBFβ. HIV-1*Δvif* reporter virus is expressed in HEK293T cells with a constituitive knockdown of CBFβ, and challenged with APOBEC3 protein from a given natural host. A rescue of APOBEC3-mediated loss of HIV-1

infectivity is performed with a cognate Vif protein (e.g. BIV Vif for bovine APOBEC3 protein) with and without exogenous CBFβ to complement the knockdown (**Figure 2.5A**). As previously observed (Hultquist et al., 2012; Jäger et al., 2012b), and consistent with our AP-MS dataset, HIV-1 infectivity can only be rescued by primate lentiviral Vif proteins (HIV-1, SIVmac) when exogenous CBFβ is expressed to complement the knockdown (**Figure 2.5B-C**). In contrast, non-primate lentiviral Vif proteins (FIV, BIV, and MVV) show a rescue of reporter virus infectivity regardless of whether or not CBFβ is present, confirming it is dispensable for non-primate lentiviral Vif activity (**Figure 2.5D-F**).

In Vitro Reconstitution of Vif-Associated CRL5 Complexes Reveals Lack of BIV Vif Requirement for a Non-Canonical Cofactor and Potential Novel Cofactors For FIV and MVV Vif Proteins

Based on the observation that CBFβ does not associate with non-primate lentivirus Vif proteins, we were left with two possibilities in terms of the biochemical requirements of these Vif proteins: (i) no non-canonical cofactor is required for their activity, or (ii) a different host factor is hijacked by these Vif proteins to play a CBFβ-like role in their activities. In order to test the first possibility, we worked with John Gross's group at UCSF to carry out an *in vitro* reconstitution strategy to determine the minimum biochemical requirements for Vif-associated CRL complex formation and ubiquitylation activity against purified natural host APOBEC3 proteins. Previous work with HIV-1 Vif showed that attempts to reconstitute the Vif-associated CRL complex with ELOB and ELOC results in protein aggregation; only with the co-expression of CBFβ is a soluble, stable, stoichiometric complex formed that can then be mixed with CUL5 and RBX2 to form a stable and functional HIV-1 Vif-associated CRL5 complex (Jäger et al., 2012b). Expression of recombinant BIV Vif with ELOB and ELOC resulted in stable formation of a trimeric complex as assessed by size-exclusion chromatography, and formed a stable CRL5

complex when mixed with CUL5 and RBX2 (**Figure 2.5G-H**). *In vitro* ubiquitylation assays with the BIV Vif-CRL5 complex showed poly-ubiquitylation activity against purified bovine APOBEC3-Z3 protein, at a level comparable to that of HIV-1 Vif-CRL5 activity against purified human APOBEC3F protein (**Figure 2.5I**). We concluded that in contrast to primate-infecting lentivirus Vif proteins, BIV Vif does not require a non-canonical cofactor for CRL5 complex formation or natural host APOBEC3 ubiquitylation activity.

Recombinant expression with ELOB and ELOC alone was also attempted with FIV and MVV proteins. Unlike the case of BIV Vif, these Vif proteins failed to form stable trimeric complexes; instead, they aggregated in a manner reminiscent of HIV-1 Vif without CBFβ. We concluded that another factor playing a CBFβ-like role is required by these Vif proteins.

DISCUSSION

Viruses are obligate intra-cellular parasites that require the use of host cellular components to undertake the complex biochemistry of viral replication. These repurposing, or "hijacking", of cellular components to facilitate viral biology are often mediated by direct physical interaction between viral and host proteins. Therefore, a list or map of physical interactions between viral proteins and host cell proteins can provide much detail in the way of understanding the myriad biochemical processes that define the virus lifecycle. While this has been performed now genome-wide for a number of viruses, including HIV-1 (Jäger et al., 2012a), HCV (Ramage et al., 2015), and KHSV (Davis et al., 2015), few studies have been performed to understand the evolution of these viral-host interactions (VHIs). In particular, to answer questions such as (i) how stable are VHIs over evolutionary time, (ii) are particular VHIs associated with increases in virulence or zoonosis, and (iii) can we make predictions or generalized models of VHI evolution. All are quite relevant to the efforts to treat and eradicate

viral pathogens, and in particular to a recent focus in targeting the VHI interface with therapeutics to block viral replication in a manner more resistant to viral escape (de Chassey et al., 2014). We selected the HIV-1 Vif protein for this pilot study due to its conservation of both presence in lentiviral genomes and in anti-APOBEC3 activity, the great body of knowledge already accumulated on HIV-1 and related virus biology, and that our group had recently carried out an AP-MS study, as well as follow-up experimental work, on HIV-1.

The initial discovery of the HIV-1 Vif-CBFβ interaction led quickly to the characterization of the interaction as required for the stable expression of Vif, assembly of a Vif-hijacked CRL5 complex, and for Vif-mediated APOBEC3 antagonism (Jäger et al., 2012b). Surprisingly, despite this intimate relationship between HIV-1 Vif and CBFβ, we were able to show though repeated AP-MS experiments that the interaction between Vif proteins and CBFβ orthologs is not conserved over the course of lentivirus evolution. We also provided functional evidence demonstrating the dispensability of CBFβ in non-primate infecting lentiviral Vif proteins for anti-APOBEC3 using a single-cycle viral replication assay; this assay captures multiple aspects of the lentiviral-APOBEC3 antagonism biology including APOBEC3 degradation, APOBEC3 packaging, and APOBEC3 antagonism of early viral lifecycle steps. We concluded the interaction between Vif and CBFβ is limited to primate-infecting lentiviruses, SIVmac and HIV-1 in this study. Other studies have also demonstrated the lineage-specific nature of the Vif-CBFβ interaction limited to primate-infecting lentiviruses only (Ai et al., 2014; Zhang et al., 2014a, 2014b), though in a direct fashion using immunoblotting assays and not through unbiased proteomics techniques. The AP-MS data provided data highly suggestive of a conserved mechanism of APOBEC3 antagonism using hijacking CRL complexes alongside the CBFβ data, showing that all of these Vif proteins were associating with a conserved CRL complex in human cells under similar experimental conditions.

Once the data strongly suggesting that CBFβ is dispensible for non-primate infecting lentiviral Vif protein activity, we implemented a reductionist approach of reconstituting Vif-CRL5 complex *in vitro* to assess what, if any, non-canonical cofactors are required for MVV, BIV, or FIV Vif proteins. A protocol for *in vitro* reconstitution of Vif-CRL5 complexes had been previously established by the Gross lab at UCSF (Jäger et al., 2012b; Kim et al., 2013), simplifying the process of screening for cofactor use using reconstitution assays. We demonstrated that BIV Vif requires no cofactor for either Vif-CRL complex assembly or poly-ubiquitylation activity against recombinant purified bovine APOBEC3 protein, indicating that a Vif protein can function without a cofactor, though it remains unclear as to whether the most recent common ancestor Vif was BIV Vif-like in not requiring a cofactor, or more primate lentiviral Vif-like in requiring a cofactor, and BIV Vif subsequently lost due some undescribed influence on BIV evolution.

Figure 2.1

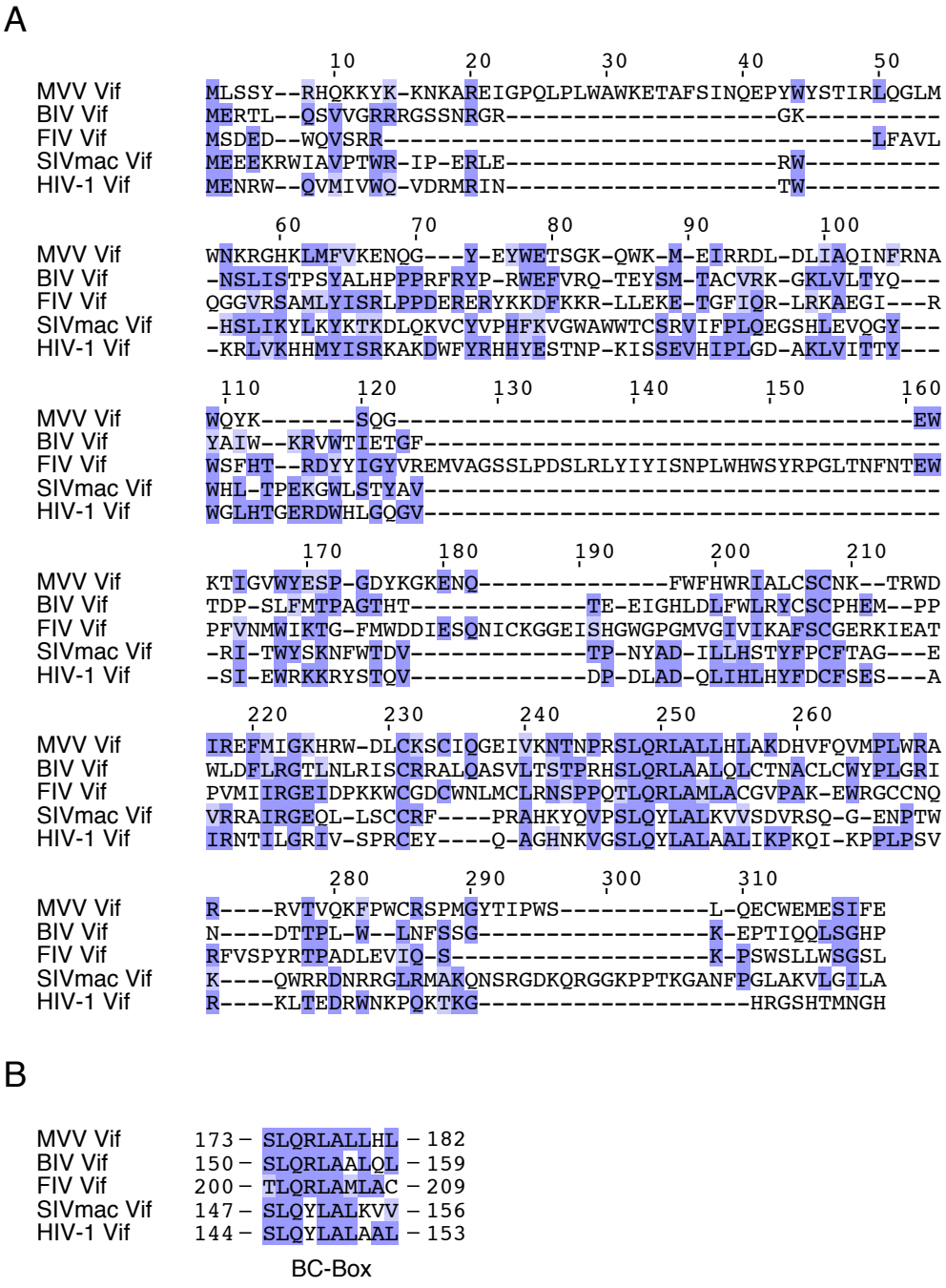
A
MVV Vif
BIV Vif
FIV Vif
SIVmac Vif
HIV-1 Vif
B
MVV Vif 173 – SLQRLALLHL – 182
BIV Vif 150 – SLQRLAALQL – 159
FIV Vif 200 – TLQRLAMLAC – 209
SIVmac Vif 147 – SLQYLALKVV – 156
HIV-1 Vif 144 – SLQYLALAAL – 153
BC-Box

Figure 2.1: Multiple Sequence Alignment of Lentivirus Vif Proteins.

(A) Multiple sequence alignment of Vif proteins used in this study. Alignment was performed by the PSI-Coffee variant of the T-Coffee alignment algorithm (Notredame et al., 2000). Residues were highlighted by BLOSUM62 similarity using the software Jalview (Waterhouse et al., 2009).

(B) BC-box motif from alignment in **A**. Numbers indicate position in Vif sequence.

Figure 2.2

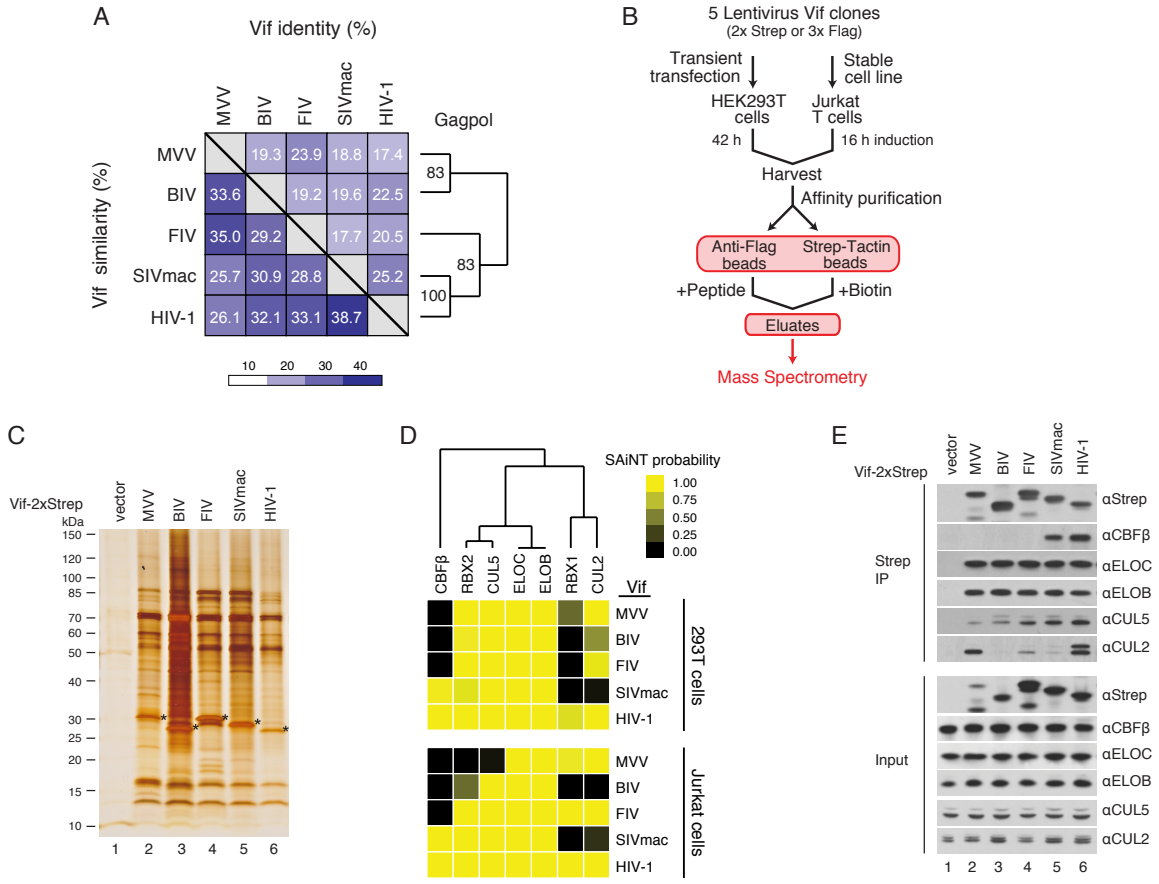
A
Vif identity (%)
MVV
BIV
FIV
SIVmac
HIV-1
Gagpol
Vif similarity (%)
MVV 19.3 23.9 18.8 17.4
BIV 33.6 19.2 19.6 22.5
FIV 35.0 29.2 17.7 20.5
SIVmac 25.7 30.9 28.8 25.2
HIV-1 26.1 32.1 33.1 38.7
83
83
100
10 20 30 40
B
5 Lentivirus Vif clones
(2x Strep or 3x Flag)
Transient transfection
Stable cell line
HEK293T cells
Jurkat T cells
42 h
16 h induction
Harvest
Affinity purification
Anti-Flag beads
Strep-Tactin beads
+Peptide
+Biotin
Eluates
Mass Spectrometry
C
Vif-2xStrep
vector
MVV
BIV
FIV
SIVmac
HIV-1
kDa
150
120
100
85
70
60
50
40
30
25
20
15
10
1 2 3 4 5 6
D
SAiNT probability
1.00
0.75
0.50
0.25
0.00
CBFβ
RBX2
CUL5
ELOC
ELOB
RBX1
CUL2
Vif
MVV
BIV
FIV
SIVmac
HIV-1
293T cells
Jurkat cells
E
Vif-2xStrep
vector
MVV
BIV
FIV
SIVmac
HIV-1
Strep IP
Input
αStrep
αCBFβ
αELOC
αELOB
αCUL5
αCUL2
1 2 3 4 5 6

Figure 2.2: Proteomic analysis of lentiviral Vif proteins.

(**A**) Percent identity and percent similarity matrix of Vif proteins used in this study. Distance tree generated from Gagpol protein sequence of viruses, with bootstrap support values.

(**B**) Flow-chart of affinity purification – mass spectrometry (AP-MS) pipeline used to identify Vif-interacting host proteins.

(**C**) Representative silver stained SDS-PAGE of eluates from a Vif-Strep purification in transiently transfected HEK293T cells. Asterisks indicate Vif proteins.

(**D**) Cullin ubiquitin ring ligase (CRL) complex proteins identified in AP-MS experiments, colored by SAINT score and clustered hierarchically by correlation.

(**E**) Immunoblot of a Strep affinity purification of Strep-tagged Vif proteins transiently expressed in HEK293T cells, probing for CRL proteins highlighted in panel (D)

Figure 2.3

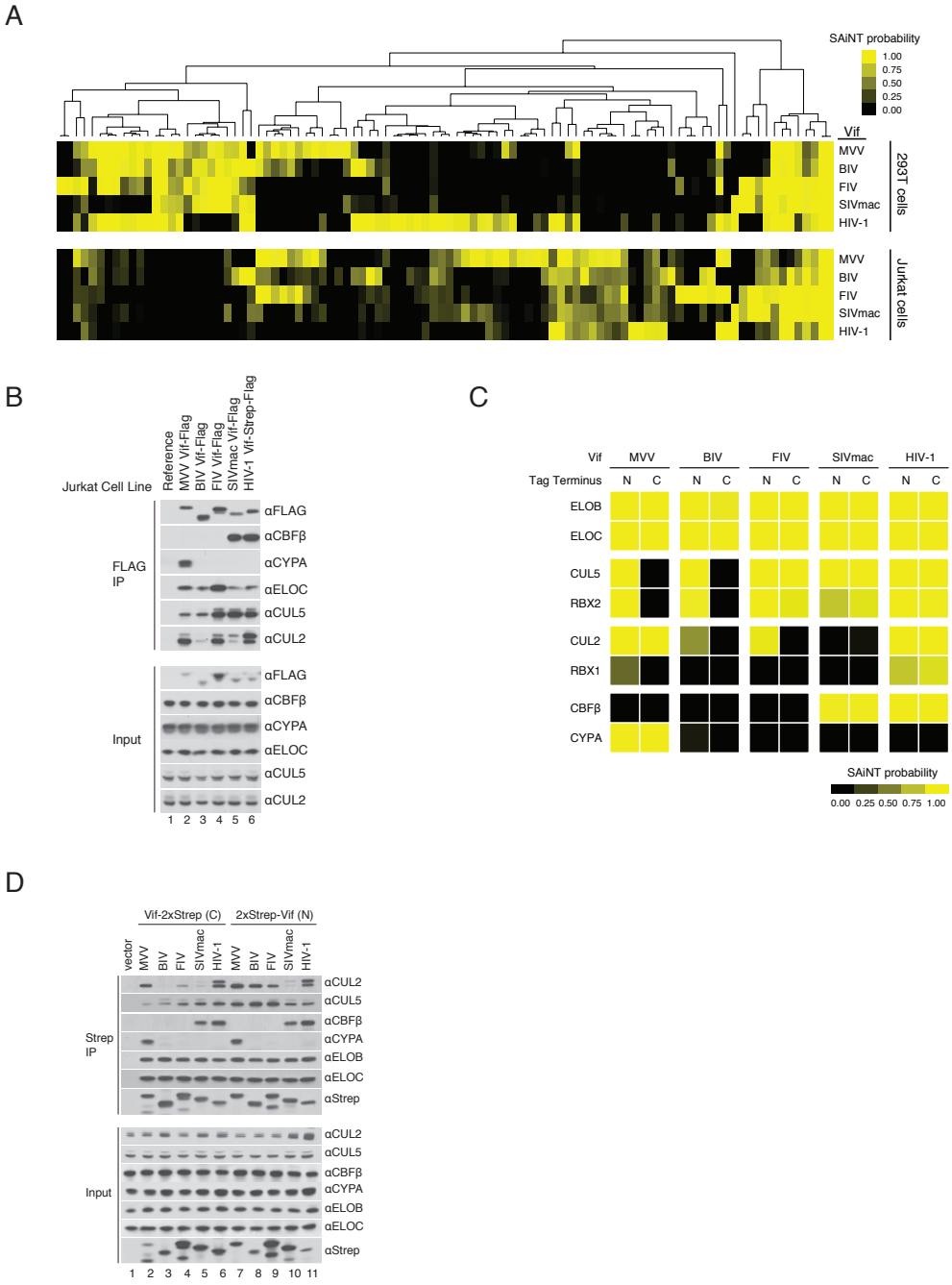
A
SAiNT probability
1.00
0.75
0.50
0.25
0.00
Vif
MVV
BIV
FIV
SIVmac
HIV-1
293T cells
Jurkat cells
B
Jurkat Cell Line
Reference
MVV Vif-Flag
BIV Vif-Flag
FIV Vif-Flag
SIVmac Vif-Flag
HIV-1 Vif-Strep-Flag
FLAG IP
Input
αFLAG
αCBFβ
αCYPA
αELOC
αCUL5
αCUL2
1 2 3 4 5 6
C
Vif
MVV
BIV
FIV
SIVmac
HIV-1
Tag Terminus
N C
ELOB
ELOC
CUL5
RBX2
CUL2
RBX1
CBFβ
CYPA
SAiNT probability
0.00 0.25 0.50 0.75 1.00
D
Vif-2xStrep (C)
2xStrep-Vif (N)
vector
MVV
BIV
FIV
SIVmac
HIV-1
Strep IP
Input
αCUL2
αCUL5
αCBFβ
αCYPA
αELOB
αELOC
αStrep
1 2 3 4 5 6 7 8 9 10 11

Figure 2.3: Affinity Tag Terminus Affects Cullin Specificity of Non-Primate Lentiviral Vif Proteins.

(A) Heatmap of analyzed data from Vif AP-MS experiments in HEK293T and Jurkat T-cell lines. AP-MS experiments were scored using the SAINT algorithm using at least 2 experiments per Vif protein per cell line, comparing Vif results to controls. HEK293T data and Jurkat data were scored separately. Interactors are colored by SAINT score and clustered hierarchically by correlation.

(B) SDS-PAGE immunoblot of a Flag affinity purification of Flag-tagged Vif proteins induced from stable Jurkat TRex cells, probing for CRL proteins highlighted in **Figure 1D**.

(C) AP-MS data comparing N-terminus (N) versus C-terminus (C) 2xStrep affinity tagging of Vif proteins. Heatmap denotes SAINT probabilities of interactions. Data from 7-10 replicate AP-MS experiments per terminus in 293T cells.

(D) Immunoblotting of affinity purifications from transient transfections of HEK293T cells comparing N-terminus versus C-terminus 2xStrep tagging of Vif proteins.

Figure 2.4

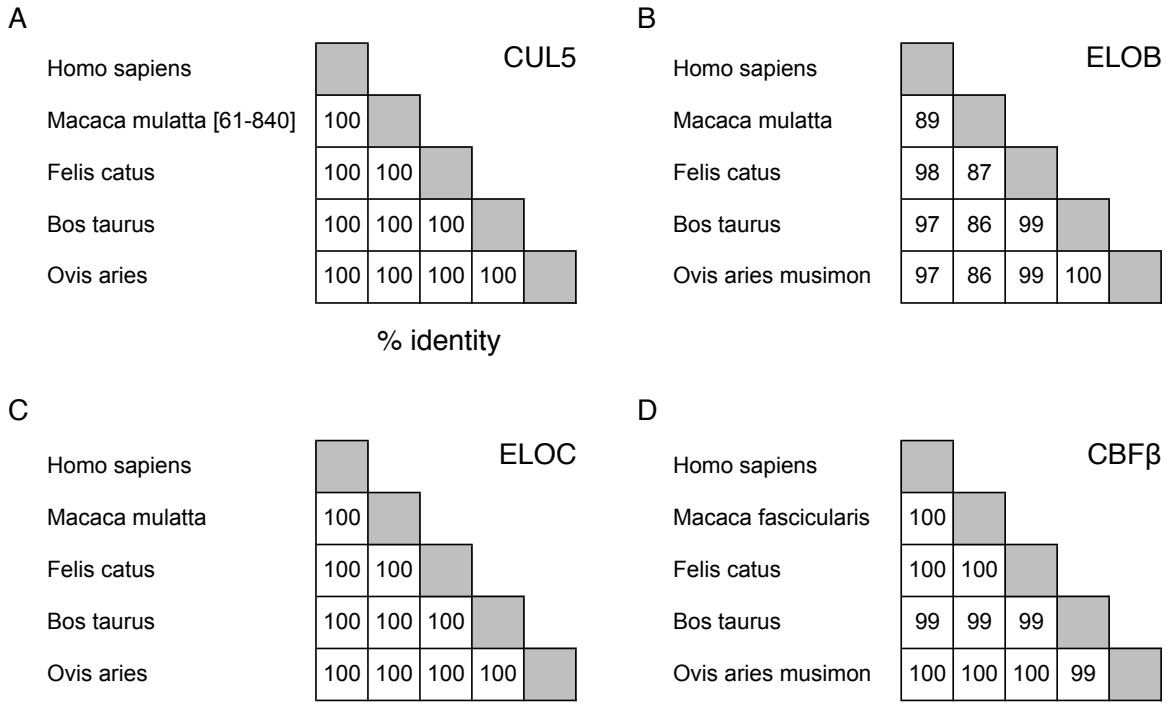
A
CUL5
Homo sapiens
Macaca mulatta [61-840] 100
Felis catus 100 100
Bos taurus 100 100 100
Ovis aries 100 100 100 100
% identity
B
ELOB
Homo sapiens
Macaca mulatta 89
Felis catus 98 87
Bos taurus 97 86 99
Ovis aries musimon 97 86 99 100
C
ELOC
Homo sapiens
Macaca mulatta 100
Felis catus 100 100
Bos taurus 100 100 100
Ovis aries 100 100 100 100
D
CBFβ
Homo sapiens
Macaca fascicularis 100
Felis catus 100 100
Bos taurus 99 99 99
Ovis aries musimon 100 100 100 99

Figure 2.4: Host factors in the HIV-1 Vif-CRL5 complex are highly conserved

Percent identity matrices of host proteins in the Vif-hijacked CRL5 complex across mammals Homo sapiens, Macaca mulatta (rhesus macaque), Felis catus (domestic cat), Bos taurus (cow), and Ovis aries (sheep), infected by HIV-1, SIVmac, FIV, BIV, and MVV, respectively.

(A) CUL5. Hs: NP_003469.2; Mm: XP_001103587.2, first 60 residues truncated;
Fc: NP_001233250.1; Bt: XP_002693012.1; Oa: XP_004016047.1.

(B) ELOB. Hs: NP_009039.1; Mm: XP_001113620.1; Fc: XP_003998980.1;
Bt: NP_001029972.1; Oam: XP_011999936.1, no sequence available for Oa, related subspecies.

(C) ELOC. Hs: NP_005639.1; Mm: NP_001185606.1; Fc: NP_001233156.1;
Bt: NP_001039958.1; Oa: XP_004011792.1

(D) CBFβ. Hs: NP_001746.1; Mf: XP_005592247.1, no sequence available for Mm, related species in Macaca genus; Fc: NP_001291957.1; Bt: NP_001178364.1; Oam: XP_011965836.1, no sequence available for Oa, related subspecies.

Figure 2.5

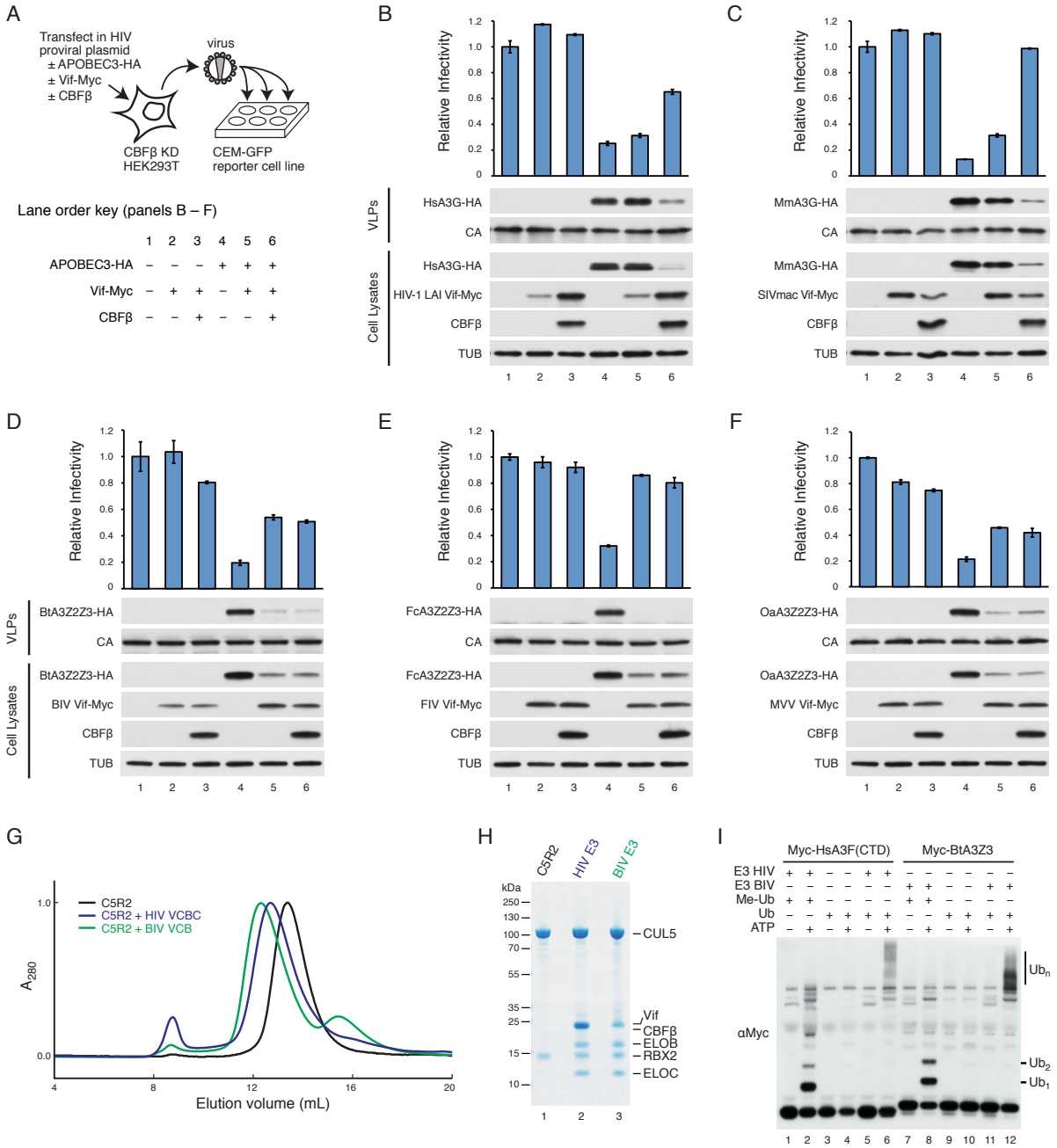
A
Transfect in HIV proviral plasmid
± APOBEC3-HA
± Vif-Myc
± CBFβ
virus
CBFβ KD HEK293T
CEM-GFP reporter cell line
Lane order key (panels B – F)
1 2 3 4 5 6
APOBEC3-HA – – – + + +
Vif-Myc – + + – + +
CBFβ – – + – – +
B
Relative Infectivity
VLPs
HsA3G-HA
CA
Cell Lysates
HsA3G-HA
HIV-1 LAI Vif-Myc
CBFβ
TUB
C
Relative Infectivity
MmA3G-HA
CA
MmA3G-HA
SIVmac Vif-Myc
CBFβ
TUB
D
Relative Infectivity
VLPs
BtA3Z2Z3-HA
CA
Cell Lysates
BtA3Z2Z3-HA
BIV Vif-Myc
CBFβ
TUB
E
Relative Infectivity
FcA3Z2Z3-HA
CA
FcA3Z2Z3-HA
FIV Vif-Myc
CBFβ
TUB
F
Relative Infectivity
OaA3Z2Z3-HA
CA
OaA3Z2Z3-HA
MVV Vif-Myc
CBFβ
TUB
G
C5R2
C5R2 + HIV VCBC
C5R2 + BIV VCB
A280
Elution volume (mL)
H
C5R2
HIV E3
BIV E3
kDa
CUL5
Vif
CBFβ
ELOB
RBX2
ELOC
I
Myc-HsA3F(CTD)
Myc-BtA3Z3
E3 HIV
E3 BIV
Me-Ub
Ub
ATP
αMyc
Ubn
Ub2
Ub1

Figure 2.5: Vif dependence on CBFβ is primate lentivirus-specific.

(**A**) Schema of single-round infection assay.

(**B-F**) Infectivity assays described in panel (A), using Vif proteins and cognate APOBEC3 proteins. Bars represent mean ± S.E. of GFP expression from virus reporter lines. Viral, A3, and CBFβ proteins are detected by immunoblot. VLPs: virus-like particles.

(**G**) UV absorbance curves are shown for gel filtration of CUL5-RBX2 (C5R2) alone, or mixed with an excess of indicated Vif complexes (HIV VCBC = Vif-ELOB-ELOC-CBFβ, BIV VCB = Vif-ELOB-ELOC. Peaks are observed at earlier elution volumes when C5R2 is mixed with Vif complexes, indicating E3 complex formation.

(**H**) Coomassie-blue stained SDS-PAGE of peak fractions collected from gel filtration runs shown in panel (G). Vif bands are indicated by an asterisk, and cofactor CBFβ is indicated by a circle.

(**I**) Immunoblot of ubiquitylation reactions with either HIV-1 Vif or BIV Vif E3, using myc-tagged C-terminal domain of human A3F (myc-HsA3F CTD) or bovine A3Z3 (myc-BtA3Z3) as substrate, respectively. Ub: ubiquitin; Me-Ub: methylated ubiquitin.

Chapter 3: Cyclophilin A is a Novel Non-Canonical Cofactor in MVV Vif-Associated CRL Complexes

SUMMARY

After establishing that the interaction between CBFβ and Vif is limited to primate-infecting lentiviruses, we performed in vitro reconstitution assays that showed BIV Vif does not require a cofactor, but that MVV and FIV Vif may require a cofactor. We examined our existing AP-MS data and found a potential MVV Vif non-canonical cofactor, cyclophilin A (CYPA). Tandem affinity purification of Vif and CUL5 proteins show CYPA associates with MVV Vif-CRL5 complexes in vivo. A limited mutagenesis screen revealed a proline-rich motif that is conserved among closely related CAEV viruses, whose Vif proteins also bind CYPA. We performed an NMR binding assay between an MVV Vif peptide containing this proline-rich motif and labeled CYPA, and found the peptide specifically binds the CYPA active site. Use of a CYPA active-site inhibitor, cyclosporine A, blocks MVV Vif binding, further indicating the interaction between the two proteins is mediated through the CYPA active site. In vitro assays confirm CYPA is required for MVV Vif-ELOB-ELOC reconstitution, CRL5 complex assembly, and ubiquitylation activity against purified sheep APOBEC3 protein. We also show that the overall structure of the MVV Vif-CYPA-CRL5 complex is similar to that of the HIV-1 Vif-CBFβ-CRL5 complex. We conclude that CYPA is a novel MVV Vif non-canonical cofactor.

INTRODUCTION

Identification of Non-Canonical Vif CRL Complex Cofactors

The discovery of the HIV-1 Vif-CBFβ interaction as an essential regulator of both Vif stability and activity was unexpected given the literature of how endogenous ubiquitin E3 ligases

operate. While endogenous E3 ligase association with CRL complexes are regulated through post-translational modification and turnover (Deshaies and Joazeiro, 2009), there does not appear to be a known example of an endogenous E3 ligase required to form a heterodimer for activity. Moreover, CBFβ is not known to associate with CRL complexes in a stoichiometric manner in the absence of HIV-1 Vif (Jäger et al., 2012b). This is the origin of the term "non-canonical cofactor" to describe host factors playing a CBFβ-like role in Vif biology. Thus, our criteria for discovery of a novel non-canonical cofactor is that the host protein should (i) not associate with CRL complexes in the absence of a Vif protein that requires it, and (ii) Vif should not be able to hijack an active CRL complex in the absence of the non-canonical cofactor.

RESULTS

AP-MS Data and Tandem Affinity Purification Reveal Cyclophilin A as Likely MVV Vif Non-Canonical Cofactor

In vitro reconstitution assays performed with MVV and FIV Vif proteins with ELOB and ELOC alone failed to generate stable, trimeric complexes, similar to the behavior of HIV-1 Vif in the absence of CBFβ (**Figure 3.5A-B**). We inferred that this was due to a requirement of a not-yet-identified non-canonical cofactor that is not CBFβ. Re-examining the AP-MS data generated for each Vif protein, we looked for candidate cofactors that (i) had high SAINT scores, and (ii) were specific for MVV or FIV Vif proteins. These criteria were chosen based on the fact that CBFβ showed these characteristics in the AP-MS dataset for HIV-1 and SIVmac Vif proteins (**Table 4**, **Table 5**). While no candidate in the FIV Vif dataset matched both of these criteria, one host factor in particular did match these criteria in the MVV Vif dataset – the cis-trans prolyl isomerase cyclophilin A (CYPA) (**Figure 3.1A**). CYPA was particularly interesting as a candidate novel non-canonical cofactor in that it is similar in size to CBFβ (18 and 20 kDa, respectively),

and CYPA has a well-documented role in HIV-1 biology, interacting with the Capsid (CA) protein to aid in cloaking the viral core from detection by the innate immune system (Luban et al., 1993; Rasaiyaah et al., 2013; Thali et al., 1994; Towers et al., 2003). We re-probed an immunoblot of Vif-2xStrep purifications and observed a specific interaction of CYPA only with MVV Vif (**Figure 3.1B**), consistent with the AP-MS results. To verify that the interaction we observed between CYPA and MVV Vif was not an artifact of performing the purifications in human cell lines, we performed an MVV Vif-2xStrep purification in sheep fetal lamb kidney (FLK) cells. We observed robust co-purification of CYPA with MVV Vif in the FLK cells (**Figure 3.1C**), demonstrating that the interaction was not an artifact of expressing MVV Vif in HEK293T or other human cells.

In addition, we asked if the interaction between MVV Vif was specific to CYPA, or if other cyclophilin molecules could substitute. CYPA is one member of a family of cyclophilin proteins (Wang and Heitman, 2005), and we entertained the idea that CYPA was purified with MVV Vif and not other cyclophilins due to expression level. To test this, we cloned three other cyclophilins of varying relatedness to CYPA with 3xFlag affinity tags: Ppeptidylprolyl isomerase A (Cyclophilin A)-Like 4G (PPIAL4G), cyclophilin B (CYPB), and cyclophilin D (CYPD) (**Figure 3.2A**). We performed a Strep affinity purification assay between MVV Vif-2xStrep and the four cyclophilin constructs, assessing co-purification of the various cyclophilins by immunoblot (**Figure 3.2B**). We observe strong co-purification from only CYPA, though a relatively low amount of PPIAL4G was also co-purified, potentially due to its close similarity to CYPA (**Figure 3.2A**). We concluded that MVV Vif specifically interacts with CYPA and not other cell cyclophilin proteins.

While the AP-MS data was demonstrated a robust and specific interaction between CYPA and MVV Vif, it did not provide information as to whether CYPA was associated with an

MVV Vif-CRL complex *in vivo*. To test this, we transfected HEK293T cells with CUL5-3xFlag and one of each of the the five Vif constructs (MVV, BIV, FIV, SIVmac, HIV-1) with a 2xStrep tag, and performed a two-step tandem affinity purification, first pulling down on the Strep tag then the Flag tag, ideally only leaving complexes containing both affinity tags (**Figure 3.1D**). We observed high peptide percent coverages from Vif and CUL5 baits, as well as from members of the CRL5 complex (ELOB, ELOC, RBX2, NEDD8) from each sample (**Figure 3.1E**, **Table 6**). We only identify CBFβ in the SIVmac and HIV-1 samples, as expected given its role as a non-canonical cofactor for these primate-infecting lentiviruses. We identified high peptide coverage of CYPA only in the MVV Vif sample, consistent with its role as a non-canonical cofactor for MVV Vif. These data were additionally verified by immunoblot (**Figure 3.1F**). We concluded that CYPA associates with MVV Vif-hijacked CRL5 complexes *in vivo*.

Site-Directed Mutagenesis Identifies Prolines 21 and 24 as Crucial for Mediating MVV Vif-CYPA Interaction

CYPA targets proline residues in client proteins as substrates for its cis-trans propyl-isomerase activity (Fischer et al., 1984, 1989; Takahashi et al., 1989). To test if any proline residues in MVV Vif were mediating the interaction with CYPA, we performed a limited alanine scan of MVV Vif proline residues, then performed a CYPA co-affinity purification assay with these constructs. Various 2xStrep-tagged MVV Vif constructs were co-transfected with CYPA-3xFlag in HEK293T cells, then a Flag immuneprecipitation was performed, and Vif association with CYPA was assessed by immunoblotting (**Figure 3.3A**). We identified two Vif constructs that showed profound loss in CYPA binding – the double mutant P21A/P24A, and P192A. We focused on the double mutant P21A / P24A as P192 appears to be more conserved (**Figure 2.1A**), whereas the $_{21}$PxxP$_{24}$ motif appears only in MVV and the closely related CAEV Vif proteins (**Figure 3.3B**). Indeed, affinity purification of CAEV Vif shows co-purification of

endogenous CYPA, consistent with the motif's role in CYPA binding (**Figure 3.6A**). Unexpectedly, a control mutant that is unable to bind ELOC through alanine mutation of the BC-Box (**Figure 2.1B**), SLQ::AAA, also showed a profound loss in CYPA binding, implying proper formation of the entire MVV Vif-CYPA-ELOB-ELOC tetramer is required for a stable interaction between MVV Vif and CYPA.

MVV Vif 21PxxP24 Region Binds CYPA Active Site

In order to more definitively assess whether the P21 and P24 residues played a direct role in binding CYPA, a peptide containing the residues, MVV Vif$^{17-26}$ (**Figure 3.3B**), was synthesized to perform NMR shift assays in the presence of labeled CYPA. Working with James Fraser's group at UCSF, two-dimensional ^{15}N-^{1}H chemical shift correlation spectroscopy was performed on labeled CYPA in the unbound state and in the presence of increasing concentrations of the MVV Vif$^{17-26}$ peptide. Vif peptide up to 300 μM induced significant chemical shift perturbations on the protein spectrum, although saturation was not reached even at the highest Vif concentration, and a binding constant could not be determined (**Figure 3.3C**). Mapping of the resonances that disappeared upon addition of the MVV Vif peptide indicated that the peptide binds to the active site of CYPA (**Figure 3.3C-D**). Additional residues surrounding the active site were observed to enter slow exchange mode, or displayed peak broadening (**Figure 3.5C**). We conclude that MVV Vif directly binds CYPA at its active site using the $_{21}$PxxP$_{24}$ motif.

As an orthogonal method to test if the MVV Vif-CYPA interaction is mediated through the host factor's active site, we treated HEK293T cells transfected with 2xStrep-tagged MVV Vif with the CYPA inhibitor cyclosporine A (CsA), a small molecule which binds to the active site of CYPA and can sterically block CYPA-substrate interactions mediated through the active site (Takahashi et al., 1989; Thériault et al., 1993). A titration of CsA followed by affinity purification of MVV Vif shows a sensitivity of the MVV Vif-CYPA interaction to CsA treatment, where co-

purification of CYPA is weakened to the point of dropping below detectable levels in the 5 – 10 μM range as assessed by immunoblotting (**Figure 3.3E**). A concomitant weakening of ELOC co-purification was also observed.

Given the well-studied interaction between CYPA and HIV-1 CA, we asked if the MVV Vif-CYPA interaction is of a similar affinity, and if the MVV CA interacts with CYPA. Interestingly, the concentration of CsA required to disrupt the MVV Vif-CYPA interaction as assessed by co-purification is an order of magnitude higher than the concentration required to disrupt the HIV-1 CA-CYPA interaction (**Figure 3.6B**). Performing an affinity purification of 2xStrep-tagged MVV CA in transfected HEK293T cells, we observe no co-purification of endogenous CYPA, whereas we readily detect co-purified CYPA with MVV Vif and HIV-1 CA (**Figure 3.6C**), indicating the lack of CYPA binding by MVV CA.

In Vivo Reconstitution Assay Confirms CYPA Role in MVV Vif-CRL5 Complex Formation and Activity

After confirming an association between CYPA and the MVV Vif-CRL5 complex in vivo, we revisited our Vif-CRL complex *in vitro* reconstitution assay to assess whether addition of CYPA can rescue the previously observed aggregation of MVV Vif-ELOB-ELOC. Co-expression of recombinant CYPA with MVV Vif, ELOB, and ELOC resulted in the formation of a stable, non-aggregating tetrameric complex as assessed by size-exclusion chromatography (**Figure 3.7B**). The MVV Vif-CYPA-ELOB-ELOC tetramer readily associated with CUL5-RBX2 to form a stable CRL5 complex (**Figure 3.4A-B**). We performed an *in vitro* ubiquitylation assay with the reconstituted MVV Vif-CYPA-CRL5 complex and observed mono-ubiquitylation activity against purified sheep APOBEC3Z3 protein, but not against human APOBEC3H (**Figure 3.4C**).

Structural Analysis of Vif-CRL Complexes Reveals Related but Potentially Distinct Complex Topologies

After generating in vitro reconstituted Vif-CRL5 complexes for MVV and HIV-1, we asked these complexes conformed to similar macromolecular organizations. To this end, we again collaborated with John Gross's group at UCSF to perform small angle X-ray scattering (SAXS) analysis on a MVV Vif-CYPA-CRL5 complex, as well as an HIV-1-CBFβ-CRL5 complex using a truncated HIV-1 Vif protein, HIV-1 Vif^{1-174}. Both the MVV and the HIV-1 complexes were monodisperse and well-folded under the experimental conditions, and therefore suitable for envelope generation (**Figure 3.7A-C**). The pair-wise distribution function revealed that both HIV-1 and MVV complexes have similar maximal dimensions (Dmax), with values of 190Å and 200Å, respectively (**Figure 3.4D**, **Table 7**). Analysis of the resulting envelopes revealed that despite different complex constituents the overall surface of the macromolecular assemblies is quite similar with an overall elongated E3 ring-ligase conformation. To determine how well the SAXS envelopes fit the available structure data, a model of HIV-1 Vif-CRL5 was generated. While the HIV-1 Vif-CRL5 model was relatively well fit into its experimental SAXS envelope, with a chi value of 1.89 (**Figure 3.7D**), there was a slightly poorer fit into the experimentally determined MVV Vif-CRL5 envelope, possibly due to differences in substrate receptor structure (**Figure 3.4E**). This likely reflects different fold of CYPA, CBFβ and possibly MVV and HIV-1 Vif. SAXS analysis was also attempted on the BIV Vif-CRL5 complex, but we were unable to concentrate the complex to a sufficiently high density without the proteins crashing out of solution.

DISCUSSION

While the observation of aggregation during *in vitro* reconstitution of MVV Vif with ELOB and ELOC alone implied the requirement of a non-canonical cofactor that was not CBFβ, the actual identification of said cofactor, CYPA, was quite unexpected. This is compounded by the observation, using the same in vitro reconstitution assay, that BIV Vif does not require a non-canonical cofactor, instead behaving as a traditional BC-Box E3 ligase directly interacting with ELOC without forming a heterodimer. The model of Vif evolution with respect to non-canonical cofactor evolution has three options without the addition of more intermediates: (i) a most recent common ancestor (MRCA) Vif that is BIV Vif-like, and cofactors CYPA and CBFβ were acquired independently along the ovine- and primate-infecting lentivirus lineages, respectively; (ii) a MRCA Vif that required CBFβ, but that was lost during the evolution of non-primate infecting lineages and a new cofactor, CYPA, was acquired in the ovine-infecting lentiviruses; or (iii) a MRCA Vif that required CYPA, but that was lost during the evolution of non-ovine infecting lentiviruses and a new cofactor, CBFβ, was acquired in the primate-infecting lentivirus lineage. While not enough data yet exists to falsify any of these three models, parsimony suggests that the MRCA Vif would be more BIV Vif (and endogenous E3)-like, and that the acquisition of CYPA and CBFβ occurred on separate lineages, rather than a series of gain, loss, then gain events for at least one of the lineages. The lack of conclusive data concerning an FIV Vif cofactor hinders this phylogenetic reconstruction as well. While the true history of cofactor acquisition during lentiviral Vif evolution may be impossible to reconstruct, more data points, in terms of more Vif proteins assayed, would give a better sense of the ancestral states of Vif. The endogenous lentivirus, pSIVgml, found in the genomes of the Madagascar native gray mouse lemur, is basal to known primate-infecting lentiviruses, and contains a *vif* gene (Gifford et al., 2008). If the protein could be synthesized and assessed for cofactor requirement, it could provide data on when the interaction between Vif and CBFβ evolved. In addition, structural information may be more useful in reconstructing Vif evolution than using

the rapidly diverging primary protein sequences, as the structures of these Vif proteins, and particularly the overall Vif-hijacked CRL complexes, may be more conserved over time. This is reflected in the similarity of the SAXS envelope data for the MVV and HIV-1 CRL5 reconstituted complexes.

A direct interaction between MVV Vif and the CYPA active site mediated by Vif residues P21 and P24 was concluded from Vif mutagenesis data, as well as direct binding assays using NMR with Vif peptide and labeled CYPA. Informatics analysis indicates that this region in MVV Vif is not to be found in other Vif proteins, save for the closely related CAEV Vif protein, potentially signifying its importance in CYPA binding. Attempts to disrupt the CYPA-MVV Vif interaction through the CYPA inhibitor CsA proved to be less efficacious than anticipated, particulary when compared with the effects of CsA treatment on disrupting the interaction between CYPA and HIV-1 CA. HIV-1 CA interacts with CYPA through a CYPA-binding loop in its N-terminus containing a GPIAP motif that is recognized by the CYPA active site (Gamble et al., 1996). Indeed, the MVV Vif putative binding motif, GPQLP, bears some resemblance to the HIV-1 CA one. The higher degree of stability in the MVV Vif-CYPA interaction during CsA treatment as compared with HIV-1 CA may indicate additional binding sites between MVV Vif and CYPA. The relatively low affinity between the MVV Vif$^{17-26}$ peptide and CYPA is consistent with this model of MVV Vif-CYPA interactions outside the active site of CYPA.

While the selective pressures that caused the acquisition of CYPA by MVV Vif are under investigation, the mechanism of capture may be related to the function of CYPA as a chaperone. Cellular chaperones interact with a large contingent of clients to catalyze their folding, and often interact with their substrates via general features, such as hydrophobic patches, rather than specific protein-protein interaction surfaces or domains (Jaya et al., 2009; Spiess et al., 2006). The relatively promiscuous interactions of CYPA combined with a high

cellular concentration may have eased the evolution of MVV Vif to capture CYPA. If the interaction between the two proteins is mechanistically unrelated to perturbing endogenous CYPA activities, this may explain the selection of CYPA by the virus. The capture of CYPA by MVV Vif would involve transition of the CYPA interaction from a potentially catalytic one in aiding Vif folding to a stoichiometric one in forming a stable complex. This model of capture is likely distinct from one responsible for the interaction between primate lentiviral Vif proteins and CBFβ, as this interaction falls in a specific protein-protein interaction surface evolved by CBFβ to interact with the runt domain of RUNX transcription factors (Guo et al., 2014). However, if both the MVV Vif-CYPA and the primate lentiviral Vif-CBFβ interactions evolved to disrupt endogenous protein binding, through the active site of CYPA and the runt domain of CBFβ, then this may be a generalizable aspect to Vif cofactor acquisition.

We are left now with a more complete understanding of Vif-associated CRL complexes, with a "core" conserved CRL module and lineage-specific requirements for assembly (**Figure 3.8**). Future work will involve elucidating the structures of the MVV Vif-CYPA-CRL5 complex, as well as the BIV Vif-CRL5 complex, hopefully to ascertain the biophysical explanation of Vif cofactor gains / losses. This may play an important role in understanding how novel viral-host interactions evolve, and may give insights to conserved Vif structural elements that would be good therapeutic targets, especially if they are shown to be highly conserved over lentivirus evolution.

Figure 3.1

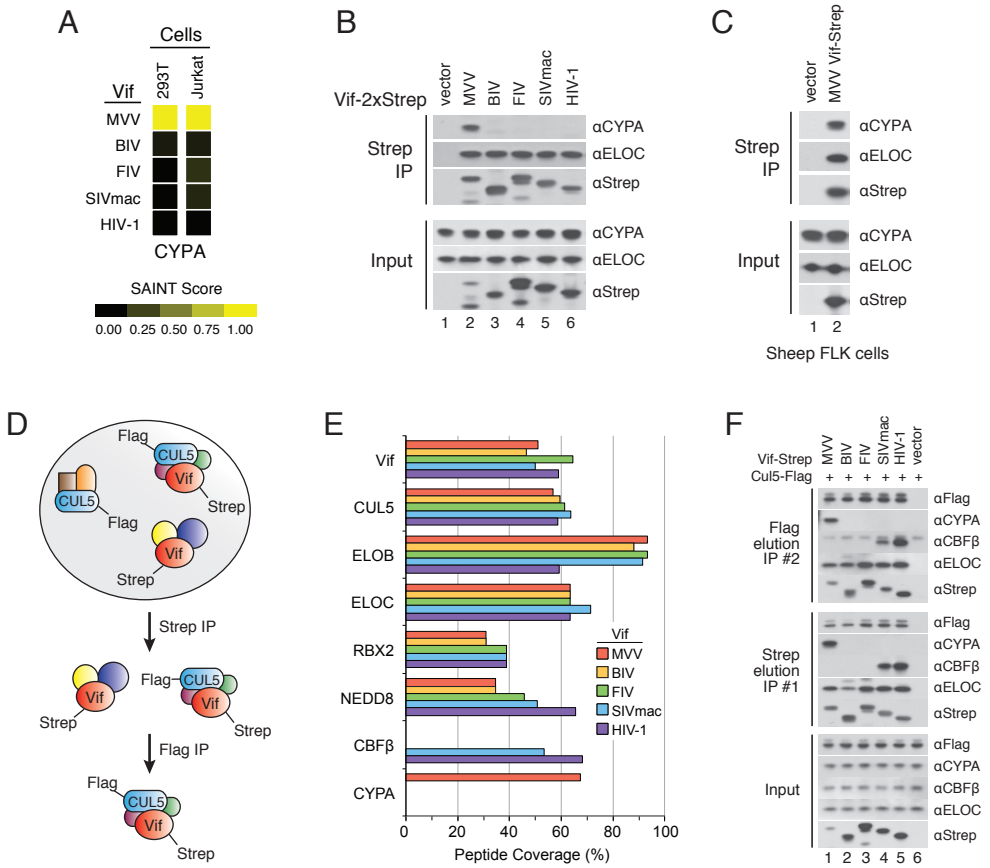
A
Cells
293T
Jurkat
Vif
MVV
BIV
FIV
SIVmac
HIV-1
CYPA
SAINT Score
0.00 0.25 0.50 0.75 1.00
B
Vif-2xStrep
vector
MVV
BIV
FIV
SIVmac
HIV-1
Strep IP
Input
αCYPA
αELOC
αStrep
1 2 3 4 5 6
C
vector
MVV Vif-Strep
Strep IP
Input
αCYPA
αELOC
αStrep
1 2
Sheep FLK cells
D
Flag
CUL5
Vif
Strep
Strep IP
Flag IP
E
Vif
CUL5
ELOB
ELOC
RBX2
NEDD8
CBFβ
CYPA
Vif
MVV
BIV
FIV
SIVmac
HIV-1
0 20 40 60 80 100
Peptide Coverage (%)
F
Vif-Strep
Cul5-Flag
MVV
BIV
FIV
SIVmac
HIV-1
vector
Flag elution IP #2
Strep elution IP #1
Input
αFlag
αCYPA
αCBFβ
αELOC
αStrep
1 2 3 4 5 6

Figure 3.1: CYPA is Tightly and Uniquely Associated with MVV Vif.

(**A**) Cartoon of double affinity purification experiment.

(**B**) LC-MS/MS mass spectrometry results from the double purification of 2xStrep-tagged Vif proteins and 3xFlag-tagged CUL5. Bars indicate peptide percent coverage of proteins identified in eluates after second purification step.

(**C**) Immunoblot of input lysates, first and second purification eluates used for MS analysis in panel (B).

(**D**) Heatmap of AP-MS data for CYPA in HEK293T and Jurkat T-cell lines. Color indicates SAINT score.

(**E**) Re-probing of immunoblot of Strep affinity purification shown in Figure 1F; ELOC is shown as a control for CRL complex interaction.

(**F**) Strep purification of MVV Vif from transient transfection of ovine FLK cells. CYPA, ELOC, and Vif are detected by immunoblot.

Figure 3.2

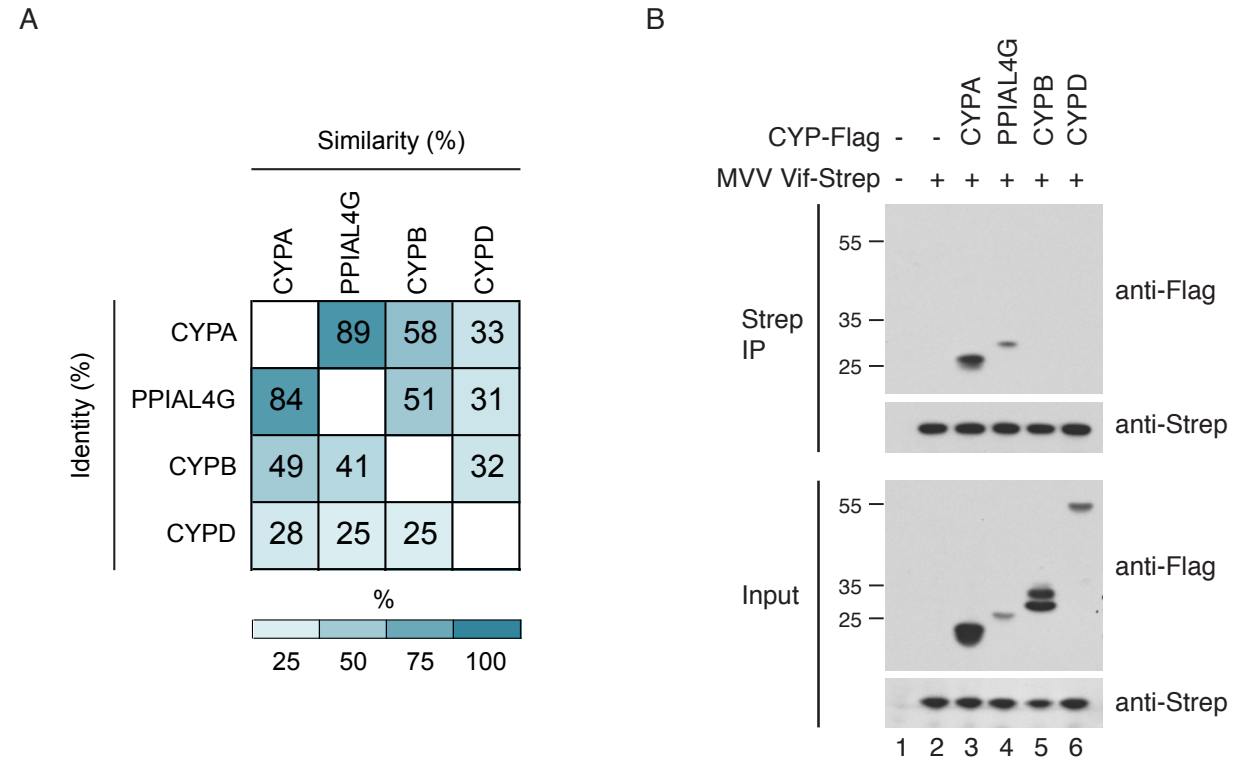
A
Similarity (%)
CYPA
PPIAL4G
CYPB
CYPD
Identity (%)
CYPA
PPIAL4G
CYPB
CYPD
89
58
33
84
51
31
49
41
32
28
25
25
%
25
50
75
100
B
CYP-Flag - - CYPA PPIAL4G CYPB CYPD
MVV Vif-Strep - + + + + +
Strep IP
55
35
25
anti-Flag
anti-Strep
Input
55
35
25
anti-Flag
anti-Strep
1 2 3 4 5 6

Figure 3.2: MVV Vif Interacts with CYPA to a High Degree of Specificity as Relative to other Cyclophilin Paralogs

(A) Similarity and identity matrix of CYPA and three paralogs: Peptidylprolyl Isomerase A (Cyclophilin A)-Like 4G (PPIAL4G), cyclophilin B (CYPB), and cyclophilin D (CYPD). Similarity and identity assessed by EMBOSS Needle tool.

(B) Strep co-affinity purification assay between MVV Vif-2xStrep and CYP-3xFlag orthologs. Co-purifications were assessed by immunoblot.

Figure 3.3

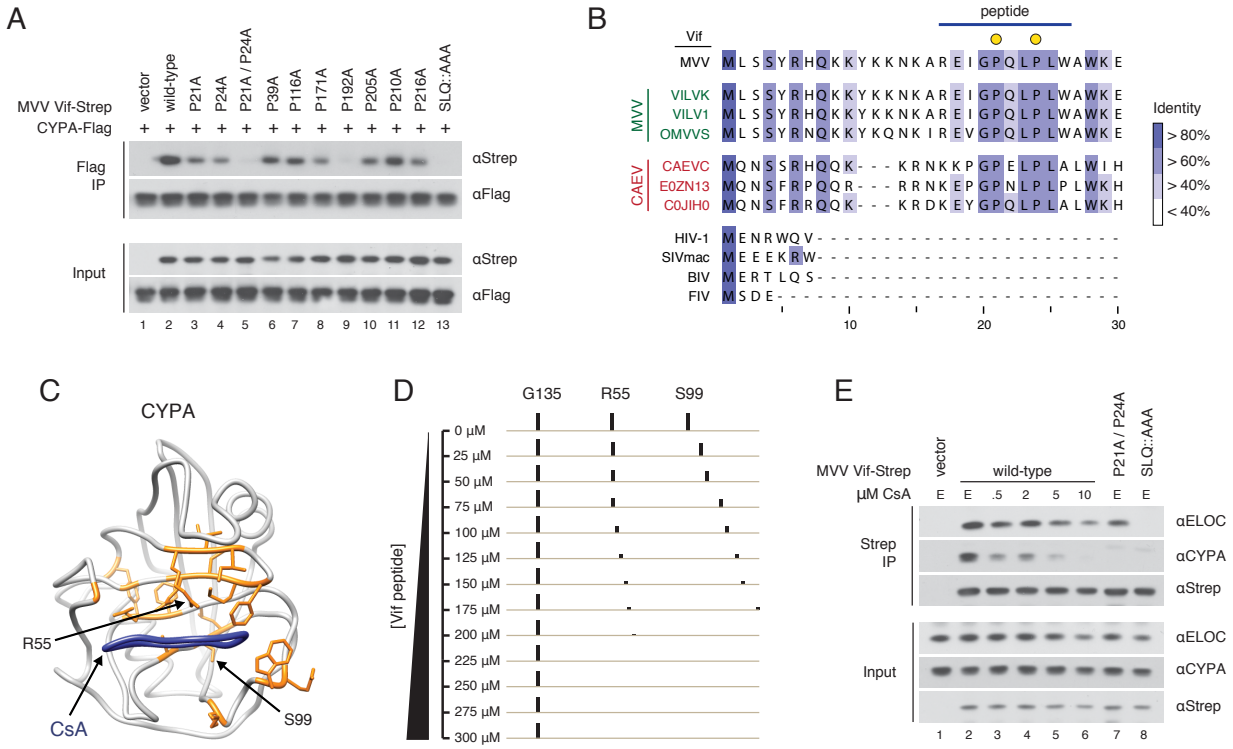
A
MVV Vif-Strep
CYPA-Flag
vector
wild-type
P21A
P24A
P21A / P24A
P39A
P116A
P171A
P192A
P205A
P210A
P216A
SLQ::AAA
Flag IP
αStrep
αFlag
Input
αStrep
αFlag
1 2 3 4 5 6 7 8 9 10 11 12 13
B
peptide
Vif
MVV
MVV
VILVK
VILV1
OMVVS
CAEV
CAEVC
E0ZN13
C0JIH0
HIV-1
SIVmac
BIV
FIV
10
20
30
Identity
> 80%
> 60%
> 40%
< 40%
C
CYPA
R55
CsA
S99
D
G135
R55
S99
[Vif peptide]
0 μM
25 μM
50 μM
75 μM
100 μM
125 μM
150 μM
175 μM
200 μM
225 μM
250 μM
275 μM
300 μM
E
MVV Vif-Strep
μM CsA
vector
wild-type
P21A / P24A
SLQ::AAA
E E .5 2 5 10 E E
Strep IP
αELOC
αCYPA
αStrep
Input
αELOC
αCYPA
αStrep
1 2 3 4 5 6 7 8

Figure 3.3: P21 and P24 of MVV Vif Mediate the Interaction With CYPA

(**A**) Co-purification testing *in vivo* interaction between CYPA and either wild-type or mutant MVV Vif. CYPA-Flag and various MVV Vif-Strep constructs are co-transfected, followed by a Flag immunoprecipation. Co-purification of MVV Vif constructs is assayed by immunoblot.

(**B**) Multiple sequence alignment of MVV, CAEV, and the other Vif proteins used in this study (BIV, FIV, SIVmac, HIV-1) referenced to the first 30 amino acids of MVV Vif. Residues P21 and P24 are highlighted, as well as the region used for CYPA-binding assay in panel (D). Residues are colored by percent identity.

(**C**) Two-dimensional ^{15}N-^{1}H chemical shift mapping of CYPA in presence of MVV Vif$^{17-26}$ peptide. The resonances of Y48, R55, I56, I57, F60, M61, C62, Q63, G65, G72, L98, S99. A101, Q111, F112, E120, W121 and K125 (orange sticks) shift, then disappear upon addition of the Vif peptide. CsA is labeled in blue. PDB: 1CWA.

(**D**) Column 1: Representative example of a CYPA residue (G135) that is not affected by the presence of the MVV Vif peptide. Column 2: By comparison, R55 and S99 undergo significant chemical shift and intensity reduction. The bars are scaled to the intensity of the HSQC peak at the corresponding Vif concentration.

(**E**) Affinity purification of MVV Vif in presence of a titration of CsA. Co-purification of endogenous Vif interactors is assayed by immunoblot. BC-box and proline mutants are used as controls for ELOC and CYPA binding, respectively. E: Ethanol.

Figure 3.4

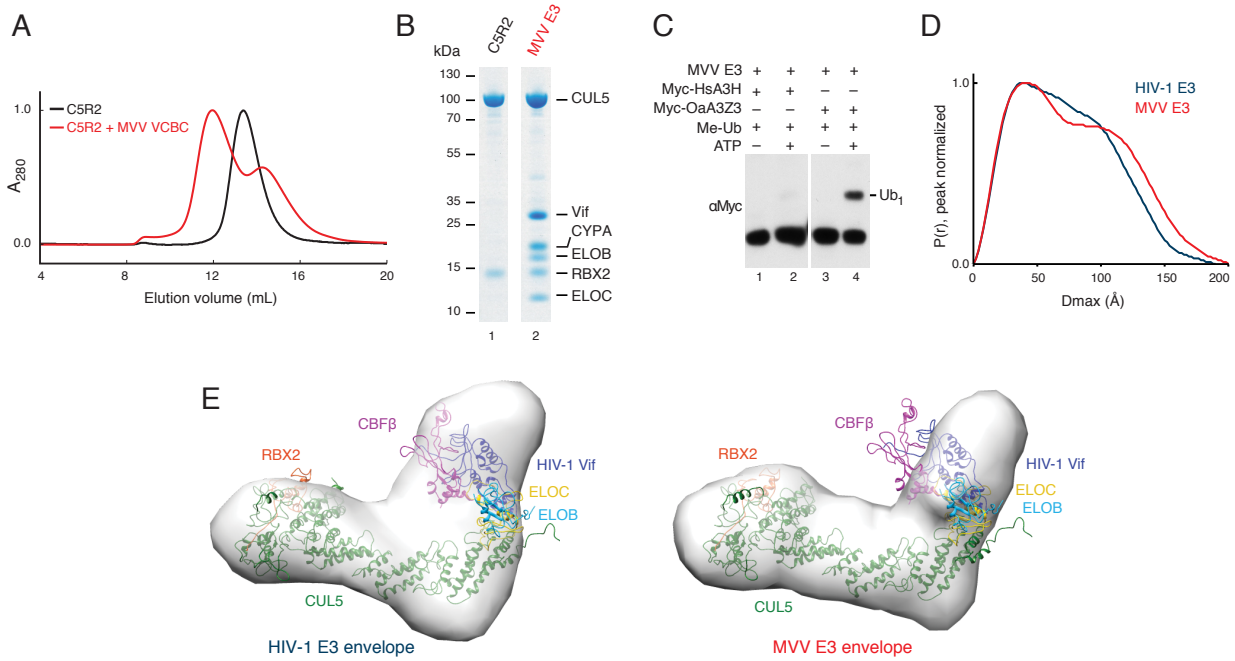
A
1.0
C5R2
C5R2 + MVV VCBC
A280
0.0
4
8
12
16
20
Elution volume (mL)
B
kDa
C5R2
MVV E3
130
100
70
55
35
25
15
10
CUL5
Vif
CYPA
ELOB
RBX2
ELOC
1
2
C
MVV E3
Myc-HsA3H
Myc-OaA3Z3
Me-Ub
ATP
αMyc
Ub1
1
2
3
4
D
1.0
0.0
P(r), peak normalized
HIV-1 E3
MVV E3
0
50
100
150
200
Dmax (Å)

E
CBFβ
RBX2
HIV-1 Vif
ELOC
ELOB
CUL5
HIV-1 E3 envelope
CBFβ
RBX2
HIV-1 Vif
ELOC
ELOB
CUL5
MVV E3 envelope

Figure 3.4: CYPA is Required for *In Vitro* Reconstitution of MVV Vif-CRL5 Complex

(A) UV absorbance curves are shown for gel filtration of CUL5-RBX2 (C5R2) alone, or mixed with an excess of indicated Vif complexes (MVV VCBC = Vif-ELOB-ELOC-CYPA). Peaks are observed at earlier elution volumes when C5R2 is mixed with Vif complexes, indicating E3 complex formation.

(B) Coomassie-blue stained SDS-PAGE of peak fractions collected from gel filtration runs shown in panel **A**.

(C) Immunoblot of methyl-ubiquitylation reactions with MVV E3 and either myc-tagged human A3H (myc-HsA3H) or ovine A3-Z3 (myc-OaA3Z3).

(D) Pair distance distribution function, P(r), calculated from SAXS intensity data.

(E) Molecular envelopes of HIV-1 Vif^{1-174}-CBFβ-CRL5 (left) and MVV Vif-CYPA-CRL5 (right) calculated from P(r). An HIV-1 E3 model was superimposed into both envelopes.

Figure 3.5

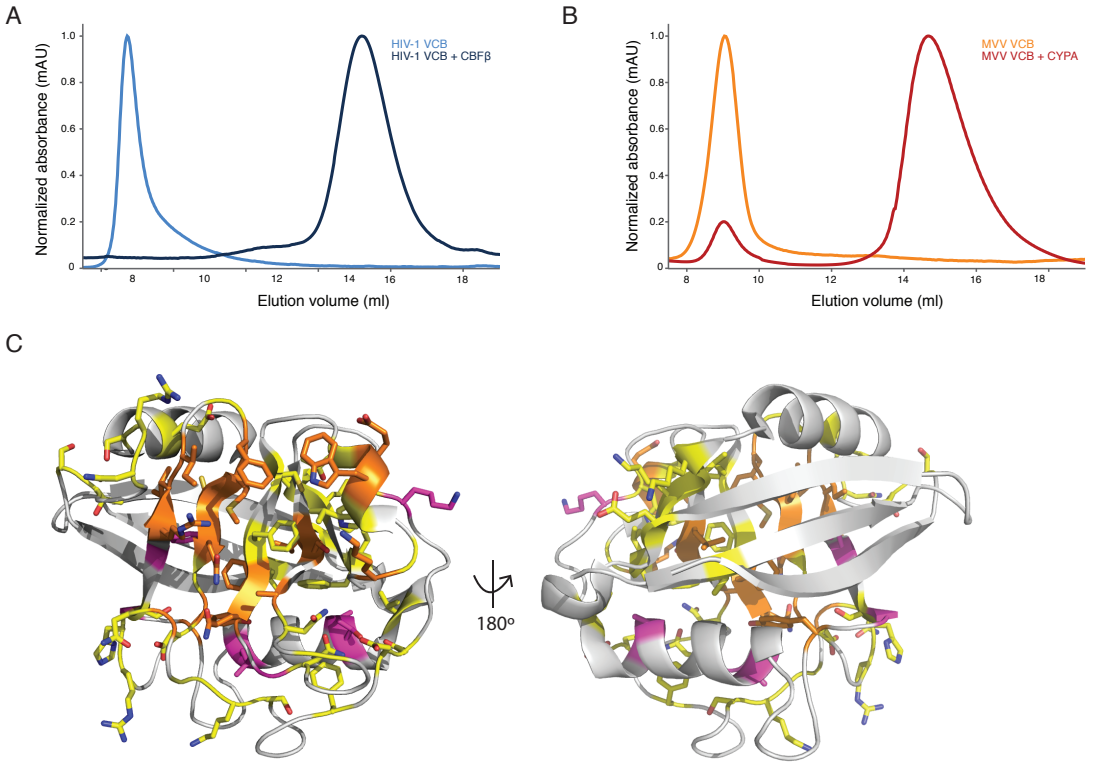
A
Normalized absorbance (mAU)
HIV-1 VCB
HIV-1 VCB + CBFβ
Elution volume (ml)
B
Normalized absorbance (mAU)
MVV VCB
MVV VCB + CYPA
Elution volume (ml)
C
180°

Figure 3.5: HIV-1 and MVV Vif-ELOB-ELOC trimers are stabilized by cofactors, and additional CYPA residues perturbed in presence of the MVV Vif peptide.

(A) UV absorbance curves for recombinantly expressed and purified HIV-1 Vif-ELOB-ELOC complex with and without CBFβ. Samples fractionated by size-exclusion chromatography.

(B) UV absorbance curves for recombinantly expressed and purified MVV Vif-ELOB-ELOC complex with and without CYPA. Samples fractionated by size-exclusion chromatography.

(C) Different types of perturbations are observed on CYPA HSQC spectrum upon addition of the MVV Vif peptide: peaks disappear (orange sticks, see also **Figure 4C**), broaden (pink sticks) or enter slow exchange (yellow sticks). All the residues affected are located in or around the active site of CYPA.

Figure 3.6

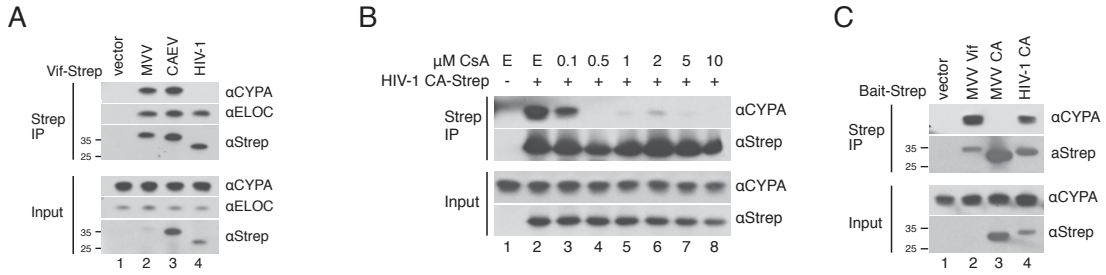
A
Vif-Strep
vector
MVV
CAEV
HIV-1
Strep IP
αCYPA
αELOC
αStrep
35
25
Input
αCYPA
αELOC
αStrep
35
25
1 2 3 4
B
μM CsA E E 0.1 0.5 1 2 5 10
HIV-1 CA-Strep - + + + + + + + +
Strep IP
αCYPA
αStrep
Input
αCYPA
αStrep
1 2 3 4 5 6 7 8
C
Bait-Strep
vector
MVV Vif
MVV CA
HIV-1 CA
Strep IP
αCYPA
aStrep
35
25
Input
αCYPA
αStrep
35
25
1 2 3 4

Figure 3.6: Blocking CYPA Interactions affects MVV Vif activity but does not affect non-interacting HIV-1 Vif activity.

(A) Strep affinity purification of MVV Vif-2xStrep, CAEV Vif-2xStrep, and HIV-1 Vif-2xStrep. Co-purification of CYPA is assayed by immunoblotting.

(B) Strep affinity purification of Strep tagged HIV-1 Capsid (CA) in the presence of a titration of CsA. Co-purification of CYPA is assayed by immunoblotting. E: ethanol.

(C) Strep affinity purification of MVV Vif-2xStrep, MVV Capsid-2xStrep, and HIV-1 Capsid-2xStrep. Co-purification of CYPA is assayed by immunoblotting. CA: Capsid.

Figure 3.7

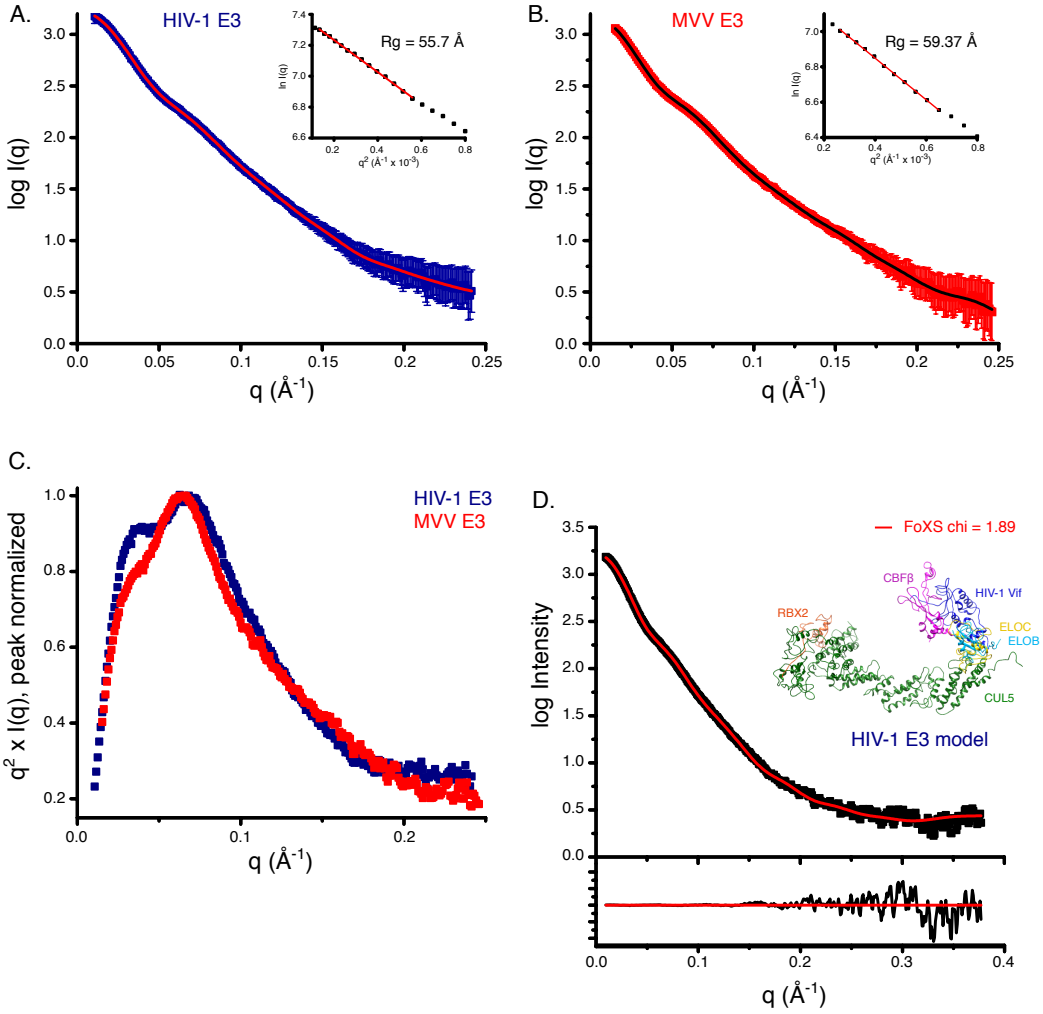
A.
HIV-1 E3
Rg = 55.7 Å
log I(q)
q (Å-1)
B.
MVV E3
Rg = 59.37 Å
log I(q)
q (Å-1)
C.
HIV-1 E3
MVV E3
q2 x I(q), peak normalized
q (Å-1)
D.
FoXS chi = 1.89
CBFβ
HIV-1 Vif
RBX2
ELOC
ELOB
CUL5
HIV-1 E3 model
log Intensity
q (Å-1)

Figure 3.7: SAXS analysis of reconstituted MVV Vif-CYPA-CRL5 and HIV-1 Vif$^{1-174}$-CBFβ-CRL5.

(A-B) SAXS experimental scattering profiles for **A** HIV-1 E3 and **B** MVV E3. The upper inset shows the SAXS profiles in the Guinier plot with an radius of gyration (Rg) fit of 55.7 ± 0.4 Å and 60.1 ± 0.1 Å for the HIV-1 E3 and MVV E3, respectively.

(C) A Kratky plot (q vs. q2I(q)) of the scattering curve indicates the complexes were all folded. The HIV-1 E3 is shown in blue, and the MVV E3 is shown in red.

(D) AllosMod FoXS server was used to refine the HIV-1 E3 model to the experimental SAXS profile. The top plot is of the experimental scattering curve and the red curve is the theoretical scattering profile calculated from the atomic resolution HIV-1 E3 model inset into the plot. The model fits the experimental scattering profile with a $\chi = 1.89$. The lower plot shows the residuals (calculated intensity / experimental intensity) of each calculated SAXS profile.

Figure 3.8

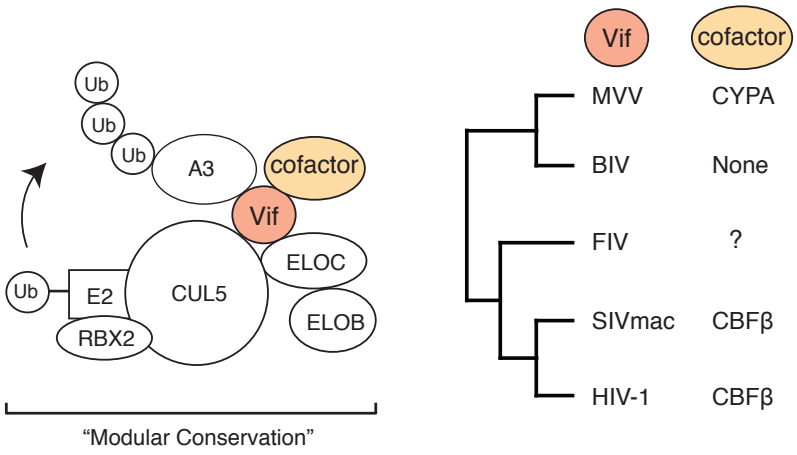
Ub
Ub
Ub
A3
cofactor
Vif
ELOC
Ub
E2
CUL5
ELOB
RBX2
"Modular Conservation"
Vif
cofactor
MVV
CYPA
BIV
None
FIV
?
SIVmac
CBFβ
HIV-1
CBFβ

Figure 3.8: Modular Conservation of CRL Hijacking and Non-Canonical Cofactor Recruitment by Vif.

The host CRL complex hijacked by Vif represents a conserved host-pathogen interaction module. Vif proteins recruit non-canonical host cofactors in a lineage-specific manner within the lentivirus genus.

Chapter 4: CYPA is Required for MVV Vif Anti-APOBEC3 Activity

SUMMARY

We established CYPA as a putative MVV Vif non-canonical cofactor, associating with MVV Vif-CRL5 complexes *in vivo* and playing a CBFβ-like role in Vif-CRL complex assembly and regulating sheep APOBEC3 ubiquitylation activity *in vitro*. However, demonstration that CYPA is required for Vif anti-APOBEC3 activity is required to confirm that CYPA plays a CBFβ-like role in regulating MVV Vif activity in vivo, particularly in the context of infection. To this end, we show that MVV Vif mutants unable to physically interact with CYPA are likewise unable to degrade sheep APOBEC3 proteins in cell culture. We introduce these mutations in the MVV genome, and find that the most severe mutant in terms of loss of CYPA binding, P21A/P24A, largely phenocopies both a BC-box mutant unable to assemble CRL complex as well as a *Δvif* virus, all being unable to promote MVV infectivity in primary sheep cell cultures. Examination of these viruses shows clear signs of APOBEC3 antagonism. We show that a combinatorial knockdown of CYPA and treatment with a CYPA inhibitor, cyclosporine A, block MVV Vif anti-APOBEC3 activity, but have no effect on HIV-1 Vif anti-APOBEC3 activity. Additionally, we show that MVV Vif is both unstable and unable to degrade sheep APOBEC3 in a CYPA knockout cell line without complemention with exogenous CYPA, and that this does not occur with HIV-1 Vif. Lastly, we show that CYPA isomerization activity likely plays a role in MVV Vif ubiquitylation activity, but is not required for association with CYPA or assembly of at least partial CRL complexes.

INTRODUCTION

Maedi-Visna Virus and Sheep Disease

Maedi-visna virus is an ovine-tropic lentivirus whose name is derived from the Icelandic descriptions of the two diseases observed in infected sheep: “maedi”, meaning dyspnea or “difficult or labored breathing; shortness of breath”, for lung infections that cause pneumonia-like symptoms; and “visna”, meaning “wasting”, for infections of the central nervous system (CNS) (Thormar, 2005). The disease caused by MVV infection had been described as early as 1915 in South Africa as a type of progressive sheep pneumonia, in 1923 in Montana as “Montana sheep disease”, and as “la bouhite” or “sheep malignant pulmonary lymphomatosis” in France in 1942, though the causative agent was unknown at the time. The disease was introduced into Iceland through an import of infected Kurakal rams from Halle, Germany in 1933. The Icelandic sheep population was particularly susceptible to the virus as they had been previously isolated from other sheep populations since their introduction to the island by Viking settlers, though due to the slow nature of MVV infection, the disease onset was not recognized until 6 – 7 years after its introduction, when flocks of sheep began to exhibit pneumonia and wasting symptoms (Petursson, 1994). Originally thought to be two distinct pathogens, visna virus isolated from cultures of infected sheep brain tissue in 1957 and maedi virus isolated from infected lung tissue in 1958, they were quickly recognized to be the same virus eliciting different disease states when infecting different tissues, and renamed maedi-visna virus.

Unlike HIV-1, MVV does not infect T-lymphocytes and does not lead to immune deficiency. Rather, the virus tropism is for monocytes and macrophages. A current model of MVV infection involves a “Trojan horse” infection where the virus infects monocytes but remains latent until the cells differentiate into macrophages and the viral replication lifecycle continues (Peluso et al., 1985). This allows dissemination of the virus into various host tissues by latently infected

monocytes without inducing an immune response. CNS-tropic virus that causes visna disease is also known to infect cells in the sheep choroid plexus.

APOBEC3 Antagonism, Hypermutation, and Sequence Specificity

APOBEC3 are a family of anti-viral restriction factors that are part of the host innate immune system. Falling under the umbrella of interferon-stimulated genes, APOBEC3 family members are expressed during viral infection and bind to viral ribonucleic complexes that form during the end-stages of the viral lifecycle, resulting in biased packaging of the APOBEC3 proteins into budding viruses from infected cells. During the subsequent cycle of infection, APOBEC3 proteins act to directly antagonize reverse transcription via deaminase-dependent and deaminase-independent mechanisms. In its more canonical activity, APOBEC3 proteins target cDNA generated during the first round of reverse-transcription from viral RNA template, hydrolyzing the primary amine on cytosine bases, resulting in a uracil base in its place. During complementary strand synthesis to form a double-stranded DNA viral genome, base-pairing with uracil in the deaminated template strand leads to a G-to-A mutation in the newly synthesized strand containing the viral open reading frames. The fate of the viral DNA may be degradation due to the presence of uracil in the viral DNA, or if integration of the viral DNA into the host genome is successful, G-to-A mutations in the viral reading frames are often lethal nonsense mutations, effectively blocking viral replication. A deaminase-independent mechanism for APOBEC3 anti-viral activity has also been reported, with current models having APOBEC3 blocking reverse transcriptase processivity, leading to inefficient reverse transcription (Gillick et al., 2013; Iwatani et al., 2007). APOBEC3 G-to-A mutation does not occur randomly in the viral genome. In humans, each APOBEC3 protein (A-H) has an associated sequence preference for cytosines targeted (Harris and Dudley, 2015); these

sequence preferences have been used to infer which APOBEC3 proteins are most important for anti-HIV activity *in vivo* (Gillick et al., 2013).

While primate genomes encode seven APOBEC3 genes, the ovine genome encodes only three: A3Z1, A3Z3, and A3Z2Z3 (LaRue et al., 2008), using deaminase-domain nomenclature (LaRue et al., 2009). Sheep APOBEC3 proteins are expressed in primary sheep cells used to study MVV, and are effective in blocking spread of *vif*-null MVV in culture, with the hallmark of APOBEC3 antagonism – G-to-A hypermutation – observed in these antagonized viruses.

RESULTS

MVV Vif Proline Mutants Deficient in CYPA Binding are Unable to Antagonize Ovine APOBEC3 Proteins

Given the role CBFβ plays in regulating HIV-1 Vif anti-APOBEC3 activity, and the apparent CBFβ-like role of CYPA in assembly of MVV Vif hijacked CRL complexes, we next asked if CYPA regulates MVV Vif anti-APOBEC3 activity as well. We first asked if Vif proline mutants we had generated that we had previously been shown to be deficient in CYPA binding would also show deficiency in APOBEC3 antagonism. We focused our analysis on the $_{21}$PxxP$_{24}$ putative CYPA binding site, co-expressing wild-type, P21A, P24A, P21A/P24A, or SLQ::AAA 2xStrep-tagged MVV Vif with 3xHA-tagged ovine APOBEC3Z2Z3 (OaA3Z2Z3) in HEK293T cells. We observed that deficiency in OaA3Z2Z3 degradation activity strongly correlated with previously assayed loss in CYPA co-purification across the mutants, with the greatest loss in OaA3Z2Z3 degradation activity observed in the P21A/P24A and SLQ::AAA mutants (**Figure 4.1A**). While we observed this strong correlation between a loss in CYPA binding and a loss in APOBEC3 antagonism activity, we were concerned the Vif proline mutations may be structurally compromising, rather than an ability to form an active CRL complex due to loss of CYPA

binding. To test if MVV Vif P21A/P24A was unable to antagonize OaA3Z2Z3 due to structural instability, or because of inability to assemble a functional CRL complex due to the loss of CYPA binding, we performed a substrate-binding assay to test if these MVV Vif mutants can still physically recognize substrates by co-affinity purification. HEK293T cells were transfected with 3xHA-tagged OaA3Z2Z3 and either P21A/P24A or SLQ::AAA 2xStrep-tagged MVV Vif, cells were lysed, and a Strep purification was performed. OaA3Z2Z3 protein co-purified with both constructs as assessed by immunoblotting despite these mutants being unable to target OaA3Z2Z3 for degradation (**Figure 4.1B**), suggesting both mutants can still physically interact with the substrate *in vivo*. We interpreted these data as indicating the inability of P21A/P24A MVV Vif to degrade OaA3Z2Z3 is due to an inability to form a functional CRL complex, and not due to a structurally compromising mutation disrupting substrate binding.

MVV Infectivity Loss Observed in Vif P21A/P24A Likely Due to APOBEC3 Antagonism In Vivo

After observing the affects of CYPA binding on MVV Vif activity, both in terms of CRL complex assembly and APOBEC3 antagonism, we moved to a more relevant platform to study this interaction in the context of MVV infection. Working with Valgerður Andrésdóttir's lab at the University of Iceland, we performed viral spreading assays with wild-type, P21A, P24A, P21A/P24A, SLQ::AAA, and *vif*-null MVV strain K1772 in two different primary sheep cells – sheep choroid plexus (SCP) and macrophages. All mutant viruses showed reduced spreading kinetics relative to the wild-type viruses, though the P21A/P24A Vif virus displayed a greater spreading defect than the P21A Vif or P24A Vif viruses, and appeared to phenocopy the SLQ::AAA Vif and *vif*-null viruses for the first 8-10 days of the experiment in both cell lines (**Figure 4.1C**; **Figure 4.2E**). To assess if the defective spreading phenotypes observed with the various MVV Vif mutants were due to ovine APOBEC3 antagonism, proviral sequences from

SCP cells were cloned and sequenced. Significant increases in G-to-A mutations were observed in P21A / P24A ($p = 1.41x10^{-4}$), SLQ::AAA ($p = 5.27x10^{-5}$), and *vif*-null ($p = 1.84x10^{-5}$) MVV relative to wild-type virus using a one-sided Wilcoxon Rank-sum test; no significant increase in G-to-A mutations was observed in either the P21A Vif or P24A Vif viruses relative to wild-type, despite these viruses displaying slower spreading kinetics compared to wild-type MVV (**Figure 4.1D**; **Figure 4.2A-C**). The tri-nucleotide sequence preference (GRA) for the site of G-to-A mutations were similar in all significantly affected viruses, implicating an identical mechanism of mutation, i.e. APOBEC3-mediated mutations (**Figure 4.1E**; **Figure 4.2D**).

Combinatorial Knockdown and Inhibitor Treatment of CYPA Block MVV Vif Anti-APOBEC3 Activity

Owing to the limited genetic tractability of sheep primary cells, we moved back to human cell lines to perform experiments perturbing the CYPA axis of the MVV Vif-CYPA interaction. We first attempted to knockdown CYPA with a constituitively expressed shRNA, but polyclonal populations of multiple shRNAs failed to achieve a sufficient knockdown to affect either APOBEC3 degradation or MVV Vif-CRL complex assembly (**Figure 4.3**). As an alternative to knocking down CYPA, we also tested small-molecule inhibition of CYPA activity with CsA, which inhibits substrate binding to the CYPA active site (Takahashi et al., 1989; Thériault et al., 1993). Titration of CsA resulted in limited inhibition of OaA3Z2Z3 antagonism by MVV Vif until toxicity became apparent at 5 μM as assayed by quantitative immunoblotting (**Figure 4.5A**); this inhibition was not observed with HIV-1 and human APOBEC3G (HsA3G) and CsA toxicity was observed at similar concentrations (**Figure 4.5B**).

As previous *in vitro* data suggested CYPA was required for MVV Vif-CRL complex assembly and ubiquitylation of OaAPOBEC3 proteins, we were puzzled as to the inefficacies of either

CYPA knockdown or treatment with the CYPA inhibitor CsA, which we attributed to the high cellular concentration of CYPA and the likely high affinity binding of the MVV Vif-CYPA complex. We reasoned that a combinatorial approach combining both protocols may give enough of a one-two punch to CYPA to inhibit MVV Vif activity. We generated a monoclonal CYPA knockdown line and treated with 2 μM CsA and assayed MVV Vif-mediated OaA3-Z2Z3 degradation (**Figure 4.4A**). A modest inhibition of MVV Vif OaA3Z2Z3 degradation activity was observed in the knockdown line relative to the non-targeting shRNA control line without CsA treatment that became a near complete inhibition of Vif activity upon treatment with CsA in the knockdown line, whereas incomplete inhibition, consistent with previous titrations of CsA in HEK293T cells, was observed in the non-targeting control line. Importantly, neither CYPA knockdown nor CsA treatment appeared to have an effect on HsA3G degradation by HIV-1 Vif (**Figure 4.5C**), consistent with a model where combined CYPA knockdown with CYPA inhibition via CsA specifically and cooperatively interfered with the MVV Vif-CYPA interaction.

CYPA Knockout Reveals Essential Requirement for In Vivo MVV Vif Stability and Anti-APOBEC3 Activity

While the combination of CYPA knockdown in a monoclonal line combined with CsA treatment was effective in inhibiting MVV Vif-mediated degradation of ovine APOBEC3 protein, the system is not ideal due to the potential off-target effects of both the shRNA and the CsA treatment. To alleviate concerns of the combined treatment, we next performed ovine APOBEC3 degradation assays in a $CYPA^{-/-}$ knockout (KO) Jurkat T-cell line (Braaten and Luban, 2001). We first confirmed the knockout by immunoblot, comparing the CYPA signal with the parental E6-1 Jurkat T-cell line (**Figure 4.4B**). Next, we used a nucleofection protocol to transfect either the $CYPA^{-/-}$ KO or the E6-1 control cells with 3xHA-tagged OaA3Z2Z3 in the presence or absence of MVV Vif, and with or without a rescue of the knockout by

complementation with exogenous 3xFlag-tagged CYPA (**Figure 4.4B**). We observed robust OaA3Z2Z3 expression even in the presence of MVV Vif in the knockout background as assayed by immunoblot; only with the complementation of exogenous CYPA is OaA3Z2Z3 degradation observed (**Figure 4.4C**, top). Interestingly, there appears to be little to no expression of MVV Vif in the CYPA KO background, and only with complementation is MVV Vif readily detected by immunoblot. These MVV Vif phenotypes were not observed in the E6-1 control Jurkat line (**Figure 4.4C**, bottom). No effect on HIV-1 Vif, both in terms of expression and HsA3G degradation activity, was observed in either the CYPA KO line or the E6-1 control (**Figure 4.4D**).

We next looked to CYPA isomerase activity, asking if simply binding MVV Vif was sufficient for stable MVV Vif-CYPA-CRL complex formation and anti-APOBEC3 activity, or if CYPA isomerase activity was also required. We created three CYPA mutants using site-directed mutagenesis – R55K, F113W, and H126A – which are all located within the CYPA active site (**Figure 4.6A**), and have all been previously reported to affect CYPA enzymatic activity (Bosco et al., 2010). We performed the same experiments as previously described in the CYPA KO Jurkat line, but complemented MVV Vif with R55K, F113W, and H126A exogenous CYPA in addition to wild-type. We found that two of the mutants, R55K and F113W, failed to rescue MVV Vif anti-OaA3Z2Z3 activity, and unexpectedly H126A mutant rescued MVV Vif activity as efficiently as wild-type CYPA (**Figure 4.4E**). We performed the same experiments in the monoclonal CYPA knockdown HEK293T cell line and obtained similar results, albeit with less effect due to incomplete loss of MVV Vif activity in the knockdown background (**Figure 4.6B**). Interestingly, both the R55K and F113W complementations, although failing to rescue Vif anti-APOBEC3 acitivity, do rescue MVV Vif stability, potentially suggestive that binding still occurs to stabilize Vif, but CYPA isomerase activity is required for MVV Vif-mediated degradation of

OaA3Z2Z3. To determine if the effect was due to a lack of MVV Vif binding by CYPA or if CYPA isomerase activity is required for an active MVV Vif-CYPA-CRL5 complex, we performed an *in vitro* reconstitution of MVV Vif-ELOB-ELOC with CYPA R55K, F113, or H126A forming the tetrameric complex, and assessing complex stability by size-exchange chromatography (**Figure 4.6C-D**). We observed complex formation in all mutants, although the mutant most deficient in promoting MVV Vif anti-APOBEC3 activity, F113W, showed a very broad elution peak relative to the others. We interpreted these results as suggesting CYPA isomerase activity is important for MVV Vif anti-APOBEC3 activity.

DISCUSSION

The canonical function of Vif with respect to Lentiviral biology is to nullify the anti-viral effects of host APOBEC3 proteins, mediated through the hijacking of a host CRL complex. The biology of Vif and non-canonical cofactors, as understood through the interaction between HIV-1 Vif and CBFβ, is one that must mediate this function through, minimally, the stable assembly of the anti-APOBEC3 Vif-CRL complex. Demonstrating CYPA acts as a non-canonical cofactor as defined by the role CBFβ directly plays in HIV-1 Vif anti-APOBEC3 activity, we showed that MVV Vif mutants that were deficient in CYPA binding were also deficient in mediating the degradation of sheep APOBEC3 proteins. In fact, the severity of the CYPA binding defect correlated strongly not only with sheep APOBEC3 degradation in cell culture transient transfections, but in MVV spreading assays performed in primary sheep cells as well. Without an atomic structure of the MVV Vif-CYPA-CRL complex, it is difficult to know if the perturbations made by proline-to-alanine mutations simply break CYPA binding, or destabilize MVV Vif structural integrity to the point of disrupting protein-protein interactions; however, we were able to capture sheep APOBEC3 substrate as assessed by a co-affinity purification assay with two distinct MVV Vif mutants, the P21A/P24A double mutant and our

BC-box mutant, SLQ::AAA, implying that an inability to assemble a functional Vif-associated CRL complex, and not an inability to bind substrates, is the defect observed with these mutants.

MVV spreading assays clearly showed a concomitant accumulation of G-to-A mutations in proviral sequences with a lack of spreading in *vif*-mutant viruses. Again, the severity of the G-to-A hypermutations correlated strongly with the defect in CYPA binding associated with the Vif mutant, with only the P21A/P24A, SLQ::AAA, and *Δvif* MVV showing a significant increase in G-to-A mutations with respect to the wild-type virus as assessed by a Wilcoxon one-sided rank-sum test. The tri-nucleotide context of the G-to-A mutations, a hallmark of the non-random cytosine preference of APOBEC3 proteins (Harris and Dudley, 2015), was nearly identical between the three hypermutated mutant MVV, providing further evidence that APOBEC3 proteins are responsible for the lack of MVV mutant spread, and not some other Vif-dependent mechanism. On the other hand, both single proline mutants tested, P21A and P24A, both reproducibly showed reduced spreading kinetics with respect to wild-type virus, but did not accumulate any G-to-A mutations. This may be due to antagonism by sheep APOBEC3 proteins in a cytosine deaminase independent manner (Gillick et al., 2013; Iwatani et al., 2007), or an unrelated function of either MVV Vif or the biology of its interaction with CYPA.

The nature of the interaction between CYPA and MVV Vif with respect to sheep APOBEC3 proteins is still unclear, especially as the evolutionary driving force for the acquisition of CYPA, or of non-canonical cofactors in general, remains unclear. There may not be a common selective pressure at all, and each acquisition (HIV/SIV and CBFβ; MVV and CYPA) may have evolved for different reasons. An interesting hypothesis that bridges both acquisitions is through the axis of APOBEC3 antagonism – aiding in substrate recognition. The

acquisition of CBFβ as a primate-infecting lentivirus Vif cofactor coincides with an expansion of *Apobec3* genes in the primate genome. The number of *Apobec3* genes in mammalian genomes varies from only a single locus in the mouse genome to seven in primates, with three in the bovine and ovine genomes, and four in the feline genome (Bogerd et al., 2008; Jarmuz et al., 2002; LaRue et al., 2008; Münk et al., 2008). A potential model for cofactor acquisition is to cope with changing numbers of Vif substrates, which may include APOBEC3 proteins or perhaps unknown, even lineage-specific, substrates.

While no direct structural evidence exists that shows CBFβ plays a direct role in recognizing APOBEC3 proteins in the HIV-1 Vif-hijacked CRL complexes, multiple structures of the SIV / HIV-2 accessory factor Vpx, which hijacks a CUL4A-DDB1-DCAF1 CRL complex to target the restriction factor SAMHD1 for poly-ubiquitylation (Laguette et al., 2011), show the host factor DCAF1 directly contacting the viral substrate covering a shared surface area of 200-500 $Å^2$ (Schwefel et al., 2014, 2015). If non-canonical cofactors can be shown to play roles in substrate recognition, the selective pressure to acquire them may be to dampen the effects of either restriction factor family expansion, positive selection diversifying restriction factor haplotypes in a natural host population (Binka et al., 2012; Ooms et al., 2013), or enabling greater rates of zoonosis through ease of recognition of restriction factor orthologues. The sheep genome does not show an expansion of *Apobec3* genes relative to the bovine genome (LaRue et al., 2008), seemingly negating a selective pressure to acquire CYPA as a means to deal with *Apobec3* family expansion, as the BIV Vif protein does not have a non-canonical cofactor and must antagonize an equal number of host APOBEC3 proteins. Intriguingly, MVV Vif has been reported to have an exceptional ability amongst Vif proteins to broadly recognize APOBEC3 proteins from numerous, non-sheep mammals (LaRue et al., 2010), though whether

this is due to its interaction with CYPA or by other means, such as directly recognizing a widely conserved APOBEC3 structural motif, is unclear.

The interaction between CYPA and HIV-1 CA is part of a cloaking strategy evolved by HIV-1 to avoid detection by the host cell innate immune system. When the interaction between CYPA and HIV-1 CA is disrupted by either mutations in CA or treatment with CYPA inhibitors such as CsA, the viral core is antagonized by a number of restriction factors including TRIM5, and an interferon response is initiated that blocks HIV-1 infectivity (Rasaiyaah et al., 2013; Sokolskaja and Luban, 2006; Towers et al., 2003). Whether or not the MVV Vif-CYPA interaction plays a role in protecting the MVV virion core during early infection is unclear. MVV CA does not appear to interact with CYPA as measured by co-affinity purification (**Figure 3.6C**), but it is not known if MVV Vif or CYPA are packaged into MVV virions. Sheep do have a TRIM5 protein that can block MVV infection and it is not known how MVV overcomes this replication block (Jáuregui et al., 2012). An intriguing clue into the relationship between Vif, CA, and CYPA in MVV biology lies in an observation that a pair of mutants in Vif and CA (P205S and L120R, respectively) result in a block to MVV infection during the early life-cycle, where neither of the mutations alone results in a block (Gudmundsson et al., 2005). The Vif mutant is still able to antagonize sheep APOBEC3. Whether this phenotype is related to the MVV Vif-CYPA interaction is currently under investigation. A difficulty remains in separating any Vif-CYPA functions from APOBEC3 antagonism as any perturbation that disrupts the interaction between MVV Vif and CYPA results in antagonism from sheep APOBEC3. A model cell line or primary tissue that is free of APOBEC3 proteins and supportive of MVV replication will be needed to test for other axes of MVV Vif-CYPA biology.

We explored the idea of whether or not the interaction between CYPA and MVV Vif may be related to the genetic conflict between lentiviruses and the host restriction factor TRIM5α

(Stremlau et al., 2004). In HIV-1, CYPA interaction with the viral capsid is involved in mitigating the anti-viral actions of TRIM5α (Sokolskaja and Luban, 2006), and some old world primate hosts have evolved a TRIM5α–CYPA fusion protein, TRIMCYP, which uses its CYPA-domain to recruit the TRIM5α domain to the viral core (Nisole et al., 2004; Sayah et al., 2004). MVV is restricted by sheep TRIM5α when overexpressed in cell culture, but the mechanism by which MVV avoids this restriction *in vivo* is unknown (Jáuregui et al., 2012). It remains possible that the interaction between CYPA and MVV Vif is to allow crosstalk of Vif between two different host restriction pathways – APOBEC3 and TRIM5α, particularly if there exists an as of yet unidentified TRIMCYP gene in the sheep genome. We searched for a potential *TRIMCYP* gene in the sheep genome using tBlastn (Altschul et al., 1990) against sheep and goat expressed sequence tag (EST) data in the GoSH DB goat and sheep DNA database (Caprera et al., 2007) for sequences matching both ovine TRIM5α and ovine CYPA, which may be indicative of a fusion protein, but were unsuccessful in identifying any candidates (data not shown).

Figure 4.1

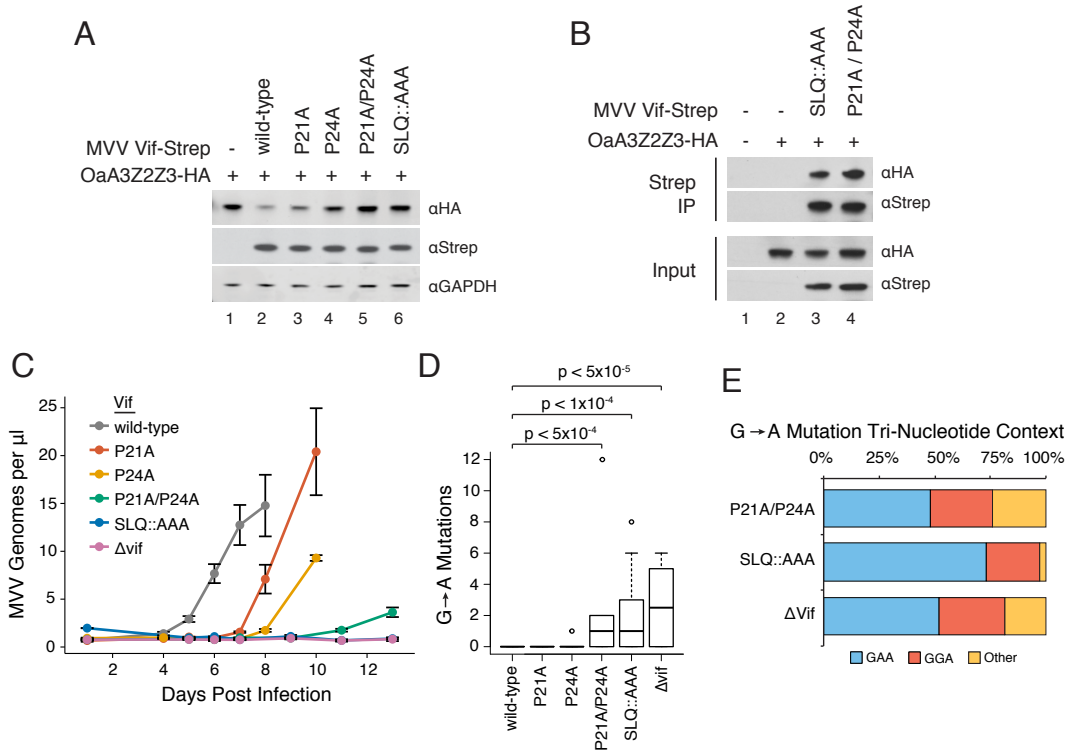
A
MVV Vif-Strep
OaA3Z2Z3-HA
wild-type
P21A
P24A
P21A/P24A
SLQ::AAA
αHA
αStrep
αGAPDH
1 2 3 4 5 6
B
MVV Vif-Strep
OaA3Z2Z3-HA
SLQ::AAA
P21A / P24A
Strep IP
Input
αHA
αStrep
1 2 3 4
C
MVV Genomes per µl
Vif
wild-type
P21A
P24A
P21A/P24A
SLQ::AAA
Δvif
Days Post Infection
D
G→A Mutations
p < 5x10-5
p < 1x10-4
p < 5x10-4
wild-type
P21A
P24A
P21A/P24A
SLQ::AAA
Δvif
E
G→A Mutation Tri-Nucleotide Context
0% 25% 50% 75% 100%
P21A/P24A
SLQ::AAA
ΔVif
GAA
GGA
Other

Figure 4.1: MVV Vif Mutants Deficient in CYPA-Binding are Deficient in APOBEC3 Antagonism and Cannot Promote MVV Infectivity *in situ*

(**A**) Co-transfection of HA-tagged ovine A3Z2Z3 (OaA3Z2Z3-HA) and either wild-type or proline mutant MVV Vif. APOBEC3 stability in the presence of Vif is assayed by immunoblot.

(**B**) Co-affinity purification between OaA3Z2Z3 and MVV Vif constructs that were deficient in OaA3Z2Z3 destabilization in panel (A). Interaction between APOBEC3 and Vif proteins is assayed by immunoblotting.

(**C**) MVV spreading assay in ovine primary macrophage cells. Lysates were harvested at various time points post-infection, and virus genome copies were quantified using TaqMan-based real-time PCR assay, mean ± S.E. (n=3).

(**D**) Hypermutation assay of MVV strain KV1772. MVV with either wild-type or mutant *vif* were subjected to a single-cycle infection assay in primary sheep choroid plexus (SCP) cells, and produced viruses were then used to infect cells, pro-viruses cloned, and assayed for A3-mediated G-to-A mutations. Wild-type, P24A: n=20; P21A: n=16; P21A/P24A: n=17; SLQ::AAA: n=19; Δvif: n=10. Significance values were determined by a one-sided Wilcoxon Rank-Sum Test compared to wild-type; no annotated p-value indicates p-value > 0.05.

(**E**) Tri-nucleotide context of G-to-A mutations measured in panel (C). Other refers to any GNN tri-nucleotide other than GGA or GAA.

Figure 4.2

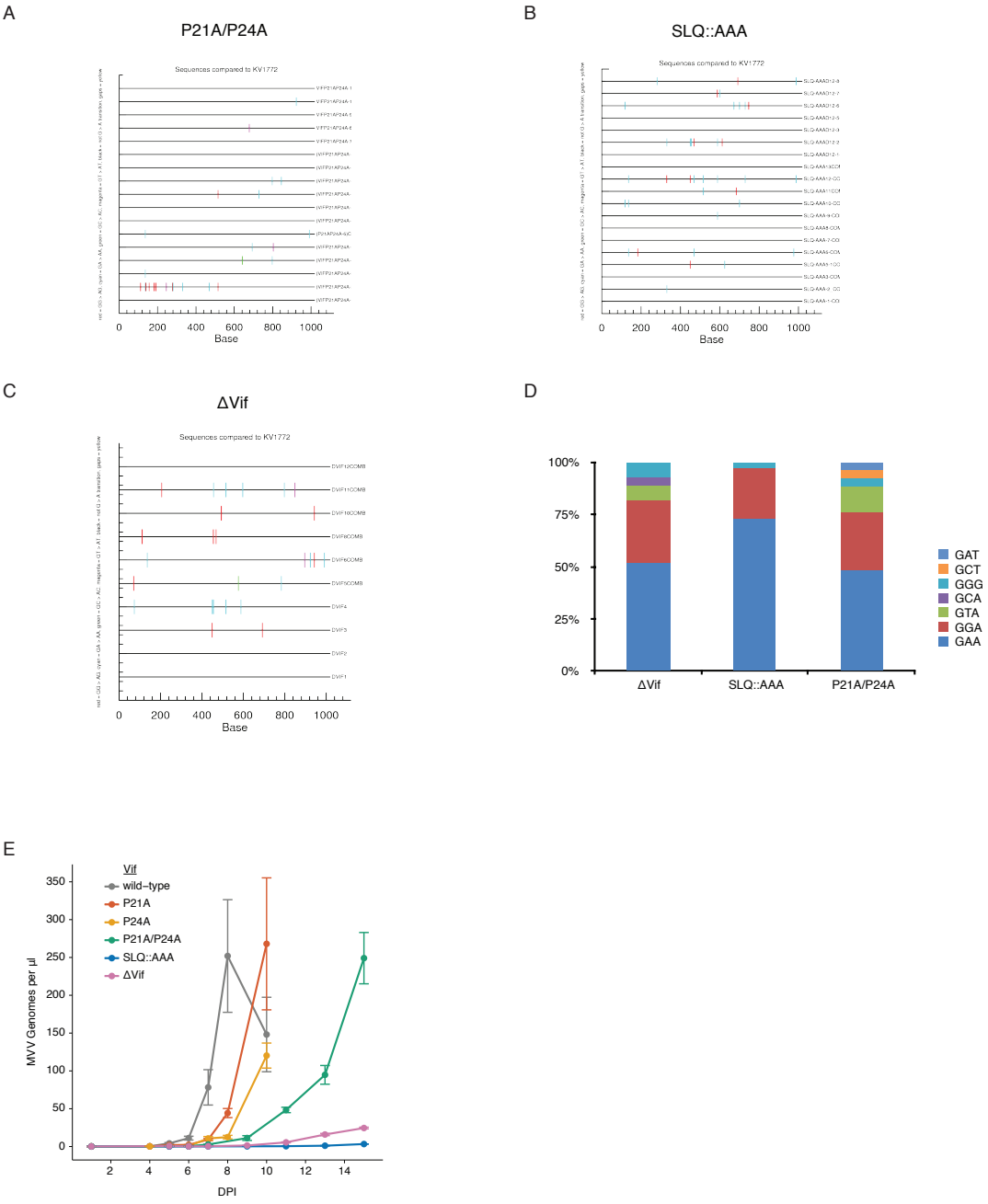
A
P21A/P24A
Sequences compared to KV1772
0
200
400
600
800
1000
Base
B
SLQ::AAA
Sequences compared to KV1772
0
200
400
600
800
1000
Base
C
ΔVif
Sequences compared to KV1772
0
200
400
600
800
1000
Base
D
100%
75%
50%
25%
0%
ΔVif
SLQ::AAA
P21A/P24A
GAT
GCT
GGG
GCA
GTA
GGA
GAA
E
Vif
wild–type
P21A
P24A
P21A/P24A
SLQ::AAA
ΔVif
MVV Genomes per µl
350
300
250
200
150
100
50
0
2
4
6
8
10
12
14
DPI

Figure 4.2: MVV Vif mutants result in A3-mediated restriction in primary sheep cells.

(A-C) Per-genome context of G-to-A mutations observed in proviral genomes with various MVV Vif mutants.

(D) Tri-nucleotide context of observed G-to-A mutations from MVV hypermutation assay in **Figure 5C**, summarized in **Figure 5D**.

(E) MVV spreading assay performed in SCP cells with various Vif mutants, identical to the experimental setup in **Figure 5E**.

Figure 4.3

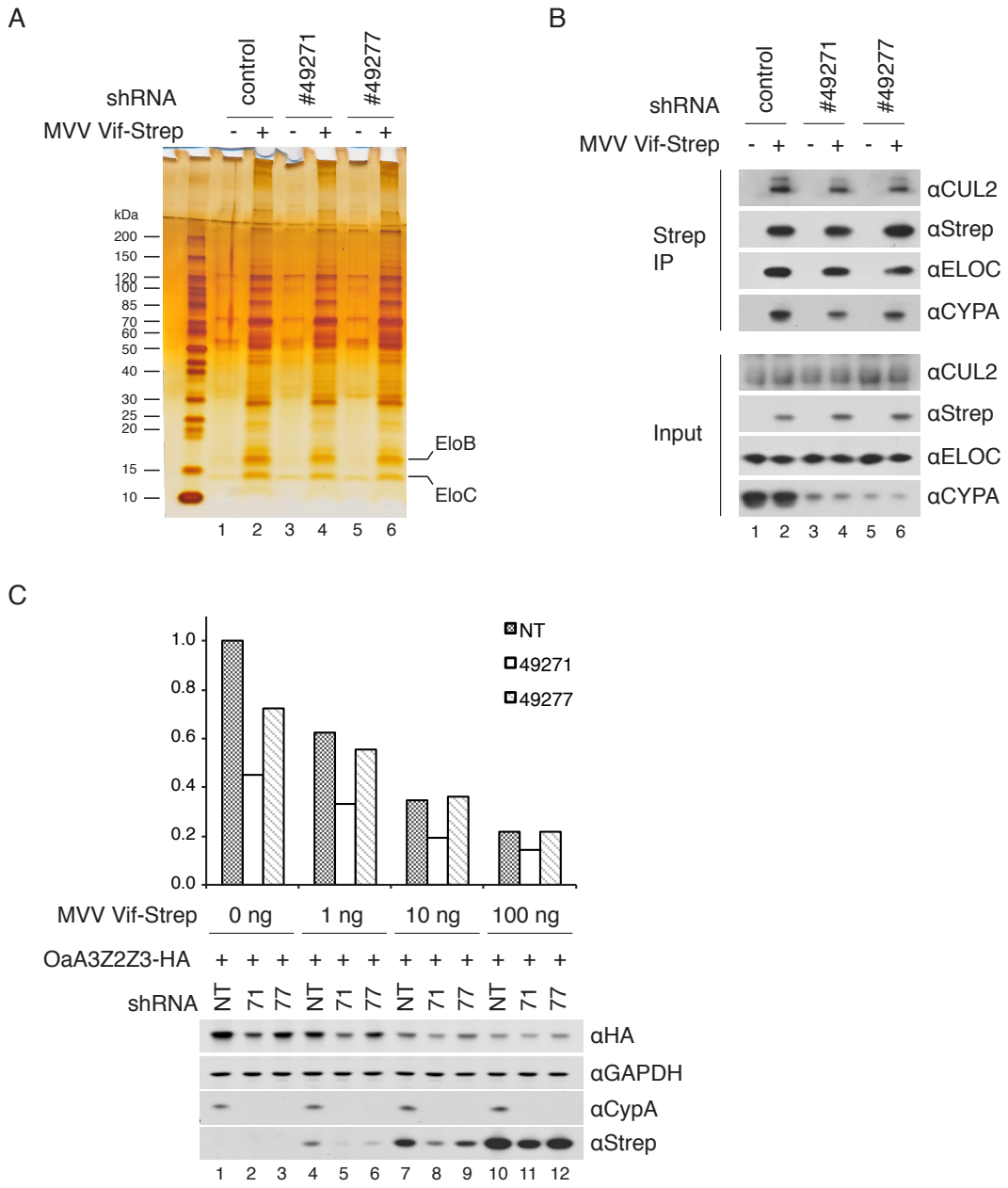
A
shRNA
MVV Vif-Strep
control
#49271
#49277
- + - + - +
kDa
200
150
120
100
85
70
60
50
40
30
25
20
15
10
EloB
EloC
1 2 3 4 5 6
B
shRNA
MVV Vif-Strep
control
#49271
#49277
- + - + - +
Strep IP
αCUL2
αStrep
αELOC
αCYPA
Input
αCUL2
αStrep
αELOC
αCYPA
1 2 3 4 5 6
C
NT
49271
49277
1.0
0.8
0.6
0.4
0.2
0.0
MVV Vif-Strep
0 ng
1 ng
10 ng
100 ng
OaA3Z2Z3-HA
+ + + + + + + + + + + +
shRNA
NT 71 77 NT 71 77 NT 71 77 NT 71 77
αHA
αGAPDH
αCypA
αStrep
1 2 3 4 5 6 7 8 9 10 11 12

Figure 4.3: Knockdown of CYPA Is Insufficient to Disrupt MVV Vif-CYPA-CRL Assembly or APOBEC3 Antagonism

(A) SDS-PAGE silver stained gel of Strep affinity purification of MVV Vif-2xStrep from polyclonal HEK293T cells transduced with either a control or one of two shRNAs targeting CYPA.

(B) Immunoblot of purification in **A**.

(C) APOBEC3 degradation assay using polyclonal HEK293T cells from **A**. Cells are co-transfected with OaA3Z2Z3-3xHA and a titration of MVV Vif-2xStrep. HA intensities are normalized to GAPDH signal, then to lane 1. NT: Non-targeting control.

Figure 4.4

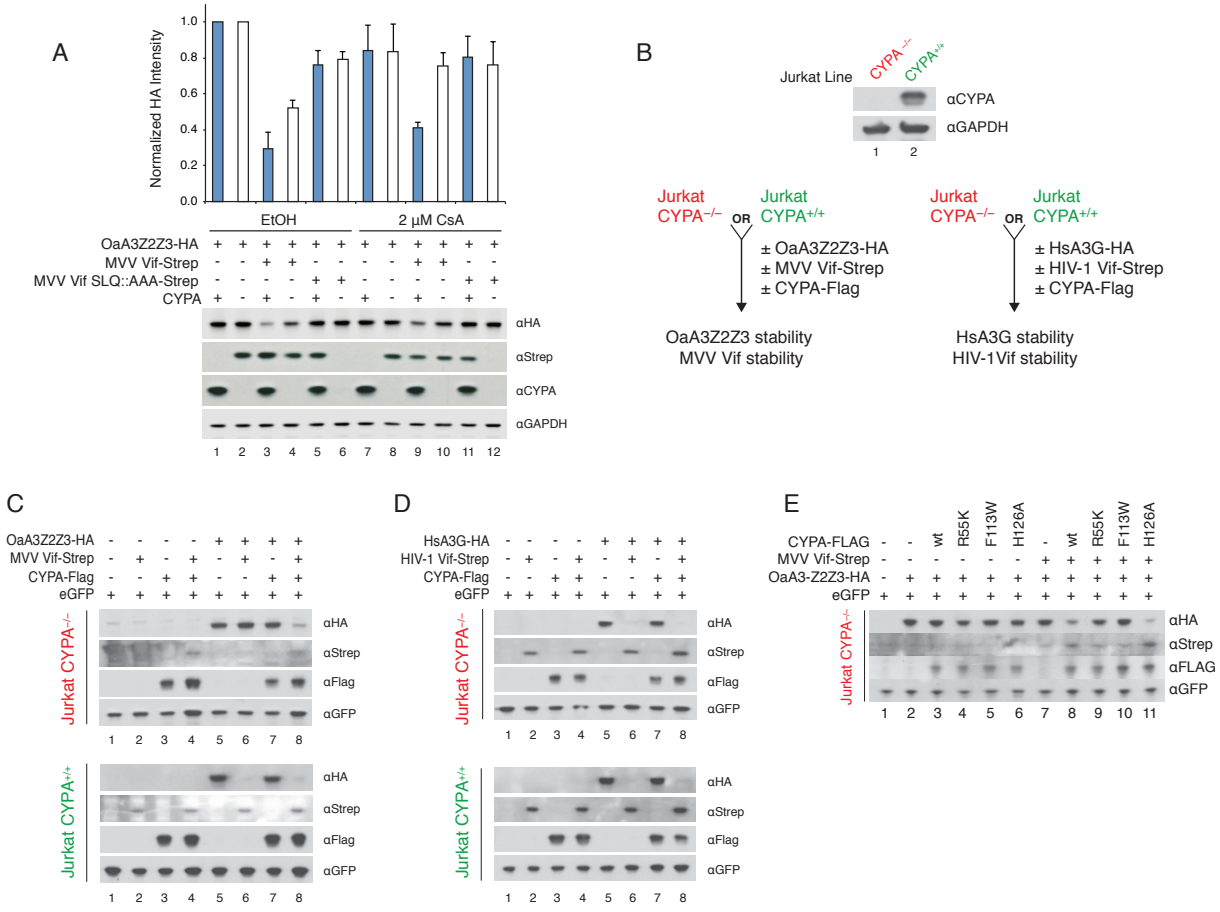
A
Normalized HA Intensity
1.0
0.8
0.6
0.4
0.2
0.0
EtOH
2 µM CsA
OaA3Z2Z3-HA
MVV Vif-Strep
MVV Vif SLQ::AAA-Strep
CYPA
αHA
αStrep
αCYPA
αGAPDH
1 2 3 4 5 6 7 8 9 10 11 12
B
Jurkat Line
CYPA−/−
CYPA+/+
αCYPA
αGAPDH
1 2
Jurkat CYPA−/− OR Jurkat CYPA+/+
± OaA3Z2Z3-HA
± MVV Vif-Strep
± CYPA-Flag
OaA3Z2Z3 stability
MVV Vif stability
Jurkat CYPA−/− OR Jurkat CYPA+/+
± HsA3G-HA
± HIV-1 Vif-Strep
± CYPA-Flag
HsA3G stability
HIV-1Vif stability
C
OaA3Z2Z3-HA
MVV Vif-Strep
CYPA-Flag
eGFP
Jurkat CYPA−/−
Jurkat CYPA+/+
αHA
αStrep
αFlag
αGFP
1 2 3 4 5 6 7 8
D
HsA3G-HA
HIV-1 Vif-Strep
CYPA-Flag
eGFP
Jurkat CYPA−/−
Jurkat CYPA+/+
αHA
αStrep
αFlag
αGFP
1 2 3 4 5 6 7 8
E
CYPA-FLAG
MVV Vif-Strep
OaA3-Z2Z3-HA
eGFP
wt
R55K
F113W
H126A
Jurkat CYPA−/−
αHA
αStrep
αFLAG
αGFP
1 2 3 4 5 6 7 8 9 10 11

Figure 4.4: CYPA is Required for MVV Vif APOBEC3 Degradation Activity

(**A**) Comparison of Vif APOBEC3 degradation activity in monoclonal CYPA knockdown versus control cells in the presence or absence of CsA. Cells were transiently transfected with HA-tagged ovine A3Z2Z3 (OaA3-Z2Z3) and either wild-type or BC-box mutant (SLQ::AAA) Strep-tagged MVV Vif, then treated 6 hours later with either ethanol (E) or 2 μM CsA overnight. Bars represent HA immunoreactivity normalized first by GAPDH loading control, then to no Vif control for each cell line; mean ± S.E. (n=3). Proteins are detected by immunoblotting.

(**B**) CYPA immunoblot in Jurkat E6-1 $CYPA^{+/+}$ "parental" line and derived E6-1 $CYPA^{-/-}$ knockout (KO) line.

(**C**) Top: Jurkat $CYPA^{-/-}$ KO cells are transiently transfected with HA-tagged OaA3Z2Z3, Strep-tagged MVV Vif, and Flag-tagged CYPA. eGFP is used as transfection control. Bottom: identical experiment performed in E6-1 $CYPA^{+/+}$ control line.

(**D**) Top: Jurkat $CYPA^{-/-}$ KO cells are transiently transfected with HA-tagged human A3G (HsA3G), Strep-tagged HIV-1 Vif, and Flag-tagged CYPA. eGFP is used as transfection control. Bottom: identical experiment performed in E6-1 $CYPA^{+/+}$ control line.

(**E**) MVV Vif activity rescue assay using mutants of CYPA. Strep-tagged MVV Vif, HA-tagged OaA3Z2Z3, and various Flag-tagged CYPA constructs are transfected into Jurkat $CYPA^{-/-}$ KO line, and Vif activity assessed through APOBEC3 stability.

Figure 4.5

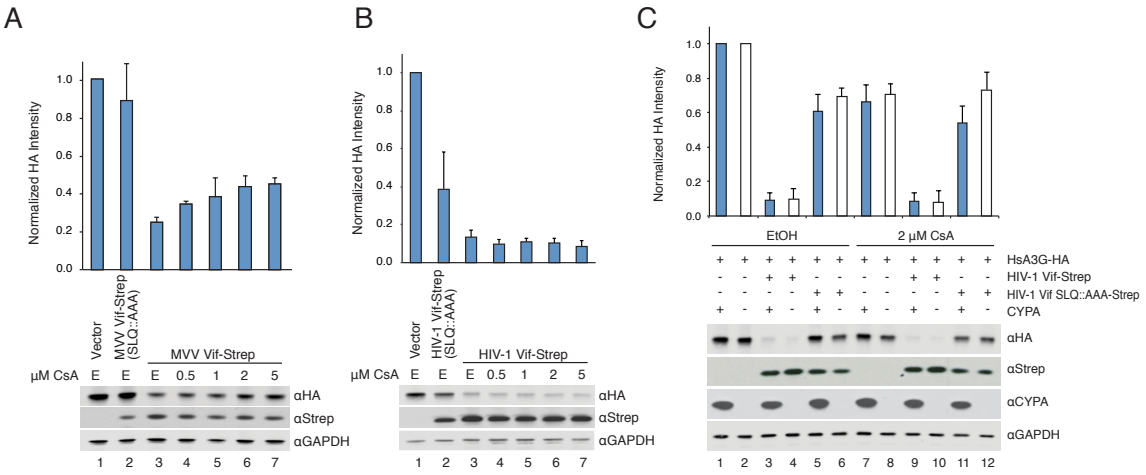
A
B
C
Normalized HA Intensity
1.0
0.8
0.6
0.4
0.2
0.0
Vector
MVV Vif-Strep (SLQ::AAA)
MVV Vif-Strep
HIV-1 Vif-Strep (SLQ::AAA)
HIV-1 Vif-Strep
µM CsA
E
0.5
1
2
5
αHA
αStrep
αGAPDH
1 2 3 4 5 6 7
EtOH
2 µM CsA
HsA3G-HA
HIV-1 Vif-Strep
HIV-1 Vif SLQ::AAA-Strep
CYPA
αCYPA
1 2 3 4 5 6 7 8 9 10 11 12

Figure 4.5: Effect of CYPA on MVV Vif Anti-APOBEC3 Activity

(A) MVV Vif-mediated degradation of OaA3Z2Z3 in the presence of a titration of CsA in HEK293T cells. APOBEC3 stability is assayed by Western blot. Bars represent HA immunoreactivity normalized first by GAPDH loading control, then to no Vif control, mean ± S.D. (n=3). E: ethanol.

(B) Assay in **A** performed with HIV-1 Vif and HsA3G.

(C) Comparison of HIV-1 Vif HsA3G degradation activity in monoclonal CYPA knockdown versus control cells in the presence or absence of CsA. Bars represent HA immunoreactivity normalized first by GAPDH loading control, then to no Vif control for each cell line; mean ± S.E. (n=3).

Figure 4.6

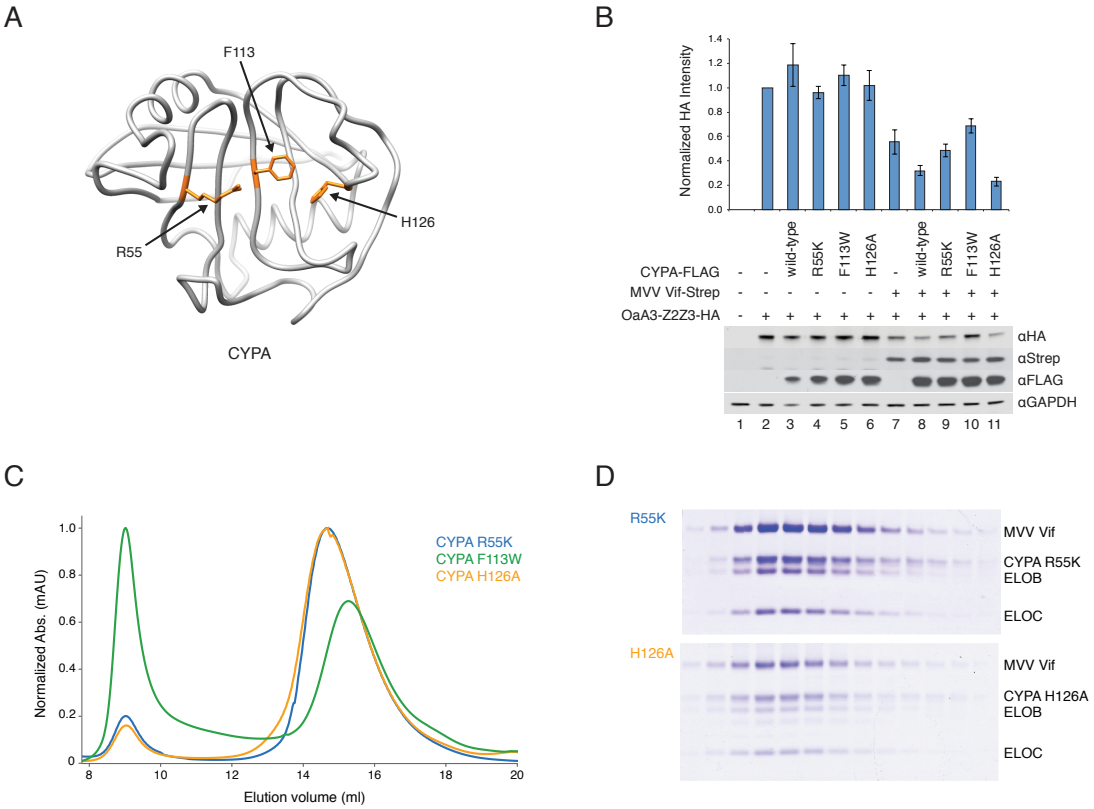
A
F113
H126
R55
CYPA
B
Normalized HA Intensity
1.4
1.2
1.0
0.8
0.6
0.4
0.2
0.0
wild-type
R55K
F113W
H126A
wild-type
R55K
F113W
H126A
CYPA-FLAG - - + + + + - + + + +
MVV Vif-Strep - - - - - - + + + + +
OaA3-Z2Z3-HA - + + + + + + + + + +
αHA
αStrep
αFLAG
αGAPDH
1 2 3 4 5 6 7 8 9 10 11
C
Normalized Abs. (mAU)
1.0
0.8
0.6
0.4
0.2
0
8 10 12 14 16 18 20
Elution volume (ml)
CYPA R55K
CYPA F113W
CYPA H126A
D
R55K
MVV Vif
CYPA R55K
ELOB
ELOC
H126A
MVV Vif
CYPA H126A
ELOB
ELOC

Figure 4.6: Active-site CYPA mutants fail to rescue MVV Vif function but still interact physically.

(A) Model of CYPA showing residues R55, F113, and H126. PDB: 1CWA

(B) Monoclonal knockdown line of CYPA is transfected with HA tagged OaA3Z2Z3, Strep-tagged MVV Vif, and various constructs of Flag-tagged CYPA. Vif activity is assessed by OaA3Z2Z3 stability. HA immunoreactivity is normalized by GAPDH signal and to lane 2 control; mean ± S.E. (n=2).

(C) UV absorbance curves for recombinantly expressed and purified MVV-ELOB-ELOC complex with either R55K, F113W, or H126A CYPA. Samples fractionated by size-exclusion chromatography.

(D) Coomassie-stained SDS-PAGE of peak fractions from **C**.

Chapter 5: Investigations into Non-APOBEC3 Vif Activities Mediated by Non-Canonical Cofactors

SUMMARY

The discovery of lineage-specific cofactor use among Vif proteins raised questions about the function of these acquisitions. As all Vif proteins act as E3 ubiquitin ligases, we took a global proteomics approach to assess cell-wide changes in ubiquitylated proteins upon Vif expression. We identify many changes in ubiquitylated proteins for each Vif both the in the presence and absence of a proteasome inhibitor, potentially indicating the presence of novel Vif substrates. We also tested the hypothesis that CBFβ sequestration to antagonize RUNX is a driving force behind its association with primate-infecting lentiviral Vif proteins. We find that CBFβ is neither necessary nor sufficient to affect the expression of a RUNX1 target gene during T-cell activation, raising questions about the veracity of this simplified model. Lastly, we investigated two host factors, FKBP5 and PTGES3, as potential FIV Vif non-canonical cofactors, as the status of whether or not FIV Vif required a non-canonical cofactor remained ambiguous. We found evidence that FIV and potentially SIVmac Vif proteins form a novel complex with FKBP5 and PTGES3 that, particulary in the case of FIV Vif, may be distinct from Vif-associated CRL complexes, potentially indicative of as-of-yet uncharacterized Vif activities.

INTRODUCTION

Global Approaches to Finding Ubiquitin Substrates

There exist two general approaches to identifying the substrates of ubiquitylation in cells. The first involves a “one-at-a-time” search where a candidate substrate is examined in the presence of its suspected E3 ligase, where the ligase can be overexpressed or knocked

down and the ubiquitylation status of the potential substrate can be measured (Bloom and Pagano, 2005). A generalized version of this search can involve a high-throughput binary search, such as a yeast two-hybrid screen, to look for physical interactions between an E3 ligase and potential substrates (Zhang et al., 2000). A downside to this approach is that many interactions with an E3 ligase will not be with substrates, so such an assay will invariably lead to many false-positive substrates in the initial screen.

A newer approach utilizes global proteomics to view all proteins in a cell at once, removing the bias of selecting candidates. In its simplest form, global protein abundances can be measured by mass spectrometry in the presence or absence of an E3 ubiquitin ligase in an attempt to see proteins that decrease in abundance in the presence of the ligase, implicating them as substrates (Yen and Elledge, 2008). A downside to this approach is a signal-to-noise issue, as most proteins will not change in abundance due to a given E3 ligase. In addition, this will only identify ubiquitylation events that lead to degradation of the substrate. Further to that point, the mass spectrometry does not detect whether or not the proteins that change in abundance are ubiquitylated; this must be determined in follow-up assays. Another approach involves tagging E3 ligases with an ubiquitin-binding UBA domain to “tether” the E3 to its substrate, and to use tagged ubiquitin to perform tandem affinity purifications to identify ubiquitylated substrates bound to the E3 (Mark et al., 2014). While this assay can directly identify ubiquitylated substrates, it requires mutant E3 and mutant ubiquitin to be expressed and is less amendable to less genetically tractable systems.

Recently, a global approach to studying ubiquitylation through mass spectrometry has been devised that does not require any mutant genes to be used and identifies proteins as being ubiquitylated when they are detected. The method, called Ubiscan, involves enrichment of ubiquitylated peptides based on an antibody that specifically recognizes a tryptic di-glycine

ubiquitin remnant on lysine residues (Lee et al., 2011). Once enriched, these peptides undergo LC-MS/MS mass spectrometry where peptides that contain the di-glycine motif can be specifically sequenced, confirming their ubiquitylation status.

Vif Antagonism of T-Cell Activation Through CBFβ Sequestration

After the discovery of the HIV-1 Vif-CBFβ interaction, a sequestration hypothesis was presented as an evolutionary driving force for the interaction. Briefly, Vif sequesters CBFβ from RUNX transcription factors, which require the transcriptional coactivator for both stability and to enhance DNA binding activity; this sequestration results in Vif-mediated antagonism of RUNX-mediated gene expression (Jäger et al., 2012b). RUNX1, a member of the RUNX family, is involved in mediating the T-cell activation gene expression program, and was chosen to test the sequestration model in this context. Kim et al. showed that RUNX1 target genes, as defined by ChIP-seq of RUNX1, are down-regulated in the presence of Vif during T-cell activation (Kim et al., 2013), and others have shown that RUNX1 negatively regulates HIV-1 LTR-driven gene expression that is alleviated by Vif sequestration of CBFβ (Klase et al., 2014)., we picked a highly down-regulated gene in the Vif-RUNX1 antagonism dataset to act as a reporter for RUNX1 antagonism activity – the transcription factor T-bet, also known as Tbx21. Upon T-cell activation, RUNX1-dependent T-bet expression is up-regulated, and is involved in regulating cytokine production, including down-regulation of IL-2 production and up-regulation of IFNγ production (Szabo et al., 2000). When HIV-1 Vif is co-expressed, T-bet expression is blocked at the transcriptional level, consistent with a model of Vif antagonism of RUNX1-mediated gene expression (Kim et al., 2013).

The Ambiguous State of the FIV Vif Non-canonical Cofactor Requirement

The investigation into Vif non-canonical cofactor use yielded the association of CBFβ with primate-infecting lentiviruses HIV-1 and SIVmac, and CYPA with the ovine-tropic MVV. Through *in vitro* reconstitution, BIV Vif was shown to not require any additional host factors beyond the "canonical" CRL5 complex of CUL5, RBX2, ELOB, and ELOC for stable, stoichiometric complex formation and ubiquitylation activity against purified recombinant bovine APOBEC3Z3 protein; we interpreted this *in vitro* data as strong evidence that BIV Vif does not require a non-canonical host cofactor, and this interpretation is consistent with both the AP-MS results, as well as the tandem affinity purification of *in vivo* BIV Vif-CUL5 complexes. However, FIV Vif remains enigmatic with respect to potential host cofactor usage. The largest Vif protein explored in this investigation, we were unable identify a condition which allowed for reconstitution of an FIV Vif-CRL5 complex *in vitro* despite strong association with this complex *in vivo* based on AP-MS data. The observed aggregation of FIV Vif with ELOB and ELOC was reminiscent of both HIV-1 and MVV Vif protein attempted reconstitution without their required non-canonical cofactors CBFβ and CYPA, respectively. Confusingly, tandem affinity purification of FIV Vif-CUL5 complexes failed to yield strong candidate cofactors (**Figure 5.8A**, **Table 6**).

RESULTS

Global Ubiquitylation Profiling of Stable Vif Jurkat Lines

Global ubiquitylation profiling of cells, or Ubiscan, is a powerful technique to enrich for and detect by mass spectrometry ubiquitylated peptides in cells. Given that all the Vif proteins are E3 ubiquitin ligases, we asked if they would share similar global ubiquitylation patterns, or if they showed differential patterns, potentially indicative of different substrates. Previous HIV-1 Vif-related Ubiscan data had been generated in the Krogan lab using the stable, inducible

Jurkat cell system that had also been used in our cross-species AP-MS Jurkat set (Kane et al. 2015). As stable, inducible Jurkat Vif lines had been generated for all the Vif constructs used in the AP-MS study, we used these for the Ubiscan as well. Jurkat T-cells stably transfected with Flag-tagged Vif genes plus a control parental line were treated with 1 μg / mL doxycline for 18 hours to induce Vif expression, then cell pellets were snap-frozen. Two biological replicates were produced without treatment of the proteasome inhibitor MG-132, and two biological replicates were treated with 10 μM MG-132 for the last four hours of Vif expression so that total induction time was identical across all samples. Cell pellets were lysed under denaturing conditions, trypsinized, and tryptic peptides containing ubiquitin remnant di-GlyGly motifs were immunoprecipitated, identified by LC-MS/MS (**Figure 5.1A**), and statistically significant up- or down-ubiquitylated peptides were assessed using the MSstats package by comparing Vif samples to the parental controls (Choi et al., 2014). Samples were tested for Vif induction and efficacy of MG-132 treatment by immunoblot (**Figure 5.1B**).

A cutoff of a log2 fold change of greater than two or less than negative two and a p-value, corrected for multiple testing, of less than 0.001 were used as cutoffs for data from the Ubiscan that would be considered (**Figure 5.2**). Each Vif protein showed distinct ubiquitylation patterns both in the MG-132 treated and untreated samples, and when analyzed for Gene Ontology (GO) category enrichment in biological processes (**Figure 5.1C-E**). Comparing each Vif for treated versus untreated with MG-132, there are immediately identifiable differences between each dataset for all five Vif proteins, and those that are significantly increased in the MG-132 treated samples may be novel substrates. No APOBEC3 proteins were identified in any dataset, potentially due to low level of expression of these proteins in Jurkat cells (Koning et al., 2009).

Testing CBFβ-Mediated Antagonism of T-Cell Activation by Vif Results in Confusing Phenotypes

After the observation that CBFβ only interacts with Vif in primate-infecting lentiviruses, we asked if the observed phenomenon of RUNX1 antagonism would be limited only to those Vif proteins. To test this, we performed a Vif antagonism of T-cell activation assay using the transcription factor T-bet as a reporter for Vif antagonism of RUNX1 function (Kim et al., 2013). Using the stable, inducible Jurkat T-cell Vif lines, Vif expression was induced with doxycycline for 18 hours, then T-cells were activated with 50 ng / mL phorbol 12-myristate 13-acetate (PMA) and 1 μg / mL phytohemagluttinin (PHA). Cells were harvested, and T-bet expression was assessed by immunoblot, with non-activated, Vif expressing cells as controls. We did not perform experimental samples that were activated but not induced, as activation appeared to de-repress Vif expression, leading to effects on T-bet expression even in samples untreated with doxycycline (**Figure 5.4B**). Unexpectedly, we observed that T-bet expression did not correlate with CBFβ interaction, as the SIVmac Vif expressing Jurkat line showed no down-regulation of T-bet in spite of Vif expression, even as the HIV-1 Vif line showed robust inhibition of T-bet expression (**Figure 5.4A**). Moreover, BIV and FIV Vif-expressing Jurkat lines also displayed down-regulation of T-bet expression during T-cell activation, despite these Vif proteins lacking any measurable interaction with CBFβ. Thus, these initial results imply that Vif interaction is neither necessary nor sufficient for affecting T-bet expression after T-cell activation. Interestingly, multiple sequence alignment of the five Vif proteins revealed a potentially critical site that is common between BIV, FIV, and HIV-1 Vif proteins but not found in MVV and SIVmac Vif proteins – a hydrophobic patch consisting of a LVI motif (**Figure 5.4C**). Previous research into the HIV-1 Vif-CBFβ interaction implicated this region as important for mediating the reported sequestration effect by Vif (Kim et al., 2013), but the later published

HIV-1 Vif structure does not implicate these residues in mediating the Vif-CBFβ interaction (Guo et al., 2014).

Search for an FIV Vif Non-Canonical Cofactor Leads to an Intriguing Interaction between FIV and SIVmac Vif Proteins and Host Factors FKBP5 and PTGES3

Entertaining the notion that we had failed to identify a non-canonical cofactor for FIV Vif, I re-examined the SAINT-scored AP-MS data and identified two host factors that showed strong associations with FIV and, interestingly, SIVmac Vif – PTGES3 and FKBP5 (**Figure 5.8B**). PTGES3, also known as p23, is a 23 kDa protein that was identified as a HIV-1 Vpu interactor in the Jager et al. dataset, and is associated with a number of functions, including binding to telomerase, acting as an HSP90 co-factor, involvement in hormone receptor signaling, prostaglandin synthesis, and RNAi pathways (Holt et al., 1999; Karagoz et al., 2011; Knoblauch and Garabedian, 1999; McLaughlin et al., 2006; Nguyen et al., 2012; Oxelmark et al., 2006; Pare et al., 2013; Tanioka et al., 2000). FKBP5 is a cis-trans propyl-isomerase like CYPA, but falls under a different family of isomerases known as immunophilins (Marks, 1996); FKBP5 has been implicated in NF-κB signaling, as well as glucocorticoid receptor (GCR) signaling, where polymorphisms in the *Fkbp5* gene have been implicated in psychological disorders (Erlejman et al., 2014; Galigniana et al., 2012; Szczepankiewicz et al., 2014; Tatro et al., 2009). FKBP5 and PTGES3 have been reported to form a complex together with HSP90 as well to regulate GCR signaling (Johnson and Toft, 1994; Ni et al., 2010). Somewhat puzzlingly, FKBP5 and PTGES3 were not readily detected in the Vif-CUL5 tandem affinity purification for either FIV or SIVmac (**Figure 5.8C**). To assess if the SAINT data correctly identified these two host factors as specific for FIV and SIVmac Vif proteins, I performed a co-affinity purification assay with Strep-tagged Vif proteins and Flag-tagged PTGES3 or FKBP5, performing a Strep purification followed by immunoblotting to assess if the Flag-tagged host factors co-purified

with Vif proteins. Consistent with the AP-MS data, both PTGES3 and FKBP5 are only observed to co-purify with FIV and SIVmac Vif proteins (**Figure 5.8D)**. Next, I performed the inverse assay focusing only on FIV and SIVmac Vif proteins, performing a Flag immunoprecipitation on FKBP5 or PTGES3 with or without FIV or SIVmac Vif proteins co-expressed and assay both by immunoblotting and LC-MS/MS mass spectrometry to identify the co-purification of Vif proteins and proteins that associate with the host factors in a Vif-dependent manner (**Figure 5.6A-B, Figure 5.7**). Two biological replicates were performed per condition, and AP-MS data was scored using SAINT, with detected proteins with a SAINT score ≥ 0.8 were included (**Table 8**). The complex data shows many proteins shared between both PTGES3 and FKBP5, but many proteins only associating with the host factors in a Vif-dependent manner (**Figure 5.7**). Interestingly, association between Vif and ELOC is only observed with SIVmac when pulling down on either FKBP5 or PTGES3; these data are confirmed by immunoblot, where a strong association between SIVmac Vif and ELOC is observed for both FKBP5 and PTGES3 purifications, compared to very weak association observed for FIV Vif (**Figure 5.6B**). The lack of association of ELOC with FIV Vif in the context of Vif association with FKBP5 or PTGES3 may explain why these host factors were not detected in the tandem purification of FIV Vif with CUL5, i.e. this VIF Vif-associated complex is distinct from the FIV Vif-CRL5 complex.

Given the association of both PTGES3 and FKBP5 with HSP90, I reasoned that the complex may be involved with the folding or stability of FIV and SIVmac Vif proteins. To test this, I first overexpressed FKBP5 or PTGES3 in the presence of FIV, SIVmac, and HIV-1 Vif proteins. If the interaction was specific, I would expect no effect to be observed with HIV-1 Vif. In addition, I used the overexpression of CBFβ, which increases HIV-1 Vif stability, as a positive control in the assay (**Figure 5.8A-B**). The results show somewhat confusing results, as very little increase in stability is observed for PTGES3 for both FIV and SIVmac Vif proteins, and FKBP5 appears

to increase the stability of all Vif proteins tested. The positive control, HIV-1 Vif and CBFβ, shows a strong increase in HIV-1 Vif stability. To test the stability hypothesis in an orthogonal manner, I treated HEK293T cells expressing either FIV, SIVmac, or HIV-1 Vif proteins with a titration of the HSP90 inhibitor geldanamycin (GA). If the HSP90-FKBP5-PTGES3 complex was specifically involved in the stability of FIV or SIVmac Vif proteins, I expected to see increased sensitivity to GA treatment compared to HIV-1 Vif. Unexpectedly, all Vif proteins tested increased in expression through the GA titration, the exact opposite of what would be expected if Vif required HSP90 for proper folding and stability (**Figure 5.8C**). As all Vif proteins responded similarly to the GA treatment and I did not provide an independent control to measure HSP90 activity, it remained possible that I did not treat the cells with enough GA to inhibit HSP90 sufficiently to result in a Vif destabilization phenotype, though my highest concentration of 5 μM was well above the reported GA IC50 in the hundred nanomolar range (Howes et al., 2006).

DISCUSSION

A goal of the Vif comparative proteomics project was to characterize potentially novel Vif biology, including novel viral-host interactions and activities. The initial AP-MS experiments and follow-up work was successful in identifying the lineage-specific use of non-canonical cofactors in Vif anti-APOBEC3 activity. However, unanswered questions remained at the conclusion of this study, including if there are novel substrates of any of these Vif proteins, aside from the canonical APOBEC3 substrates, if the antagonism of RUNX activity observed with HIV-1 Vif is conserved across lentiviruses, if there is an FIV Vif cofactor (undetermined by the aforementioned study).

Global proteomics is a powerful tool to unbiasedly observe cell-wide changes in the proteome. As all Vif proteins act as E3 ubiquitin ligases, we employed a global proteomics method known as Ubiscan to measure ubiquitylated proteins in a cell and ask if any change in their abundance during Vif expression occur. We identified a large set of proteins that are undergoing changes in ubiquitylation state upon expression of the five Vif proteins examined in this study, both in the presence and in the absence of a proteasome inhibitor. The observation that many proteins only observe increases in ubiquitylation state upon MG-132 treatment may indicate the existence of novel Vif substrates. An important caveat to these data is that Vif may not be directly involved in the ubiquitylation of these proteins, as the ubiquitylation state of many cellular proteins may be indirectly affected by the expression of Vif proteins. However, with gene enrichment analyses, affected pathways may become apparent and a mechanism implicated if the action is indirect from Vif. More follow-up work is required to assess the implications of these data, particularly the potential existence of novel Vif substrates. An additional caveat to the Ubiscan technique is that information about the type of ubiquitylation, whether mono or poly-ubiquitylated, and if a chain, what type, is lost during trypsinization. This also prevents the discrimination between ubiquitin remnants and remnants from other, ubiquitin-like proteins such as SUMO or ISG15 (Schwartz and Hochstrasser, 2003). A work-around to this is the use of multiple proteases that will leave moieties that discriminate between different ubiquitin-like proteins (Swaney et al., 2010), or the use of mutant ubiquitin-like proteins that only form a di-glycine motif in the presence of a non-trypsin protease (Tammsalu et al., 2015).

The observation of the interaction between HIV-1 Vif and CBFβ, and the presentation of a sequestration model that enabled Vif to perform a “dual-hijack” and antagonize both APOBEC3 proteins and RUNX-mediated gene expression, implied a simple model – that if a Vif

protein interacts with CBFβ, then it should affect the RUNX pathway, and vice versa. We tested this assumption using an assay developed in part to validate the Vif dual-hijack hypothesis (Kim et al., 2013), using a transcription factor, T-bet, that was shown to be repressed during T-cell activation when HIV-1 Vif is co-expressed. To our surprise, we found that CBFβ was neither necessary nor sufficient for T-bet repression after T-cell activation. Two Vif proteins that do not interact with CBFβ nor require it for APOBEC3 antagonism, from BIV and FIV, showed robust T-bet repression during activation of Jurkat cells with PMA / PHA. Conversely, we did not observe any T-bet repression during Jurkat T-cell activation with SIVmac Vif, which does interact with CBFβ and does require it for APOBEC3 antagonism. Clearly, if the observation of RUNX1 antagonism by HIV-1 Vif is correct, either the sequestration model is an oversimplification of the mechanism, or other mechanisms are employed, such as degradation of an unidentified substrate. More work is required to understand this confusing aspect of Vif biology. Starting points for this include leveraging the Ubiscan and AP-MS data, as well as developing a more robust assay to measure the effect of RUNX antagonism, i.e. measuring more parameters than solely T-bet protein expression.

The inability to definitely assess the cofactor requirement for FIV Vif made it more difficult to say with certainty the timing of various cofactor acquisitions during Vif evolution. In particular, whether or not the most recent common ancestor Vif had a cofactor, and if FIV Vif does in fact have a cofactor, give a stronger notion to what trends may drive cofactor gains or losses across the lentivirus phylogeny. In exploring potential FIV cofactors from generated AP-MS data, we found two host proteins, FKBP5 and PTGES3, that appeared to have robust and specific interactions with FIV and SIVmac Vif proteins. Further investigation using proteomics techniques reveals that the interaction between FIV Vif and these two host factors may also involve the chaperone HSP90, and this complex appears to exclude members of the FIV Vif-

associated CRL5 complex, as ELOB and ELOC appear to be de-enriched relative to both what would appear in a typical FIV Vif AP-MS experiment, and relative to the co-purification of ELOB and ELOC with SIVmac Vif in the same context. Whether this is a bona fide novel Vif complex that is distinct from the FIV Vif-CRL5 complex, or an intermediate between de novo synthesis of FIV Vif and its assembly of a hijacked CRL5 complex, is unclear. Attempts to inhibit HSP90 to observe a potential sensitivity to HSP90-mediated folding for FIV and SIVmac Vif, relative to HIV-1 Vif, were at best ambiguous and at worst showed an anti-correlation between inhibition of HSP90 and expression of these Vif proteins. We did not test Vif activity in terms of CRL5 complex assembly nor APOBEC3 degradation activity in the presence of the HSP90 inhibitor GA, and it remains possible that while at a population level Vif becomes more stable, these Vif molecules may be less active in mediating APOBEC3 degradation. The endogenous function shared by both PTGES3 and FKBP5, in regulating the response of glucocorticoid receptor after ligand binding (Johnson and Toft, 1994; Knoblauch and Garabedian, 1999), may play a role in FIV and SIVmac Vif targeting these proteins. Further research needs to be performed to assess if the interaction is a more trivial aspect of expression of these Vif proteins out of the context of infection in human cells, or a glimpse into deeper, novel Vif biology.

Figure 5.1

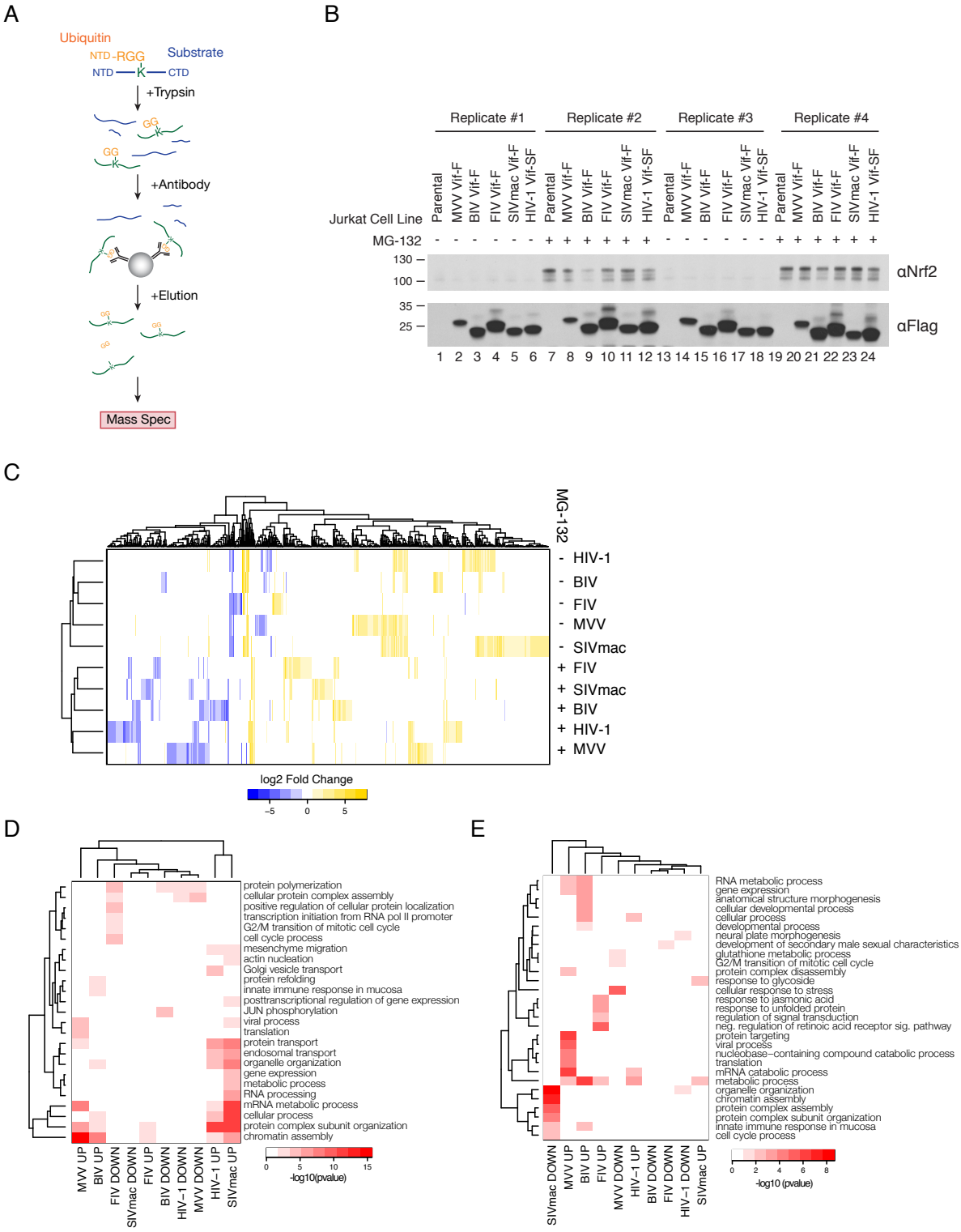
A
Ubiquitin
NTD-RGG
Substrate
NTD — K — CTD
+Trypsin
+Antibody
+Elution
Mass Spec
B
Replicate #1
Replicate #2
Replicate #3
Replicate #4
Jurkat Cell Line
Parental
MVV Vif-F
BIV Vif-F
FIV Vif-F
SIVmac Vif-F
HIV-1 Vif-SF
MG-132
130
100
35
25
αNrf2
αFlag
1 2 3 4 5 6 7 8 9 10 11 12 13 14 15 16 17 18 19 20 21 22 23 24
C
MG-132
- HIV-1
- BIV
- FIV
- MVV
- SIVmac
+ FIV
+ SIVmac
+ BIV
+ HIV-1
+ MVV
log2 Fold Change
−5 0 5
D
protein polymerization
cellular protein complex assembly
positive regulation of cellular protein localization
transcription initiation from RNA pol II promoter
G2/M transition of mitotic cell cycle
cell cycle process
mesenchyme migration
actin nucleation
Golgi vesicle transport
protein refolding
innate immune response in mucosa
posttranscriptional regulation of gene expression
JUN phosphorylation
viral process
translation
protein transport
endosomal transport
organelle organization
gene expression
metabolic process
RNA processing
mRNA metabolic process
cellular process
protein complex subunit organization
chromatin assembly
MVV UP
BIV UP
FIV DOWN
SIVmac DOWN
FIV UP
BIV DOWN
HIV−1 DOWN
MVV DOWN
HIV−1 UP
SIVmac UP
0 5 10 15
-log10(pvalue)
E
RNA metabolic process
gene expression
anatomical structure morphogenesis
cellular developmental process
cellular process
developmental process
neural plate morphogenesis
development of secondary male sexual characteristics
glutathione metabolic process
G2/M transition of mitotic cell cycle
protein complex disassembly
response to glycoside
cellular response to stress
response to jasmonic acid
response to unfolded protein
regulation of signal transduction
neg. regulation of retinoic acid receptor sig. pathway
protein targeting
viral process
nucleobase−containing compound catabolic process
translation
mRNA catabolic process
metabolic process
organelle organization
chromatin assembly
protein complex assembly
protein complex subunit organization
innate immune response in mucosa
cell cycle process
SIVmac DOWN
MVV UP
BIV UP
FIV UP
MVV DOWN
HIV−1 UP
BIV DOWN
FIV DOWN
HIV−1 DOWN
SIVmac UP
0 2 4 6 8
-log10 (pvalue)

Figure 5.1: Overview of Vif Ubiscan Data

(A) Schema of Ubiscan technique. Ubiquitylate proteins typically have the carboxy-terminus of ubiquitin conjugated to the e-amine in lysine residues. After trypsinization, ubiquitylated lysines will have a di-glycine motif conjugated to them. An antibody specifically recognizing this motif is used to immunoprecipitate ubiquitylated peptides, which are then detected using LC-MS/MS mass spectrometry.

(B) Four biological replicates were used in the Vif Ubiscan experiment. Jurkat T-cells stably transfected with Vif constructs were induced with doxycycline for 18 hours before cells were harvested and lysed. Two sets were without the proteasome inhibitor MG-132, and two were with MG-132 for four hours. Nrf2 is an unstable protein that is used to detect proteasome inhibition. F: 3xFlag; SF: 2xStrep-3xFlag.

(C) Heatmap of ubiquitylated proteins identified in Ubiscan that had log2 fold changes greater than 2 or less than -2 and p-values, corrected for multiple testing, less than 0.001 as assessed by the MSstats package. Fold changes were relative to control Jurkat T-cell samples.

(D) Gene ontology (GO) biological process enrichment for Ubiscan data in **C** for samples untreated with MG-132. “UP” refers to ubiquitylated proteins that were enriched in a sample (i.e. log2 fold change greater than 2) and “DOWN” refers to ubiquitylated proteins that were de-enriched in a sample (i.e. log2 fold change less than -2).

(E) Same plot as **D** with MG-132 treated samples.

Figure 5.2

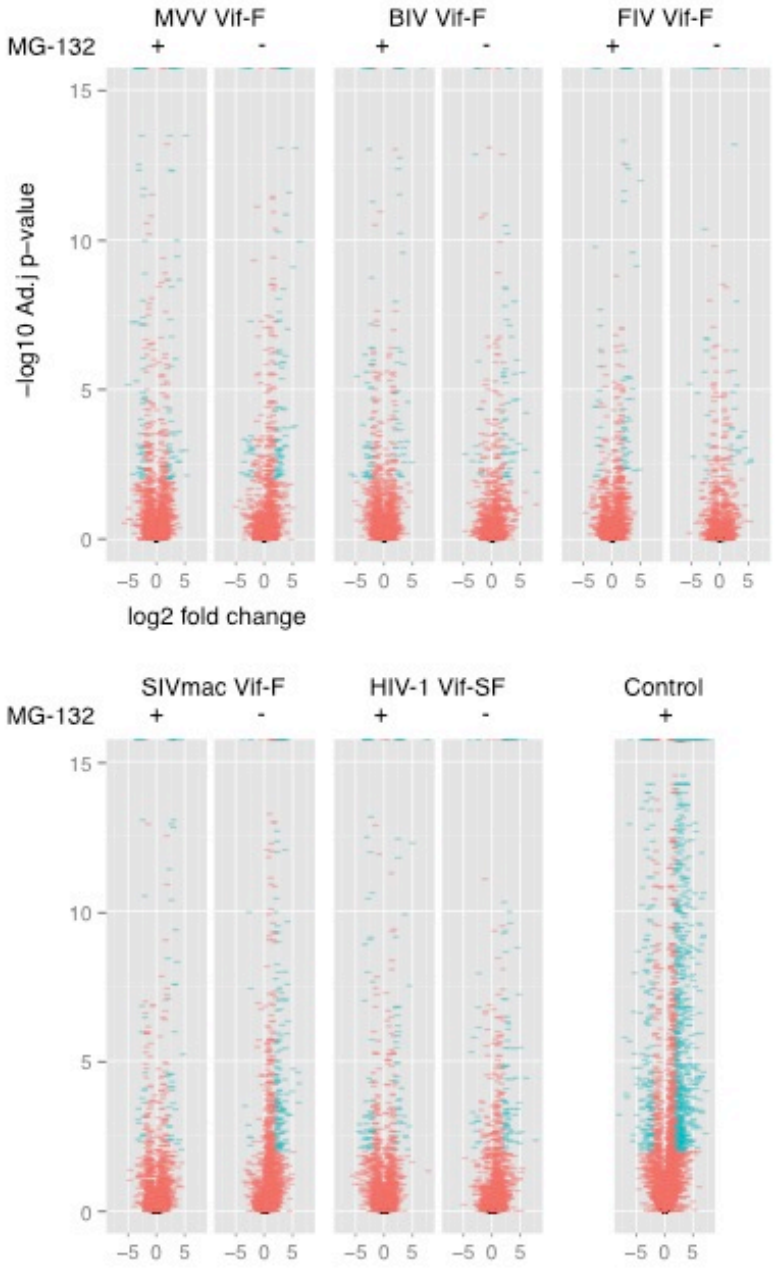
MVV Vif-F
BIV Vif-F
FIV Vif-F
MG-132
+
-
15
10
5
0
−log10 Ad.j p−value
−5 0 5
log2 fold change
SIVmac Vif-F
HIV-1 Vif-SF
Control

Figure 5.2: Volcano Plots of Relative Fold Changes of Ubiquitylated Proteins in Jurkat Cells Expressing Vif Proteins

P-values corrected for multiple testing and log2 fold changes in ubiquitylated proteins were calculated using the MSstats package, comparing Vif expressing cells treated with the proteasome inhibitor MG-132 to control cells treated with MG-132, and Vif expressing cells not treated with MG-132 with untreated control cells. Control cell volcano plot is comparing control cells treated with MG-132 to untreated control cells. Data points in blue indicate fold changes greater than 2 or less than -2, with an adjusted p-value less than 0.001.

Figure 5.3

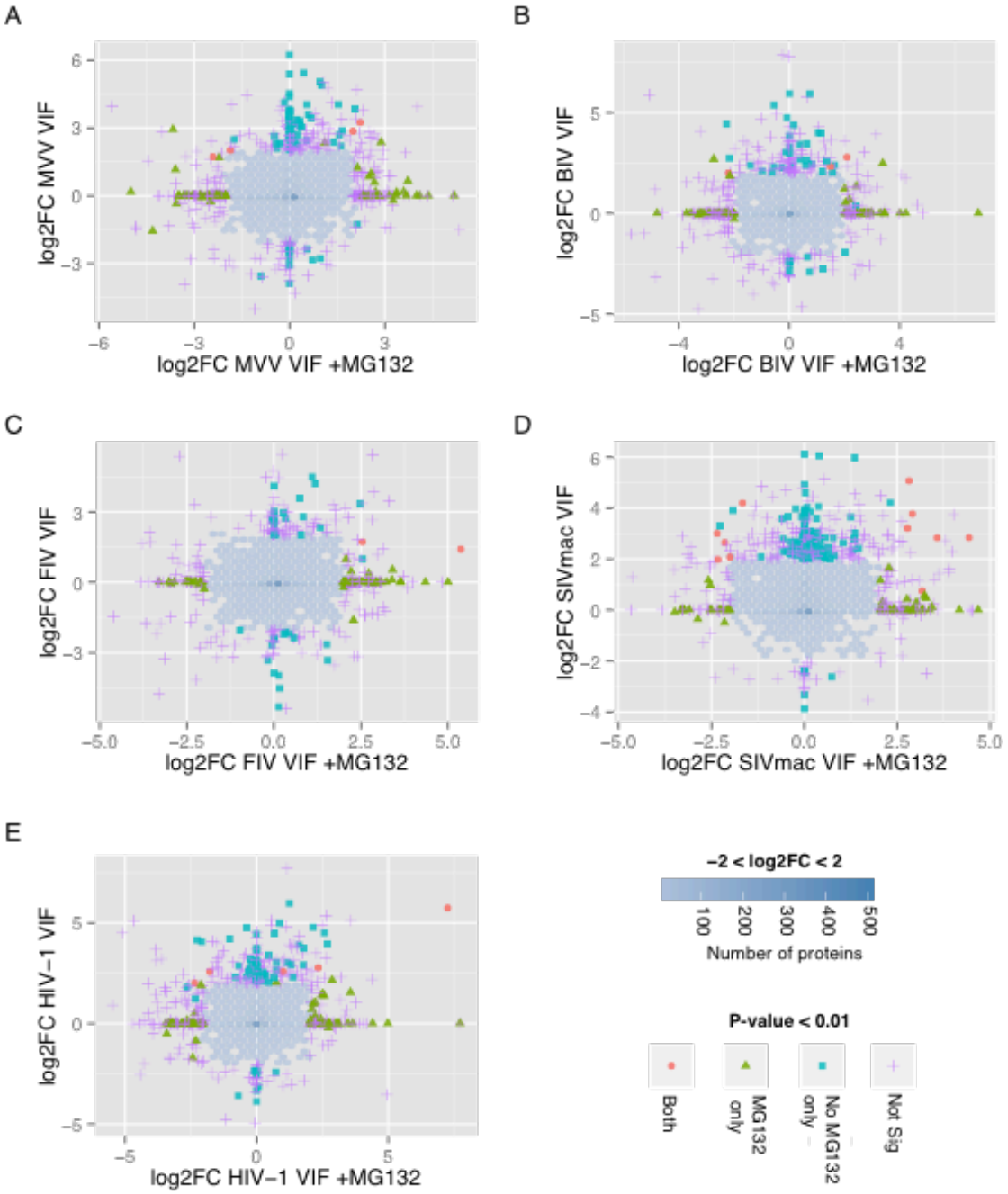
A
log2FC MVV VIF
log2FC MVV VIF +MG132
B
log2FC BIV VIF
log2FC BIV VIF +MG132
C
log2FC FIV VIF
log2FC FIV VIF +MG132
D
log2FC SIVmac VIF
log2FC SIVmac VIF +MG132
E
log2FC HIV−1 VIF
log2FC HIV−1 VIF +MG132
−2 < log2FC < 2
100
200
300
400
500
Number of proteins
P-value < 0.01
Both
MG132 only
No MG132 only
Not Sig

Figure 5.3: Scatterplots Comparing Vif Sample Ubiquitylated Proteins With and Without MG-132 Treatment

(A–E) Scatterplots comparing significantly increased or decreased fold changes in ubiquitylated proteins in Jurkat T-cells expressing Vif proteins. Individual data points represent ubiquitylated proteins that have a log2 fold change greater than 2 or less than -2, otherwise they are binned. Log2 fold changes and p-values corrected for multiple testing were obtained through the MSstats package. Log2fc: Log2 fold change.

Figure 5.4

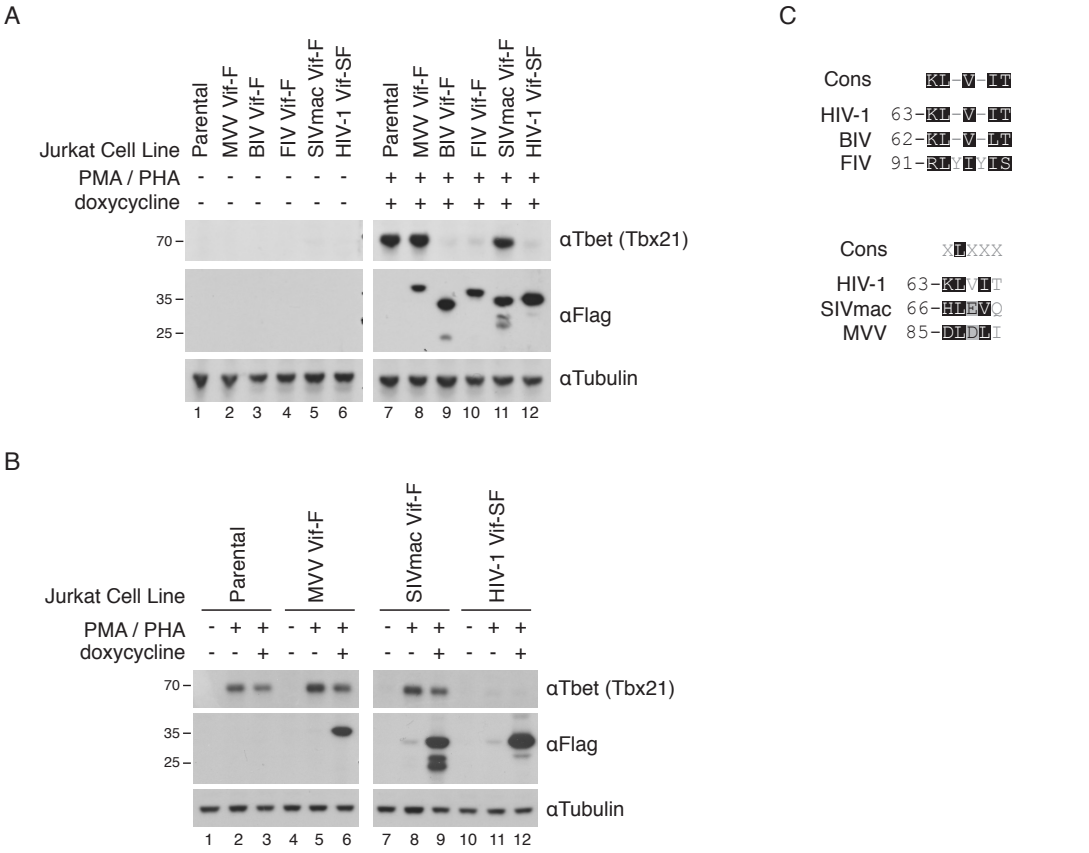
A
Parental
MVV Vif-F
BIV Vif-F
FIV Vif-F
SIVmac Vif-F
HIV-1 Vif-SF
Jurkat Cell Line
PMA / PHA
doxycycline
70
35
25
αTbet (Tbx21)
αFlag
αTubulin
1 2 3 4 5 6 7 8 9 10 11 12
B
Parental
MVV Vif-F
SIVmac Vif-F
HIV-1 Vif-SF
Jurkat Cell Line
PMA / PHA
doxycycline
70
35
25
αTbet (Tbx21)
αFlag
αTubulin
1 2 3 4 5 6 7 8 9 10 11 12
C
Cons
HIV-1 63-KL-V-LT
BIV 62-KL-V-LT
FIV 91-RLYLYLS
Cons
HIV-1 63-KLVLT
SIVmac 66-HLEVQ
MVV 85-DLDLI

Figure 5.4: CBFβ is Neither Necessary Nor Sufficient for T-bet Suppression During T-Cell Activation

(A) Jurkat T-cells stably transfected with doxycycline-inducible *vif* genes are treated with doxycycline for 16 hours, then treated with PMA and PHA to activate the T-cells. Vif and T-bet expression is detected by immunoblotting. F: 3xFlag; SF: 2xStrep-3xFlag.

(B) A subset of the Vif proteins assayed in **A** are tested for T-bet suppression during T-cell activation with and without doxycycline treatment.

(C) A motif appears to be conserved in Vif proteins that suppress T-bet expression (HIV-1, BIV, FIV), but not in Vif proteins that fail to suppress T-bet in the assay in **A** (SIVmac, MVV). Color indicates extent of conservation in sequences.

Figure 5.5

A

	MVV Vif	BIV Vif	FIV Vif	SIVmac Vif	HIV-1 Vif
1	**CUL5**	**CUL5**	**CUL5**	**CUL5**	**CUL5**
2	**CYPA**	TBB5	**FIV Vif**	TBB2C	**CBFβ**
3	HSP71	TBA1B	TBA1B	HSP71	**ELOC**
4	**MVV Vif**	HSP71	HSP71	TBA1B	KRT85
5	**ELOC**	**ELOC**	TBB2C	**ELOC**	HSP71
6	TBA1B	**ELOB**	**ELOC**	**CBFβ**	**ELOB**
7	TBB5	K2C1	**ELOB**	**ELOB**	PABP1
8	**ELOB**	**BIV Vif**	K2C1	**SIVmac239 Vif**	TBB5
9	K2C1	K1C9	HS90B	K2C1	**HIV1-NL43 Vif**
10	HNRPF	PABP1	K1C9	HS90B	KT33B

B

	HEK293T cells					Jurkat T-cells				
Vif	MVV	BIV	FIV	SIV	HIV-1	MVV	BIV	FIV	SIV	HIV-1
FKBP5	0.00	0.00	1.00	1.00	0.00	0.00	0.00	1.00	1.00	0.00
PTGES3	0.00	0.00	1.00	1.00	0.00	0.00	0.00	0.74	0.75	0.00

C

Vif	MVV	BIV	FIV	SIV	HIV-1
ELOC	41	46	57	51	53
CYPA	65	0	0	0	0
CBFβ	0	0	0	41	69
PTGES3	0	0	3	1	0
FKBP5	0	0	0	1	0

D

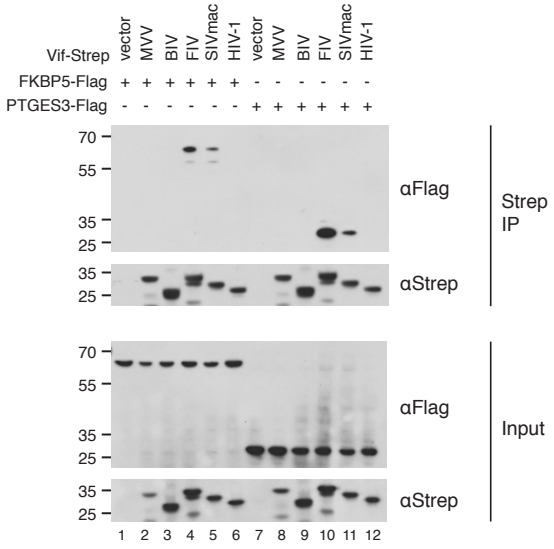

Figure 5.5: Host Factors FKBP5 and PTGES3 Are FIV and SIVmac Vif Specific Interactors

(A) Top ten proteins identified in Vif-CUL5 tandem affinity purification performed in **Figure 3.1D**. Numbers indicate spectral counts of proteins identified by LC-MS/MS mass spectrometry. Protein names in bold are known members of Vif-associated CRL5 complexes; Vif proteins are highlighted in green, and non-canonical cofactors are highlighted in red.

(B) Vif AP-MS data for FBKP5 and PTGES3. Numbers indicate SAINT scores from **Table 4** and **Table 5**.

(C) Spectral counts of select proteins detected in Vif-CUL5 tandem affinity purification performed in **Figure 3.1D**.

(D) Strep purification of Vif-2xStrep proteins in the presence of either FKBP5-3xFlag or PTGES3-3xFlag in HEK293T cells. Proteins are detect by immunoblot.

Figure 5.6

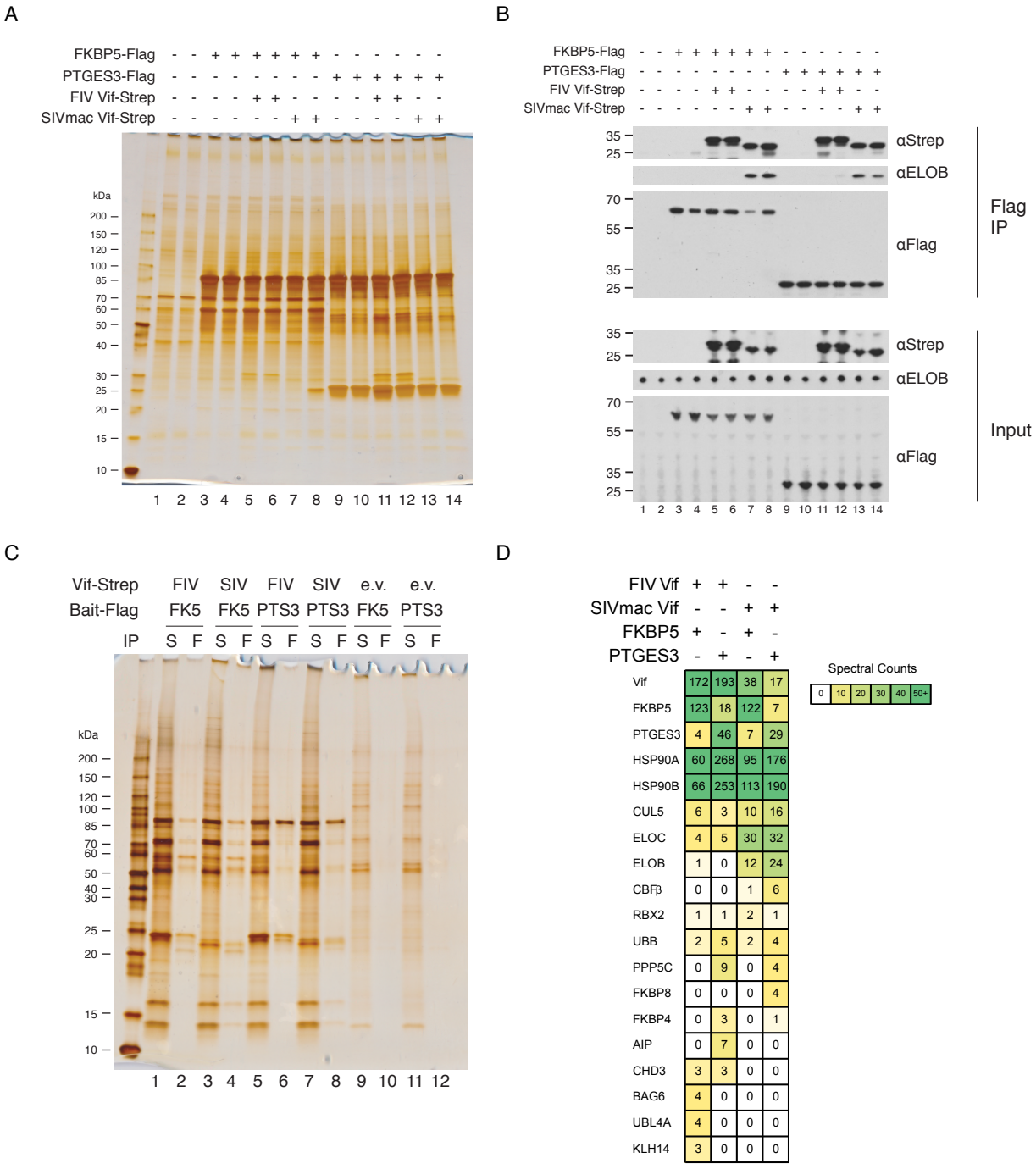
A
FKBP5-Flag
PTGES3-Flag
FIV Vif-Strep
SIVmac Vif-Strep
kDa
200
150
120
100
85
70
60
50
40
30
25
20
15
10
1 2 3 4 5 6 7 8 9 10 11 12 13 14
B
FKBP5-Flag
PTGES3-Flag
FIV Vif-Strep
SIVmac Vif-Strep
35
25
αStrep
αELOB
70
55
αFlag
Flag IP
Input
1 2 3 4 5 6 7 8 9 10 11 12 13 14
C
Vif-Strep FIV SIV FIV SIV e.v. e.v.
Bait-Flag FK5 FK5 PTS3 PTS3 FK5 PTS3
IP S F S F S F S F S F S F
kDa
200
150
120
100
85
70
60
50
40
30
25
20
15
10
1 2 3 4 5 6 7 8 9 10 11 12
D
FIV Vif + + - -
SIVmac Vif - - + +
FKBP5 + - + -
PTGES3 - + - +
Spectral Counts
0 10 20 30 40 50+
Vif 172 193 38 17
FKBP5 123 18 122 7
PTGES3 4 46 7 29
HSP90A 60 268 95 176
HSP90B 66 253 113 190
CUL5 6 3 10 16
ELOC 4 5 30 32
ELOB 1 0 12 24
CBFβ 0 0 1 6
RBX2 1 1 2 1
UBB 2 5 2 4
PPP5C 0 9 0 4
FKBP8 0 0 0 4
FKBP4 0 3 0 1
AIP 0 7 0 0
CHD3 3 3 0 0
BAG6 4 0 0 0
UBL4A 4 0 0 0
KLH14 3 0 0 0

Figure 5.6: FKBP5 and PTGES3 Appear to Associate with Vif-CRL Complex for SIVmac but not FIV Vif

(A) SDS-PAGE silver stained gel showing Flag purification of either FKBP5-3xFlag or PTGES3-3xFlag co-expressed with either an empty vector control, FIV Vif-2xStrep, or SIVmac Vif-2xStrep. Each doublet are replicates of the same condition.

(B) Immunoblot of affinity purification experiment shown in **A**.

(C) SDS-PAGE silver stained gel showing tandem affinity purification of FKBP5-3xFlag or PTGES3-3xFlag with either FIV Vif-2xStrep or SIVmac Vif-2xStrep. e.v.: empty vector; FK: FKBP5-3xFlag; PTS3: PTGES3-3xFlag; F: Flag; S: Strep.

(D) Mass spectrometry results from tandem affinity purification shown in **C**. Numbers indicate spectral counts detected by mass spectrometer.

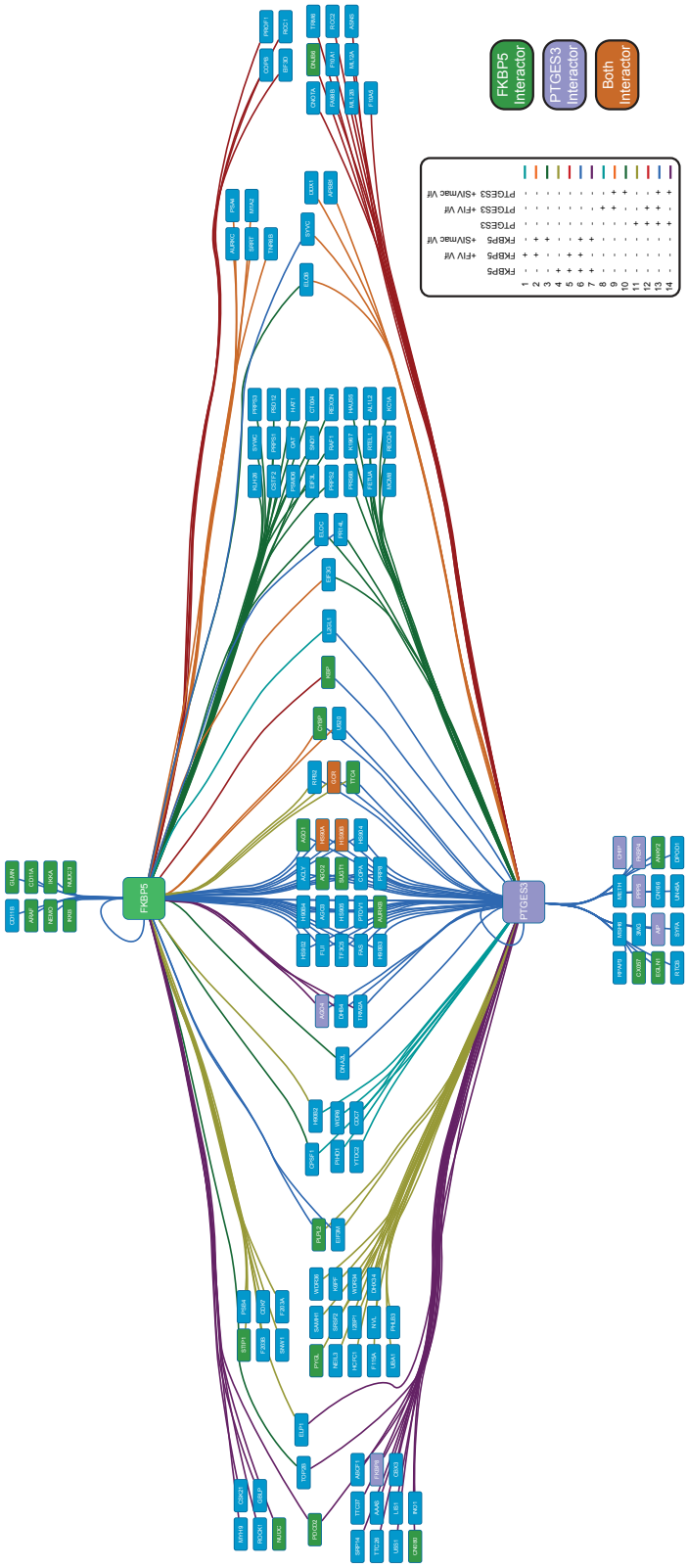
FKBP5 Interactor
PTGES3 Interactor
Both Interactor
FKBP5
FKBP5 +FLV Vif
FKBP5 +SIVmac Vif
PTGES3
PTGES3 +FLV Vif
PTGES3 +SIVmac Vif
FKBP5
PTGES3

Figure 5.7

Figure 5.7: Interaction Map of SAINT-Scored FKBP5-Vif and PTGES3-Vif AP-MS Data

Interaction map of AP-MS data generated from affinity purification shown in **Figure 5.6A-B**. Data is shown for interacting proteins with SAINT scores ≥ 0.8. Edges are color-coded to indicate which dataset they were discovered in. Nodes colored in green, purple, or orange indicate previously reported interactions in BioGrid for FKBP5, PTGES3, or both proteins, respectively.

Figure 5.8

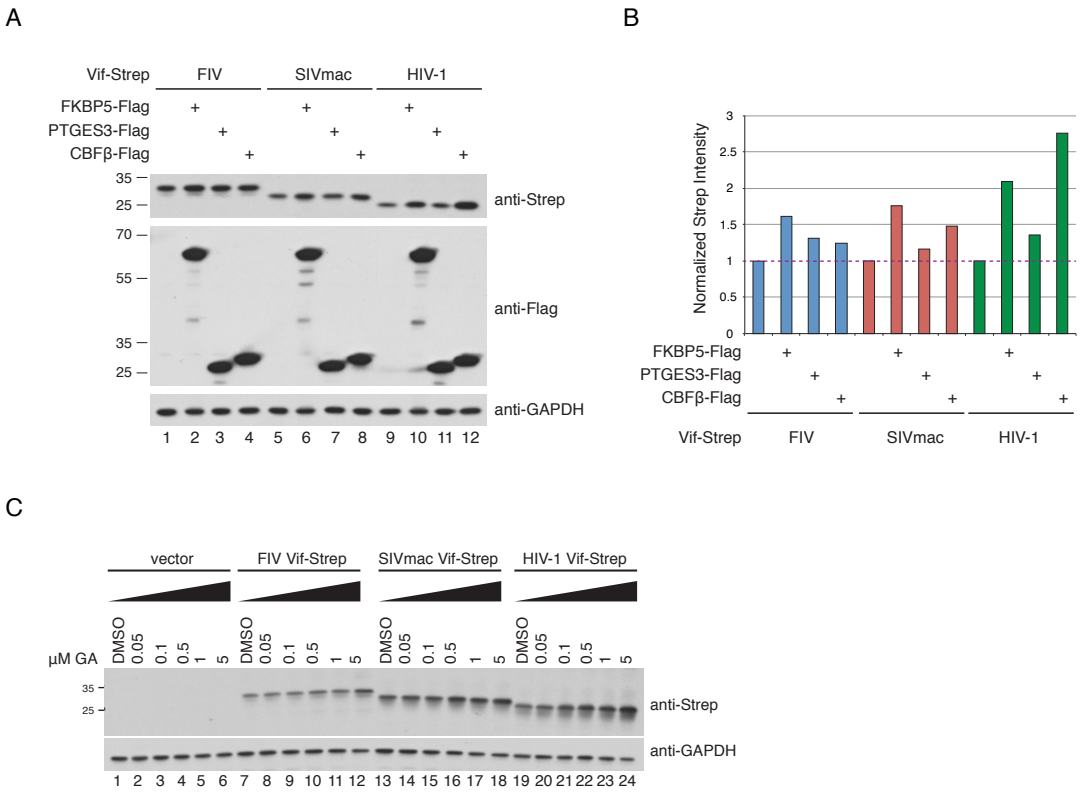
A
Vif-Strep
FIV
SIVmac
HIV-1
FKBP5-Flag
PTGES3-Flag
CBFβ-Flag
35
25
70
55
35
25
anti-Strep
anti-Flag
anti-GAPDH
1 2 3 4 5 6 7 8 9 10 11 12
B
Normalized Strep Intensity
3
2.5
2
1.5
1
0.5
0
FKBP5-Flag
PTGES3-Flag
CBFβ-Flag
Vif-Strep
FIV
SIVmac
HIV-1
C
vector
FIV Vif-Strep
SIVmac Vif-Strep
HIV-1 Vif-Strep
μM GA
DMSO
0.05
0.1
0.5
1
5
35
25
anti-Strep
anti-GAPDH
1 2 3 4 5 6 7 8 9 10 11 12 13 14 15 16 17 18 19 20 21 22 23 24

Figure 5.8: Effects of FKBP5 and PTGES3 on Vif Stability

(A) Vif-host factor stability assay. 3xFlag host factors are overexpressed in the presence of either FIV, SIVmac, or HIV-1 Vif-2xStrep in HEK293T cells. Protein stability is assessed by immunoblot.

(B) Quantification of Vif expression in **D**. Strep band intensities are normalized to GAPDH signal then to Vif co-expressed with vector control.

(C) Testing the requirement of HSP90 for Vif expression. HEK293T cells were transfected with FIV, SIVmac, or HIV-1 Vif-2xStrep and treated with a titration of the HSP90 inhibitor geldanamycin (GA). Vif expression is measured by immunoblot.

Chapter 6: Conclusions

Viruses are obligate intra-cellular parasites that must overcome multiple barriers to infection in order to successfully complete their lifecycles. These barriers include not only successfully carrying out the complex biochemical processes of the viral lifecycle, including viral fusion and entry into host cells, genome replication, expression of viral genes and viral protein synthesis, assembly of viral factors at cell membranes, and budding of matured, infectious particles, but also host defined barriers to viral replication. These barriers can originate from both the innate immune system in the form of restriction factors and virus-detecting receptors (Douville and Hiscott, 2010; Kawai and Akira, 2006), and from the adaptive immune system (Bowen and Walker, 2005; McMichael et al., 2010; McNab et al., 2015). One of these barriers is presented by the APOBEC3 family of anti-viral proteins, which inhibit viral infections by antagonizing viral genome replication through cytosine deamination of viral DNA and interference with viral polymerase processivity (Harris and Dudley, 2015).

The retrovirus family infects a diverse set of mammalian hosts, with each viral lineage required to evolve a mechanism to nullify the host barrier to infection presented by APOBEC3 proteins in order to remain viable. Most lentiviruses use the protein Vif to target APOBEC3 proteins for proteasomal degradation (LaRue et al., 2010; Sheehy et al., 2002; Yu et al., 2003). Foamy viruses sequester APOBEC3 proteins away from virions using the protein Bet (Löchelt et al., 2005). MuLV and HTLV-1 block APOBEC3 packaging by masking interfaces the host factors recognize in the virions (Derse et al., 2007; Doehle et al., 2005). This viral diversity to solve a host barrier to infection extends even into the *Lentivirus* genus, with the equine infectious anemia virus (EIAV) having evolved a Vif-independent, non-degrading mechanism of escaping APOBEC3 restriction (Bogerd et al., 2008).

As the activity of Vif proteins across the Lentivirus genus, that of APOBEC3 antagonism through mediation of poly-ubiquitylation and subsequent proteasomal degradation, was observed to be conserved (LaRue et al., 2010), an assumption was generally made that the core modules facilitating this activity would be conserved as well. Early on in the discovery of Vif-host interactions, recognition that a host CRL complex associated with Vif proteins from multiple lentiviruses was established, with some debate about whether the make-up of these CRL complexes involved CUL2 or CUL5 (Luo et al., 2005). This was not an unreasonable model to have, as recent research into genome evolution has shown many complexes form conserved evolutionary units over time (Beltrao et al., 2010; Roguev et al., 2008; Ryan et al., 2012). In fact, a recent gene-swapping experiment from humans to yeast has shown that nearly 50% of the 400+ human orthologues tested were able to rescue their counterpart knockout in yeast, two species separated by nearly a billion years of evolution (Kachroo et al., 2015). It came then as a great surprise that, through a series of proteomic, virological, biochemical and structural approaches targeting five evolutionarily distinct lentiviral Vif proteins from HIV-1, SIVmac, MVV, BIV and FIV, we discovered lineage-specific non-canonical host factor interactions that show a great plasticity to the biochemical requirements of Vif-CRL assembly and activity, even though, consistent with the original model, all show strong and conserved interactions with CRL proteins. These acquisition events of non-canonical cofactors may be a form of exaptation, where a novel biological function evolves from an existing one (Gould and Vrba, 1982); in this case, by including additional factors in hijacked CRL complexes, Vif may be able to exert influence on multiple pathways simultaneously; a type of viral-host interaction pleiotropy.

HIV-1 Vif potentially exhibits pleiotropy by hijacking a host CRL complex to target host anti-viral APOBEC3 proteins for proteasomal degradation, through recruitment of the

transcriptional activator CBFβ to the same CRL complex. HIV-1 Vif is then able to antagonize endogenous CBFβ function, activation of RUNX transcription factors, by a sequestration mechanism, leading to repression of RUNX-mediated gene expression (Kim et al 2013; Klase et al. 2014). A pleotropic mechanism through host factor sequestration is not unique to Vif in HIV-1 biology. The HIV-1 accessory factor Vpu, which hijacks the Cul1-Skp1-βTrCP (CRL1$^{\beta TrCP}$) complex to mediate the ubiquitylation of the T-cell receptor CD4 and the restriction factor Tetherin (Dubé et al., 2010), also utilizes a sequestration mechanism with the βTrCP subunit. βTrCP plays an important role in NF-κB signaling by targeting the NF-κB inhibitor IκBα for ubiquitylation and subsequent proteasomal degradation (Rahman and McFadden, 2011). By sequestering βTrCP, Vpu blocks NF-κB signaling and the subsequent innate immune response (Sauter et al., 2015). A similar mechanism of sequestering βTrCP by hijacking the CRL1$^{\beta TrCP}$ complex is observed with Vaccinia Virus (VacV) A49 as well (Mansur et al., 2013), although the substrate(s) of the VACV A49-CRL1$^{\beta TrCP}$ complex have not been identified. Curiously, unlike the Vpu and A49 examples where the endogenous CRL1$^{\beta TrCP}$ complex is stabilized to the point of βTrCP sequestration, the Vif-CBFβ is an additive interaction as CBFβ is only a stoichiometric member of the CRL in the presence of Vif (Jäger et al., 2012b).

Although the interaction between HIV-1 Vif and CBFβ can now be associated with a RUNX antagonism activity, this does not necessarily indicate that said activity was the driving force for the acquisition of CBFβ as a primate lentiviral Vif non-canonical cofactor. There are inconsistences with this hypothesis, namely our own observations that CBFβ appeared neither necessary nor sufficient for Vif proteins to exhibit RUNX1 antagonism as assessed by T-bet expression during T-cell activation. HIV-1 Vif underwent dramatic change in its recent evolution relative to other primate lentiviruses, where a deletion and overprinting event created a novel C-terminus for the protein in the evolution of the inferred HIV-1 progenitor virus, the

chimpanzee-infecting SIVcpz (Etienne et al., 2013); this may have led to novel activities of HIV-1 Vif that include the RUNX1 antagonism. The observation of primate-infecting lentiviral Vif proteins interacting with CBFβ concomitant with an expansion of the APOBEC3 family in primate genomes has led some to speculate that the selective pressure to neutralize a greater number of substrates drove Vif acquisition of CBFβ (Ai et al., 2014). While compelling, this model fails to explain the acquisition of MVV Vif and CYPA, as the number of *Apobec3* genes in ovine genomes is identical to those in the bovine genome (LaRue et al., 2008), and BIV Vif does not require a non-canonical cofactor for activity. However, a generalized model of this is one where cofactors increase the substrate repertoire of Vif proteins. One manner in which this could occur is by expanding the substrate binding surface as is observed with the interaction of SIV / HIV-2 Vpx proteins and the host factor DCAF1 to target the restriction factor SAMHD1 (Schwefel et al., 2014, 2015). This model may be tested by structural analysis, if one can demonstrate non-canonical cofactors play a direct role in binding APOBEC3, or potentially novel, substrates. Another model is one where non-canonical cofactors increase the "evolvability" of Vif by allowing Vif proteins to sample mutations that would otherwise compromise the structure or activity of Vif proteins. This would allow for greater diversity of Vif sequences in a given viral population, increasing the likelihood a Vif protein would recognize different APOBEC3 haplotypes (Binka et al., 2012; Ooms et al., 2013), non-host APOBEC3 orthologues (LaRue et al., 2010; Sharp and Hahn, 2011; Xu et al., 2004), or potentially recognition of novel substrates that lead to an increase in viral fitness.

This work helps to establish the stability of viral-host interactions over the evolution of a well-studied viral genus. While other studies have been performed comparing viral protein function between viral strains (Ayllon et al., 2012; Greninger et al., 2012, 2013; White et al., 2014, 2012), the scope, depth, and inter-disciplinary methodologies of this study revealed an

unexpected dichotomy in Vif biology – one that consists of strong conservation of APOBEC3 antagonism through a hijacked host CRL complex complemented with high plasticity in viral-protein interactions. Future research investigating the consequences of non-canonical cofactor acquisition may lead to answers about the evolutionary forces that drive the acquisitions. Given the large about of data generated in this study, much follow-up work remains to be performed in this biochemical dance of virus and host.

i

Chapter 7: Experimental Procedures

Expression Constructs

HIV-1_{LAI}, SIV_{mac239}, BIV, FIV, and MVV Vif constructs with C-terminal Myc tags in pVR1012 (Vical Co.) have been reported previously (LaRue et al., 2010). All but HIV-1_{LAI} sequence were subcloned into pcDNA4/TO expression vectors (Invitrogen) using the restriction sites HindIII / ApaI to match HIV-1_{NL4-3} Vif plasmids used in previous affinity purification / mass spectrometry (AP-MS) studies (Jäger et al., 2012a, 2012b). Human *APOBEC3G*, rhesus *APOBEC3G*, cow *APOBEC3Z2Z3*, cat *APOBEC3Z2Z3*, and sheep *APOBEC3Z2Z3* constructs with C-terminal 3xHA tags in pcDNA3.1(+) (Invitrogen) have been previously reported (Hultquist et al., 2011; LaRue et al., 2008; Stenglein and Harris, 2006). The HIV-1 Capsid construct has been previously reported (Jäger et al., 2012a). The CBFβ complementation construct in pcDNA3.1(+) has been previously reported (Jäger et al., 2012b). *CYPA*, *PTGES3* was cloned from cDNA generated from HEK293T cells and cloned into pcDNA4/TO vector. *FKBP5* was cloned from cDNA generated from Jurkat T-cells cells and cloned into pcDNA4/TO vector. CAEV Vif and MVV Capsid sequences were codon-optimized for human cell expression and synthesized using gBlocks (IDT) from Uniprot entries P33462 and P35955 |144-363, respectively, and subcloned into pcDNA4/TO 2xStrep vectors. See **Table 2**.

Cell Lines

Human Embryonic Kidney (HEK) 293T cells were maintained in high glucose Dulbecco's Modified Eagle Medium (DMEM) containing 10% fetal bovine serum (FBS), 2mM sodium pyruvate, and 1% penicillin/streptomycin (Pen/Strep). CBFβ knockdown HEK293T cells [reported previously (Jäger et al., 2012b)] were maintained in identical conditions. CYPA knockdown 293T cells were maintained in identical conditions, with 0.375 µg / mL puromycin

(Calbiochem) added to maintain shRNA insert. CEM-GFP cells (obtained from the AIDS Research and Reference Reagent Program) were maintained in RPMI with 10% FBS and 0.5% Pen/Strep. Jurkat TRex cells (Invitrogen) were cultured in RPMI-1640 media, 10% FBS, 4 mM glutamine, 1% Pen/Strep, and 10 µg / mL blasticidin (reported previously (Jäger et al., 2012b)). Jurkat E6-1 and Jurkat *CYPA*$^{-/-}$ knockout cells (obtained from the AIDS Research Reagent Program, #177 and #10095, respectively) were maintained in RPMI-1640 media, 10% FBS, 4 mM glutamine, and 1% Pen/Strep. Fetal lamb kidney (FLK) cells were cultured in DMEM high glucose media, 10% FBS, and 1% Pen/Strep. Cell lines were maintained at 37°C and 5% CO_2.

Generation of Stable Jurkat TRex Vif Lines

pcDNA4/TO Vif-3xFlag plasmids (MVV, BIV, FIV, SIVmac) were linearized by digestion with ScaI (NEB). $5x10^6$ Jurkat TRex cells were then electroporated with 20 µg plasmid in 1 mL electroporation buffer (150 mM sucrose, 5 mM potassium phosphate, 25 mM HEPES-KOH, 5 mM $MgCl_2$, 2 mM EDTA, 1% DMSO, 2 mM MgATP, pH 7.4) in a 12-well electroporation plate with a GenePulser MXCell (Bio-Rad) at 250V, 300 µF, and 1000 Ω. Cells were then placed under 300 µg / mL Zeocin (Invitrogen) selection for 3 weeks, then subjected to limiting dilution to generate monoclonal lines.

Affinity Purifications

Affinity purifications (AP) were generally performed as described previously (Jäger et al., 2012a). For affinity purification, $4x10^6$ cells were seeded in 15 cm tissue culture plates and transfected the next day with 5 – 10 µg plasmid using either calcium phosphate (Kingston et al., 2003) or Polyjet transfection reagent (SignaGen). After approx. 42 hours post-transfection, cells were detached using 10 mM EDTA in PBS buffer and rinsed in cold PBS buffer. Stable Jurkat TRex cells were grown in 250 mL media in spinner flasks. $2.5x10^8$ cells were induced with 1 µg / mL doxycycline for 16 hours prior to harvesting by centrifugation for 10 minutes at

4°C at 650 rpm, followed by rinsing in PBS. Cells were lysed in 1 mL cold lysis buffer [150 mM NaCl, 50 mM Tris-HCl, pH 7.4, 1 mM EDTA, 0.5% NP40, protease inhibitor (cOmplete-mini, Roche), phosphatase inhibitor (phosSTOP, Roche)]. Cells were then either allowed to passively lyse on ice for 20 minutes or disrupted using ice-bath sonication, followed by lysate clearing at 2800 RCF for 30 minutes. Cells were then precleared with 70µl agarose mouse IgG beads (Sigma) for Flag APs, or 70 µl sepharose 4B beads (Sigma) for Strep APs for 1 hour. Preclear lysates were then incubated with 35 µl M2 mouse anti-Flag agarose beads (Sigma) for Flag IP or 35 µl StrepTactin beads (IBA) for Strep AP; lysates and beads were rotated for 2 hours at 4°C. Beads were rinsed 3x times with wash buffer (150 mM NaCl, 50 mM Tris-HCl, pH 7.4, 1 mM EDTA, 0.05% NP40), followed by 1x rinse with wash buffer without detergent. Proteins were eluted with 40 µl elution buffer [150 mM NaCl, 50 mM Tris-HCl, pH 7.4, 1 mM EDTA; for Flag elutions, 0.05% RapiGest (Waters) and 0.1 mg / mL 3xFlag peptide (Elimbio); for Strep elutions, 2.5 mM D-desthiobiotin (IBA)]. 4 µl of the eluate were analyzed by 4-20% SDS-PAGE (Bio-Rad) followed by silver stain (Thermo).

Immunoblotting

6x sample buffer (Morganville Scientific, 9% 2-mercaptoethanol added fresh) was added to samples prior to boiling for 5-10 minutes at 95°, and diluted with 1x sample buffer if samples were concentrated or dilutions previously calculated by BCA Assay (Thermo). SDS-PAGE was performed with denatured samples were run on 4-12% NuPAGE gels in MOPS SDS running buffer (Invitrogen) at 170V for approximately 1 hr. Samples were transferred to either PVDF or nitrocellulose (Bio-Rad) in 48 mM Tris base, 39 mM glycine, 20% methanol at 100V for 60-90 minutes. Membranes were blocked in 5% BSA in TBS, 0.1% Tween-20 for 30 minutes. Immunoblotting was performed with the following antibodies: HA (H3663, Sigma), Gapdh (#2118, CST), Strep (#34850, Qiagen), ELOB (ab154854, Abcam), ELOC (#610760, BD

Transduction Laboratories), CUL2 (A302-476A, Bethyl), CUL5 (A302-173A, Bethyl), Flag (F7425, A8592, Sigma), CBFβ (sc-56751, SCBT), CYPA (ab41684, Abcam), GFP (kind gift of Dr. Andrew A. Peden, University of Sheffield). Immunoreactive bands were detected either by chemiluminescence (Pierce; Amersham) using anti-mouse or anti-rabbit horseradish peroxidase (HRP) conjugated secondary antibodies (Bio-Rad), or quantitatively by digital infrared scanner (LI-COR) using anti-mouse or anti-rabbit fluorophore-conjugated secondary antibodies (LI-COR). Quantitative immunoblotting bands were quantified using ImageJ software (Rasband, 2007). For infectivity assays, cell lysates were prepared by resuspension of washed cell pellets directly in 2.5x Laemmli Sample Buffer (32.5mM Tris pH 6.8, 10% glycerol, 1.0% SDS, 2.5% 2-mercaptoethanol, 0.05% bromophenol blue), and homogenization at 95°C for 30 minutes. Virus-like particles were isolated from culture supernatants by purification through 0.45 μm PVDF filters (Millipore) followed by centrifugation (13,000 rpm for 2 hours) through a 20% sucrose, 1x PBS cushion and lysis directly in 2.5x Laemmli Sample Buffer. Samples were run on 12.5% Tris-HCl SDS-PAGE resolving gels with 4% stacking gels each at a 37.5 acrylamide : 1 bis-acrylamide ratio (Bio-Rad Criterion) at 150V for 90 minutes. Proteins were transferred to PVDF membranes by methanol-based electrotransfer (Bio-Rad Criterion Blotter) at 90V for 2 hours. Membranes were blocked in 4% Milk in PBS, 0.1% Tween-20 overnight prior to overnight incubation with primary antibody against HA to detect HA-tagged APOBEC3 (HA.11; Covance), Myc to detect Myc-tagged Vif (9E10; Sigma), to detect CBFβ complementation (T1832; Epitomics), TUB (tubulin; Covance), or p24/capsid (NIH ARRRP 3537 courtesy of B. Chesebro and K. Wehrly). Anti-mouse and anti-rabbit horseradish peroxidase (HRP)-conjugated secondary antibodies (Bio-Rad) were detected using Hyglo HRP detection reagents (Denville Scientific). Blots were incubated in a 1xPBS, 0.2M glycine, 1.0% SDS, 1.0% Tween-20, pH 2.2 stripping buffer before reprobing.

Tandem Affinity Purification

Four 15 cm plates per transfection were seeded with $4x10^6$ HEK293T cells, followed by a next day transfection of 5 – 10 µg plasmid per plate using Polyjet transfection reagent (SignaGen). 42 hours later, cells were harvested using 10 mM EDTA / PBS and pooled. Cells were pelleted at 400 RCF at 4°C for 5 minutes and resuspended by gentle pipetting in 6 mL lysis buffer [150 mM NaCl, 50 mM Tris-HCl, pH 7.4, 1 mM EDTA, 0.5% NP40, protease inhibitor (cOmplete-mini, Roche), phosphatase inhibitor (phosSTOP, Roche)] and passively lysed by rotating at 4°C for 20 minutes. Lysates were cleared with 2800 RCF, 45 minute, 4°C centrifugation. Cleared lysate was incubated with 120 µl StrepTactin beads for 3 hours rotating at 4°C. Beads were washed 3x with wash buffer (150 mM NaCl, 50 mM Tris-HCl, pH 7.4, 1 mM EDTA, 0.1% NP40), and eluted in 200 µl Strep elution buffer [150 mM NaCl, 50 mM Tris-HCl, pH 7.4, 1 mM EDTA, 2.5 mM D-desthiobiotin (IBA)] for 30 minutes at 4°C. Strep AP eluates were then incubated with 20 µl M2 magnetic anti-Flag beads (Sigma) overnight. Flag beads were washed 3x with wash buffer (described previously) and 2x in wash buffer with no detergent. Proteins were eluted in 40 µl Flag elution buffer [150 mM NaCl, 50 mM Tris-HCl, pH 7.4, 1 mM EDTA, 0.05% RapiGest (Waters) and 0.1 mg / mL 3xFlag peptide (Elimbio)]. Eluates were analyzed by immunoblotting and mass spectrometry as described.

Mass spectrometry analysis

Purified proteins eluates were digested with trypsin for LC-MS/MS analysis. Samples were denatured and reduced in 2M urea, 10 mM NH_4HCO_3, 2 mM DTT for 30 minutes at 60°C, then alkylated with 2 mM iodoacetamide for 45 at room temperature. Trypsin (Promega) was added at a 1:100 enzyme:substrate ratio and digested overnight at 37°C. Following digestion, samples were concentrated using C18 ZipTips (Millipore) according to the manufacturer's specifications. Digested peptide mixtures were analyzed by LC-MS/MS on either a Thermo

Scientific Velos Pro or a Thermo Scientific LTQ XL ion trap mass spectrometry system equipped with a Proxeon Easy nLC high pressure liquid chromatography and autosampler system. Samples were injected onto a pre-column (2 cm x 100 um I.D. packed with ReproSil Pur C18 AQ 5um particles) in 0.1% formic acid and then separated with a two-hour gradient from 5% to 30% ACN in 0.1% formic acid on an analytical column (10 cm x 75 um I.D. packed with ReproSil Pur C18 AQ 3 um particles). The mass spectrometer collected data in a data-dependent fashion, collecting one full scan followed by 20 collision-induced dissociation MS/MS scans of the 20 most intense peaks from the full scan. Dynamic exclusion was enabled for 30 seconds with a repeat count of 1. The results raw data was matched to protein sequences by the Protein Prospector algorithm. Data were searched against a database containing SwissProt Human protein sequences (downloaded March 6, 2012) and lentivirus sequences, concatenated to a decoy database where each sequence was randomized in order to estimate the false positive rate. The searches considered a precursor mass tolerance of 1 Da and fragment ion tolerances of 0.8 Da, and considered variable modifications for protein N-terminal acetylation, protein N-terminal acetylation and oxidation, glutamine to pyroglutamate conversion for peptide N-terminal glutamine residues, protein N-terminal methionine loss, protein N-terminal acetylation and methionine loss, and methionine oxidation, and constant modification for carbamidomethyl cysteine. Prospector data was filtered using a maximum protein expectation value of 0.01 and a maximum peptide expectation value of 0.05.

Mass Spectrometry Data Analysis

Interactions were scored using the SAINT algorithm (Choi et al., 2011) with prey identified spectral counts, using empty vector and HIV-1 Nef transfections as negative controls; for Jurkat T-cell data, reference Jurkat cells AP-MS results were also included. A threshold SAINT probability ≥ 0.9 for at least one bait-prey interaction was set the cut-off for prey inclusion in

the final dataset. Data was hierarchically clustered by correlation using the Cluster3 program (de Hoon et al., 2004) and visualized using the Java TreeView program (Saldanha, 2004).

HIV-1 Single Cycle Assay with Replication Proficient Virus

At 50% confluency, CBFβ knockdown HEK293T cells were transfected (TransIt, Mirus) with 1 mg Vif-deficient ($X_{26}X_{27}$) HIV-1_{IIIB} A200C proviral construct (Haché et al., 2008) in the presence or absence of 50 ng of the indicated C-terminal HA-tagged APOBEC3 expression construct, 25 ng of the species cognate C-terminal Myc-tagged Vif expression construct, and 50 ng untagged human CBFβ. After 48 hours to allow for virus production, portions of the virus-containing supernatants were used to infect 25,000 CEM-GFP cells in 96-well plates to titer. The rest of the viral supernatant and the cells were processed for immunoblotting. After another 48 hours, the CEM-GFP cells were fixed in 4% paraformaldehyde and GFP positive cells quantified by flow cytometry (see below). Data was normalized to the no A3, no Vif, no CBFβ control for each species as 100% infectivity.

Flow Cytometry

HIV-1-infected CEM-GFP cells were prepared for flow cytometry by fixation in 4% paraformaldehyde, 1x PBS. GFP fluorescence was measured on a Becton Dickinson FACS Canto II flow cytometer. All data was analyzed using FlowJo Flow Cytometry Analysis Software (Version 8.8.6). Quantification was done by first gating the live cell population, followed by gating on the GFP^+ cells.

Vif Site-Directed Mutagenesis

BC-mutant proteins were generated using site-directed mutagenesis via a quick-change PCR (QC-PCR) protocol. pcDNA4/TO Vif-2xStrepII plasmids were amplified using PfuUltra (Agilent)

and primers targeting Vif BC-box S/TLQ motifs (Suppl. Figure 1B). Products were DpnI (NEB) digested then transformed into Top10 cells (Invitrogen). See Table 3.

For MVV Vif proline-to-alanine mutants, the same QC-PCR protocol was used with the pcDNA4/TO MVV Vif-2xStrep template. See Table 3.

Generation of CYPA Mutants

Following the same protocol as with Vif site-directed mutagenesis, we generated CYPA active-site point mutants R55K, F113W, and H126A. See Table 3. To generate shRNA resistant constructs in order to perform rescue experiments in CYPA knockdown background, we targeted the region in CYPA CDS targeted by the shRNA used in the monoclonal knockdown line (#49277; 349-GCCAAGACTGAGTGGTTGGAT-369). See Table 3.

Generation of CYPA Knockdown Lines

Lentiviruses were generated using HEK293T cells. Cells were transfected in 6-well format with pCMV-VSV-G, pCMV-dR8.91, and pLKO.1 lentivirus vector using Polyjet transfection reagent (SignaGen). Lentiviruses were titered, polybrene added to increase transduction efficiency, and HEK293T cells were transduced with lentiviruses expressing either an shRNA against CYPA (TRCN0000049271; TRCN0000049277) or a scrambled control (SHC002; Sigma), and subjected to puromycin selection. Verification of knockdown was assessed by immunoblotting. A monoclonal line was generated from the TRCN0000049277 transduced cells by limiting dilution.

CYPA Co-Immunoprecipitation Assays

$5x10^6$ cells were seeded in 6-well plates and transfected the following day with 0.5 µg CYPA-3xFlag and 1 µg MVV Vif-2xStrepII constructs. 42 hours post-transfection, cells were harvested and Strep AP performed as described above using 10 µl StrepTactin beads and a 2 hour

incubation at 4°C, eluting in 20 µl Strep elution buffer [150 mM NaCl, 50 mM Tris-HCl, pH 7.4, 1 mM EDTA, 2.5 mM D-desthiobiotin (IBA)].

Cyclosporine A Affinity Purification Assays

Approximately $5x10^6$ HEK293T cells were seeded in 15 cm plates, and transfected the next day with 7.5 µg MVV Vif-2xStrepII constructs or a vector control using calcium phosphate precipitation. 4-6 hours post-transfection, media was replaced with fresh media containing either ethanol or appropriate concentration of cyclosporine A (CsA) (#9973, CST). 24 hours post-transfection, cells were harvested and Strep AP performed as described, with ethanol or CsA was added to lysis buffer of appropriate samples to prevent washing out of CsA and re-association of MVV Vif-CYPA complexes *ex vivo*.

Cyclosporine A – APOBEC3 Degradation Assays

$2.5x10^5$ HEK293T cells were seeded in 12-well plates and transfected the following day with 200 ng of pcDNA3.1-OaA3Z2Z3-3xHA and 100 ng pcDNA4/TO-MVV-Vif-2xStrep constructs using Polyjet transfection reagent (SignaGen); for control experiments, 200 ng pcDNA3.1-Hs-A3G-3xHA and 20 ng pcDNA4/TO-HIV1-Vif-2xStrep constructs were used. 6 hours post-transfection, cells were treated with cyclosporine A (#9973, CST) or ethanol. 25 hours post-transfection, cells were harvested and lysed in RIPA buffer [150 mM NaCl, 50 mM Tris-HCl pH 7.4, 1 mM EDTA, 1% NP40, 0.5% sodium deoxycholate, 0.1% SDS, protease inhibitor (cOmplete-mini, Roche), phosphatase inhibitor (phosSTOP, Roche)]. Cells were lysed for 20 minutes on ice followed by 20,000 RCF, 4°C, 5 minutes lysate clearing. Prior to adding 6x sample buffer, a BCA assay (Thermo) was performed to calculate protein concentration using a bovine serum albumin standard. Supernatant was boiled in sample buffer and 4-12% SDS-PAGE (Invitrogen) was performed loading approx. 4 µg of protein per sample, followed by transfer to nitrocellulose membrane (Bio-Rad). HA immunoreactivity bands were measured

quantitatively by digital infrared scanner (LI-COR), then normalized by GAPDH, and these values were normalized to no Vif controls for each line (A3-3xHA alone). Additional immunoprobing of membranes (Strep, CYPA) were developed by chemiluminescence.

Jurkat Nucleofections

Jurkat E6-1 and *CYPA*$^{-/-}$ knockout lines were transfected using the Lonza nucleofection kit (Cell Line Nucleofector V, Lonza) and following their Jurkat optimized protocol (X-005). Briefly, 1x10^{6} Jurkat cells were pelleted at 500 rpm for 10 minutes at room temperature, then resuspended in nucleofection reagent. 2 µg of DNA was then added to the resuspended cells, and cells were nucleofected using the X-005 protocol, incubated with DNA and reagent for 10 minutes, and resuspended in 0.5 mL pre-warmed media and added to 12-well plate well containing 1 mL pre-warmed media. Cells were harvested approximately 40 hours post-nucleofection.

Jurkat CYPA Knockout APOBEC3 Degradation and Rescue Assays

Jurkat E6-1 or *CYPA*$^{-/-}$ knockout lines were transfected with 1 µg OaA3Z2Z3-3xHA, HsA3G-3xHA, or vector; 0.4 µg MVV Vif-2xStrep, 0.2 µg HIV-1 Vif-2xStrep, or vector; 0.5 µg CYPA-3xFlag or vector; 0.1 µg eGFP; and vector to total 2 µg per nucleofection. Cells were harvested approximately 40 hours post-nucleofection, pelleted at 400 RCF for 10 minutes at room temperature, and lysed in 50 µl 1x sample buffer (Morganville Scientific) and boiled for 30 minutes prior to SDS-PAGE and subsequent immunoblotting. CYPA rescue experiments were performed with 0.5 µg of either wild-type, R55K, F113W, or H126A CYPA-3xFlag; mutants were generated as described previously.

CYPA Monoclonal Knockdown Rescue Assay

2x10^{5} monoclonal CYPA knockdown line (shRNA TRCN0000049277) in 293T background cells were seeded per well in a 12-well plate (Costar). 24 hours later, cells were transfected with 200

ng OaA3Z2Z3-3xHA plasmid or vector; 25 ng MVV Vif-2xStrep or vector; and 250 ng wild-type, R55K, F113W, or H126A shRNA-resistant CYPA-3xFlag or vector using Polyjet transfection reagent (SignaGen). Cells were harvested 24 hours later, lysed in RIPA buffer (150 mM NaCl, 50 mM Tris-HCl, pH 7.4, 1 mM EDTA, 1% NP40, 0.5% Sodium Deoxycholate, 0.1% SDS), and lysates subjected to SDS-PAGE.

Recombinant Protein Expression Vectors

Cow and sheep A3Z3 genes have been described (Jónsson et al., 2006; LaRue et al., 2008, 2010). The cDNA were PCR amplified with following primers: cow A3Z3, forward 5'-nnnnGAATTCGCCACCATGACCGAGGGCTGG -3', reverse 5'-nnnnAAGCTT AATTGGGGCCGTTAG-3'; sheep A3Z3, forward 5'-nnnnGAATTCGCCACCATGACGGAGGGCTGG-3', reverse 5'-nnnnAAGCTTAGTCGGCGCCGTCAG-3'. The PCR products were digested with EcoRI and HindIII, gel-purified and inserted into eukaryotic expression vector pcDNA3.1-Myc-His (Invitrogen) digested with the same enzymes.

APOBEC3 Protein Purification

A3Z3-Myc-His proteins were purified with previously described protocol (Li et al., 2012; Nowarski et al., 2008; Stenglein et al., 2010). Briefly, $1x10^8$ of HEK-293T cells transiently transfected with pcDNA3.1-BtA3Z3-myc-His or pcDNA3.1-OaA3Z3-Myc-His were harvested, washed with PBS and resuspended in 10ml of cell lysis buffer (25mM HEPES, pH7.4, 150mM NaCl, 0.5% Triton X-100, 1mM EDTA, 1mM $MgCl_2$, 1mM $ZnCl_2$, 10% Glycerol, Roche EDTA-free complete protease inhibitor cocktail) supplemented with 50 μg/ml RNase A (Qiagen). The cell suspension was incubated on ice for 1 hour with periodic vortexing, followed by incubation at 25°C for 20 min. The lysates were then clarified by centrifugation (12,000g, 4°C, 10 min). NaCl was added to the lysates to bring the final concentration to 0.8 M. The lysates were then

mixed with 50 µl Ni-NTA agarose (Qiagen) by rotating over night at 4˚C. The suspension was then loaded onto a Poly-Prep chromatography column (Bio-Rad). Following extensive washing with wash buffer (50 mM Tris, pH 8.0, 0.3 M NaCl, 10% glycerol, 0.5% Triton X-100, 50 mM imidazole), each A3-Myc-His protein was eluted with elution buffer (50 mM Tris, pH 8.0, 0.3 M NaCl, 10% glycerol, 0.5% Triton X-100, 250 mM imidazole). Protein purity was assessed by SDS-PAGE and Coomassie blue R250 staining. Protein concentration was determined by densitometry compared to bovine serum albumin standards and by the Bradford assay (Bio-Rad).

Cullin Ligase Protein Expression and Purification

Vif complexes for *in vitro* work were produced by coexpression in BL21-Star(DE3)pLysS cells. For trimers (Vif-ELOB-ELOC), Vif was expressed from a pET28a-derived vector as a fusion protein with an N-terminal 6xHis-GST tag. For tetramers (Vif-CYPA/CBFβ-ELOB-ELOC), a pETDuet vector was used that encoded both untagged Vif and either CYPA or CBFβ as a fusion protein with an N-terminal 6xHis-TRX tag. All tags were removed by cleavage with TEV protease as a purification step. A previously described pCDFDuet vector encoding both ElonginB and ElonginC was used in all cases (Kim et. al 2013). All protein expression was induced at OD~1.0 at a temperature of 16°C, and allowed to proceed for 15-18 hours. Cells were harvested by centrifugation, and washed once with 1X PBS. Washed cell pellets were immediately flash frozen and stored at -20°C. Cells were resuspended in roughly 20 mL lysis buffer (25 mM HEPES pH 7.5, 0.5 M NaCl, 5% glycerol, 20 mM imidazole, 2mM DTT) per liter of cell culture, and lysed by sonication. Cell debris was pelleted by centrifugation at 16,000 RCF for 40 minutes, and the resulting supernatant was loaded onto a 5 mL NiNTA HisTrap column (GE Healthcare). Following extensive washing with lysis buffer, bound proteins were eluted by an imidazole gradient. At this stage fusion tags were removed by incubation with TEV

protease, and further purified by a combination of heparin affinity and/or size exclusion chromatography. A notable exception was the purification of the MVV Vif tetrameric complex, in which heparin affinity chromatography was performed immediately after the NiNTA step, in order to isolate tetrameric complex from the large excess of free TRX-CYPA. E3 ligase complexes were assembled by mixing an excess of Vif subcomplexes with CUL5-RBX2, followed by size exclusion chromatography to isolate the resultant pentamer or hexamer. All purifications were finished by size exclusion chromatography into a final buffer of 25 mM HEPES pH 7.5, 0.3 M NaCl, 5% glycerol, 2mM DTT. CUL5-RBX2, and all ubiquitin and Nedd8 pathway components used in ubiquitylation assays were obtained as previously described (Stanley et al., 2012).

In vitro ubiquitylation assays

Assays for ubiquitylation activity of reconstituted Vif E3 ligases were initiated out by mixing together separate NEDD8-charging and ubiquitin-charging reactions with myc-tagged APOBEC3 substrate. Prior to mixing, the charging reactions were incubated at room temperature for 30 minutes to fully charge E2 enzymes and fully NEDD8ylate E3s. This final mixture contained the following components in a buffer of 25 mM HEPES pH 7.5, 50 mM NaCl, 2.5 mM $MgCl_2$: 50 nM NAE1, 5 μM UBE2F, 12.5 μM NEDD8, 300 nM Vif E3, 50 nM UBE1, 5 μM UBE2R1, 12.5 μM UBIQUITIN, 2 mM ATP, 1 mg/mL BSA. The reaction was allowed to incubate at room temperature for 2 hours, and stopped with SDS-PAGE loading dye and heat denaturation. Reaction products were visualized by immunoblotting with an anti-c-Myc mAb (M4439, Sigma).

Small-angle X-ray Scattering

Samples for small-angle X-ray scattering (SAXS) were dialyzed extensively against 20 mM Tris-HCl (pH 8.0), 500 mM NaCl, 10% (w/v) glycerol, and 2 mM TCEP, and filtered through 0.1 μm

membranes (Millipore, Bedford, MA) prior to data collection. SAXS profiles of HIV-1 E3 and MVV E3 were measured at concentrations of 0.5, 1.0, 1.5, 2.0, and 4.4 mg/ml at 10°C, using up to 15, 1 second exposures at Beamline 4-2 of the Stanford Synchrotron Radiation Lightsource (SSRL) in the SLAC National Accelerator Laboratory (Menlo Park, CA). The buffer profile was obtained in the same manner and subtracted from a protein profile. The merged scattering profiles were processed using software in the ATSAS package (Konarev et al., 2006). 20 independent *ab initio* envelopes were generated using DAMMIF (Franke and Svergun, 2009) and consensus models were obtained using DAMAVER (Volkov and Svergun, 2003). The DAMAVER output was refined against using DAMMIN (Svergun, 1999). The final NSD values for the HIV-1 E3 and MVV E3 envelopes were 0.679 and 0.820, respectively. All plots were generated using ORIGIN 8.0 (OriginLab, Northampton, MA), and final SAXS envelopes were draw in Chimera (Pettersen et al., 2004). The HIV E3 atomic resolution model used to fit the SAXS envelopes was constructed based on the HIV-1 Vif, CBFβ, ELOB, ELOC, CUL5 N-terminal crystal structure (PDB ID: 4N9F). The full-length CUL5 model was generated using MODELER (Sali and Blundell, 1993) with HIV-1 Vif complex (PDB ID:4N9F), CUL5 CTD (PDB ID: 2WZK), and full-length Cullin-1 and Cullin-4 (PDB IDs: 1LDJ and 2HYE). The HIV-1 E3 model was further refined using the AllosMod-FoXS server (http://salilab.org/allosmod) (Schneidman-Duhovny et al., 2010; Weinkam et al., 2012) to obtain a model which fit our experimental SAXS profile with a Chi value of 1.89.

Informatics

Percent identity / similarity matrix for Vif proteins used in this study was generated using by the EMBOSS tool Needle (Rice et al., 2000) using the following settings – Gap-open: 8.0, Gap-extend: 0.5, End-open: 10.0, End-extend: 0.5, Matrix: Blosum45. Multiple sequence alignment of Vif sequences was performed using the PSI-Coffee variant of the T-Coffee alignment

algorithm (Notredame et al., 2000) and visualized using JalView (Waterhouse et al., 2009). Lentivirus Gagpol tree was generated from the sequence entries in Uniprot (P05897, P12497, P16087, P16088, P19560, P35955, P35956). Sequences were aligned using PSI-Coffee, curated using Gblocks (Castresana, 2000) on *Phylogeny.fr* (Dereeper et al., 2008), and a maximum likelihood tree with bootstrap values generated using the RAxML Blackbox (Stamatakis et al., 2008). Statistics on MVV KV1772 hypermutation was performed using the statistical software package R (R Core Team, 2014) using a one-sided Wilcoxon Ranked-Sum test.

Construction of mutant viruses

The MVV molecular clone KV1772 is split between two plasmids, p8XSp5-RK1 and p67r, as has been described previously (Skraban et al., 1999). For construction of the single mutants Vif P21A and Vif P24A and the double mutant Vif P21A/P24A, a subclone of p8XSp5-RK1 containing nucleotides 4587-6392 was used for PCR-based mutagenesis. Briefly, complementary oligos containing the respective mutations were used for amplification. The PCR products were treated with DpnI to degrade parental DNA, and transformed into E. coli. The resulting plasmids were cleaved with MluI and BglII and the $MluI_{4680}$ - $BglII_{5841}$ fragment was isolated and exchanged for the equivalent fragment in p8XSp5-RK1. All constructs were verified by DNA sequencing.

For transfections, equimolar quantities of the two plasmids containing the viral genome, a total of 6 µg, were cut with XbaI and ligated. Transfections of primary sheep choroid plexus (SCP) cells were carried out using Lipofectamine 2000 in T25 tissue culture flasks as specified by the manufacturer (Invitrogen). Supernatants were clarified by centrifugation at 3000 rpm for 3 min. and kept at -80°C.

Ovine cells and MVV infections

Primary sheep choroid plexus (SCP) cells were cultured in Dulbecco's modified Eagle's medium supplemented with antibiotics and 10% and 1% lamb serum for growth and maintenance respectively. Sheep blood-derived macrophage cultures were established as described previously (Skraban et al 1999). SCP cells and sheep blood-derived macrophages were infected with RT-normalized wild-type and mutant viruses for spreading infection assays. 500 µl samples were taken every day for Taqman qPCR analysis and replaced by the same volume of fresh medium.

RT assay

Viral particles from 200 µl of cell-free supernatants from infected cells were pelleted at 14,000 rpm for 1 hour in a microfuge. The pelleted virus was resuspended in TNE (10mM Tris-HCl (pH7.5), 100 mM NaCl, 1 mM EDTA) containing 0.1% Triton X-100. RT activity was assayed on a poly (A) template, adding oligo-dT primer and dTTP. The resulting RNA-DNA heteroduplexes were detected by PicoGreen reagent as specified by the manufacturer (Molecular Probes Inc., Eugene, Oregon).

MVV Genome Copy Quantification

Viral particles from 200 µl cell-free supernatants from infected cells were pelleted at 14,000 rpm for 1 hour in a microfuge. The pellet was dissolved in 10 µl TNE (10 mM Tris pH 7.5; 100 mM NaCl; 1 mM EDTA) with 0.1% Triton X-100. This lysate was used for generating cDNA using MultiScribe reverse transcriptase (Applied Biosystems) and a primer from the gag gene (V-1818; 5'-CGGGGTACCTTACAACATAGGGGGCGCGG-3'). Real-time PCR was carried out in a final volume of 20 µl. The primers and Taqman probe were as follows: Forward primer: V1636; 5'-TAAATCAAAAGTGTTATAATTGTGGGA-3', reverse primer: V-1719; 5'-TCCCACAATGATGGCATATTATTC-3', Taqman probe: V1665 Taqman; 5'-FAM-

CCAGGACATCTCGCAAGACAGTGTAGACA-BHQ-1-3'. Calibration curves were derived by running 10-fold dilutions of specific cDNA over the range of 6x10 - $6x10^7$ copies. Each assay included triplicate wells for each dilution of calibration DNA and for each cDNA sample.

MVV Proviral DNA sequence analysis

Genomic DNA was prepared from MVV infected SCP cells using the Gentra Puregene Cell Kit (Qiagen). A 1034 bp fragment from the *env* gene (nt 6911-7945) of integrated proviruses was amplified using Phusion DNA polymerase and treated with Taq DNA polymerase before being cloned into TOPO-TA vectors (Invitrogen). Ten to twenty clones were sequenced for each virus strain. Sequences were analyzed using Sequencher, version 5.0 (Genes Codes Corp.).

NMR

NMR spectra were recorded at 10ºC on a Bruker 800 MHz equipped with a cryogenic probe. A 440 µM sample was prepared in 50 mM phosphate buffer pH 7.0, 10% D_2O. $^{1}H–^{15}N$ HSQC spectra were recorded on CYPA, in presence of increasing amounts of MVV Vif peptide (17-REIGPQLPLW-26) (from 0 to 300 µM, adding 25 µM at a time). All NMR spectra were processed with Topspin3 (Bruker) and analyzed with the CCPN suite (Vranken et al., 2005).

Ubiscan

Ubiscan was performed with Jurkat TRex cells previously described and generally followed the manufacturer protocol (PTMScan Ubiquitin Remnant Motif (K-ε-GG) Kit, CST #5562). Cells were cultured in T175 flasks to a final, harvesting number of 6-8x10^7 cells. Cells were treated for 18 hours with 1 μg / mL doxycycline to induce Vif expression. MG-132 subjected cells were treated with 10 μM MG-132 (Calbiochem) suspended in DMSO for the last 4 hours of doxycycline treatment. Cells were counted, then snap-frozen in liquid nitrogen until ready for use. Cells were lysed by brief sonication in denaturing urea buffer (8M urea, 150 mM NaCl, 100

mM NH_4HCO_3, phosSTOP, mini-c0mplete protease inhibitor cocktail, in HPLC-grade H_2O) on ice. Proteins were then reduced for 30 minutes with 4 mM TCEP, followed by alkylation with 10 mM iodoacetamide for 30 minutes, and quenching of the alkylation reaction with 10 mM DTT, all at room temperature. Protein content measured by Bradford assay, and 10 mg of protein from each sample and diluted with 100 mM NH_4HCO_3 to a final urea concentration of 2M. Trypsin (Promega) was added at a 1:100 enzyme:substrate ratio and samples digested overnight at 37°C. Samples were desalted using C18 ZipTips (Millipore) according to the manufacturer's specifications, then lyophilized for two days. Samples were resuspended at 10 mg / mL in IAP buffer (50 mM MOPS, 10 mM HNa_2PO_4, 50 mM NaCl, pH 7.2 in HPLC-grade water). 80 μl of PTMScan Ubiquitin Branch Motif (K-ε-GG) Immunoaffinity Beads (CST #5562) were added, incubated for 90 minutes at 4°C, then washed three times with IAP buffer. Peptides were eluted using 0.15% Trifluoroacetic acid (TFA, Sigma). Peptides were desalted using custom mini-C18 columns (Millipore). Digested peptide mixtures were analyzed by LC-MS/MS using a Thermo Fisher Orbitrap Elite mass spectrometer.

Ubiscan Data Analysis

MS1 peptide intensities from MaxQuant were analyzed using the MSstats package (Choi et al., 2014), modified using wrappers specifically for Ubiscan data (https://github.com/everschueren/RMSQ/) under the following settings: normalization_method : equalizeMedians; missing_action : impute; interference : 0; scopeOfTechReplication : restricted; scopeOfBioReplication : restricted; equalFeatureVar : 0. Data was stored in an sqlite database, and proteins with log2 fold changes greater than 2 or less than negative 2 and p-values corrected for multiple testing less than 0.001. Data was visualized in R using the gplots and ggplots2 packages (R Core Team, 2014). Gene Ontology (GO) analysis was performed using AmiGO (Carbon et al., 2009) in June 2015.

T-bet Assays

T-bet repression assays were performed with Jurkat TRex cells previously described. Cells were seeded $4x10^5$ cells per mL in 6-well plate format, and treated for 18 hours with 1 μg / mL doxycycline to induce Vif expression. Cells were treated with 50 ng / mL phorbol 12-myristate 13-acetate (PMA) (Sigma, L8902) and 1 μg / mL phytohemagluttinin (PHA) (LC Laboratories, P-1680), or PBS and DMSO, for 6 hours to activate T-cells. Cells were then harvested, lysed in sample buffer, boiled, and analyzed by immunoblot. T-bet (Tbx21) was detected using an endogenous antibody (CST #5214S).

Geldanamycin Treatment Assay

HEK293T cells were seeded in a 24-well plate at a density of $1x10^5$ cells per well. Cells were transfected the following day with either 30 ng of FIV or HIV-1 -2xStrep plasmid, or 150 ng SIVmac Vif-2xStrep plasmid or empty-vector control. 3 hours post-transfection, cells were treated with a titration of geldanamycin (Invivogen, Cat # ant-gl-5) or DMSO. Cells were harvested 24 hours after transfection and analyzed by immunoblot.

Appendix: Supplemental Tables

Table 1: Overview of *Lentiviruses* Examined in this Study

Lentivirus	Strain	Host	Primary Cell Tropism	Disease	Vif Length (a.a.'s)	No. of Host APOBEC3 (Degraded by Vif)
Maedi-Visna Virus (MVV)	Iceland	*Ovis aries*	Monocytes/ Macrophages[a]	Dyspnea, Paraplegia[a]	230	4 (2)[g,h]
Bovine Immunodeficiency Virus (BIV)	p127	*Bos taurus*	Monocytes/ Macrophages[b]	Lymphocytosis, emaciation, CNS lesions[b]	198	4 (2)[g,h]
Feline Immunodeficiency Virus (FIV)	NCSU	*Felis sp.*	T Lymphocytes[c]	AIDS[c]	251	5 (2)[h,i]
Simian Immunodeficiency Virus (SIV)	mac239	*Macaca mulatta*	T Lymphocytes[d]	AIDS[4]	214	7 (5)[h,j]
Human Immunodeficiency Virus 1 (HIV-1)	NL4-3	*Homo sapiens*	T Lymphocytes[e,f]	AIDS[e,f]	192	7 (5)[j,k]

a. (Torsteinsdottir et al., 2007), b. (St-Louis et al., 2004), c. (Ackley et al., 1990), d. (Letvin et al., 1985), e. (Barré-Sinoussi et al., 1983), f. (Gallo et al., 1983), g. (Jónsson et al., 2006), h. (LaRue et al., 2008), i. (Münk et al., 2008), j. (Hultquist et al., 2011), k. (Jarmuz et al., 2002)

Table 2: Plasmids Used in this Study

Name	Plasmid	Resistance	Source	Notes
MVV Vif-2xStrep	pcDNA4/TO	AmpR	R. Harris	Subcloned from LaRue et al., 2010
MVV Vif-3xFlag	pcDNA4/TO	AmpR	R. Harris	Subcloned from LaRue et al., 2010
MVV Vif SLQ::AAA-2xStrep	pcDNA4/TO	AmpR	This study	
MVV Vif P21A-2xStrep	pcDNA4/TO	AmpR	This study	
MVV Vif P24A-2xStrep	pcDNA4/TO	AmpR	This study	
MVV Vif P21A/P24A-2xStrep	pcDNA4/TO	AmpR	This study	
MVV Vif P39A-2xStrep	pcDNA4/TO	AmpR	This study	
MVV Vif P116A-2xStrep	pcDNA4/TO	AmpR	This study	
MVV Vif P171A-2xStrep	pcDNA4/TO	AmpR	This study	
MVV Vif P192A-2xStrep	pcDNA4/TO	AmpR	This study	
MVV Vif P205A-2xStrep	pcDNA4/TO	AmpR	This study	
MVV Vif P210A-2xStrep	pcDNA4/TO	AmpR	This study	
MVV Vif P216A-2xStrep	pcDNA4/TO	AmpR	This study	
BIV Vif-2xStrep	pcDNA4/TO	AmpR	R. Harris	Subcloned from LaRue et al., 2010
BIV Vif-3xFlag	pcDNA4/TO	AmpR	R. Harris	Subcloned from LaRue et al., 2010
BIV Vif SLQ::AAA-2xStrep	pcDNA4/TO	AmpR	This study	
FIV Vif-2xStrep	pcDNA4/TO	AmpR	R. Harris	Subcloned from LaRue et al., 2010
FIV Vif-3xFlag	pcDNA4/TO	AmpR	R. Harris	Subcloned from LaRue et al., 2010
FIV Vif SLQ::AAA-2xStrep	pcDNA4/TO	AmpR	This study	
SIVmac Vif-2xStrep	pcDNA4/TO	AmpR	R. Harris	Subcloned from LaRue et al., 2010
SIVmac Vif-3xFlag	pcDNA4/TO	AmpR	R. Harris	Subcloned from LaRue et al., 2010
SIVmac Vif SLQ::AAA-2xStrep	pcDNA4/TO	AmpR	This study	
HIV-1 Vif-2xStrep	pcDNA4/TO	AmpR	This study	
HIV-1 Vif-2xStrep-3xFlag	pcDNA4/TO	AmpR	stef's paper	
HIV-1 Vif SLQ::AAA-2xStrep	pcDNA4/TO	AmpR	This study	
CBFβ-3xFlag	pcDNA4/TO	AmpR	stef's paper	
CYPA-3xFlag	pcDNA4/TO	AmpR	This study	Cloned as part of Jäger et al., 2012a
CYPA R55K-3xFlag	pcDNA4/TO	AmpR	This study	
CYPA F113W-3xFlag	pcDNA4/TO	AmpR	This study	
CYPA H126A-3xFlag	pcDNA4/TO	AmpR	This study	
PPIAL4G-3xFlag	pcDNA4/TO	AmpR	DNASU	Subcloned into pcDNA4 vector
CYPB-3xFlag	pcDNA4/TO	AmpR	DNASU	Subcloned into pcDNA4 vector

CYPD-3xFlag	pcDNA4/TO	AmpR	DNASU	Subcloned into pcDNA4 vector
FKBP5-3xFlag	pcDNA4/TO	AmpR	This study	
PTGES3-3xFlag	pcDNA4/TO	AmpR	This study	Cloned as part of Jäger et al., 2012a
CUL5-3xFlag	pcDNA4/TO	AmpR	This study	Cloned as part of Jäger et al., 2012a
HIV-1 CA-2xStrep	pcDNA4/TO	AmpR	Jäger et al., 2012a	
MVV CA-2xStrep	pcDNA4/TO	AmpR	This study	
CAEV Vif-2xStrep	pcDNA4/TO	AmpR	This study	
OaA3Z2Z3-3xHA	pcDNA3.1	AmpR	LaRue et al., 2008	
BtA3Z2Z3-3xHA	pcDNA3.1	AmpR	LaRue et al., 2008	
FcA3Z2Z3-3xHA	pcDNA3.1	AmpR	LaRue et al., 2008	
MmA3G-3xHA	pcDNA3.1	AmpR	LaRue et al., 2008	
HsA3G-3xHA	pcDNA3.1	AmpR	LaRue et al., 2008	

Table 3: Primers Used in this Study

Primer	Sequence (5'-to-3')
mvv-vif-qc-slq-fw	TAACCCCAGAGCCGCGGCGAGACTTGCCCTGCTTCACCTCG
mvv-vif-qc-slq-rv	GGGCAAGTCTCGCCGCGGCTCTGGGGTTAGTGTTTTTGAC
biv-vif-qc-slq-fw	CCCACGCCACGCCGCGGCGCGGCTGGCAGCTCTGCAGCTC
biv-vif-qc-slq-rv	CTGCCAGCCGCGCCGCGGCGTGGCGTGGGGTAGAGGTCAG
fiv-vif-qc-tlq-fw	CCCACCACAGGCCGCGGCGCGGCTGGCCATGCTGGCTTGTG
fiv-vif-qc-tlq-rv	TGGCCAGCCGCGCCGCGGCCTGTGGTGGGCTGTTCCGCAG
siv-vif-qc-slq-fw	CCAGGTTCCTGCTGCGGCGTATCTGGCACTCAAAGTCGTTTC
siv-vif-qc-slq-rv	GTGCCAGATACGCCGCAGCAGGAACCTGGTACTTGTGAGC
hiv-qc-slq-fw	CAAGGTCGGGGCCGCGGCGTATCTGGCACTGGCAGCCCTG
hiv-qc-slq-rv	GTGCCAGATACGCCGCGGCCCCGACCTTGTTGTGGCCGGC
mvv-vif-P21A-P24A-fw	GGAGATAGGCGCCCAGCTGGCACTGTGGGCATGGAAAGAAAC
mvv-vif-P21A-P24A-rv	ATGCCCACAGTGCCAGCTGGGCGCCTATCTCCCGGGCCTTGTTC
mvv-vif-P171A-fw	AAACACTAACGCCAGAAGCCTGCAGAGACTTGC
mvv-vif-P171A-rv	GCAGGCTTCTGGCGTTAGTGTTTTTGACAATC
mvv-vif-P216A-fw	ATACACCATCGCCTGGAGTCTGCAGGAGTGTTG
mvv-vif-P216A-rv	GCAGACTCCAGGCGATGGTGTATCCCATTGGAG
mvv-vif-P21A-fw	GGAGATAGGCGCCCAGCTGCCACTGTGGGCATGGAAAGAAAC
mvv-vif-P21A-rv	ATGCCCACAGTGGCAGCTGGGCGCCTATCTCCCGGGCCTTGTTC
mvv-vif-P24A-fw	GGAGATAGGCCCCCAGCTGGCACTGTGGGCATGGAAAGAAAC
mvv-vif-P24A-rv	ATGCCCACAGTGCCAGCTGGGGGCCTATCTCCCGGGCCTTGTTC
mvv-vif-P39A-fw	CAATCAGGAGGCCTACTGGTATAGCACTATTAGAC
mvv-vif-P39A-rv	TATACCAGTAGGCCTCCTGATTGATAGAGAATGCTG
mvv-vif-P116A-fw	GTACGAGAGCGCCGGAGACTACAAGGGAAAAGAG
mvv-vif-P116A-rv	TGTAGTCTCCGGCGCTCTCGTACCACACCCCAATTG
mvv-vif-P192A-fw	CCAGGTCATGGCTCTTTGGAGGGCACGGAGGGTG
mvv-vif-P192A-rv	CCCTCCAAAGAGCCATGACCTGGAACACATGATC
mvv-vif-P205A-fw	GCAAAAGTTCGCATGGTGCAGGTCTCCAATGGGATAC
mvv-vif-P205A-rv	ACCTGCACCATGCGAACTTTTGCACAGTCACCCTC
mvv-vif-P210A-fw	GTGCAGGTCTGCAATGGGATACACCATCCCCTGGAG
mvv-vif-P210A-rv	TGTATCCCATTGCAGACCTGCACCATGGGAACTTTTG
CYPA-R55K-fw	GTTCCTGCTTTCACAAAATTATTCCAGGGTTTATGTGTC
CYPA-R55K-rv	CCCTGGAATAATTTTGTGAAAGCAGGAACCCTTATAAC
CYPA-F113W-fw	GGTTCCCAGTTTTGGATCTGCACTGCCAAGACTGAGTG
CYPA-F113W-rv	CTTGGCAGTGCAGATCCAAAACTGGGAACCATTTGTGTTGGG
CYPA-H126A-fw	GTTGGATGGCAAGGCTGTGGTGTTTGGCAAAGTGAAAGAAG
CYPA-H126-rv	CTTTGCCAAACACCACAGCCTTGCCATCCAACCACTCAGTCTTG
CYPA wt+R55K sh-resist-fw	CATCTGCACTGCGAAAACAGAATGGCTCGACGGCAAGCATGTGGTGTTTG
CYPA wt+R55K sh-resist-rv	ACATGCTTGCCGTCGAGCCATTCTGTTTTCGCAGTGCAGATGAAAAACTG
CYPA F113W sh-resist-fw	CATCTGCACTGCGAAAACAGAATGGCTCGACGGCAAGCATGTGGTGTTTG
CYPA F113W sh-resist-rv	ACATGCTTGCCGTCGAGCCATTCTGTTTTCGCAGTGCAGATCCAAAACTG

CYPA H126A sh-resist-fw	CATCTGCACTGCGAAAACAGAATGGCTCGACGGCAAGGCTGTGGTGTTTG
CYPA H126A sh-resist-rv	ACAGCCTTGCCGTCGAGCCATTCTGTTTTCGCAGTGCAGATGAAAAACTG

Table 4: SAINT Scored AP-MS Data For HEK293T Cells

Uniprot ID	Uniprot Name	MVV Vif	BIV Vif	FIV Vif	SIVmac Vif	HIV-1 Vif
P02768	ALBU	0.21	0.28	0.46	0.07	0.93
Q9C0C7	AMRA1	0.00	0.00	0.00	0.00	0.99
O95816	BAG2	0.00	1.00	0.34	0.94	1.00
Q13951	CBFβ	0.00	0.00	0.00	0.99	1.00
Q9UNE7	CHIP	0.64	1.00	0.00	0.15	1.00
Q9H078	CLPB	0.00	0.00	0.00	0.13	1.00
Q9Y224	CN166	0.00	0.00	0.00	0.00	0.92
Q13098	CSN1	0.89	0.00	0.00	0.00	0.00
P61201	CSN2	0.71	0.58	0.00	0.00	0.00
Q9UNS2	CSN3	0.98	0.36	0.00	0.00	0.00
Q9BT78	CSN4	1.00	0.89	0.00	0.00	0.00
Q92905	CSN5	0.74	0.24	0.00	0.00	0.00
Q7L5N1	CSN6	0.86	0.52	0.00	0.00	0.00
Q99627	CSN8	0.97	0.74	0.00	0.00	0.00
Q13617	CUL2	1.00	0.57	0.93	0.05	1.00
Q93034	CUL5	1.00	1.00	1.00	1.00	1.00
Q9HB71	CYBP	0.00	0.00	0.52	0.00	0.16
Q16531	DDB1	0.00	0.00	0.00	0.13	1.00
Q5TDH0	DDI2	0.00	0.00	0.00	0.00	1.00
P09622	DLDH	0.99	0.71	0.60	0.76	1.00
Q99615	DNJC7	0.00	0.64	0.00	0.09	1.00
Q15717	ELAV1	0.06	0.00	0.00	0.00	0.69
Q15370	ELOB	1.00	1.00	1.00	1.00	1.00
Q15369	ELOC	1.00	1.00	1.00	1.00	1.00
Q13451	FKBP5	0.00	0.00	1.00	1.00	0.00
Q58FF8	H90B2	0.92	0.99	1.00	1.00	0.00
Q58FF7	H90B3	0.82	0.91	1.00	1.00	0.00
Q58FF6	H90B4	0.57	0.75	0.99	1.00	0.91
O00165	HAX1	0.00	0.00	0.00	0.00	0.93
O60812	HNRCL	0.00	0.00	0.00	0.00	0.92
P31942	HNRH3	0.00	0.00	0.00	0.00	0.96
P52597	HNRPF	0.73	0.00	0.00	0.00	0.39
O60506	HNRPQ	0.84	0.00	0.00	0.12	0.80
O43390	HNRPR	0.03	0.00	0.00	0.00	0.67
Q92598	HS105	0.00	0.98	0.00	0.08	1.00
O95757	HS74L	0.00	0.00	0.00	0.00	0.94
Q14568	HS902	0.88	0.88	1.00	1.00	0.21
Q58FG1	HS904	0.96	0.77	1.00	1.00	0.00

Q58FG0	HS905	0.37	0.43	0.97	0.97	0.82
P07900	HS90A	0.01	0.17	1.00	1.00	0.95
P08238	HS90B	0.00	0.00	0.72	0.52	0.00
P34932	HSP74	0.00	0.20	0.00	0.00	0.95
P48741	HSP77	0.81	1.00	0.89	0.75	0.19
Q7Z6Z7	HUWE1	0.00	0.00	0.00	0.00	1.00
Q12906	ILF3	0.40	0.00	0.00	0.00	0.94
P00338	LDHA	0.06	0.50	0.00	0.00	0.00
P55209	NP1L1	0.10	0.10	0.09	0.29	1.00
Q99733	NP1L4	0.00	0.00	0.00	0.00	1.00
Q02218	ODO1	1.00	1.00	1.00	0.83	1.00
P36957	ODO2	1.00	1.00	1.00	1.00	1.00
Q9Y536	PAL4A	0.98	0.00	0.00	0.00	0.00
Q15366	PCBP2	0.00	0.01	0.00	0.00	0.18
Q9BY77	PDIP3	0.00	0.00	0.00	0.00	0.97
P62937	PPIA	1.00	0.09	0.00	0.00	0.00
P28072	PSB6	0.00	0.00	0.00	0.00	0.30
Q13200	PSMD2	0.00	0.00	0.00	0.00	0.33
P61289	PSME3	0.98	1.00	0.53	0.99	1.00
Q15185	PTGES3	0.00	0.00	1.00	1.00	0.00
P62877	RBX1	0.41	0.00	0.00	0.00	0.87
Q9UBF6	RBX2	1.00	0.97	1.00	0.89	1.00
P35268	RL22	0.00	0.00	0.00	0.01	0.00
Q9UNX3	RL26L	0.97	0.00	0.00	0.00	0.00
P62987	RL40	0.72	0.57	0.99	0.43	0.10
Q13151	ROA0	0.00	0.00	0.00	0.00	0.35
P51991	ROA3	0.17	0.00	0.00	0.00	0.93
P62280	RS11	0.99	0.14	0.05	0.18	0.91
P25398	RS12	0.95	0.00	0.00	0.00	0.38
P0CW22	RS17L	0.98	0.38	0.00	0.46	0.00
P62979	RS27A	0.61	0.13	0.90	0.12	0.59
Q71UM5	RS27L	0.68	0.91	0.96	0.97	0.00
P82909	RT36	0.97	0.50	0.65	0.78	0.81
P31948	STIP1	1.00	1.00	1.00	1.00	1.00
Q9H853	TBA4B	0.61	0.93	0.80	0.92	0.09
P17987	TCPA	0.92	0.67	0.18	0.00	0.98
P78371	TCPB	1.00	1.00	0.98	0.01	1.00
P50991	TCPD	1.00	0.98	0.60	0.00	1.00
P48643	TCPE	0.91	0.91	0.53	0.00	0.95
P49368	TCPG	0.98	0.57	0.07	0.00	0.82
Q99832	TCPH	1.00	0.96	0.33	0.00	0.92

P50990	TCPQ	1.00	1.00	1.00	0.03	1.00
P40227	TCPZ	1.00	1.00	0.99	0.00	1.00
P10599	THIO	0.00	0.00	0.03	0.00	0.00
Q9Y5L4	TIM13	0.00	0.19	0.00	0.00	0.59
Q9NS69	TOM22	0.00	0.00	0.99	0.00	0.00
O96008	TOM40	0.00	0.00	1.00	0.00	0.00
P0CG48	UBC	0.70	0.50	0.98	0.40	0.00

Table 5: SAINT Scored AP-MS Data For Jurkat T-Cells

Uniprot ID	Uniprot Name	MVV Vif	BIV Vif	FIV Vif	SIVmac Vif	HIV-1 Vif
P49902	5NTC	0.32	0.32	0.24	0.45	0.92
P02768	ALBU	0.31	0.00	0.23	0.18	0.00
Q9C0C7	AMRA1	0.37	0.81	0.47	0.35	1.00
Q99873	ANM1	0.83	0.99	0.17	0.53	0.59
Q13510	ASAH1	0.00	0.00	1.00	0.00	0.00
O95816	BAG2	0.00	1.00	0.28	0.47	0.13
Q13951	CBFβ	0.00	0.00	0.00	1.00	1.00
Q9UNE7	CHIP	0.00	0.51	0.00	0.00	0.00
Q14011	CIRBP	0.93	0.53	0.16	0.50	0.75
Q9Y224	CN166	0.85	0.00	0.19	0.62	0.00
Q13098	CSN1	0.90	0.26	0.50	0.00	0.00
P61201	CSN2	1.00	0.51	0.99	0.00	0.00
Q9UNS2	CSN3	0.97	0.25	0.76	0.00	0.00
Q9BT78	CSN4	1.00	0.50	1.00	0.46	0.00
Q92905	CSN5	0.70	0.22	0.99	0.38	0.00
Q7L5N1	CSN6	0.99	0.00	0.93	0.00	0.00
Q99627	CSN8	0.59	0.12	0.80	0.00	0.00
Q13617	CUL2	1.00	0.00	1.00	0.19	1.00
Q93034	CUL5	0.05	1.00	1.00	1.00	1.00
Q9HB71	CYBP	0.14	0.26	0.98	0.24	0.00
Q16531	DDB1	1.00	0.74	0.75	0.76	1.00
Q99615	DNJC7	0.00	1.00	0.24	0.00	0.00
Q15717	ELAV1	0.98	0.00	0.00	0.29	0.00
Q15370	ELOB	1.00	1.00	1.00	1.00	1.00
Q15369	ELOC	1.00	1.00	1.00	1.00	1.00
P37268	FDFT	0.00	0.84	1.00	0.30	0.00
Q13451	FKBP5	0.00	0.00	1.00	1.00	0.00
P16401	H15	0.95	0.00	0.00	0.00	0.00
Q58FF7	H90B3	0.33	0.26	0.00	0.49	0.00
Q58FF6	H90B4	0.70	0.78	1.00	1.00	0.50
O00165	HAX1	0.00	0.31	0.00	0.00	0.00
O60812	HNRCL	0.62	0.00	0.00	0.29	0.00
P31942	HNRH3	0.88	0.00	0.00	0.39	0.41
Q9BUJ2	HNRL1	0.96	0.00	0.00	0.03	0.00
P52597	HNRPF	0.99	0.75	0.26	0.71	0.65
O60506	HNRPQ	1.00	0.10	0.00	0.03	0.08
O43390	HNRPR	0.99	0.09	0.03	0.09	0.23
Q92598	HS105	0.00	0.48	0.07	0.16	0.06

O95757	HS74L	0.00	0.12	0.23	0.01	0.22
Q14568	HS902	0.35	0.70	1.00	1.00	0.48
Q58FG0	HS905	0.83	0.99	0.98	0.99	0.83
P07900	HS90A	0.64	0.60	0.90	0.99	0.23
P08238	HS90B	0.50	0.56	1.00	1.00	0.29
P34932	HSP74	0.03	0.80	0.15	0.21	0.01
P48741	HSP77	0.00	0.73	0.00	0.00	0.00
Q7Z6Z7	HUWE1	0.00	0.16	0.15	0.00	0.00
Q12906	ILF3	0.77	0.00	0.00	0.00	0.00
P05455	LA	0.95	0.44	0.62	0.49	0.39
P00338	LDHA	0.32	0.99	0.10	0.11	0.00
Q8NCE2	MTMRE	0.00	0.07	0.00	0.08	0.98
Q15843	NEDD8	0.00	0.00	0.00	0.00	0.98
P55209	NP1L1	0.42	0.64	0.30	0.30	0.00
Q99733	NP1L4	0.49	0.48	0.22	0.25	0.00
Q15366	PCBP2	0.92	0.55	0.05	0.19	0.01
Q9BY77	PDIP3	0.35	0.26	0.26	0.24	0.00
P62937	PPIA	1.00	0.10	0.19	0.14	0.00
P28072	PSB6	0.66	0.53	0.91	0.61	0.39
Q13200	PSMD2	0.59	0.50	0.56	0.48	0.90
P61289	PSME3	0.00	1.00	0.00	0.00	0.01
Q15185	PTGES3	0.00	0.00	0.74	0.75	0.00
P62877	RBX1	0.96	0.00	1.00	0.00	1.00
Q9UBF6	RBX2	0.00	0.42	1.00	1.00	1.00
P35268	RL22	0.96	0.48	0.38	0.31	0.51
Q9UNX3	RL26L	0.00	0.22	0.00	0.00	0.00
P62987	RL40	0.62	0.00	0.24	0.25	0.47
Q13151	ROA0	0.99	0.00	0.00	0.00	0.00
P51991	ROA3	0.98	0.00	0.00	0.46	0.00
P62280	RS11	0.74	0.54	0.49	0.55	0.51
P25398	RS12	0.65	0.25	0.00	0.25	0.00
P62979	RS27A	0.86	0.24	0.25	0.47	0.00
P31948	STIP1	0.36	0.76	0.95	0.52	0.48
P78371	TCPB	0.12	0.17	0.00	0.06	0.02
P50991	TCPD	0.20	0.16	0.00	0.01	0.00
P49368	TCPG	0.46	0.50	0.18	0.11	0.16
Q99832	TCPH	0.23	0.20	0.00	0.17	0.00
P40227	TCPZ	0.28	0.24	0.22	0.00	0.00
P10599	THIO	0.00	0.00	1.00	0.00	0.00
Q9Y5L4	TIM13	0.00	0.95	0.93	0.00	0.00
O75643	U520	0.97	0.48	0.53	0.49	0.24

Q93009	UBP7	0.00	0.78	0.31	0.32	0.92

Table 6: Mass Spectrometry Results for Vif-CUL5 Tandem Affinity Purification

Bait 1	Bait 2	Prey Name	Acc #	Rank	Spectral Count	Num Unique	Uniq Pep	% Cov
MVV VIF	CUL5	CUL5	Q93034	[1]	157	54		56.7
MVV VIF	CUL5	HSP71	P08107	[2]	61	31		55.4
MVV VIF	CUL5	HSP7C	P11142	[2-2]	37	23	20	42.4
MVV VIF	CUL5	HS71L	P34931	[2-4]	26	13	1	26.2
MVV VIF	CUL5	HSP76	P17066	[2-6]	16	9	1	14
MVV VIF	CUL5	HSP77	P48741	[2-8]	11	6	0	15.3
MVV VIF	CUL5	HSP72	P54652	[2-10]	16	9	6	13
MVV VIF	CUL5	TBB5	P07437	[3]	36	26		65.3
MVV VIF	CUL5	TBB2C	P68371	[3-2]	30	23	3	55.5
MVV VIF	CUL5	TBB4	P04350	[3-4]	26	19	2	46.2
MVV VIF	CUL5	TBB2A	Q13885	[3-6]	23	17	2	47
MVV VIF	CUL5	TBB2B	Q9BVA1	[3-7]	23	17	2	47
MVV VIF	CUL5	TBB2A	Q13885	[3-8]	23	17	2	47
MVV VIF	CUL5	TBB2B	Q9BVA1	[3-9]	23	17	2	47
MVV VIF	CUL5	TBB8	Q3ZCM7	[3-10]	13	9	1	16.4
MVV VIF	CUL5	TBB3	Q13509	[3-12]	13	12	0	22.2
MVV VIF	CUL5	TBB6	Q9BUF5	[3-14]	11	7	1	12.6
MVV VIF	CUL5	TBB8B	A6NNZ2	[3-15]	11	8	0	13.1
MVV VIF	CUL5	TBB6	Q9BUF5	[3-17]	10	6	0	8.7
MVV VIF	CUL5	YI016	A6NKZ8	[3-18]	8	5	0	6.7
MVV VIF	CUL5	TBB1	Q9H4B7	[3-20]	4	4	1	6.2
MVV VIF	CUL5	TBA1B	P68363	[4]	37	18		50.8
MVV VIF	CUL5	TBA1C	Q9BQE3	[4-2]	33	16	2	47.2
MVV VIF	CUL5	TBA1A	Q71U36	[4-4]	32	18	2	50.8
MVV VIF	CUL5	TBA4A	P68366	[4-6]	29	14	0	39.1
MVV VIF	CUL5	TBA3C	Q13748	[4-8]	27	15	2	43.6
MVV VIF	CUL5	TBA3E	Q6PEY2	[4-10]	22	12	2	39.8
MVV VIF	CUL5	TBA8	Q9NY65	[4-12]	17	9	1	26.3
MVV VIF	CUL5	TBA4B	Q9H853	[4-14]	6	2	0	10.8
MVV VIF	CUL5	TBAL3	A6NHL2	[4-16]	1	1	0	2
MVV VIF	CUL5	PPIA	P62937	[5]	65	15		67.3
MVV VIF	CUL5	PAL4A	Q9Y536	[5-2]	8	2	0	8.5
MVV VIF	CUL5	ELOC	Q15369	[6]	41	12		63.4
MVV VIF	CUL5	K2C1	P04264	[7]	22	18		30.4
MVV VIF	CUL5	K22E	P35908	[7-2]	6	5	4	11.6
MVV VIF	CUL5	K2C6B	P04259	[7-4, 88-2]	3	2	1	3.9
MVV VIF	CUL5	K2C1B	Q7Z794	[7-6]	2	1	0	2.1
MVV VIF	CUL5	K2C8	P05787	[7-8]	1	1	0	2.3
MVV VIF	CUL5	K2C7	P08729	[7-9]	1	1	0	2.3
MVV VIF	CUL5	GFAP	P14136	[7-10]	1	1	0	2.5
MVV VIF	CUL5	K2C4	P19013	[7-11]	1	1	0	2.1
MVV VIF	CUL5	K2C80	Q6KB66	[7-12]	1	1	0	2.4
MVV VIF	CUL5	K2C8	P05787	[7-13]	1	1	0	2.3

MVV VIF	CUL5	K2C7	P08729	[7-14]	1	1	0	2.3
MVV VIF	CUL5	GFAP	P14136	[7-15]	1	1	0	2.5
MVV VIF	CUL5	K2C4	P19013	[7-16]	1	1	0	2.1
MVV VIF	CUL5	K2C80	Q6KB66	[7-17]	1	1	0	2.4
MVV VIF	CUL5	RS3A	P61247	[8]	20	13		43.9
MVV VIF	CUL5	HNRPF	P52597	[9]	21	13		40.7
MVV VIF	CUL5	HNRH1	P31943	[9-2]	16	10	8	33.4
MVV VIF	CUL5	HNRH2	P55795	[9-4]	7	6	5	18.7
MVV VIF	CUL5	MVV Vif	N/A	[10]	53	15		50.9
MVV VIF	CUL5	ELOB	Q15370	[11]	33	15		93.2
MVV VIF	CUL5	NUCL	P19338	[12]	16	11		19.3
MVV VIF	CUL5	RS2	P15880	[13]	16	10		37.2
MVV VIF	CUL5	PABP1	P11940	[14]	14	12		22.2
MVV VIF	CUL5	PABP4	Q13310	[14-2]	11	9	2	16
MVV VIF	CUL5	PABP3	Q9H361	[14-4]	7	6	0	9.7
MVV VIF	CUL5	PAP1L	Q4VXU2	[14-6]	4	3	0	5.5
MVV VIF	CUL5	PAP1M	Q5JQF8	[14-8]	1	1	0	5.5
MVV VIF	CUL5	K1C9	P35527	[15]	11	11		35.5
MVV VIF	CUL5	YBOX1	P67809	[16]	13	8		52.8
MVV VIF	CUL5	DBPA	P16989	[16-2]	7	6	3	36.6
MVV VIF	CUL5	YBOX2	Q9Y2T7	[16-4]	4	3	0	11
MVV VIF	CUL5	RS3	P23396	[17]	17	13		63
MVV VIF	CUL5	RS5	P46782	[18]	15	8		41.2
MVV VIF	CUL5	HNRPU	Q00839	[19]	11	9		18.2
MVV VIF	CUL5	RS4X	P62701	[20]	19	10		35.4
MVV VIF	CUL5	RS4Y1	P22090	[20-2]	3	3	0	11.4
MVV VIF	CUL5	RS4Y2	Q8TD47	[20-4]	2	2	0	7.2
MVV VIF	CUL5	RS17	P08708	[21]	14	8		65.9
MVV VIF	CUL5	RS17L	P0CW22	[21-1]	14	8	0	65.9
MVV VIF	CUL5	RS17	P08708	[21-2]	14	8	0	65.9
MVV VIF	CUL5	RS17L	P0CW22	[21-3]	14	8	0	65.9
MVV VIF	CUL5	RS8	P62241	[22]	9	7		42.3
MVV VIF	CUL5	IF2B1	Q9NZI8	[23]	11	9		19.9
MVV VIF	CUL5	IF2B2	Q9Y6M1	[23-2]	3	2	1	4.8
MVV VIF	CUL5	IF2B3	O00425	[23-4]	2	1	0	2.2
MVV VIF	CUL5	RCN2	Q14257	[24]	8	7		24
MVV VIF	CUL5	HNRPQ	O60506	[25]	10	9		26.3
MVV VIF	CUL5	HNRPR	O43390	[25-2]	6	6	5	10.6
MVV VIF	CUL5	RS19	P39019	[26]	16	11		57.2
MVV VIF	CUL5	RS6	P62753	[27]	9	8		35.7
MVV VIF	CUL5	RS16	P62249	[28]	19	11		57.5
MVV VIF	CUL5	RS18	P62269	[29]	18	9		49.3
MVV VIF	CUL5	RS12	P25398	[30]	6	5		41.7
MVV VIF	CUL5	DHX9	Q08211	[31]	8	8		8.1
MVV VIF	CUL5	TCPB	P78371	[32]	5	5		16.3
MVV VIF	CUL5	RL23	P62829	[33]	7	5		33.6
MVV VIF	CUL5	TCPH	Q99832	[34]	5	5		13.4

MVV VIF	CUL5	RL12	P30050	[35]	6	6		54.5
MVV VIF	CUL5	RS9	P46781	[36]	9	7		27.8
MVV VIF	CUL5	RLA0	P05388	[37]	6	4		19.2
MVV VIF	CUL5	RLA0L	Q8NHW5	[37-2]	5	3	0	13.9
MVV VIF	CUL5	TCPE	P48643	[38]	7	6		25.5
MVV VIF	CUL5	RL10	P27635	[39]	5	5		25.2
MVV VIF	CUL5	RL10L	Q96L21	[39-2]	1	1	0	5.1
MVV VIF	CUL5	RS7	P62081	[40]	10	7		41.8
MVV VIF	CUL5	RS25	P62851	[41]	9	6		39.2
MVV VIF	CUL5	RLA2	P05387	[42]	8	4		69.6
MVV VIF	CUL5	RS14	P62263	[43]	8	7		40.4
MVV VIF	CUL5	RL7	P18124	[44]	6	5		19.4
MVV VIF	CUL5	RS15A	P62244	[45]	11	6		54.6
MVV VIF	CUL5	ILF3	Q12906	[46]	7	6		11.6
MVV VIF	CUL5	STRBP	Q96SI9	[46-2]	1	1	0	1.6
MVV VIF	CUL5	ILF2	Q12905	[47]	7	6		26.7
MVV VIF	CUL5	RL11	P62913	[48]	7	4		27.5
MVV VIF	CUL5	RS27A	P62979	[49]	4	4		39.1
MVV VIF	CUL5	UBB	P0CG47	[49-2]	2	2	0	12.7
MVV VIF	CUL5	UBC	P0CG48	[49-3]	2	2	0	4.2
MVV VIF	CUL5	RL40	P62987	[49-4]	2	2	0	22.7
MVV VIF	CUL5	UBB	P0CG47	[49-5]	2	2	0	12.7
MVV VIF	CUL5	UBC	P0CG48	[49-6]	2	2	0	4.2
MVV VIF	CUL5	RL40	P62987	[49-7]	2	2	0	22.7
MVV VIF	CUL5	ACTB	P60709	[50]	3	2		10.4
MVV VIF	CUL5	ACTG	P63261	[50-1]	3	2	0	10.4
MVV VIF	CUL5	POTEE	Q6S8J3	[50-2]	3	2	0	3.6
MVV VIF	CUL5	ACTB	P60709	[50-3]	3	2	0	10.4
MVV VIF	CUL5	ACTG	P63261	[50-4]	3	2	0	10.4
MVV VIF	CUL5	POTEE	Q6S8J3	[50-5]	3	2	0	3.6
MVV VIF	CUL5	RS11	P62280	[51]	4	3		23.4
MVV VIF	CUL5	SRP14	P37108	[52]	3	3		25.7
MVV VIF	CUL5	RL10A	P62906	[53]	6	4		17.1
MVV VIF	CUL5	RL35	P42766	[54]	5	4		29.3
MVV VIF	CUL5	RS24	P62847	[55]	9	4		29.3
MVV VIF	CUL5	TCPA	P17987	[56]	4	3		8.1
MVV VIF	CUL5	XRCC5	P13010	[57]	5	5		13.4
MVV VIF	CUL5	TCPQ	P50990	[58]	5	5		12.2
MVV VIF	CUL5	RL19	P84098	[59]	3	2		9.2
MVV VIF	CUL5	NPM	P06748	[60]	4	4		29.6
MVV VIF	CUL5	RBX2	Q9UBF6	[61]	2	2		31
MVV VIF	CUL5	RL13	P26373	[62]	5	4		15.2
MVV VIF	CUL5	TCPG	P49368	[63]	5	5		14.5
MVV VIF	CUL5	RL30	P62888	[64]	4	4		34.8
MVV VIF	CUL5	RS10	P46783	[65]	6	4		24.2
MVV VIF	CUL5	RS10L	Q9NQ39	[65-2]	5	3	0	17.6
MVV VIF	CUL5	TCPD	P50991	[66]	4	4		11.3

MVV VIF	CUL5	RL37A	P61513	[67]	3	3		42.4
MVV VIF	CUL5	DNJA1	P31689	[68]	5	4		18.6
MVV VIF	CUL5	H2B1K	O60814	[69]	3	2		11.9
MVV VIF	CUL5	H2B1J	P06899	[69-1]	3	2	-1	11.9
MVV VIF	CUL5	H2B1O	P23527	[69-2]	3	2	-1	11.9
MVV VIF	CUL5	H2B1B	P33778	[69-3]	3	2	-1	11.9
MVV VIF	CUL5	H2BFS	P57053	[69-4]	3	2	-1	11.9
MVV VIF	CUL5	H2B1D	P58876	[69-5]	3	2	-1	11.9
MVV VIF	CUL5	H2B1C	P62807	[69-6]	3	2	-1	11.9
MVV VIF	CUL5	H2B2E	Q16778	[69-7]	3	2	-1	11.9
MVV VIF	CUL5	H2B2F	Q5QNW6	[69-8]	3	2	-1	11.9
MVV VIF	CUL5	H2B3B	Q8N257	[69-9]	3	2	-1	11.9
MVV VIF	CUL5	H2B1H	Q93079	[69-10]	3	2	-1	11.9
MVV VIF	CUL5	H2B1N	Q99877	[69-11]	3	2	-1	11.9
MVV VIF	CUL5	H2B1M	Q99879	[69-12]	3	2	-1	11.9
MVV VIF	CUL5	H2B1L	Q99880	[69-13]	3	2	-1	11.9
MVV VIF	CUL5	H2B1K	O60814	[69-14]	3	2	-1	11.9
MVV VIF	CUL5	H2B1J	P06899	[69-15]	3	2	-1	11.9
MVV VIF	CUL5	H2B1O	P23527	[69-16]	2	2	0	11.9
MVV VIF	CUL5	H2B1B	P33778	[69-17]	3	2	-1	11.9
MVV VIF	CUL5	H2BFS	P57053	[69-18]	2	2	0	11.9
MVV VIF	CUL5	H2B1D	P58876	[69-19]	3	2	-1	11.9
MVV VIF	CUL5	H2B1C	P62807	[69-20]	3	2	-1	11.9
MVV VIF	CUL5	H2B2E	Q16778	[69-21]	2	2	0	11.9
MVV VIF	CUL5	H2B2F	Q5QNW6	[69-22]	2	2	0	11.9
MVV VIF	CUL5	H2B3B	Q8N257	[69-23]	2	2	0	11.9
MVV VIF	CUL5	H2B1H	Q93079	[69-24]	3	2	-1	11.9
MVV VIF	CUL5	H2B1N	Q99877	[69-25]	3	2	-1	11.9
MVV VIF	CUL5	H2B1M	Q99879	[69-26]	3	2	-1	11.9
MVV VIF	CUL5	H2B1L	Q99880	[69-27]	3	2	-1	11.9
MVV VIF	CUL5	RL7A	P62424	[70]	5	4		15
MVV VIF	CUL5	RL27A	P46776	[71]	5	4		24.3
MVV VIF	CUL5	ADT2	P05141	[72]	3	3		11.4
MVV VIF	CUL5	RS15	P62841	[73]	8	3		40.7
MVV VIF	CUL5	DDX5	P17844	[74]	5	5		9.9
MVV VIF	CUL5	DDX17	Q92841	[74-2]	3	3	1	5.8
MVV VIF	CUL5	RL31	P62899	[75]	6	4		31.2
MVV VIF	CUL5	RL14	P50914	[76]	3	3		15.3
MVV VIF	CUL5	RBX1	P62877	[77]	3	2		18.5
MVV VIF	CUL5	RL4	P36578	[78]	2	2		9.1
MVV VIF	CUL5	RLA1	P05386	[79]	4	2		51.8
MVV VIF	CUL5	NP1L1	P55209	[80]	2	2		7.4
MVV VIF	CUL5	DNJA2	O60884	[81]	4	4		16.3
MVV VIF	CUL5	H2A1B	P04908	[82]	5	2		21.5
MVV VIF	CUL5	H2A1	P0C0S8	[82-1]	5	2	0	21.5
MVV VIF	CUL5	H2A1D	P20671	[82-2]	5	2	0	21.5

MVV VIF	CUL5	H2A2C	Q16777	[82-3]	5	2	0	21.7
MVV VIF	CUL5	H2A2A	Q6FI13	[82-4]	5	2	0	21.5
MVV VIF	CUL5	H2A3	Q7L7L0	[82-5]	5	2	0	21.5
MVV VIF	CUL5	H2A1C	Q93077	[82-6]	5	2	0	21.5
MVV VIF	CUL5	H2A1H	Q96KK5	[82-7]	5	2	0	21.9
MVV VIF	CUL5	H2A1J	Q99878	[82-8]	5	2	0	21.9
MVV VIF	CUL5	H2AJ	Q9BTM1	[82-9]	5	2	0	21.7
MVV VIF	CUL5	H2A1B	P04908	[82-10]	5	2	0	21.5
MVV VIF	CUL5	H2A1	P0C0S8	[82-11]	5	2	0	21.5
MVV VIF	CUL5	H2A1D	P20671	[82-12]	5	2	0	21.5
MVV VIF	CUL5	H2A2C	Q16777	[82-13]	5	2	0	21.7
MVV VIF	CUL5	H2A2A	Q6FI13	[82-14]	5	2	0	21.5
MVV VIF	CUL5	H2A3	Q7L7L0	[82-15]	5	2	0	21.5
MVV VIF	CUL5	H2A1C	Q93077	[82-16]	5	2	0	21.5
MVV VIF	CUL5	H2A1H	Q96KK5	[82-17]	5	2	0	21.9
MVV VIF	CUL5	H2A1J	Q99878	[82-18]	5	2	0	21.9
MVV VIF	CUL5	H2AJ	Q9BTM1	[82-19]	5	2	0	21.7
MVV VIF	CUL5	RL23A	P62750	[83]	5	3		19.9
MVV VIF	CUL5	RL21	P46778	[84]	3	2		20.6
MVV VIF	CUL5	HS90A	P07900	[85]	3	3		5.3
MVV VIF	CUL5	HS90B	P08238	[85-1]	3	3	0	5.4
MVV VIF	CUL5	HS90A	P07900	[85-2]	3	3	0	5.3
MVV VIF	CUL5	HS90B	P08238	[85-3]	3	3	0	5.4
MVV VIF	CUL5	HS904	Q58FG1	[85-4]	1	1	0	3.1
MVV VIF	CUL5	TRAP1	Q12931	[85-6]	1	1	0	2
MVV VIF	CUL5	HS902	Q14568	[85-8]	1	1	0	3.5
MVV VIF	CUL5	H90B2	Q58FF8	[85-9]	1	1	0	3.1
MVV VIF	CUL5	HS902	Q14568	[85-10]	1	1	0	3.5
MVV VIF	CUL5	H90B2	Q58FF8	[85-11]	1	1	0	3.1
MVV VIF	CUL5	ROA1	P09651	[86]	2	2		7
MVV VIF	CUL5	RA1L2	Q32P51	[86-1]	2	2	0	8.1
MVV VIF	CUL5	ROA1	P09651	[86-2]	2	2	0	7
MVV VIF	CUL5	RA1L2	Q32P51	[86-3]	2	2	0	8.1
MVV VIF	CUL5	RS13	P62277	[87]	5	4		21.2
MVV VIF	CUL5	K2C5	P13647	[88]	2	2		4.6
MVV VIF	CUL5	K2C6B	P04259	[7-4, 88-2]	3	2	1	3.9
MVV VIF	CUL5	K2C75	O95678	[88-4]	1	1	0	2.2
MVV VIF	CUL5	K2C6A	P02538	[88-5]	1	1	0	2.1
MVV VIF	CUL5	K2C6C	P48668	[88-6]	1	1	0	2.1
MVV VIF	CUL5	K2C79	Q5XKE5	[88-7]	1	1	0	2.2
MVV VIF	CUL5	K2C75	O95678	[88-8]	1	1	0	2.2
MVV VIF	CUL5	K2C6A	P02538	[88-9]	1	1	0	2.1
MVV VIF	CUL5	K2C6C	P48668	[88-10]	1	1	0	2.1
MVV VIF	CUL5	K2C79	Q5XKE5	[88-11]	1	1	0	2.2
MVV VIF	CUL5	RL18A	Q02543	[89]	2	2		15.3
MVV VIF	CUL5	RL36	Q9Y3U8	[90]	2	2		20
MVV VIF	CUL5	RL22	P35268	[91]	3	3		30.5

MVV VIF	CUL5	RL13A	P40429	[92]	3	3		15.3
MVV VIF	CUL5	R13AX	Q6NVV1	[92-2]	2	2	0	18.6
MVV VIF	CUL5	RL8	P62917	[93]	3	3		22.2
MVV VIF	CUL5	NEDD8	Q15843	[94]	3	2		34.6
MVV VIF	CUL5	XRCC6	P12956	[95]	3	3		7.1
MVV VIF	CUL5	KV201	P01614	[96]	5	1		11.3
MVV VIF	CUL5	KV204	P01617	[96-1]	5	1	0	11.5
MVV VIF	CUL5	KV205	P06309	[96-2]	5	1	0	11.1
MVV VIF	CUL5	KV206	P06310	[96-3]	5	1	0	9.8
MVV VIF	CUL5	KV201	P01614	[96-4]	5	1	0	11.3
MVV VIF	CUL5	KV204	P01617	[96-5]	5	1	0	11.5
MVV VIF	CUL5	KV205	P06309	[96-6]	5	1	0	11.1
MVV VIF	CUL5	KV206	P06310	[96-7]	5	1	0	9.8
MVV VIF	CUL5	SRP09	P49458	[97]	3	2		26.7
MVV VIF	CUL5	RL26	P61254	[98]	4	4		20.7
MVV VIF	CUL5	RL26L	Q9UNX3	[98-1]	4	4	0	20.7
MVV VIF	CUL5	RL26	P61254	[98-2]	4	4	0	20.7
MVV VIF	CUL5	RL26L	Q9UNX3	[98-3]	4	4	0	20.7
MVV VIF	CUL5	K1C10	P13645	[99]	3	3		7
MVV VIF	CUL5	K1C28	Q7Z3Y7	[99-2]	1	1	0	1.9
MVV VIF	CUL5	K1C27	Q7Z3Y8	[99-3]	1	1	0	2
MVV VIF	CUL5	K1C25	Q7Z3Z0	[99-4]	1	1	0	2
MVV VIF	CUL5	K1C28	Q7Z3Y7	[99-5]	1	1	0	1.9
MVV VIF	CUL5	K1C27	Q7Z3Y8	[99-6]	1	1	0	2
MVV VIF	CUL5	K1C25	Q7Z3Z0	[99-7]	1	1	0	2
MVV VIF	CUL5	RL24	P83731	[100]	6	4		26.8
MVV VIF	CUL5	TCPZ	P40227	[101]	2	2		4.9
MVV VIF	CUL5	TCPW	Q92526	[101-2]	1	1	0	2.5
MVV VIF	CUL5	PAIRB	Q8NC51	[102]	1	1		3.9
MVV VIF	CUL5	RS28	P62857	[103]	2	2		30.4
MVV VIF	CUL5	RS26	P62854	[104]	3	2		20.9
MVV VIF	CUL5	RL9	P32969	[105]	3	3		22.4
MVV VIF	CUL5	PRP19	Q9UMS4	[106]	2	2		10.9
MVV VIF	CUL5	RL28	P46779	[107]	3	2		16.8
MVV VIF	CUL5	LSR	Q86X29	[108]	3	2		1.8
MVV VIF	CUL5	2xStrep	N/A	[109]	7	1		71.4
MVV VIF	CUL5	TIM13	Q9Y5L4	[110]	1	1		14.7
MVV VIF	CUL5	PFD2	Q9UHV9	[111]	2	2		16.9
MVV VIF	CUL5	RL35A	P18077	[112]	2	2		20
MVV VIF	CUL5	RL27	P61353	[113]	5	4		32.4
MVV VIF	CUL5	PURA	Q00577	[114]	2	2		22.4
MVV VIF	CUL5	RL17	P18621	[115]	2	2		10.9
MVV VIF	CUL5	ERH	P84090	[116]	1	1		11.5
MVV VIF	CUL5	ANM5	O14744	[117]	2	2		3.6
MVV VIF	CUL5	DREB	Q16643	[118]	1	1		4.3
MVV VIF	CUL5	RS23	P62266	[119]	2	1		7.7
MVV VIF	CUL5	CAPR1	Q14444	[120]	1	1		1.6

MVV VIF	CUL5	TFAM	Q00059	[121]	1	1		4.1
MVV VIF	CUL5	ELAV1	Q15717	[122]	2	2		8.3
MVV VIF	CUL5	HNRPM	P52272	[123]	2	2		7.1
MVV VIF	CUL5	LA	P05455	[124]	1	1		3.4
MVV VIF	CUL5	MEP50	Q9BQA1	[125]	1	1		4.1
MVV VIF	CUL5	BAG2	O95816	[127]	1	1		5.2
MVV VIF	CUL5	LSM12	Q3MHD2	[128]	1	1		6.7
MVV VIF	CUL5	ML12B	O14950	[129]	2	1		11.6
MVV VIF	CUL5	ML12A	P19105	[129-1]	2	1	0	11.7
MVV VIF	CUL5	ML12B	O14950	[129-2]	2	1	0	11.6
MVV VIF	CUL5	ML12A	P19105	[129-3]	2	1	0	11.7
MVV VIF	CUL5	PSME3	P61289	[130]	1	1		5.9
MVV VIF	CUL5	H12	P16403	[131]	2	2		13.6
MVV VIF	CUL5	H14	P10412	[131-2]	2	2	1	13.2
MVV VIF	CUL5	H13	P16402	[131-4]	1	1	0	5.4
MVV VIF	CUL5	RTCB	Q9Y3I0	[132]	1	1		2.2
MVV VIF	CUL5	ROAA	Q99729	[134]	2	2		5.4
MVV VIF	CUL5	HNRDL	O14979	[134-2]	1	1	0	2.4
MVV VIF	CUL5	HNRPD	Q14103	[134-3]	1	1	0	2.8
MVV VIF	CUL5	HNRDL	O14979	[134-4]	1	1	0	2.4
MVV VIF	CUL5	HNRPD	Q14103	[134-5]	1	1	0	2.8
MVV VIF	CUL5	RL18	Q07020	[135]	2	2		12.8
MVV VIF	CUL5	HNRCL	O60812	[136]	1	1		4.1
MVV VIF	CUL5	HNRPC	P07910	[136-1]	1	1	0	3.9
MVV VIF	CUL5	HNRCL	O60812	[136-2]	1	1	0	4.1
MVV VIF	CUL5	HNRPC	P07910	[136-3]	1	1	0	3.9
MVV VIF	CUL5	HNRPK	P61978	[137]	1	1		2.6
MVV VIF	CUL5	H1X	Q92522	[138]	1	1		4.7
MVV VIF	CUL5	GRP78	P11021	[140]	1	1		2.4
MVV VIF	CUL5	HNRL1	Q9BUJ2	[141]	1	1		1.8
MVV VIF	CUL5	DHX36	Q9H2U1	[142]	1	1		1.4
MVV VIF	CUL5	TSR1	Q2NL82	[143]	1	1		1.9
MVV VIF	CUL5	DIMT1	Q9UNQ2	[144]	1	1		3.5
MVV VIF	CUL5	CHIP	Q9UNE7	[145]	2	1		3.6
MVV VIF	CUL5	ALBU	P02768	[146]	1	1		2.5
MVV VIF	CUL5	RL39	P62891	[147]	1	1		19.6
MVV VIF	CUL5	R39L5	Q59GN2	[147-1]	1	1	0	19.6
MVV VIF	CUL5	RL39	P62891	[147-2]	1	1	0	19.6
MVV VIF	CUL5	R39L5	Q59GN2	[147-3]	1	1	0	19.6
MVV VIF	CUL5	RRAS	P10301	[149]	2	1		5
BIV VIF	CUL5	CUL5	Q93034	[1]	218	64		59.5
BIV VIF	CUL5	TBB5	P07437	[2]	103	42		74.3
BIV VIF	CUL5	TBB2C	P68371	[2-2]	92	42	9	74.2
BIV VIF	CUL5	TBB2A	Q13885	[2-4]	77	35	6	66.1
BIV VIF	CUL5	TBB2B	Q9BVA1	[2-5]	77	35	6	66.1
BIV VIF	CUL5	TBB2A	Q13885	[2-6]	77	35	6	66.1
BIV VIF	CUL5	TBB2B	Q9BVA1	[2-7]	77	35	6	66.1

BIV VIF	CUL5	TBB4	P04350	[2-8]	74	32	7	62.2
BIV VIF	CUL5	TBB3	Q13509	[2-10]	49	22	3	33.8
BIV VIF	CUL5	TBB8	Q3ZCM7	[2-12]	35	15	2	24.5
BIV VIF	CUL5	TBB6	Q9BUF5	[2-14]	31	14	5	28.5
BIV VIF	CUL5	TBB8B	A6NNZ2	[2-16]	32	13	0	21.2
BIV VIF	CUL5	YI016	A6NKZ8	[2-18]	19	7	0	11.6
BIV VIF	CUL5	TBB1	Q9H4B7	[2-20]	12	5	0	6.4
BIV VIF	CUL5	HSP71	P08107	[3]	70	31		53.5
BIV VIF	CUL5	HSP7C	P11142	[3-2]	54	30	27	44.6
BIV VIF	CUL5	HS71L	P34931	[3-4]	29	12	1	25.4
BIV VIF	CUL5	HSP76	P17066	[3-6]	22	9	1	14.6
BIV VIF	CUL5	HSP72	P54652	[3-8]	18	10	7	15.2
BIV VIF	CUL5	HSP77	P48741	[3-10]	15	6	0	16.3
BIV VIF	CUL5	GRP78	P11021	[3-12]	3	2	1	4.1
BIV VIF	CUL5	TBA1B	P68363	[4]	87	29		71
BIV VIF	CUL5	TBA1A	Q71U36	[4-2]	81	28	2	70.7
BIV VIF	CUL5	TBA4A	P68366	[4-4]	71	23	0	45.8
BIV VIF	CUL5	TBA1C	Q9BQE3	[4-6]	77	24	2	60.8
BIV VIF	CUL5	TBA3C	Q13748	[4-8]	65	21	2	48.7
BIV VIF	CUL5	TBA8	Q9NY65	[4-10]	47	17	2	38.5
BIV VIF	CUL5	TBA3E	Q6PEY2	[4-12]	50	15	2	41.3
BIV VIF	CUL5	TBA4B	Q9H853	[4-14]	8	3	0	10.8
BIV VIF	CUL5	TBAL3	A6NHL2	[4-16]	9	6	0	5.8
BIV VIF	CUL5	K2C1	P04264	[5]	26	20		35.6
BIV VIF	CUL5	K22E	P35908	[5-2]	6	5	4	8.5
BIV VIF	CUL5	K2C6B	P04259	[5-4]	4	3	2	5.9
BIV VIF	CUL5	K2C1B	Q7Z794	[5-6]	2	1	0	2.1
BIV VIF	CUL5	K2C8	P05787	[5-8]	1	1	0	2.3
BIV VIF	CUL5	K2C7	P08729	[5-9]	1	1	0	2.3
BIV VIF	CUL5	GFAP	P14136	[5-10]	1	1	0	2.5
BIV VIF	CUL5	K2C4	P19013	[5-11]	1	1	0	2.1
BIV VIF	CUL5	K2C80	Q6KB66	[5-12]	1	1	0	2.4
BIV VIF	CUL5	K2C8	P05787	[5-13]	1	1	0	2.3
BIV VIF	CUL5	K2C7	P08729	[5-14]	1	1	0	2.3
BIV VIF	CUL5	GFAP	P14136	[5-15]	1	1	0	2.5
BIV VIF	CUL5	K2C4	P19013	[5-16]	1	1	0	2.1
BIV VIF	CUL5	K2C80	Q6KB66	[5-17]	1	1	0	2.4
BIV VIF	CUL5	ELOC	Q15369	[6]	46	12		63.4
BIV VIF	CUL5	K1C9	P35527	[7]	20	15		38.5
BIV VIF	CUL5	ELOB	Q15370	[8]	31	13		88.1
BIV VIF	CUL5	PABP1	P11940	[9]	17	13		24.1
BIV VIF	CUL5	PABP4	Q13310	[9-2]	8	6	0	10.4
BIV VIF	CUL5	PABP3	Q9H361	[9-4]	7	5	0	10.1
BIV VIF	CUL5	PAP1L	Q4VXU2	[9-6]	4	3	0	5.7
BIV VIF	CUL5	PAP1M	Q5JQF8	[9-8]	1	1	0	5.5
BIV VIF	CUL5	RCN2	Q14257	[10]	13	9		37.9
BIV VIF	CUL5	BIV Vif	N/A	[11]	24	9		46.5

BIV VIF	CUL5	DNJA1	P31689	[12]	13	10		41.3
BIV VIF	CUL5	HNRPM	P52272	[13]	11	9		19.2
BIV VIF	CUL5	ADT2	P05141	[14]	8	7		26.8
BIV VIF	CUL5	ADT3	P12236	[14-2]	5	5	2	17.4
BIV VIF	CUL5	TCPE	P48643	[15]	5	5		19.4
BIV VIF	CUL5	TCPB	P78371	[16]	6	6		16.8
BIV VIF	CUL5	HNRPF	P52597	[17]	5	5		21.7
BIV VIF	CUL5	HNRH1	P31943	[17-2]	6	6	5	15.1
BIV VIF	CUL5	IF2B1	Q9NZI8	[18]	5	5		12.8
BIV VIF	CUL5	IF2B3	O00425	[18-2]	1	1	0	2.2
BIV VIF	CUL5	IF2B2	Q9Y6M1	[18-3]	1	1	0	2.2
BIV VIF	CUL5	IF2B3	O00425	[18-4]	1	1	0	2.2
BIV VIF	CUL5	IF2B2	Q9Y6M1	[18-5]	1	1	0	2.2
BIV VIF	CUL5	BAG2	O95816	[19]	10	7		48.3
BIV VIF	CUL5	K1C10	P13645	[20]	6	5		12.8
BIV VIF	CUL5	K1C28	Q7Z3Y7	[20-2]	1	1	0	1.9
BIV VIF	CUL5	K1C27	Q7Z3Y8	[20-3]	1	1	0	2
BIV VIF	CUL5	K1C25	Q7Z3Z0	[20-4]	1	1	0	2
BIV VIF	CUL5	K1C28	Q7Z3Y7	[20-5]	1	1	0	1.9
BIV VIF	CUL5	K1C27	Q7Z3Y8	[20-6]	1	1	0	2
BIV VIF	CUL5	K1C25	Q7Z3Z0	[20-7]	1	1	0	2
BIV VIF	CUL5	AKP8L	Q9ULX6	[21]	6	6		16.6
BIV VIF	CUL5	RBX1	P62877	[22]	4	4		31.5
BIV VIF	CUL5	RL23	P62829	[23]	4	4		27.9
BIV VIF	CUL5	YBOX1	P67809	[24]	3	3		36.7
BIV VIF	CUL5	RL12	P30050	[25]	5	4		33.9
BIV VIF	CUL5	RS5	P46782	[26]	5	3		26
BIV VIF	CUL5	RLA0	P05388	[27]	7	7		32.2
BIV VIF	CUL5	RLA0L	Q8NHW5	[27-2]	5	5	0	21.8
BIV VIF	CUL5	NUCL	P19338	[28]	5	5		11.5
BIV VIF	CUL5	RBX2	Q9UBF6	[29]	2	2		31
BIV VIF	CUL5	RLA2	P05387	[30]	6	4		70.4
BIV VIF	CUL5	RLA1	P05386	[30-2]	2	2	1	28.9
BIV VIF	CUL5	RS16	P62249	[31]	6	6		42.5
BIV VIF	CUL5	RS4X	P62701	[32]	5	5		26.6
BIV VIF	CUL5	TCPG	P49368	[33]	3	3		10.5
BIV VIF	CUL5	EMD	P50402	[34]	4	3		18.1
BIV VIF	CUL5	DNJA3	Q96EY1	[35]	5	5		11.7
BIV VIF	CUL5	RS3	P23396	[36]	4	4		18.1
BIV VIF	CUL5	RS2	P15880	[37]	3	3		11.9
BIV VIF	CUL5	TCPZ	P40227	[38]	3	3		5.5
BIV VIF	CUL5	TCPW	Q92526	[38-2]	2	2	0	2.5
BIV VIF	CUL5	RS3A	P61247	[39]	6	6		25.8
BIV VIF	CUL5	RL30	P62888	[40]	5	3		34.8
BIV VIF	CUL5	TCPA	P17987	[41]	4	3		8.3
BIV VIF	CUL5	C1QBP	Q07021	[42]	5	2		14.9
BIV VIF	CUL5	RS18	P62269	[43]	7	5		34.2

BIV VIF	CUL5	RS17	P08708	[44]	4	3		32.6
BIV VIF	CUL5	RS17L	P0CW22	[44-1]	4	3	0	32.6
BIV VIF	CUL5	RS17	P08708	[44-2]	4	3	0	32.6
BIV VIF	CUL5	RS17L	P0CW22	[44-3]	4	3	0	32.6
BIV VIF	CUL5	TCPQ	P50990	[45]	4	4		10.9
BIV VIF	CUL5	CH60	P10809	[46]	3	3		7.2
BIV VIF	CUL5	DNJA2	O60884	[47]	3	3		15.5
BIV VIF	CUL5	YTHD2	Q9Y5A9	[48]	3	3		15.4
BIV VIF	CUL5	MEP50	Q9BQA1	[49]	3	3		15.5
BIV VIF	CUL5	RS24	P62847	[50]	3	3		28.6
BIV VIF	CUL5	RL35A	P18077	[51]	4	4		28.2
BIV VIF	CUL5	CLPB	Q9H078	[52]	4	4		7.8
BIV VIF	CUL5	RS27	P42677	[53]	3	2		15.5
BIV VIF	CUL5	RS27L	Q71UM5	[53-1]	3	2	0	15.5
BIV VIF	CUL5	RS27	P42677	[53-2]	3	2	0	15.5
BIV VIF	CUL5	RS27L	Q71UM5	[53-3]	3	2	0	15.5
BIV VIF	CUL5	RS8	P62241	[54]	2	2		13.5
BIV VIF	CUL5	NEDD8	Q15843	[55]	2	2		34.6
BIV VIF	CUL5	K2C5	P13647	[56]	3	3		6.4
BIV VIF	CUL5	K2C75	O95678	[56-2]	2	2	0	4.2
BIV VIF	CUL5	K2C6A	P02538	[56-3]	2	2	0	4.1
BIV VIF	CUL5	K2C6C	P48668	[56-4]	2	2	0	4.1
BIV VIF	CUL5	K2C79	Q5XKE5	[56-5]	2	2	0	4.3
BIV VIF	CUL5	K2C75	O95678	[56-6]	2	2	0	4.2
BIV VIF	CUL5	K2C6A	P02538	[56-7]	2	2	0	4.1
BIV VIF	CUL5	K2C6C	P48668	[56-8]	2	2	0	4.1
BIV VIF	CUL5	K2C79	Q5XKE5	[56-9]	2	2	0	4.3
BIV VIF	CUL5	K2C3	P12035	[56-10]	1	1	0	1.8
BIV VIF	CUL5	K22O	Q01546	[56-11]	1	1	0	1.7
BIV VIF	CUL5	K2C3	P12035	[56-12]	1	1	0	1.8
BIV VIF	CUL5	K22O	Q01546	[56-13]	1	1	0	1.7
BIV VIF	CUL5	UBB	P0CG47	[57]	2	2		12.7
BIV VIF	CUL5	UBC	P0CG48	[57-1]	2	2	0	4.2
BIV VIF	CUL5	RS27A	P62979	[57-2]	2	2	0	18.6
BIV VIF	CUL5	RL40	P62987	[57-3]	2	2	0	22.7
BIV VIF	CUL5	UBB	P0CG47	[57-4]	2	2	0	12.7
BIV VIF	CUL5	UBC	P0CG48	[57-5]	2	2	0	4.2
BIV VIF	CUL5	RS27A	P62979	[57-6]	2	2	0	18.6
BIV VIF	CUL5	RL40	P62987	[57-7]	2	2	0	22.7
BIV VIF	CUL5	ANM5	O14744	[58]	3	3		6.4
BIV VIF	CUL5	ACTB	P60709	[59]	1	1		6.1
BIV VIF	CUL5	ACTG	P63261	[59-1]	1	1	0	6.1
BIV VIF	CUL5	POTEE	Q6S8J3	[59-2]	1	1	0	2.1
BIV VIF	CUL5	ACTB	P60709	[59-3]	1	1	0	6.1
BIV VIF	CUL5	ACTG	P63261	[59-4]	1	1	0	6.1
BIV VIF	CUL5	POTEE	Q6S8J3	[59-5]	1	1	0	2.1
BIV VIF	CUL5	RUVB1	Q9Y265	[60]	3	3		8.8

BIV VIF	CUL5	KV201	P01614	[61]	5	1		11.3
BIV VIF	CUL5	KV204	P01617	[61-1]	5	1	0	11.5
BIV VIF	CUL5	KV205	P06309	[61-2]	5	1	0	11.1
BIV VIF	CUL5	KV206	P06310	[61-3]	5	1	0	9.8
BIV VIF	CUL5	KV201	P01614	[61-4]	5	1	0	11.3
BIV VIF	CUL5	KV204	P01617	[61-5]	5	1	0	11.5
BIV VIF	CUL5	KV205	P06309	[61-6]	5	1	0	11.1
BIV VIF	CUL5	KV206	P06310	[61-7]	5	1	0	9.8
BIV VIF	CUL5	RL13	P26373	[62]	3	3		15.2
BIV VIF	CUL5	RL13A	P40429	[63]	2	2		11.3
BIV VIF	CUL5	R13AX	Q6NVV1	[63-2]	1	1	0	10.8
BIV VIF	CUL5	PSME3	P61289	[64]	3	3		16.1
BIV VIF	CUL5	HORN	Q86YZ3	[65]	2	2		1.4
BIV VIF	CUL5	RL37A	P61513	[66]	1	1		19.6
BIV VIF	CUL5	EF1A1	P68104	[67]	4	4		16.9
BIV VIF	CUL5	EF1A3	Q5VTE0	[67-1]	4	4	0	16.9
BIV VIF	CUL5	EF1A1	P68104	[67-2]	4	4	0	16.9
BIV VIF	CUL5	EF1A3	Q5VTE0	[67-3]	4	4	0	16.9
BIV VIF	CUL5	EF1A2	Q05639	[67-4]	2	2	0	5.6
BIV VIF	CUL5	ATD3A	Q9NVI7	[68]	2	2		3.2
BIV VIF	CUL5	ATD3B	Q5T9A4	[68-2]	1	1	0	1.7
BIV VIF	CUL5	ATD3C	Q5T2N8	[68-4]	1	1	0	2.2
BIV VIF	CUL5	HNRPC	P07910	[69]	2	2		8.8
BIV VIF	CUL5	CMC2	Q9UJS0	[70]	2	2		4.6
BIV VIF	CUL5	RS19	P39019	[71]	6	6		33.8
BIV VIF	CUL5	TIM13	Q9Y5L4	[72]	1	1		14.7
BIV VIF	CUL5	ILF2	Q12905	[73]	2	2		9.5
BIV VIF	CUL5	RS11	P62280	[74]	3	3		24.7
BIV VIF	CUL5	TCPH	Q99832	[75]	2	2		4.4
BIV VIF	CUL5	ATPA	P25705	[76]	1	1		2.7
BIV VIF	CUL5	2xStrep	N/A	[77]	3	1		71.4
BIV VIF	CUL5	RL31	P62899	[78]	2	2		18.4
BIV VIF	CUL5	ILF3	Q12906	[79]	3	3		3.9
BIV VIF	CUL5	STRBP	Q96SI9	[79-2]	1	1	0	1.6
BIV VIF	CUL5	RS25	P62851	[80]	2	2		16
BIV VIF	CUL5	RL7	P18124	[81]	2	2		7.7
BIV VIF	CUL5	RL10A	P62906	[82]	3	2		9.7
BIV VIF	CUL5	RL14	P50914	[83]	1	1		5.6
BIV VIF	CUL5	RL9	P32969	[84]	1	1		9.9
BIV VIF	CUL5	H2B1K	O60814	[85]	2	1		11.9
BIV VIF	CUL5	H2B1J	P06899	[85-1]	2	1	-1	11.9
BIV VIF	CUL5	H2B1O	P23527	[85-2]	2	1	-1	11.9
BIV VIF	CUL5	H2B1B	P33778	[85-3]	2	1	-1	11.9
BIV VIF	CUL5	H2BFS	P57053	[85-4]	2	1	-1	11.9
BIV VIF	CUL5	H2B1D	P58876	[85-5]	2	1	-1	11.9
BIV VIF	CUL5	H2B1C	P62807	[85-6]	2	1	-1	11.9
BIV VIF	CUL5	H2B2E	Q16778	[85-7]	2	1	-1	11.9

BIV VIF	CUL5	H2B2F	Q5QNW6	[85-8]	2	1	-1	11.9
BIV VIF	CUL5	H2B3B	Q8N257	[85-9]	2	1	-1	11.9
BIV VIF	CUL5	H2B1H	Q93079	[85-10]	2	1	-1	11.9
BIV VIF	CUL5	H2B1N	Q99877	[85-11]	2	1	-1	11.9
BIV VIF	CUL5	H2B1M	Q99879	[85-12]	2	1	-1	11.9
BIV VIF	CUL5	H2B1L	Q99880	[85-13]	2	1	-1	11.9
BIV VIF	CUL5	H2B1K	O60814	[85-14]	2	1	-1	11.9
BIV VIF	CUL5	H2B1J	P06899	[85-15]	2	1	-1	11.9
BIV VIF	CUL5	H2B1O	P23527	[85-16]	1	1	0	11.9
BIV VIF	CUL5	H2B1B	P33778	[85-17]	2	1	-1	11.9
BIV VIF	CUL5	H2BFS	P57053	[85-18]	1	1	0	11.9
BIV VIF	CUL5	H2B1D	P58876	[85-19]	2	1	-1	11.9
BIV VIF	CUL5	H2B1C	P62807	[85-20]	2	1	-1	11.9
BIV VIF	CUL5	H2B2E	Q16778	[85-21]	1	1	0	11.9
BIV VIF	CUL5	H2B2F	Q5QNW6	[85-22]	1	1	0	11.9
BIV VIF	CUL5	H2B3B	Q8N257	[85-23]	1	1	0	11.9
BIV VIF	CUL5	H2B1H	Q93079	[85-24]	2	1	-1	11.9
BIV VIF	CUL5	H2B1N	Q99877	[85-25]	2	1	-1	11.9
BIV VIF	CUL5	H2B1M	Q99879	[85-26]	2	1	-1	11.9
BIV VIF	CUL5	H2B1L	Q99880	[85-27]	2	1	-1	11.9
BIV VIF	CUL5	RL11	P62913	[86]	2	2		12.9
BIV VIF	CUL5	DDX17	Q92841	[87]	2	2		4.2
BIV VIF	CUL5	DDX5	P17844	[87-2]	1	1	0	2
BIV VIF	CUL5	HNRH2	P55795	[88]	1	1		2.9
BIV VIF	CUL5	RS10	P46783	[89]	2	2		14.5
BIV VIF	CUL5	RS10L	Q9NQ39	[89-2]	1	1	0	8.5
BIV VIF	CUL5	TIM8B	Q9Y5J9	[90]	1	1		16.9
BIV VIF	CUL5	RL21	P46778	[91]	1	1		9.4
BIV VIF	CUL5	IRS4	O14654	[92]	2	2		4.9
BIV VIF	CUL5	DNJB5	O75953	[93]	1	1		7.8
BIV VIF	CUL5	STAU1	O95793	[94]	1	1		2.8
BIV VIF	CUL5	HS90A	P07900	[95]	2	2		4.4
BIV VIF	CUL5	HS90B	P08238	[95-1]	2	2	0	4.4
BIV VIF	CUL5	HS902	Q14568	[95-2]	2	2	0	9.3
BIV VIF	CUL5	HS90A	P07900	[95-3]	2	2	0	4.4
BIV VIF	CUL5	HS90B	P08238	[95-4]	2	2	0	4.4
BIV VIF	CUL5	HS902	Q14568	[95-5]	2	2	0	9.3
BIV VIF	CUL5	PCBP2	Q15366	[96]	2	2		7.9
BIV VIF	CUL5	APC11	Q9NYG5	[97]	1	1		17.9
BIV VIF	CUL5	RL10	P27635	[98]	2	2		17.8
BIV VIF	CUL5	ANM1	Q99873	[99]	3	3		11.6
BIV VIF	CUL5	TIM50	Q3ZCQ8	[100]	1	1		4.8
BIV VIF	CUL5	PGAM5	Q96HS1	[101]	1	1		3.5
BIV VIF	CUL5	DJB11	Q9UBS4	[102]	1	1		9.5
BIV VIF	CUL5	LSM12	Q3MHD2	[103]	2	2		19
BIV VIF	CUL5	RL27A	P46776	[104]	1	1		7.4

BIV VIF	CUL5	HNRPU	Q00839	[105]	1	1		1.8
BIV VIF	CUL5	RS7	P62081	[106]	1	1		6.2
BIV VIF	CUL5	RS12	P25398	[107]	1	1		6.8
BIV VIF	CUL5	TCPD	P50991	[108]	1	1		3
BIV VIF	CUL5	NP1L1	P55209	[109]	1	1		2.6
BIV VIF	CUL5	NP1L4	Q99733	[109-1]	1	1	0	2.7
BIV VIF	CUL5	NP1L1	P55209	[109-2]	1	1	0	2.6
BIV VIF	CUL5	NP1L4	Q99733	[109-3]	1	1	0	2.7
BIV VIF	CUL5	RS14	P62263	[110]	1	1		13.9
BIV VIF	CUL5	PRP19	Q9UMS4	[111]	2	2		10.1
BIV VIF	CUL5	ACTA	P62736	[112]	1	1		6.1
BIV VIF	CUL5	ACTH	P63267	[112-1]	1	1	0	6.1
BIV VIF	CUL5	ACTC	P68032	[112-2]	1	1	0	6.1
BIV VIF	CUL5	ACTS	P68133	[112-3]	1	1	0	6.1
BIV VIF	CUL5	ACTA	P62736	[112-4]	1	1	0	6.1
BIV VIF	CUL5	ACTH	P63267	[112-5]	1	1	0	6.1
BIV VIF	CUL5	ACTC	P68032	[112-6]	1	1	0	6.1
BIV VIF	CUL5	ACTS	P68133	[112-7]	1	1	0	6.1
BIV VIF	CUL5	RS23	P62266	[113]	1	1		7.7
BIV VIF	CUL5	HAX1	O00165	[114]	1	1		9
BIV VIF	CUL5	RFOX2	O43251	[115]	1	1		3.8
BIV VIF	CUL5	RFOX1	Q9NWB1	[115-1]	1	1	0	3.8
BIV VIF	CUL5	RFOX2	O43251	[115-2]	1	1	0	3.8
BIV VIF	CUL5	RFOX1	Q9NWB1	[115-3]	1	1	0	3.8
BIV VIF	CUL5	CN166	Q9Y224	[116]	1	1		5.7
BIV VIF	CUL5	DPM1	O60762	[117]	2	2		8.5
BIV VIF	CUL5	RL27	P61353	[118]	2	2		22.1
BIV VIF	CUL5	GRP75	P38646	[119]	2	2		3.8
BIV VIF	CUL5	DREB	Q16643	[120]	1	1		4.3
BIV VIF	CUL5	DNJC7	Q99615	[121]	1	1		5.3
BIV VIF	CUL5	HS105	Q92598	[123]	1	1		1.6
BIV VIF	CUL5	HNRPR	O43390	[124]	3	3		4.9
BIV VIF	CUL5	HNRPQ	O60506	[124-2]	2	2	0	3.2
BIV VIF	CUL5	HSPB1	P04792	[125]	1	1		8.3
BIV VIF	CUL5	RS13	P62277	[126]	1	1		7.9
BIV VIF	CUL5	RL28	P46779	[127]	1	1		8
BIV VIF	CUL5	PHB2	Q99623	[128]	1	1		4.3
BIV VIF	CUL5	SRP14	P37108	[129]	1	1		11
BIV VIF	CUL5	MSI1H	O43347	[131]	1	1		4.7
BIV VIF	CUL5	RS6	P62753	[132]	1	1		4
BIV VIF	CUL5	SSRD	P51571	[133]	1	1		6.4
BIV VIF	CUL5	HIG1A	Q9Y241	[134]	1	1		20.4
BIV VIF	CUL5	1433E	P62258	[135]	1	1		4.7
BIV VIF	CUL5	F195B	C9JLW8	[136]	1	1		11.3
BIV VIF	CUL5	RL18A	Q02543	[137]	1	1		8
BIV VIF	CUL5	RL24	P83731	[139]	1	1		5.1

BIV VIF	CUL5	SERA	O43175	[140]	2	1		2.8
BIV VIF	CUL5	DHX9	Q08211	[141]	1	1		0.9
BIV VIF	CUL5	FEZF2	Q8TBJ5	[143]	1	1		7
BIV VIF	CUL5	SC16A	O15027	[145]	1	1		0.5
BIV VIF	CUL5	PRKDC	P78527	[146]	1	1		0.3
BIV VIF	CUL5	SUGP2	Q8IX01	[147]	1	1		1
BIV VIF	CUL5	BAHC1	Q9P281	[148]	1	1		0.6
FIV VIF	CUL5	CUL5	Q93034	[1]	273	70		61.4
FIV VIF	CUL5	HSP71	P08107	[2]	64	29		50.7
FIV VIF	CUL5	HSP7C	P11142	[2-2]	52	32	30	45
FIV VIF	CUL5	HS71L	P34931	[2-4]	27	11	1	22.2
FIV VIF	CUL5	HSP76	P17066	[2-6]	14	8	1	13.7
FIV VIF	CUL5	HSP72	P54652	[2-8]	14	9	7	13.8
FIV VIF	CUL5	HSP77	P48741	[2-10]	11	5	0	14.2
FIV VIF	CUL5	GRP78	P11021	[2-12]	3	3	2	6.3
FIV VIF	CUL5	TBB2C	P68371	[3]	62	35		68.8
FIV VIF	CUL5	TBB5	P07437	[3-1]	71	34	6	68.9
FIV VIF	CUL5	TBB2C	P68371	[3-3]	61	34	-1	68.8
FIV VIF	CUL5	TBB4	P04350	[3-4]	56	32	1	62.2
FIV VIF	CUL5	TBB2A	Q13885	[3-6]	49	28	5	64
FIV VIF	CUL5	TBB2B	Q9BVA1	[3-7]	49	28	5	64
FIV VIF	CUL5	TBB2A	Q13885	[3-8]	49	28	5	64
FIV VIF	CUL5	TBB2B	Q9BVA1	[3-9]	49	28	5	64
FIV VIF	CUL5	TBB3	Q13509	[3-10]	35	21	2	33.1
FIV VIF	CUL5	TBB8	Q3ZCM7	[3-12]	25	15	-1	22.7
FIV VIF	CUL5	TBB8B	A6NNZ2	[3-14]	23	13	-1	19.4
FIV VIF	CUL5	TBB6	Q9BUF5	[3-16]	18	11	1	19.5
FIV VIF	CUL5	YI016	A6NKZ8	[3-18]	12	6	0	9.4
FIV VIF	CUL5	TBB1	Q9H4B7	[3-20]	6	4	0	4.7
FIV VIF	CUL5	FIV VIV	N/A	[4]	157	28		64.5
FIV VIF	CUL5	TBA1B	P68363	[5]	70	30		78.3
FIV VIF	CUL5	TBA1A	Q71U36	[5-2]	63	29	2	78
FIV VIF	CUL5	TBA1C	Q9BQE3	[5-4]	61	26	3	71.9
FIV VIF	CUL5	TBA4A	P68366	[5-6]	54	23	0	44.6
FIV VIF	CUL5	TBA3C	Q13748	[5-8]	51	23	2	57.3
FIV VIF	CUL5	TBA3E	Q6PEY2	[5-10]	39	17	2	50
FIV VIF	CUL5	TBA8	Q9NY65	[5-12]	38	17	1	33.4
FIV VIF	CUL5	TBA4B	Q9H853	[5-14]	8	3	0	10.8
FIV VIF	CUL5	TBAL3	A6NHL2	[5-16]	9	6	0	6.5
FIV VIF	CUL5	K2C1	P04264	[6]	27	22		40.1
FIV VIF	CUL5	K22E	P35908	[6-2]	7	6	5	13.1
FIV VIF	CUL5	K2C6B	P04259	[6-4]	3	3	2	5.9
FIV VIF	CUL5	K2C1B	Q7Z794	[6-6]	2	1	0	2.1
FIV VIF	CUL5	K2C8	P05787	[6-8]	1	1	0	2.3
FIV VIF	CUL5	K2C7	P08729	[6-9]	1	1	0	2.3
FIV VIF	CUL5	GFAP	P14136	[6-10]	1	1	0	2.5
FIV VIF	CUL5	K2C4	P19013	[6-11]	1	1	0	2.1

FIV VIF	CUL5	K2C80	Q6KB66	[6-12]	1	1	0	2.4
FIV VIF	CUL5	K2C8	P05787	[6-13]	1	1	0	2.3
FIV VIF	CUL5	K2C7	P08729	[6-14]	1	1	0	2.3
FIV VIF	CUL5	GFAP	P14136	[6-15]	1	1	0	2.5
FIV VIF	CUL5	K2C4	P19013	[6-16]	1	1	0	2.1
FIV VIF	CUL5	K2C80	Q6KB66	[6-17]	1	1	0	2.4
FIV VIF	CUL5	ELOC	Q15369	[7]	57	13		63.4
FIV VIF	CUL5	HS90B	P08238	[8]	27	18		34.7
FIV VIF	CUL5	HS90A	P07900	[8-2]	26	20	12	32.8
FIV VIF	CUL5	H90B2	Q58FF8	[8-4]	6	4	0	13.4
FIV VIF	CUL5	HS902	Q14568	[8-6]	7	4	1	16
FIV VIF	CUL5	H90B3	Q58FF7	[8-8]	7	5	0	11.2
FIV VIF	CUL5	TRAP1	Q12931	[8-10]	3	1	0	2
FIV VIF	CUL5	H90B4	Q58FF6	[8-12]	2	2	1	7.1
FIV VIF	CUL5	HS904	Q58FG1	[8-14]	4	2	0	5.7
FIV VIF	CUL5	ENPL	P14625	[8-16]	1	1	0	1.5
FIV VIF	CUL5	K1C9	P35527	[9]	18	15		40.1
FIV VIF	CUL5	ELOB	Q15370	[10]	38	13		93.2
FIV VIF	CUL5	K1C10	P13645	[11]	11	10		27.9
FIV VIF	CUL5	K1C16	P08779	[11-2]	3	3	2	7.8
FIV VIF	CUL5	K1C14	P02533	[11-4]	3	3	2	7.8
FIV VIF	CUL5	K1C28	Q7Z3Y7	[11-6]	2	2	0	3.9
FIV VIF	CUL5	K1C27	Q7Z3Y8	[11-7]	2	2	0	3.9
FIV VIF	CUL5	K1C25	Q7Z3Z0	[11-8]	2	2	0	4
FIV VIF	CUL5	K1C28	Q7Z3Y7	[11-9]	2	2	0	3.9
FIV VIF	CUL5	K1C27	Q7Z3Y8	[11-10]	2	2	0	3.9
FIV VIF	CUL5	K1C25	Q7Z3Z0	[11-11]	2	2	0	4
FIV VIF	CUL5	DNJA1	P31689	[12]	15	12		42.8
FIV VIF	CUL5	RCN2	Q14257	[13]	8	8		36.9
FIV VIF	CUL5	RBX2	Q9UBF6	[14]	4	3		38.9
FIV VIF	CUL5	ADT2	P05141	[15]	8	7		26.8
FIV VIF	CUL5	ADT3	P12236	[15-2]	4	4	2	14.1
FIV VIF	CUL5	ADT1	P12235	[15-4]	2	2	1	7.7
FIV VIF	CUL5	ADT4	Q9H0C2	[15-6]	1	1	0	3.8
FIV VIF	CUL5	RBX1	P62877	[16]	5	4		31.5
FIV VIF	CUL5	GRP75	P38646	[17]	4	4		8
FIV VIF	CUL5	ASB6	Q9NWX5	[18]	5	4		13.5
FIV VIF	CUL5	CLPB	Q9H078	[19]	4	4		8.3
FIV VIF	CUL5	NEDD8	Q15843	[20]	5	3		45.7
FIV VIF	CUL5	DNJA2	O60884	[21]	3	3		12.6
FIV VIF	CUL5	DDB1	Q16531	[22]	3	3		5
FIV VIF	CUL5	TEBP	Q15185	[23]	3	3		20
FIV VIF	CUL5	KV201	P01614	[24]	3	1		11.3
FIV VIF	CUL5	KV204	P01617	[24-1]	3	1	0	11.5
FIV VIF	CUL5	KV205	P06309	[24-2]	3	1	0	11.1
FIV VIF	CUL5	KV206	P06310	[24-3]	3	1	0	9.8
FIV VIF	CUL5	KV201	P01614	[24-4]	3	1	0	11.3

FIV VIF	CUL5	KV204	P01617	[24-5]	3	1	0	11.5
FIV VIF	CUL5	KV205	P06309	[24-6]	3	1	0	11.1
FIV VIF	CUL5	KV206	P06310	[24-7]	3	1	0	9.8
FIV VIF	CUL5	UBB	P0CG47	[25]	3	2		12.7
FIV VIF	CUL5	UBC	P0CG48	[25-1]	3	2	0	4.2
FIV VIF	CUL5	RS27A	P62979	[25-2]	3	2	0	18.6
FIV VIF	CUL5	RL40	P62987	[25-3]	3	2	0	22.7
FIV VIF	CUL5	UBB	P0CG47	[25-4]	3	2	0	12.7
FIV VIF	CUL5	UBC	P0CG48	[25-5]	3	2	0	4.2
FIV VIF	CUL5	RS27A	P62979	[25-6]	3	2	0	18.6
FIV VIF	CUL5	RL40	P62987	[25-7]	3	2	0	22.7
FIV VIF	CUL5	TIM13	Q9Y5L4	[26]	2	2		25.3
FIV VIF	CUL5	NP1L1	P55209	[27]	2	2		6.9
FIV VIF	CUL5	RLA0	P05388	[28]	2	2		7.6
FIV VIF	CUL5	RLA0L	Q8NHW5	[28-1]	2	2	0	7.6
FIV VIF	CUL5	RLA0	P05388	[28-2]	2	2	0	7.6
FIV VIF	CUL5	RLA0L	Q8NHW5	[28-3]	2	2	0	7.6
FIV VIF	CUL5	HS905	Q58FG0	[29]	2	2		7.5
FIV VIF	CUL5	2xStrep	N/A	[30]	6	1		71.4
FIV VIF	CUL5	AT1A1	P05023	[31]	3	3		4.3
FIV VIF	CUL5	AT1A3	P13637	[31-2]	1	1	0	1.8
FIV VIF	CUL5	AT1A2	P50993	[31-3]	1	1	0	1.8
FIV VIF	CUL5	AT1A3	P13637	[31-4]	1	1	0	1.8
FIV VIF	CUL5	AT1A2	P50993	[31-5]	1	1	0	1.8
FIV VIF	CUL5	PABP1	P11940	[32]	2	2		4.1
FIV VIF	CUL5	PAP1L	Q4VXU2	[32-1]	2	2	0	4.2
FIV VIF	CUL5	PABP3	Q9H361	[32-2]	2	2	0	4.1
FIV VIF	CUL5	PABP1	P11940	[32-3]	2	2	0	4.1
FIV VIF	CUL5	PAP1L	Q4VXU2	[32-4]	2	2	0	4.2
FIV VIF	CUL5	PABP3	Q9H361	[32-5]	2	2	0	4.1
FIV VIF	CUL5	PAP1M	Q5JQF8	[32-6]	1	1	0	5.5
FIV VIF	CUL5	PABP4	Q13310	[32-8]	1	1	0	2.3
FIV VIF	CUL5	DNJC7	Q99615	[33]	2	2		8.9
FIV VIF	CUL5	TOM40	O96008	[34]	2	2		12.2
FIV VIF	CUL5	RS5	P46782	[35]	3	2		16.2
FIV VIF	CUL5	EF1A1	P68104	[36]	5	3		11.7
FIV VIF	CUL5	EF1A3	Q5VTE0	[36-1]	5	3	0	11.7
FIV VIF	CUL5	EF1A1	P68104	[36-2]	5	3	0	11.7
FIV VIF	CUL5	EF1A3	Q5VTE0	[36-3]	5	3	0	11.7
FIV VIF	CUL5	EF1A2	Q05639	[36-4]	3	2	0	5.6
FIV VIF	CUL5	ASB13	Q8WXK3	[37]	2	2		6.8
FIV VIF	CUL5	K2C75	O95678	[38]	2	2		4.2
FIV VIF	CUL5	K2C6A	P02538	[38-1]	2	2	0	4.1
FIV VIF	CUL5	K2C5	P13647	[38-2]	2	2	0	3.9
FIV VIF	CUL5	K2C6C	P48668	[38-3]	2	2	0	4.1
FIV VIF	CUL5	K2C79	Q5XKE5	[38-4]	2	2	0	4.3

FIV VIF	CUL5	K2C75	O95678	[38-5]	2	2	0	4.2
FIV VIF	CUL5	K2C6A	P02538	[38-6]	2	2	0	4.1
FIV VIF	CUL5	K2C5	P13647	[38-7]	2	2	0	3.9
FIV VIF	CUL5	K2C6C	P48668	[38-8]	2	2	0	4.1
FIV VIF	CUL5	K2C79	Q5XKE5	[38-9]	2	2	0	4.3
FIV VIF	CUL5	K2C3	P12035	[38-10]	1	1	0	1.8
FIV VIF	CUL5	K22O	Q01546	[38-11]	1	1	0	1.7
FIV VIF	CUL5	K2C3	P12035	[38-12]	1	1	0	1.8
FIV VIF	CUL5	K22O	Q01546	[38-13]	1	1	0	1.7
FIV VIF	CUL5	FEM1B	Q9UK73	[39]	2	2		3.7
FIV VIF	CUL5	BAG2	O95816	[40]	2	2		12.8
FIV VIF	CUL5	RL12	P30050	[41]	2	2		19.4
FIV VIF	CUL5	RPB2	P30876	[42]	2	2		4
FIV VIF	CUL5	SSRA	P43307	[43]	1	1		5.2
FIV VIF	CUL5	FETUA	P02765	[44]	1	1		3.5
FIV VIF	CUL5	AT2A2	P16615	[45]	2	2		2.5
FIV VIF	CUL5	AT2A3	Q93084	[45-2]	1	1	0	1.4
FIV VIF	CUL5	LSM12	Q3MHD2	[46]	3	3		28.2
FIV VIF	CUL5	RL23	P62829	[47]	2	2		25
FIV VIF	CUL5	CH60	P10809	[48]	2	2		4.2
FIV VIF	CUL5	RS27	P42677	[49]	2	1		15.5
FIV VIF	CUL5	RS27L	Q71UM5	[49-1]	2	1	0	15.5
FIV VIF	CUL5	RS27	P42677	[49-2]	2	1	0	15.5
FIV VIF	CUL5	RS27L	Q71UM5	[49-3]	2	1	0	15.5
FIV VIF	CUL5	APC11	Q9NYG5	[50]	3	2		31
FIV VIF	CUL5	PPP5	P53041	[51]	2	2		5.2
FIV VIF	CUL5	SSRD	P51571	[52]	1	1		6.4
FIV VIF	CUL5	PYR1	P27708	[53]	1	1		1.2
FIV VIF	CUL5	K0664	O75153	[54]	1	1		1
FIV VIF	CUL5	NUBP2	Q9Y5Y2	[55]	1	1		10
FIV VIF	CUL5	C1QBP	Q07021	[56]	1	1		9.6
FIV VIF	CUL5	ODO2	P36957	[57]	1	1		2.6
FIV VIF	CUL5	YBOX1	P67809	[58]	1	1		9.3
FIV VIF	CUL5	HIG1A	Q9Y241	[59]	1	1		20.4
FIV VIF	CUL5	CHD3	Q12873	[60]	4	1		0.7
FIV VIF	CUL5	ANM5	O14744	[61]	1	1		2
FIV VIF	CUL5	TIM50	Q3ZCQ8	[62]	1	1		4.8
FIV VIF	CUL5	DNJA3	Q96EY1	[63]	1	1		3.3
FIV VIF	CUL5	SF3B3	Q15393	[64]	1	1		2
FIV VIF	CUL5	GET4	Q7L5D6	[65]	1	1		4.3
FIV VIF	CUL5	K1C19	P08727	[66]	1	1		2.2
FIV VIF	CUL5	K1C15	P19012	[66-1]	1	1	0	2
FIV VIF	CUL5	K1C17	Q04695	[66-2]	1	1	0	2.1
FIV VIF	CUL5	K1C19	P08727	[66-3]	1	1	0	2.2
FIV VIF	CUL5	K1C15	P19012	[66-4]	1	1	0	2
FIV VIF	CUL5	K1C17	Q04695	[66-5]	1	1	0	2.1
FIV VIF	CUL5	RS3	P23396	[67]	1	1		5.8

FIV VIF	CUL5	TCPQ	P50990	[68]	2	2		4
FIV VIF	CUL5	HPBP1	Q9NZL4	[69]	1	1		4.4
FIV VIF	CUL5	SERA	O43175	[70]	1	1		2.8
FIV VIF	CUL5	CYBP	Q9HB71	[71]	1	1		6.1
FIV VIF	CUL5	RL11	P62913	[72]	2	2		12.9
FIV VIF	CUL5	THIO	P10599	[73]	1	1		8.6
FIV VIF	CUL5	RS19	P39019	[74]	1	1		6.2
FIV VIF	CUL5	TOM22	Q9NS69	[75]	1	1		7.7
FIV VIF	CUL5	NDUA4	O00483	[76]	1	1		12.3
FIV VIF	CUL5	SRP09	P49458	[77]	1	1		12.8
FIV VIF	CUL5	PGAM5	Q96HS1	[78]	1	1		3.5
FIV VIF	CUL5	RLA1	P05386	[79]	1	1		14
FIV VIF	CUL5	TERA	P55072	[80]	1	1		1.6
FIV VIF	CUL5	TCPH	Q99832	[81]	2	2		6.3
FIV VIF	CUL5	TRY1	P07477	[82]	1	1		3.2
FIV VIF	CUL5	TMPSD	Q9BYE2	[82-1]	1	1	0	1.4
FIV VIF	CUL5	TRY1	P07477	[82-2]	1	1	0	3.2
FIV VIF	CUL5	TMPSD	Q9BYE2	[82-3]	1	1	0	1.4
FIV VIF	CUL5	LSR	Q86X29	[83]	2	1		1.5
FIV VIF	CUL5	PPP6	O00743	[84]	1	1		4.3
FIV VIF	CUL5	SOCS2	O14508	[85]	1	1		9.1
FIV VIF	CUL5	HNRH1	P31943	[86]	1	1		2.9
FIV VIF	CUL5	HNRH2	P55795	[86-1]	1	1	0	2.9
FIV VIF	CUL5	HNRH1	P31943	[86-2]	1	1	0	2.9
FIV VIF	CUL5	HNRH2	P55795	[86-3]	1	1	0	2.9
SIVmac VIF	CUL5	CUL5	Q93034	[1]	257	68		63.8
SIVmac VIF	CUL5	TBB2C	P68371	[2]	114	43		81.1
SIVmac VIF	CUL5	TBB5	P07437	[2-2]	118	42	8	81.3
SIVmac VIF	CUL5	TBB2B	Q9BVA1	[2-4]	95	38	8	78.4
SIVmac VIF	CUL5	TBB2A	Q13885	[2-6]	95	38	9	72.4
SIVmac VIF	CUL5	TBB4	P04350	[2-8]	97	36	4	74.5
SIVmac VIF	CUL5	TBB3	Q13509	[2-10]	60	23	4	35.8
SIVmac VIF	CUL5	TBB8	Q3ZCM7	[2-12]	42	16	0	22.7
SIVmac VIF	CUL5	TBB6	Q9BUF5	[2-14]	38	18	7	36.1
SIVmac VIF	CUL5	TBB8B	A6NNZ2	[2-16]	38	14	0	19.4
SIVmac VIF	CUL5	YI016	A6NKZ8	[2-18]	19	6	0	9.4
SIVmac VIF	CUL5	TBB1	Q9H4B7	[2-20]	10	4	0	4.7
SIVmac	CUL5	HSP71	P08107	[3]	105	36		57.4

VIF								
SIVmac VIF	CUL5	HSP7C	P11142	[3-2]	56	31	28	44.1
SIVmac VIF	CUL5	HS71L	P34931	[3-4]	47	16	1	29.2
SIVmac VIF	CUL5	HSP76	P17066	[3-6]	23	9	1	14.6
SIVmac VIF	CUL5	HSP72	P54652	[3-8]	20	10	7	15.2
SIVmac VIF	CUL5	HSP77	P48741	[3-10]	15	6	0	16.3
SIVmac VIF	CUL5	GRP78	P11021	[3-12]	3	2	1	4.1
SIVmac VIF	CUL5	TBA1B	P68363	[4]	89	31		71.4
SIVmac VIF	CUL5	TBA1A	Q71U36	[4-2]	82	30	2	71.2
SIVmac VIF	CUL5	TBA1C	Q9BQE3	[4-4]	74	28	4	71
SIVmac VIF	CUL5	TBA4A	P68366	[4-6]	72	25	0	46.2
SIVmac VIF	CUL5	TBA3C	Q13748	[4-8]	68	24	2	50.4
SIVmac VIF	CUL5	TBA8	Q9NY65	[4-10]	44	19	2	36.5
SIVmac VIF	CUL5	TBA3E	Q6PEY2	[4-12]	51	16	2	41.3
SIVmac VIF	CUL5	TBAL3	A6NHL2	[4-14]	9	8	1	10.3
SIVmac VIF	CUL5	TBA4B	Q9H853	[4-16]	9	3	0	10.8
SIVmac VIF	CUL5	ELOC	Q15369	[5]	51	14		71.4
SIVmac VIF	CUL5	K2C1	P04264	[6]	26	20		35.4
SIVmac VIF	CUL5	K22E	P35908	[6-2]	13	11	10	25.7
SIVmac VIF	CUL5	K2C6B	P04259	[6-4]	5	4	3	7.4
SIVmac VIF	CUL5	K2C4	P19013	[6-6, 84-4]	2	2	1	3.7
SIVmac VIF	CUL5	K2C1B	Q7Z794	[6-8]	2	1	0	2.1
SIVmac VIF	CUL5	K2C8	P05787	[6-10]	1	1	0	2.3
SIVmac VIF	CUL5	K2C7	P08729	[6-11]	1	1	0	2.3
SIVmac VIF	CUL5	GFAP	P14136	[6-12]	1	1	0	2.5
SIVmac VIF	CUL5	K2C80	Q6KB66	[6-13]	1	1	0	2.4
SIVmac VIF	CUL5	K2C8	P05787	[6-14]	1	1	0	2.3

SIVmac VIF	CUL5	K2C7	P08729	[6-15]	1	1	0	2.3
SIVmac VIF	CUL5	GFAP	P14136	[6-16]	1	1	0	2.5
SIVmac VIF	CUL5	K2C80	Q6KB66	[6-17]	1	1	0	2.4
SIVmac VIF	CUL5	HS90B	P08238	[7]	25	17		33.8
SIVmac VIF	CUL5	HS90A	P07900	[7-2]	21	15	7	26.9
SIVmac VIF	CUL5	H90B3	Q58FF7	[7-4]	7	5	0	11.1
SIVmac VIF	CUL5	HS904	Q58FG1	[7-6]	5	2	0	5.7
SIVmac VIF	CUL5	H90B2	Q58FF8	[7-8]	7	4	0	13.4
SIVmac VIF	CUL5	HS902	Q14568	[7-10]	8	4	1	16
SIVmac VIF	CUL5	H90B4	Q58FF6	[7-12]	3	3	2	7.3
SIVmac VIF	CUL5	TRAP1	Q12931	[7-14]	1	1	0	2
SIVmac VIF	CUL5	ENPL	P14625	[7-16]	1	1	0	1.5
SIVmac VIF	CUL5	PEBB	Q13951	[8]	41	12		53.3
SIVmac VIF	CUL5	K1C9	P35527	[9]	25	18		41.6
SIVmac VIF	CUL5	ELOB	Q15370	[10]	38	14		91.5
SIVmac VIF	CUL5	DNJA1	P31689	[11]	23	16		54.7
SIVmac VIF	CUL5	PABP1	P11940	[12]	17	13		27
SIVmac VIF	CUL5	PABP4	Q13310	[12-2]	10	8	1	16.1
SIVmac VIF	CUL5	PABP3	Q9H361	[12-4]	10	7	0	13.9
SIVmac VIF	CUL5	PAP1L	Q4VXU2	[12-6]	4	3	0	5.5
SIVmac VIF	CUL5	PAP1M	Q5JQF8	[12-8]	1	1	0	5.5
SIVmac VIF	CUL5	SIVmac Vif	N/A	[13]	27	12		50
SIVmac VIF	CUL5	RCN2	Q14257	[14]	12	8		37.5
SIVmac VIF	CUL5	RS4X	P62701	[15]	14	13		47.9
SIVmac VIF	CUL5	RS4Y1	P22090	[15-2]	4	4	0	12.5
SIVmac VIF	CUL5	RS4Y2	Q8TD47	[15-4]	4	4	0	14.1
SIVmac	CUL5	RLA0	P05388	[16]	8	8		35.6

VIF								
SIVmac VIF	CUL5	RLA0L	Q8NHW 5	[16-2]	6	6	0	25.2
SIVmac VIF	CUL5	ABC3C	Q9NRW 3	[17]	15	6		54.2
SIVmac VIF	CUL5	ABC3F	Q8IUX4	[17-2]	4	1	0	3.2
SIVmac VIF	CUL5	ABC3D	Q96AK3	[17-3]	4	1	0	3.1
SIVmac VIF	CUL5	ABC3F	Q8IUX4	[17-4]	4	1	0	3.2
SIVmac VIF	CUL5	ABC3D	Q96AK3	[17-5]	4	1	0	3.1
SIVmac VIF	CUL5	DNJA2	O60884	[18]	13	10		35.9
SIVmac VIF	CUL5	RS5	P46782	[19]	10	6		32.8
SIVmac VIF	CUL5	RS2	P15880	[20]	9	8		32.1
SIVmac VIF	CUL5	YBOX1	P67809	[21]	8	6		39.2
SIVmac VIF	CUL5	DBPA	P16989	[21-2]	2	2	0	6.7
SIVmac VIF	CUL5	YBOX2	Q9Y2T7	[21-3]	2	2	0	6.9
SIVmac VIF	CUL5	DBPA	P16989	[21-4]	2	2	0	6.7
SIVmac VIF	CUL5	YBOX2	Q9Y2T7	[21-5]	2	2	0	6.9
SIVmac VIF	CUL5	ADT2	P05141	[22]	12	7		25.8
SIVmac VIF	CUL5	ADT3	P12236	[22-2]	10	8	4	30.5
SIVmac VIF	CUL5	ADT1	P12235	[22-4]	7	5	2	19.8
SIVmac VIF	CUL5	ADT4	Q9H0C2	[22-6]	2	1	0	3.8
SIVmac VIF	CUL5	HNRH1	P31943	[23]	9	8		24.1
SIVmac VIF	CUL5	HNRPF	P52597	[23-2]	7	6	4	25.3
SIVmac VIF	CUL5	HNRH2	P55795	[23-4]	4	3	0	8.7
SIVmac VIF	CUL5	RS3	P23396	[24]	10	7		46.1
SIVmac VIF	CUL5	HNRPU	Q00839	[25]	6	5		13
SIVmac VIF	CUL5	IRS4	O14654	[26]	9	9		14.3
SIVmac VIF	CUL5	AKP8L	Q9ULX6	[27]	7	7		17
SIVmac VIF	CUL5	HNRPM	P52272	[28]	6	6		13.2

SIVmac VIF	CUL5	NP1L1	P55209	[29]	8	6		22
SIVmac VIF	CUL5	NP1L4	Q99733	[29-2]	4	4	3	15.5
SIVmac VIF	CUL5	NUCL	P19338	[30]	10	7		13.8
SIVmac VIF	CUL5	RL30	P62888	[31]	6	6		58.3
SIVmac VIF	CUL5	RS8	P62241	[32]	6	6		37
SIVmac VIF	CUL5	EMD	P50402	[33]	4	4		29.9
SIVmac VIF	CUL5	IPO4	Q8TEX9	[34]	6	6		9.8
SIVmac VIF	CUL5	DDB1	Q16531	[35]	8	8		10.8
SIVmac VIF	CUL5	IF2B1	Q9NZI8	[36]	5	5		12.3
SIVmac VIF	CUL5	IF2B3	O00425	[36-2]	1	1	0	2.2
SIVmac VIF	CUL5	IF2B2	Q9Y6M1	[36-3]	1	1	0	2.2
SIVmac VIF	CUL5	IF2B3	O00425	[36-4]	1	1	0	2.2
SIVmac VIF	CUL5	IF2B2	Q9Y6M1	[36-5]	1	1	0	2.2
SIVmac VIF	CUL5	RBX1	P62877	[37]	8	4		31.5
SIVmac VIF	CUL5	RS3A	P61247	[38]	8	7		26.1
SIVmac VIF	CUL5	ANM5	O14744	[39]	6	6		15.4
SIVmac VIF	CUL5	HNRPQ	O60506	[40]	7	7		16.7
SIVmac VIF	CUL5	HNRPR	O43390	[40-2]	4	4	2	7.4
SIVmac VIF	CUL5	RL12	P30050	[41]	6	5		43
SIVmac VIF	CUL5	RS19	P39019	[42]	8	8		49
SIVmac VIF	CUL5	RL10A	P62906	[43]	7	5		26.3
SIVmac VIF	CUL5	MEP50	Q9BQA1	[44]	7	6		28.4
SIVmac VIF	CUL5	RS16	P62249	[45]	7	6		39.7
SIVmac VIF	CUL5	RLA2	P05387	[46]	5	4		69.6
SIVmac VIF	CUL5	BAG2	O95816	[47]	11	7		48.3
SIVmac VIF	CUL5	RL23	P62829	[48]	5	3		25.7
SIVmac	CUL5	K1C10	P13645	[49]	10	8		18.5

VIF								
SIVmac VIF	CUL5	K1C28	Q7Z3Y7	[49-2]	3	3	1	7.5
SIVmac VIF	CUL5	K1C27	Q7Z3Y8	[49-4]	2	2	0	3.9
SIVmac VIF	CUL5	K1C25	Q7Z3Z0	[49-5]	2	2	0	4
SIVmac VIF	CUL5	K1C27	Q7Z3Y8	[49-6]	2	2	0	3.9
SIVmac VIF	CUL5	K1C25	Q7Z3Z0	[49-7]	2	2	0	4
SIVmac VIF	CUL5	FKBP8	Q14318	[50]	3	3		11.4
SIVmac VIF	CUL5	RBX2	Q9UBF6	[51]	4	3		38.9
SIVmac VIF	CUL5	RS12	P25398	[52]	5	4		41.7
SIVmac VIF	CUL5	NEDD8	Q15843	[53]	6	4		50.6
SIVmac VIF	CUL5	RS6	P62753	[54]	4	4		22.5
SIVmac VIF	CUL5	DHX9	Q08211	[55]	8	8		8.3
SIVmac VIF	CUL5	GRP75	P38646	[56]	6	6		12.8
SIVmac VIF	CUL5	RL11	P62913	[57]	4	4		20.8
SIVmac VIF	CUL5	ECHA	P40939	[58]	6	6		15.9
SIVmac VIF	CUL5	RL7	P18124	[59]	6	5		24.6
SIVmac VIF	CUL5	RS18	P62269	[60]	7	6		41.4
SIVmac VIF	CUL5	EF1A1	P68104	[61]	7	4		17.1
SIVmac VIF	CUL5	EF1A3	Q5VTE0	[61-1]	7	4	0	17.1
SIVmac VIF	CUL5	EF1A1	P68104	[61-2]	7	4	0	17.1
SIVmac VIF	CUL5	EF1A3	Q5VTE0	[61-3]	7	4	0	17.1
SIVmac VIF	CUL5	EF1A2	Q05639	[61-4]	3	2	0	5.8
SIVmac VIF	CUL5	C1QBP	Q07021	[62]	4	3		19.5
SIVmac VIF	CUL5	PYR1	P27708	[63]	4	4		3
SIVmac VIF	CUL5	RS27	P42677	[64]	4	3		25
SIVmac VIF	CUL5	RS27L	Q71UM5	[64-1]	4	3	0	25
SIVmac VIF	CUL5	RS27	P42677	[64-2]	4	3	0	25

SIVmac VIF	CUL5	RS27L	Q71UM5	[64-3]	4	3	0	25
SIVmac VIF	CUL5	RL9	P32969	[65]	5	5		43.8
SIVmac VIF	CUL5	RL10	P27635	[66]	4	4		24.3
SIVmac VIF	CUL5	RL13	P26373	[67]	4	4		19.9
SIVmac VIF	CUL5	RS27A	P62979	[68]	4	4		32.7
SIVmac VIF	CUL5	UBB	P0CG47	[68-2]	3	3	0	16.6
SIVmac VIF	CUL5	UBC	P0CG48	[68-3]	3	3	0	5.5
SIVmac VIF	CUL5	RL40	P62987	[68-4]	3	3	0	29.7
SIVmac VIF	CUL5	UBB	P0CG47	[68-5]	3	3	0	16.6
SIVmac VIF	CUL5	UBC	P0CG48	[68-6]	3	3	0	5.5
SIVmac VIF	CUL5	RL40	P62987	[68-7]	3	3	0	29.7
SIVmac VIF	CUL5	RL7A	P62424	[69]	4	3		15
SIVmac VIF	CUL5	RLA1	P05386	[70]	3	2		51.8
SIVmac VIF	CUL5	DNJC7	Q99615	[71]	6	6		16.6
SIVmac VIF	CUL5	RS9	P46781	[72]	3	3		16
SIVmac VIF	CUL5	RS17	P08708	[73]	7	4		40
SIVmac VIF	CUL5	RS17L	P0CW22	[73-1]	7	4	0	40
SIVmac VIF	CUL5	RS17	P08708	[73-2]	7	4	0	40
SIVmac VIF	CUL5	RS17L	P0CW22	[73-3]	7	4	0	40
SIVmac VIF	CUL5	RL21	P46778	[74]	3	2		20.6
SIVmac VIF	CUL5	NPM	P06748	[75]	2	2		16.7
SIVmac VIF	CUL5	ILF3	Q12906	[76]	4	4		5
SIVmac VIF	CUL5	RL18A	Q02543	[77]	2	2		15.3
SIVmac VIF	CUL5	RS7	P62081	[78]	5	3		18
SIVmac VIF	CUL5	ILF2	Q12905	[79]	3	3		14.6
SIVmac VIF	CUL5	CLPB	Q9H078	[80]	6	5		9.6
SIVmac	CUL5	RL23A	P62750	[81]	3	3		20.5

VIF								
SIVmac VIF	CUL5	RS26	P62854	[82]	5	4		44.3
SIVmac VIF	CUL5	RS26L	Q5JNZ5	[82-2]	3	3	0	31.3
SIVmac VIF	CUL5	RS25	P62851	[83]	3	3		16
SIVmac VIF	CUL5	K2C6A	P02538	[84]	3	3		5.7
SIVmac VIF	CUL5	K2C6C	P48668	[84-1]	3	3	0	5.7
SIVmac VIF	CUL5	K2C6A	P02538	[84-2]	3	3	0	5.7
SIVmac VIF	CUL5	K2C6C	P48668	[84-3]	3	3	0	5.7
SIVmac VIF	CUL5	K2C4	P19013	[6-6, 84-4]	2	2	1	3.7
SIVmac VIF	CUL5	K2C75	O95678	[84-6]	2	2	0	4.2
SIVmac VIF	CUL5	K2C5	P13647	[84-7]	2	2	0	3.9
SIVmac VIF	CUL5	K2C79	Q5XKE5	[84-8]	2	2	0	4.3
SIVmac VIF	CUL5	K2C75	O95678	[84-9]	2	2	0	4.2
SIVmac VIF	CUL5	K2C5	P13647	[84-10]	2	2	0	3.9
SIVmac VIF	CUL5	K2C79	Q5XKE5	[84-11]	2	2	0	4.3
SIVmac VIF	CUL5	K22O	Q01546	[84-12]	2	2	0	3.1
SIVmac VIF	CUL5	K2C3	P12035	[84-14]	1	1	0	1.8
SIVmac VIF	CUL5	RS14	P62263	[85]	4	4		30.5
SIVmac VIF	CUL5	RS24	P62847	[86]	3	2		20.3
SIVmac VIF	CUL5	RL19	P84098	[87]	1	1		8.7
SIVmac VIF	CUL5	RL31	P62899	[88]	3	3		25.6
SIVmac VIF	CUL5	RL36	Q9Y3U8	[89]	2	2		20
SIVmac VIF	CUL5	RS15	P62841	[90]	4	3		40.7
SIVmac VIF	CUL5	H2B1K	O60814	[91]	2	1		11.9
SIVmac VIF	CUL5	H2B1J	P06899	[91-1]	2	1	-1	11.9
SIVmac VIF	CUL5	H2B1O	P23527	[91-2]	2	1	-1	11.9
SIVmac VIF	CUL5	H2B1B	P33778	[91-3]	2	1	-1	11.9

SIVmac VIF	CUL5	H2BFS	P57053	[91-4]	2	1	-1	11.9
SIVmac VIF	CUL5	H2B1D	P58876	[91-5]	2	1	-1	11.9
SIVmac VIF	CUL5	H2B1C	P62807	[91-6]	2	1	-1	11.9
SIVmac VIF	CUL5	H2B2E	Q16778	[91-7]	2	1	-1	11.9
SIVmac VIF	CUL5	H2B2F	Q5QNW 6	[91-8]	2	1	-1	11.9
SIVmac VIF	CUL5	H2B3B	Q8N257	[91-9]	2	1	-1	11.9
SIVmac VIF	CUL5	H2B1H	Q93079	[91-10]	2	1	-1	11.9
SIVmac VIF	CUL5	H2B1N	Q99877	[91-11]	2	1	-1	11.9
SIVmac VIF	CUL5	H2B1M	Q99879	[91-12]	2	1	-1	11.9
SIVmac VIF	CUL5	H2B1L	Q99880	[91-13]	2	1	-1	11.9
SIVmac VIF	CUL5	H2B1K	O60814	[91-14]	2	1	-1	11.9
SIVmac VIF	CUL5	H2B1J	P06899	[91-15]	2	1	-1	11.9
SIVmac VIF	CUL5	H2B1O	P23527	[91-16]	1	1	0	11.9
SIVmac VIF	CUL5	H2B1B	P33778	[91-17]	2	1	-1	11.9
SIVmac VIF	CUL5	H2BFS	P57053	[91-18]	1	1	0	11.9
SIVmac VIF	CUL5	H2B1D	P58876	[91-19]	2	1	-1	11.9
SIVmac VIF	CUL5	H2B1C	P62807	[91-20]	2	1	-1	11.9
SIVmac VIF	CUL5	H2B2E	Q16778	[91-21]	1	1	0	11.9
SIVmac VIF	CUL5	H2B2F	Q5QNW 6	[91-22]	1	1	0	11.9
SIVmac VIF	CUL5	H2B3B	Q8N257	[91-23]	1	1	0	11.9
SIVmac VIF	CUL5	H2B1H	Q93079	[91-24]	2	1	-1	11.9
SIVmac VIF	CUL5	H2B1N	Q99877	[91-25]	2	1	-1	11.9
SIVmac VIF	CUL5	H2B1M	Q99879	[91-26]	2	1	-1	11.9
SIVmac VIF	CUL5	H2B1L	Q99880	[91-27]	2	1	-1	11.9
SIVmac VIF	CUL5	PRKDC	P78527	[92]	4	4		1.3
SIVmac VIF	CUL5	HS105	Q92598	[93]	3	3		5.2
SIVmac	CUL5	RL13A	P40429	[94]	3	2		11.3

VIF								
SIVmac VIF	CUL5	R13AX	Q6NVV1	[94-2]	1	1	0	10.8
SIVmac VIF	CUL5	RS11	P62280	[95]	3	2		17.7
SIVmac VIF	CUL5	MAGD1	Q9Y5V3	[96]	2	2		5
SIVmac VIF	CUL5	MSI1H	O43347	[97]	2	2		8.8
SIVmac VIF	CUL5	ATPA	P25705	[98]	2	2		5.6
SIVmac VIF	CUL5	RL37A	P61513	[99]	1	1		19.6
SIVmac VIF	CUL5	RBBP4	Q09028	[100]	2	2		5.6
SIVmac VIF	CUL5	RBBP7	Q16576	[100-2]	1	1	0	2.1
SIVmac VIF	CUL5	IPO5	O00410	[101]	3	3		4.7
SIVmac VIF	CUL5	PPM1G	O15355	[102]	3	3		11
SIVmac VIF	CUL5	IPO7	O95373	[103]	3	3		3.4
SIVmac VIF	CUL5	IPO8	O15397	[103-2]	1	1	0	1
SIVmac VIF	CUL5	RS15A	P62244	[104]	2	2		22.3
SIVmac VIF	CUL5	HORN	Q86YZ3	[105]	3	2		1.4
SIVmac VIF	CUL5	RPAC1	O15160	[106]	2	2		8.1
SIVmac VIF	CUL5	RL27A	P46776	[107]	2	2		15.5
SIVmac VIF	CUL5	RL8	P62917	[108]	4	3		23.7
SIVmac VIF	CUL5	AT1A1	P05023	[109]	3	3		3.7
SIVmac VIF	CUL5	RL35A	P18077	[110]	2	2		19.1
SIVmac VIF	CUL5	HNRPK	P61978	[111]	2	2		6.7
SIVmac VIF	CUL5	RS28	P62857	[112]	2	2		33.3
SIVmac VIF	CUL5	2xStrep	N/A	[113]	5	1		71.4
SIVmac VIF	CUL5	AIFM1	O95831	[114]	2	2		4.6
SIVmac VIF	CUL5	DPM1	O60762	[115]	2	2		12.7
SIVmac VIF	CUL5	RL28	P46779	[116]	2	2		16.8
SIVmac VIF	CUL5	DDX5	P17844	[117]	3	3		6.4

SIVmac VIF	CUL5	DDX17	Q92841	[117-2]	2	2	0	3.7
SIVmac VIF	CUL5	RUVB1	Q9Y265	[118]	3	3		9.6
SIVmac VIF	CUL5	SEC13	P55735	[119]	2	2		13
SIVmac VIF	CUL5	CMC2	Q9UJS0	[120]	2	2		4.3
SIVmac VIF	CUL5	M2OM	Q02978	[121]	1	1		5.1
SIVmac VIF	CUL5	RL14	P50914	[122]	2	2		10.2
SIVmac VIF	CUL5	RL18	Q07020	[123]	2	2		12.8
SIVmac VIF	CUL5	MSI2H	Q96DH6	[124]	1	1		4.6
SIVmac VIF	CUL5	RS23	P62266	[125]	1	1		7.7
SIVmac VIF	CUL5	TIM50	Q3ZCQ8	[126]	2	2		7.9
SIVmac VIF	CUL5	ELAV1	Q15717	[127]	2	2		7.7
SIVmac VIF	CUL5	IF4A1	P60842	[128]	1	1		3.2
SIVmac VIF	CUL5	IF4A2	Q14240	[128-1]	1	1	0	3.2
SIVmac VIF	CUL5	IF4A1	P60842	[128-2]	1	1	0	3.2
SIVmac VIF	CUL5	IF4A2	Q14240	[128-3]	1	1	0	3.2
SIVmac VIF	CUL5	TEBP	Q15185	[129]	1	1		8.1
SIVmac VIF	CUL5	SRP09	P49458	[130]	1	1		12.8
SIVmac VIF	CUL5	TCPE	P48643	[131]	1	1		3
SIVmac VIF	CUL5	ICLN	P54105	[132]	1	1		13.1
SIVmac VIF	CUL5	RL35	P42766	[133]	2	2		10.6
SIVmac VIF	CUL5	RL4	P36578	[134]	2	2		7.3
SIVmac VIF	CUL5	RL22	P35268	[135]	1	1		10.2
SIVmac VIF	CUL5	FEM1B	Q9UK73	[136]	1	1		1.8
SIVmac VIF	CUL5	RL17	P18621	[137]	1	1		8.7
SIVmac VIF	CUL5	HNRPC	P07910	[138]	2	2		9.2
SIVmac VIF	CUL5	HNRCL	O60812	[138-2]	1	1	0	4.1
SIVmac	CUL5	RS10	P46783	[139]	2	2		14.5

VIF								
SIVmac VIF	CUL5	RS10L	Q9NQ39	[139-2]	1	1	0	8.5
SIVmac VIF	CUL5	ATPB	P06576	[140]	2	2		6.2
SIVmac VIF	CUL5	APC11	Q9NYG5	[141]	1	1		25
SIVmac VIF	CUL5	TCPQ	P50990	[142]	2	2		5.7
SIVmac VIF	CUL5	IPO9	Q96P70	[143]	2	2		2.6
SIVmac VIF	CUL5	P5CR2	Q96C36	[144]	1	1		5.3
SIVmac VIF	CUL5	LSM12	Q3MHD2	[145]	1	1		6.7
SIVmac VIF	CUL5	HAX1	O00165	[146]	3	3		17.2
SIVmac VIF	CUL5	STAU1	O95793	[147]	2	2		4.7
SIVmac VIF	CUL5	NDUA4	O00483	[148]	2	2		27.2
SIVmac VIF	CUL5	RT09	P82933	[149]	3	3		12.1
SIVmac VIF	CUL5	NPM3	O75607	[150]	1	1		9.6
SIVmac VIF	CUL5	HACD3	Q9P035	[151]	1	1		4.1
SIVmac VIF	CUL5	TCPB	P78371	[152]	2	2		5.6
SIVmac VIF	CUL5	YTHD2	Q9Y5A9	[153]	1	1		2.1
SIVmac VIF	CUL5	APBA2	Q99767	[154]	1	1		2.1
SIVmac VIF	CUL5	SF3B3	Q15393	[155]	2	2		2.5
SIVmac VIF	CUL5	KV201	P01614	[156]	1	1		11.3
SIVmac VIF	CUL5	KV204	P01617	[156-1]	1	1	0	11.5
SIVmac VIF	CUL5	KV205	P06309	[156-2]	1	1	0	11.1
SIVmac VIF	CUL5	KV206	P06310	[156-3]	1	1	0	9.8
SIVmac VIF	CUL5	KV201	P01614	[156-4]	1	1	0	11.3
SIVmac VIF	CUL5	KV204	P01617	[156-5]	1	1	0	11.5
SIVmac VIF	CUL5	KV205	P06309	[156-6]	1	1	0	11.1
SIVmac VIF	CUL5	KV206	P06310	[156-7]	1	1	0	9.8
SIVmac VIF	CUL5	TIM13	Q9Y5L4	[157]	1	1		14.7

SIVmac VIF	CUL5	MOV10	Q9HCE1	[158]	2	2		2.7
SIVmac VIF	CUL5	RL38	P63173	[159]	1	1		17.1
SIVmac VIF	CUL5	RT17	Q9Y2R5	[160]	1	1		15.4
SIVmac VIF	CUL5	FKBP5	Q13451	[161]	1	1		4.6
SIVmac VIF	CUL5	ROA1	P09651	[162]	1	1		4.3
SIVmac VIF	CUL5	RA1L2	Q32P51	[162-1]	1	1	0	5
SIVmac VIF	CUL5	ROA1	P09651	[162-2]	1	1	0	4.3
SIVmac VIF	CUL5	RA1L2	Q32P51	[162-3]	1	1	0	5
SIVmac VIF	CUL5	HS905	Q58FG0	[163]	1	1		3
SIVmac VIF	CUL5	DNJB1	P25685	[164]	1	1		4.7
SIVmac VIF	CUL5	H2A1B	P04908	[165]	1	1		14.6
SIVmac VIF	CUL5	H2A1	P0C0S8	[165-1]	1	1	0	14.6
SIVmac VIF	CUL5	H2A1D	P20671	[165-2]	1	1	0	14.6
SIVmac VIF	CUL5	H2A2C	Q16777	[165-3]	1	1	0	14.7
SIVmac VIF	CUL5	H2A2A	Q6FI13	[165-4]	1	1	0	14.6
SIVmac VIF	CUL5	H2A3	Q7L7L0	[165-5]	1	1	0	14.6
SIVmac VIF	CUL5	H2A1C	Q93077	[165-6]	1	1	0	14.6
SIVmac VIF	CUL5	H2A1H	Q96KK5	[165-7]	1	1	0	14.8
SIVmac VIF	CUL5	H2A1J	Q99878	[165-8]	1	1	0	14.8
SIVmac VIF	CUL5	H2AJ	Q9BTM1	[165-9]	1	1	0	14.7
SIVmac VIF	CUL5	H2A1B	P04908	[165-10]	1	1	0	14.6
SIVmac VIF	CUL5	H2A1	P0C0S8	[165-11]	1	1	0	14.6
SIVmac VIF	CUL5	H2A1D	P20671	[165-12]	1	1	0	14.6
SIVmac VIF	CUL5	H2A2C	Q16777	[165-13]	1	1	0	14.7
SIVmac VIF	CUL5	H2A2A	Q6FI13	[165-14]	1	1	0	14.6
SIVmac VIF	CUL5	H2A3	Q7L7L0	[165-15]	1	1	0	14.6
SIVmac	CUL5	H2A1C	Q93077	[165-16]	1	1	0	14.6

VIF								
SIVmac VIF	CUL5	H2A1H	Q96KK5	[165-17]	1	1	0	14.8
SIVmac VIF	CUL5	H2A1J	Q99878	[165-18]	1	1	0	14.8
SIVmac VIF	CUL5	H2AJ	Q9BTM1	[165-19]	1	1	0	14.7
SIVmac VIF	CUL5	ATX2L	Q8WWM7	[166]	1	1		2.1
SIVmac VIF	CUL5	DNJA3	Q96EY1	[167]	3	3		10.6
SIVmac VIF	CUL5	HIG1A	Q9Y241	[168]	1	1		20.4
SIVmac VIF	CUL5	ERH	P84090	[169]	1	1		11.5
SIVmac VIF	CUL5	RL3	P39023	[170]	1	1		5.5
SIVmac VIF	CUL5	AF1Q	Q13015	[171]	1	1		25.6
SIVmac VIF	CUL5	PRP19	Q9UMS4	[172]	1	1		2.8
SIVmac VIF	CUL5	PCNA	P12004	[173]	1	1		5.7
SIVmac VIF	CUL5	DYL1	P63167	[174]	1	1		24.7
SIVmac VIF	CUL5	RL27	P61353	[176]	1	1		6.6
SIVmac VIF	CUL5	NOM1	Q5C9Z4	[177]	1	1		2.8
SIVmac VIF	CUL5	TIM23	O14925	[178]	1	1		19.6
SIVmac VIF	CUL5	TI23B	Q5SRD1	[178-1]	1	1	0	16
SIVmac VIF	CUL5	TIM23	O14925	[178-2]	1	1	0	19.6
SIVmac VIF	CUL5	TI23B	Q5SRD1	[178-3]	1	1	0	16
SIVmac VIF	CUL5	RT23	Q9Y3D9	[179]	1	1		5.3
SIVmac VIF	CUL5	RFOX2	O43251	[180]	1	1		3.8
SIVmac VIF	CUL5	RFOX1	Q9NWB1	[180-1]	1	1	0	3.8
SIVmac VIF	CUL5	RFOX2	O43251	[180-2]	1	1	0	3.8
SIVmac VIF	CUL5	RFOX1	Q9NWB1	[180-3]	1	1	0	3.8
SIVmac VIF	CUL5	TADBP	Q13148	[181]	1	1		4.3
SIVmac VIF	CUL5	NDKA	P15531	[182]	1	1		7.9
SIVmac VIF	CUL5	NDKB	P22392	[182-1]	1	1	0	7.9

SIVmac VIF	CUL5	NDKA	P15531	[182-2]	1	1	0	7.9
SIVmac VIF	CUL5	NDKB	P22392	[182-3]	1	1	0	7.9
SIVmac VIF	CUL5	YMEL1	Q96TA2	[183]	1	1		1.7
SIVmac VIF	CUL5	TIM8B	Q9Y5J9	[184]	1	1		16.9
SIVmac VIF	CUL5	RSSA	P08865	[185]	1	1		3.7
SIVmac VIF	CUL5	PCBP2	Q15366	[186]	1	1		4.4
SIVmac VIF	CUL5	CSN3	Q9UNS2	[187]	1	1		3.1
SIVmac VIF	CUL5	DNJB4	Q9UDY4	[188]	1	1		4.7
SIVmac VIF	CUL5	TTC16	Q8NEE8	[189]	1	1		1.4
SIVmac VIF	CUL5	SUGP2	Q8IX01	[190]	1	1		1
SIVmac VIF	CUL5	DIMT1	Q9UNQ2	[191]	1	1		3.5
SIVmac VIF	CUL5	SRP14	P37108	[192]	1	1		7.4
SIVmac VIF	CUL5	ELP1	O95163	[193]	1	1		1.3
HIV-1 VIF	CUL5	CUL5	Q93034	[1]	221	64		58.6
HIV-1 VIF	CUL5	PEBB	Q13951	[2]	69	20		68.1
HIV-1 VIF	CUL5	PABP1	P11940	[3]	34	22		35.5
HIV-1 VIF	CUL5	PABP4	Q13310	[3-2]	19	14	4	24.7
HIV-1 VIF	CUL5	PABP3	Q9H361	[3-4]	12	9	0	16.8
HIV-1 VIF	CUL5	PAP1L	Q4VXU2	[3-6]	6	4	0	7
HIV-1 VIF	CUL5	PAP1M	Q5JQF8	[3-8]	1	1	0	5.5
HIV-1 VIF	CUL5	TBB5	P07437	[4]	33	24		59
HIV-1 VIF	CUL5	TBB2C	P68371	[4-2]	27	21	3	54.8
HIV-1 VIF	CUL5	TBB4	P04350	[4-4]	23	18	2	48.2
HIV-1 VIF	CUL5	TBB2A	Q13885	[4-6]	18	13	1	36.9
HIV-1 VIF	CUL5	TBB2B	Q9BVA1	[4-7]	18	13	1	36.9
HIV-1 VIF	CUL5	TBB2A	Q13885	[4-8]	18	13	1	36.9
HIV-1 VIF	CUL5	TBB2B	Q9BVA1	[4-9]	18	13	1	36.9
HIV-1 VIF	CUL5	TBB3	Q13509	[4-10]	14	11	1	22
HIV-1 VIF	CUL5	TBB8B	A6NNZ2	[4-12]	8	6	0	12.8
HIV-1 VIF	CUL5	TBB8	Q3ZCM7	[4-13]	8	6	0	12.8
HIV-1 VIF	CUL5	TBB8B	A6NNZ2	[4-14]	8	6	0	12.8
HIV-1 VIF	CUL5	TBB8	Q3ZCM7	[4-15]	8	6	0	12.8
HIV-1 VIF	CUL5	TBB6	Q9BUF5	[4-16]	6	4	0	8.5
HIV-1 VIF	CUL5	YI016	A6NKZ8	[4-18]	5	3	0	6.5
HIV-1 VIF	CUL5	TBB1	Q9H4B7	[4-20]	1	1	0	2.2
HIV-1 VIF	CUL5	HSP71	P08107	[5]	37	24		50.2
HIV-1 VIF	CUL5	HSP7C	P11142	[5-2]	19	15	13	30

HIV-1 VIF	CUL5	HS71L	P34931	[5-4]	16	10	0	21.5
HIV-1 VIF	CUL5	HSP76	P17066	[5-6]	10	6	1	11.7
HIV-1 VIF	CUL5	HSP72	P54652	[5-8]	8	6	4	9.5
HIV-1 VIF	CUL5	HSP77	P48741	[5-10]	7	4	0	13.6
HIV-1 VIF	CUL5	ELOC	Q15369	[6]	53	14		63.4
HIV-1 VIF	CUL5	KRT85	P78386	[7]	39	17		29
HIV-1 VIF	CUL5	KRT86	O43790	[7-2]	34	16	4	31.3
HIV-1 VIF	CUL5	KRT83	P78385	[7-4]	34	18	5	28
HIV-1 VIF	CUL5	KT81L	A6NCN2	[7-6]	21	13	5	24.3
HIV-1 VIF	CUL5	KRT81	Q14533	[7-8]	28	15	5	28.7
HIV-1 VIF	CUL5	KRT82	Q9NSB4	[7-10]	11	4	2	7.6
HIV-1 VIF	CUL5	K2C7	P08729	[7-12]	4	3	2	5.1
HIV-1 VIF	CUL5	KRT84	Q9NSB2	[7-14]	5	2	0	3.8
HIV-1 VIF	CUL5	ELOB	Q15370	[8]	36	13		59.3
HIV-1 VIF	CUL5	TBA1B	P68363	[9]	18	13		39.9
HIV-1 VIF	CUL5	TBA1A	Q71U36	[9-2]	16	12	1	37
HIV-1 VIF	CUL5	TBA1C	Q9BQE3	[9-4]	16	11	1	37.2
HIV-1 VIF	CUL5	TBA4A	P68366	[9-6]	14	10	0	30.4
HIV-1 VIF	CUL5	TBA3C	Q13748	[9-8]	12	9	1	29.8
HIV-1 VIF	CUL5	TBA3E	Q6PEY2	[9-10]	8	7	1	25.1
HIV-1 VIF	CUL5	TBA8	Q9NY65	[9-12]	8	5	0	16.5
HIV-1 VIF	CUL5	TBA4B	Q9H853	[9-14]	2	1	0	5.8
HIV-1 VIF	CUL5	TBAL3	A6NHL2	[9-16]	1	1	0	2
HIV-1 VIF	CUL5	K2C1	P04264	[10]	13	13		25.9
HIV-1 VIF	CUL5	K22E	P35908	[10-2]	4	4	2	6.9
HIV-1 VIF	CUL5	K2C6B	P04259	[10-4, 52-2]	3	3	2	6.9
HIV-1 VIF	CUL5	K2C1B	Q7Z794	[10-6]	1	1	0	2.1
HIV-1 VIF	CUL5	RS2	P15880	[11]	12	10		34.5
HIV-1 VIF	CUL5	KT33B	Q14525	[12]	29	14		23.5
HIV-1 VIF	CUL5	K1H1	Q15323	[12-2]	37	13	5	27.4
HIV-1 VIF	CUL5	KRT35	Q92764	[12-4]	26	13	8	25.5
HIV-1 VIF	CUL5	KT33A	O76009	[12-6]	20	10	2	23.3
HIV-1 VIF	CUL5	K1H2	Q14532	[12-8]	15	7	3	11.2
HIV-1 VIF	CUL5	KRT36	O76013	[12-10]	13	8	7	13.1
HIV-1 VIF	CUL5	KRT34	O76011	[12-12]	15	6	2	7.6
HIV-1 VIF	CUL5	KRT37	O76014	[12-14]	3	2	1	4.2
HIV-1 VIF	CUL5	KRT38	O76015	[12-15]	3	2	1	4.2
HIV-1 VIF	CUL5	KRT37	O76014	[12-16]	3	2	1	4.2
HIV-1 VIF	CUL5	KRT38	O76015	[12-17]	3	2	1	4.2
HIV-1 VIF	CUL5	RS4X	P62701	[13]	15	12		40.3
HIV-1 VIF	CUL5	RS4Y2	Q8TD47	[13-2]	3	2	0	7.6
HIV-1 VIF	CUL5	RS4Y1	P22090	[13-4]	1	1	0	3.8
HIV-1 VIF	CUL5	YBOX1	P67809	[14]	10	7		38.9
HIV-1 VIF	CUL5	DBPA	P16989	[14-2]	5	5	3	32.5
HIV-1 VIF	CUL5	YBOX2	Q9Y2T7	[14-4]	2	2	0	6.9
HIV-1 VIF	CUL5	HIV-1 Vif	N/A	[15]	32	10		58.9
HIV-1 VIF	CUL5	RS3A	P61247	[16]	15	12		40.5

HIV-1 VIF	CUL5	IF2B1	Q9NZI8	[17]	8	8		18.4
HIV-1 VIF	CUL5	IF2B3	O00425	[17-2]	3	3	2	7.9
HIV-1 VIF	CUL5	IF2B2	Q9Y6M1	[17-4]	2	2	1	4.5
HIV-1 VIF	CUL5	HNRPQ	O60506	[18]	11	10		28.6
HIV-1 VIF	CUL5	HNRPR	O43390	[18-2]	8	7	4	11.8
HIV-1 VIF	CUL5	RS12	P25398	[19]	8	5		41.7
HIV-1 VIF	CUL5	HNRPU	Q00839	[20]	7	7		15.8
HIV-1 VIF	CUL5	HNRPC	P07910	[21]	7	7		27.1
HIV-1 VIF	CUL5	HNRCL	O60812	[21-2]	4	4	0	14.3
HIV-1 VIF	CUL5	RS6	P62753	[22]	5	5		22.1
HIV-1 VIF	CUL5	RS16	P62249	[23]	11	9		49.3
HIV-1 VIF	CUL5	RBX1	P62877	[24]	9	5		31.5
HIV-1 VIF	CUL5	RT09	P82933	[25]	6	5		19.2
HIV-1 VIF	CUL5	K1C9	P35527	[26]	6	6		17.5
HIV-1 VIF	CUL5	NP1L1	P55209	[27]	6	6		32
HIV-1 VIF	CUL5	NP1L4	Q99733	[27-2]	3	3	2	12.5
HIV-1 VIF	CUL5	DNJA1	P31689	[28]	8	7		28.5
HIV-1 VIF	CUL5	RLA0	P05388	[29]	7	7		36.3
HIV-1 VIF	CUL5	RLA0L	Q8NHW5	[29-2]	4	4	0	17.7
HIV-1 VIF	CUL5	ILF3	Q12906	[30]	7	7		12.9
HIV-1 VIF	CUL5	STRBP	Q96SI9	[30-2]	1	1	0	1.6
HIV-1 VIF	CUL5	HNRH1	P31943	[31]	5	4		12.9
HIV-1 VIF	CUL5	HNRH2	P55795	[31-2]	2	2	0	6
HIV-1 VIF	CUL5	HNRPF	P52597	[31-4]	5	5	3	21.4
HIV-1 VIF	CUL5	NUCL	P19338	[32]	8	8		14.8
HIV-1 VIF	CUL5	RS5	P46782	[33]	6	4		25.5
HIV-1 VIF	CUL5	RS8	P62241	[34]	6	4		26.4
HIV-1 VIF	CUL5	RBX2	Q9UBF6	[35]	5	3		38.9
HIV-1 VIF	CUL5	RL12	P30050	[36]	5	5		43
HIV-1 VIF	CUL5	H2B1K	O60814	[37]	6	4		11.9
HIV-1 VIF	CUL5	H2B1J	P06899	[37-1]	6	4	0	11.9
HIV-1 VIF	CUL5	H2B1O	P23527	[37-2]	6	4	0	11.9
HIV-1 VIF	CUL5	H2B1B	P33778	[37-3]	6	4	0	11.9
HIV-1 VIF	CUL5	H2BFS	P57053	[37-4]	6	4	0	11.9
HIV-1 VIF	CUL5	H2B1D	P58876	[37-5]	6	4	0	11.9
HIV-1 VIF	CUL5	H2B1C	P62807	[37-6]	6	4	0	11.9
HIV-1 VIF	CUL5	H2B2E	Q16778	[37-7]	6	4	0	11.9
HIV-1 VIF	CUL5	H2B2F	Q5QNW6	[37-8]	6	4	0	11.9
HIV-1 VIF	CUL5	H2B3B	Q8N257	[37-9]	6	4	0	11.9
HIV-1 VIF	CUL5	H2B1H	Q93079	[37-10]	6	4	0	11.9
HIV-1 VIF	CUL5	H2B1N	Q99877	[37-11]	6	4	0	11.9
HIV-1 VIF	CUL5	H2B1M	Q99879	[37-12]	6	4	0	11.9
HIV-1 VIF	CUL5	H2B1L	Q99880	[37-13]	6	4	0	11.9
HIV-1 VIF	CUL5	H2B1K	O60814	[37-14]	6	4	0	11.9
HIV-1 VIF	CUL5	H2B1J	P06899	[37-15]	6	4	0	11.9
HIV-1 VIF	CUL5	H2B1B	P33778	[37-16]	6	4	0	11.9

HIV-1 VIF	CUL5	H2B1D	P58876	[37-17]	6	4	0	11.9
HIV-1 VIF	CUL5	H2B1C	P62807	[37-18]	6	4	0	11.9
HIV-1 VIF	CUL5	H2B1H	Q93079	[37-19]	6	4	0	11.9
HIV-1 VIF	CUL5	H2B1N	Q99877	[37-20]	6	4	0	11.9
HIV-1 VIF	CUL5	H2B1M	Q99879	[37-21]	6	4	0	11.9
HIV-1 VIF	CUL5	H2B1L	Q99880	[37-22]	6	4	0	11.9
HIV-1 VIF	CUL5	H2B1O	P23527	[37-23]	4	3	0	11.9
HIV-1 VIF	CUL5	H2BFS	P57053	[37-24]	4	3	0	11.9
HIV-1 VIF	CUL5	H2B2E	Q16778	[37-25]	4	3	0	11.9
HIV-1 VIF	CUL5	H2B2F	Q5QNW6	[37-26]	4	3	0	11.9
HIV-1 VIF	CUL5	H2B3B	Q8N257	[37-27]	4	3	0	11.9
HIV-1 VIF	CUL5	DDX5	P17844	[38]	9	8		17.3
HIV-1 VIF	CUL5	DDX17	Q92841	[38-2]	5	5	1	9.5
HIV-1 VIF	CUL5	DDX3X	O00571	[38-4]	1	1	0	1.7
HIV-1 VIF	CUL5	DDX3Y	O15523	[38-5]	1	1	0	1.7
HIV-1 VIF	CUL5	DDX3X	O00571	[38-6]	1	1	0	1.7
HIV-1 VIF	CUL5	DDX3Y	O15523	[38-7]	1	1	0	1.7
HIV-1 VIF	CUL5	RS9	P46781	[39]	6	5		22.2
HIV-1 VIF	CUL5	RS3	P23396	[40]	9	6		35.4
HIV-1 VIF	CUL5	ILF2	Q12905	[41]	4	4		17.7
HIV-1 VIF	CUL5	RCN2	Q14257	[42]	4	4		22.1
HIV-1 VIF	CUL5	RLA2	P05387	[43]	6	3		40.9
HIV-1 VIF	CUL5	RL24	P83731	[44]	5	4		26.8
HIV-1 VIF	CUL5	RS25	P62851	[45]	5	5		29.6
HIV-1 VIF	CUL5	RS19	P39019	[46]	7	7		49.7
HIV-1 VIF	CUL5	NEDD8	Q15843	[47]	8	5		65.4
HIV-1 VIF	CUL5	RL23	P62829	[48]	4	4		32.9
HIV-1 VIF	CUL5	RS18	P62269	[49]	9	5		32.2
HIV-1 VIF	CUL5	LARP1	Q6PKG0	[50]	2	2		5
HIV-1 VIF	CUL5	LAR1B	Q659C4	[50-2]	1	1	0	1.5
HIV-1 VIF	CUL5	ADT2	P05141	[51]	3	3		11.4
HIV-1 VIF	CUL5	K2C75	O95678	[52]	3	3		4.4
HIV-1 VIF	CUL5	K2C6B	P04259	[10-4, 52-2]	3	3	2	6.9
HIV-1 VIF	CUL5	K2C6A	P02538	[52-4]	2	2	1	5.1
HIV-1 VIF	CUL5	K2C6C	P48668	[52-5]	2	2	1	5.1
HIV-1 VIF	CUL5	K2C6A	P02538	[52-6]	2	2	1	5.1
HIV-1 VIF	CUL5	K2C6C	P48668	[52-7]	2	2	1	5.1
HIV-1 VIF	CUL5	K2C5	P13647	[52-8]	2	2	1	3.9
HIV-1 VIF	CUL5	K2C79	Q5XKE5	[52-10]	1	1	0	2.2
HIV-1 VIF	CUL5	RL14	P50914	[53]	4	3		15.8
HIV-1 VIF	CUL5	RL19	P84098	[54]	2	2		9.2
HIV-1 VIF	CUL5	ELAV1	Q15717	[55]	4	4		18.4
HIV-1 VIF	CUL5	RL23A	P62750	[56]	3	3		21.8
HIV-1 VIF	CUL5	RL31	P62899	[57]	6	4		31.2
HIV-1 VIF	CUL5	RL7	P18124	[58]	3	3		14.9
HIV-1 VIF	CUL5	RL10A	P62906	[59]	4	3		14.7

HIV-1 VIF	CUL5	DNJA2	O60884	[60]	3	3		17.5
HIV-1 VIF	CUL5	RS11	P62280	[61]	4	3		22.2
HIV-1 VIF	CUL5	RENT1	Q92900	[62]	6	6		8.5
HIV-1 VIF	CUL5	ABC3C	Q9NRW3	[63]	3	2		13.7
HIV-1 VIF	CUL5	ABC3F	Q8IUX4	[63-2]	2	1	0	3.2
HIV-1 VIF	CUL5	ABC3D	Q96AK3	[63-3]	2	1	0	3.1
HIV-1 VIF	CUL5	ABC3F	Q8IUX4	[63-4]	2	1	0	3.2
HIV-1 VIF	CUL5	ABC3D	Q96AK3	[63-5]	2	1	0	3.1
HIV-1 VIF	CUL5	APC11	Q9NYG5	[64]	2	2		31
HIV-1 VIF	CUL5	ATX2L	Q8WWM7	[65]	2	2		4.5
HIV-1 VIF	CUL5	DHX9	Q08211	[66]	4	4		4.4
HIV-1 VIF	CUL5	ZCCHV	Q7Z2W4	[67]	2	2		3.1
HIV-1 VIF	CUL5	RL8	P62917	[68]	3	3		23.7
HIV-1 VIF	CUL5	RS7	P62081	[69]	4	3		33
HIV-1 VIF	CUL5	KV201	P01614	[70]	1	1		11.3
HIV-1 VIF	CUL5	KV204	P01617	[70-1]	1	1	0	11.5
HIV-1 VIF	CUL5	KV205	P06309	[70-2]	1	1	0	11.1
HIV-1 VIF	CUL5	KV206	P06310	[70-3]	1	1	0	9.8
HIV-1 VIF	CUL5	KV201	P01614	[70-4]	1	1	0	11.3
HIV-1 VIF	CUL5	KV204	P01617	[70-5]	1	1	0	11.5
HIV-1 VIF	CUL5	KV205	P06309	[70-6]	1	1	0	11.1
HIV-1 VIF	CUL5	KV206	P06310	[70-7]	1	1	0	9.8
HIV-1 VIF	CUL5	RS14	P62263	[71]	4	4		38.4
HIV-1 VIF	CUL5	RS28	P62857	[72]	2	2		33.3
HIV-1 VIF	CUL5	RL7A	P62424	[73]	2	2		10.2
HIV-1 VIF	CUL5	H2A1	P0C0S8	[74]	3	3		30
HIV-1 VIF	CUL5	H2A1D	P20671	[74-1]	3	3	0	30
HIV-1 VIF	CUL5	H2A2C	Q16777	[74-2]	3	3	0	30.2
HIV-1 VIF	CUL5	H2A2A	Q6FI13	[74-3]	3	3	0	30
HIV-1 VIF	CUL5	H2A1H	Q96KK5	[74-4]	3	3	0	30.5
HIV-1 VIF	CUL5	H2A1J	Q99878	[74-5]	3	3	0	30.5
HIV-1 VIF	CUL5	H2AJ	Q9BTM1	[74-6]	3	3	0	30.2
HIV-1 VIF	CUL5	H2A1	P0C0S8	[74-7]	3	3	0	30
HIV-1 VIF	CUL5	H2A1D	P20671	[74-8]	3	3	0	30
HIV-1 VIF	CUL5	H2A2C	Q16777	[74-9]	3	3	0	30.2
HIV-1 VIF	CUL5	H2A2A	Q6FI13	[74-10]	3	3	0	30
HIV-1 VIF	CUL5	H2A1H	Q96KK5	[74-11]	3	3	0	30.5
HIV-1 VIF	CUL5	H2A1J	Q99878	[74-12]	3	3	0	30.5
HIV-1 VIF	CUL5	H2AJ	Q9BTM1	[74-13]	3	3	0	30.2
HIV-1 VIF	CUL5	H2A1B	P04908	[74-14]	2	2	0	21.5
HIV-1 VIF	CUL5	H2A3	Q7L7L0	[74-15]	2	2	0	21.5
HIV-1 VIF	CUL5	H2A1C	Q93077	[74-16]	2	2	0	21.5
HIV-1 VIF	CUL5	H2A1B	P04908	[74-17]	2	2	0	21.5
HIV-1 VIF	CUL5	H2A3	Q7L7L0	[74-18]	2	2	0	21.5
HIV-1 VIF	CUL5	H2A1C	Q93077	[74-19]	2	2	0	21.5
HIV-1 VIF	CUL5	RL13	P26373	[75]	2	2		9

HIV-1 VIF	CUL5	RL13A	P40429	[76]	2	2		11.3
HIV-1 VIF	CUL5	RS23	P62266	[77]	2	2		27.3
HIV-1 VIF	CUL5	RS17	P08708	[78]	3	2		25.2
HIV-1 VIF	CUL5	RS17L	P0CW22	[78-1]	3	2	0	25.2
HIV-1 VIF	CUL5	RS17	P08708	[78-2]	3	2	0	25.2
HIV-1 VIF	CUL5	RS17L	P0CW22	[78-3]	3	2	0	25.2
HIV-1 VIF	CUL5	NUFP2	Q7Z417	[79]	3	3		8.5
HIV-1 VIF	CUL5	RL11	P62913	[80]	5	3		17.4
HIV-1 VIF	CUL5	G3BP2	Q9UN86	[81]	2	2		6.8
HIV-1 VIF	CUL5	RS13	P62277	[82]	3	2		8.6
HIV-1 VIF	CUL5	RT29	P51398	[83]	3	3		8
HIV-1 VIF	CUL5	RL35A	P18077	[84]	2	2		19.1
HIV-1 VIF	CUL5	2xStrep	N/A	[85]	8	1		71.4
HIV-1 VIF	CUL5	HNRPM	P52272	[86]	3	3		6.6
HIV-1 VIF	CUL5	RT23	Q9Y3D9	[87]	3	3		18.4
HIV-1 VIF	CUL5	RLA1	P05386	[88]	4	2		51.8
HIV-1 VIF	CUL5	RT22	P82650	[89]	2	2		10
HIV-1 VIF	CUL5	PTCD3	Q96EY7	[90]	1	1		1.9
HIV-1 VIF	CUL5	RS24	P62847	[91]	3	2		20.3
HIV-1 VIF	CUL5	SRP14	P37108	[92]	3	3		25.7
HIV-1 VIF	CUL5	RS27	P42677	[93]	1	1		15.5
HIV-1 VIF	CUL5	RS27L	Q71UM5	[93-1]	1	1	0	15.5
HIV-1 VIF	CUL5	RS27	P42677	[93-2]	1	1	0	15.5
HIV-1 VIF	CUL5	RS27L	Q71UM5	[93-3]	1	1	0	15.5
HIV-1 VIF	CUL5	RT07	Q9Y2R9	[94]	2	2		10.3
HIV-1 VIF	CUL5	RS15	P62841	[95]	2	1		18.6
HIV-1 VIF	CUL5	PABP2	Q86U42	[96]	2	2		9.2
HIV-1 VIF	CUL5	RL21	P46778	[97]	1	1		9.4
HIV-1 VIF	CUL5	UBE2O	Q9C0C9	[98]	2	2		3.6
HIV-1 VIF	CUL5	RL10	P27635	[99]	2	2		17.8
HIV-1 VIF	CUL5	RL10L	Q96L21	[99-2]	1	1	0	5.1
HIV-1 VIF	CUL5	KR111	Q8IUC1	[100]	1	1		6.7
HIV-1 VIF	CUL5	KR132	Q52LG2	[101]	1	1		7.4
HIV-1 VIF	CUL5	KR131	Q8IUC0	[101-1]	1	1	0	7.6
HIV-1 VIF	CUL5	KR132	Q52LG2	[101-2]	1	1	0	7.4
HIV-1 VIF	CUL5	KR131	Q8IUC0	[101-3]	1	1	0	7.6
HIV-1 VIF	CUL5	RL9	P32969	[102]	1	1		9.9
HIV-1 VIF	CUL5	RSSA	P08865	[103]	1	1		5.8
HIV-1 VIF	CUL5	K2C72	Q14CN4	[104]	3	2		2.3
HIV-1 VIF	CUL5	RL18A	Q02543	[105]	1	1		8
HIV-1 VIF	CUL5	RS27A	P62979	[106]	2	2		22.4
HIV-1 VIF	CUL5	UBB	P0CG47	[106-2]	1	1	0	7
HIV-1 VIF	CUL5	UBC	P0CG48	[106-3]	1	1	0	2.3
HIV-1 VIF	CUL5	RL40	P62987	[106-4]	1	1	0	12.5
HIV-1 VIF	CUL5	UBB	P0CG47	[106-5]	1	1	0	7
HIV-1 VIF	CUL5	UBC	P0CG48	[106-6]	1	1	0	2.3
HIV-1 VIF	CUL5	RL40	P62987	[106-7]	1	1	0	12.5

HIV-1 VIF	CUL5	RT27	Q92552	[107]	1	1		3.6
HIV-1 VIF	CUL5	RL30	P62888	[108]	3	2		24.3
HIV-1 VIF	CUL5	RT34	P82930	[109]	3	2		21.1
HIV-1 VIF	CUL5	RL27A	P46776	[110]	1	1		7.4
HIV-1 VIF	CUL5	PRP19	Q9UMS4	[111]	2	2		11.7
HIV-1 VIF	CUL5	H14	P10412	[112]	2	2		9.6
HIV-1 VIF	CUL5	H13	P16402	[112-1]	2	2	0	9.5
HIV-1 VIF	CUL5	H12	P16403	[112-2]	2	2	0	9.9
HIV-1 VIF	CUL5	H14	P10412	[112-3]	2	2	0	9.6
HIV-1 VIF	CUL5	H13	P16402	[112-4]	2	2	0	9.5
HIV-1 VIF	CUL5	H12	P16403	[112-5]	2	2	0	9.9
HIV-1 VIF	CUL5	H1T	P22492	[112-6]	1	1	0	5.3
HIV-1 VIF	CUL5	H11	Q02539	[112-7]	1	1	0	5.1
HIV-1 VIF	CUL5	H1T	P22492	[112-8]	1	1	0	5.3
HIV-1 VIF	CUL5	H11	Q02539	[112-9]	1	1	0	5.1
HIV-1 VIF	CUL5	BAG2	O95816	[113]	1	1		5.2
HIV-1 VIF	CUL5	RL36	Q9Y3U8	[114]	1	1		10.5
HIV-1 VIF	CUL5	RL28	P46779	[115]	1	1		8
HIV-1 VIF	CUL5	DDB1	Q16531	[116]	1	1		2.6
HIV-1 VIF	CUL5	RT18B	Q9Y676	[117]	1	1		7.4
HIV-1 VIF	CUL5	RS26	P62854	[118]	2	2		20.9
HIV-1 VIF	CUL5	HCD2	Q99714	[119]	1	1		7.7
HIV-1 VIF	CUL5	RT31	Q92665	[120]	1	1		2.8
HIV-1 VIF	CUL5	DDX1	Q92499	[121]	1	1		1.8
HIV-1 VIF	CUL5	SRP09	P49458	[122]	1	1		12.8
HIV-1 VIF	CUL5	HNRL1	Q9BUJ2	[123]	1	1		2.3
HIV-1 VIF	CUL5	CLPB	Q9H078	[124]	2	2		4.7
HIV-1 VIF	CUL5	HS90A	P07900	[125]	1	1		1.9
HIV-1 VIF	CUL5	HS90B	P08238	[125-1]	1	1	0	1.9
HIV-1 VIF	CUL5	TRAP1	Q12931	[125-2]	1	1	0	2
HIV-1 VIF	CUL5	HS90A	P07900	[125-3]	1	1	0	1.9
HIV-1 VIF	CUL5	HS90B	P08238	[125-4]	1	1	0	1.9
HIV-1 VIF	CUL5	TRAP1	Q12931	[125-5]	1	1	0	2
HIV-1 VIF	CUL5	RL37A	P61513	[126]	1	1		19.6
HIV-1 VIF	CUL5	RS10	P46783	[127]	1	1		5.5
HIV-1 VIF	CUL5	RL35	P42766	[128]	1	1		10.6
HIV-1 VIF	CUL5	RT25	P82663	[129]	2	2		14.5
HIV-1 VIF	CUL5	HAX1	O00165	[130]	1	1		9
HIV-1 VIF	CUL5	RT14	O60783	[131]	1	1		11.7
HIV-1 VIF	CUL5	SMD3	P62318	[132]	1	1		7.9
HIV-1 VIF	CUL5	SRS10	O75494	[133]	1	1		6.1
HIV-1 VIF	CUL5	ROA1	P09651	[134]	1	1		2.7
HIV-1 VIF	CUL5	RA1L2	Q32P51	[134-1]	1	1	0	3.1
HIV-1 VIF	CUL5	ROA1	P09651	[134-2]	1	1	0	2.7
HIV-1 VIF	CUL5	RA1L2	Q32P51	[134-3]	1	1	0	3.1
HIV-1 VIF	CUL5	TCPZ	P40227	[135]	1	1		3
HIV-1 VIF	CUL5	TRA2A	Q13595	[136]	1	1		5

HIV-1 VIF	CUL5	RL27	P61353	[137]	1	1		6.6
HIV-1 VIF	CUL5	K1C40	Q6A162	[138]	1	1		2.8
HIV-1 VIF	CUL5	MEP50	Q9BQA1	[140]	1	1		4.1
HIV-1 VIF	CUL5	PGAM5	Q96HS1	[142]	1	1		4.2
HIV-1 VIF	CUL5	CSN3	Q9UNS2	[143]	1	1		3.5
HIV-1 VIF	CUL5	RT06	P82932	[144]	1	1		6.4
HIV-1 VIF	CUL5	FA40A	Q5VSL9	[145]	2	1		1.4
HIV-1 VIF	CUL5	GP133	Q6QNK2	[147]	1	1		1.3
HIV-1 VIF	CUL5	RT18C	Q9Y3D5	[148]	1	1		13.4
HIV-1 VIF	CUL5	LA	P05455	[149]	1	1		3.4
HIV-1 VIF	CUL5	RM12	P52815	[150]	1	1		6.1
HIV-1 VIF	CUL5	PURA	Q00577	[152]	1	1		2.8
HIV-1 VIF	CUL5	IPO5	O00410	[153]	1	1		1.4
HIV-1 VIF	CUL5	ELAV2	Q12926	[154]	1	1		3.1
HIV-1 VIF	CUL5	DNJA3	Q96EY1	[155]	1	1		3.3
HIV-1 VIF	CUL5	WFDC1	Q9HC57	[156]	1	1		5.9
HIV-1 VIF	CUL5	ZCHC3	Q9NUD5	[157]	1	1		4
HIV-1 VIF	CUL5	SEC62	Q99442	[158]	1	1		1.5
None	CUL5	K2C1	P04264	[1]	43	27		44.4
None	CUL5	K2C6B	P04259	[1-2, 4-4]	16	11	1	23.6
None	CUL5	K22E	P35908	[1-4, 4-6]	12	9	5	18.9
None	CUL5	K2C1B	Q7Z794	[1-6, 4-18]	5	3	1	3.6
None	CUL5	K2C8	P05787	[1-8, 4-20]	4	3	1	4.1
None	CUL5	K2C7	P08729	[1-9, 4-21]	4	3	1	4.3
None	CUL5	K2C8	P05787	[1-10, 4-22]	4	3	1	4.1
None	CUL5	K2C7	P08729	[1-11, 4-23]	4	3	1	4.3
None	CUL5	K2C4	P19013	[1-12, 4-24]	3	2	1	3.4
None	CUL5	GFAP	P14136	[1-14]	2	1	0	2.5
None	CUL5	K2C80	Q6KB66	[1-15]	2	1	0	2.4
None	CUL5	GFAP	P14136	[1-16]	2	1	0	2.5
None	CUL5	K2C80	Q6KB66	[1-17]	2	1	0	2.4
None	CUL5	K1C16	P08779	[2]	21	18		49.7
None	CUL5	K1C10	P13645	[2-2]	10	9	7	22.9
None	CUL5	K1C14	P02533	[2-4]	17	14	8	39.6
None	CUL5	K1C17	Q04695	[2-6]	8	7	4	21.3
None	CUL5	K1C15	P19012	[2-8]	6	4	0	9
None	CUL5	K1C19	P08727	[2-10]	3	2	0	4.5
None	CUL5	K1C13	P13646	[2-12]	3	2	0	5
None	CUL5	K1C12	Q99456	[2-14]	1	1	0	1.8
None	CUL5	K1C28	Q7Z3Y7	[2-16]	2	2	1	3.9
None	CUL5	K1C27	Q7Z3Y8	[2-17]	2	2	1	3.9
None	CUL5	K1C25	Q7Z3Z0	[2-18]	2	2	1	4
None	CUL5	K1C28	Q7Z3Y7	[2-19]	2	2	1	3.9
None	CUL5	K1C27	Q7Z3Y8	[2-20]	2	2	1	3.9
None	CUL5	K1C25	Q7Z3Z0	[2-21]	2	2	1	4

None	CUL5	K1C9	P35527	[3]	31	19		41.1
None	CUL5	K2C6C	P48668	[4]	17	13		28.2
None	CUL5	K2C6A	P02538	[4-2]	16	12	0	26.4
None	CUL5	K2C6B	P04259	[1-2, 4-4]	16	11	1	23.6
None	CUL5	K22E	P35908	[1-4, 4-6]	12	9	5	18.9
None	CUL5	K2C5	P13647	[4-8]	8	7	1	11.2
None	CUL5	K2C79	Q5XKE5	[4-10]	7	5	1	8.8
None	CUL5	K2C75	O95678	[4-12]	6	5	0	7.6
None	CUL5	K22O	Q01546	[4-14]	4	4	1	5.5
None	CUL5	K2C72	Q14CN4	[4-16]	4	3	0	4.7
None	CUL5	K2C1B	Q7Z794	[1-6, 4-18]	5	3	1	3.6
None	CUL5	K2C8	P05787	[1-8, 4-20]	4	3	1	4.1
None	CUL5	K2C7	P08729	[1-9, 4-21]	4	3	1	4.3
None	CUL5	K2C8	P05787	[1-10, 4-22]	4	3	1	4.1
None	CUL5	K2C7	P08729	[1-11, 4-23]	4	3	1	4.3
None	CUL5	K2C4	P19013	[1-12, 4-24]	3	2	1	3.4
None	CUL5	K2C3	P12035	[4-26]	3	3	0	3.2
None	CUL5	KRT84	Q9NSB2	[4-28]	4	3	1	3.3
None	CUL5	K2C71	Q3SY84	[4-30]	2	2	0	1.7
None	CUL5	K2C74	Q7RTS7	[4-31]	2	2	0	1.7
None	CUL5	K2C73	Q86Y46	[4-32]	2	2	0	1.7
None	CUL5	K2C71	Q3SY84	[4-33]	2	2	0	1.7
None	CUL5	K2C74	Q7RTS7	[4-34]	2	2	0	1.7
None	CUL5	K2C73	Q86Y46	[4-35]	2	2	0	1.7
None	CUL5	CUL5	Q93034	[5]	12	7		13.6
None	CUL5	HORN	Q86YZ3	[6]	6	5		3.1
None	CUL5	KV201	P01614	[7]	6	1		11.3
None	CUL5	KV204	P01617	[7-1]	6	1	0	11.5
None	CUL5	KV205	P06309	[7-2]	6	1	0	11.1
None	CUL5	KV206	P06310	[7-3]	6	1	0	9.8
None	CUL5	KV201	P01614	[7-4]	6	1	0	11.3
None	CUL5	KV204	P01617	[7-5]	6	1	0	11.5
None	CUL5	KV205	P06309	[7-6]	6	1	0	11.1
None	CUL5	KV206	P06310	[7-7]	6	1	0	9.8
None	CUL5	LSM12	Q3MHD2	[8]	3	3		28.2
None	CUL5	PEBB	Q13951	[9]	3	2		21.4
None	CUL5	CAV1	Q03135	[10]	1	1		5.6
None	CUL5	ODB2	P11182	[11]	3	3		8.1
None	CUL5	RT36	P82909	[12]	3	2		12.6
None	CUL5	KRT86	O43790	[13]	2	1		2.3
None	CUL5	KRT83	P78385	[13-1]	2	1	0	2.2
None	CUL5	KRT85	P78386	[13-2]	2	1	0	2.2
None	CUL5	KRT81	Q14533	[13-3]	2	1	0	2.2
None	CUL5	KRT82	Q9NSB4	[13-4]	2	1	0	2.1
None	CUL5	KRT86	O43790	[13-5]	2	1	0	2.3

None	CUL5	KRT83	P78385	[13-6]	2	1	0	2.2
None	CUL5	KRT85	P78386	[13-7]	2	1	0	2.2
None	CUL5	KRT81	Q14533	[13-8]	2	1	0	2.2
None	CUL5	KRT82	Q9NSB4	[13-9]	2	1	0	2.1
None	CUL5	RS5	P46782	[14]	1	1		7.4
None	CUL5	HSP71	P08107	[19]	1	1		2
None	CUL5	HSP7C	P11142	[19-1]	1	1	0	2
None	CUL5	HSP76	P17066	[19-2]	1	1	0	2
None	CUL5	HS71L	P34931	[19-3]	1	1	0	2
None	CUL5	HSP77	P48741	[19-4]	1	1	0	3.5
None	CUL5	HSP72	P54652	[19-5]	1	1	0	2
None	CUL5	HSP71	P08107	[19-6]	1	1	0	2
None	CUL5	HSP7C	P11142	[19-7]	1	1	0	2
None	CUL5	HSP76	P17066	[19-8]	1	1	0	2
None	CUL5	HS71L	P34931	[19-9]	1	1	0	2
None	CUL5	HSP77	P48741	[19-10]	1	1	0	3.5
None	CUL5	HSP72	P54652	[19-11]	1	1	0	2
None	CUL5	TMCC3	Q9ULS5	[22]	1	1		2.7
None	CUL5	TBA1B	P68363	[23]	1	1		3.1
None	CUL5	TBA4A	P68366	[23-1]	1	1	0	3.1
None	CUL5	TBA1C	Q9BQE3	[23-2]	1	1	0	3.1
None	CUL5	TBA4B	Q9H853	[23-3]	1	1	0	5.8
None	CUL5	TBA8	Q9NY65	[23-4]	1	1	0	3.1
None	CUL5	TBA1B	P68363	[23-5]	1	1	0	3.1
None	CUL5	TBA4A	P68366	[23-6]	1	1	0	3.1
None	CUL5	TBA1C	Q9BQE3	[23-7]	1	1	0	3.1
None	CUL5	TBA4B	Q9H853	[23-8]	1	1	0	5.8
None	CUL5	TBA8	Q9NY65	[23-9]	1	1	0	3.1

Table 7: SAXS Envelope Data

	Rg, from Guinier (Å)	Rg, from P(r) (Å)	Dmax (Å)
HIV-1 E3	55.7	56.94	190
MVV E3	59.37	61.47	200

Second and third columns indicate the radius of gyration (Rg) calculated from Guinier plot and pair distance distribution function P(r), respectively. The fourth column indicates the maximum distance in P(r), Dmax.

Table 8: AP-MS Data for FKBP5 and PTGES3 with FIV and SIVmac Vif Proteins, SAINT Scores ≥ 0.8

Protein Name	Uniprot Accn	FKBP5	FKBP5 + FIV VIF	FKBP5 + SIVmac VIF	PTGES3	PTGES3 + FIV VIF	PTGES3 + SIVmac VIF
1433B	P31946	0.00	0.00	0.00	0.00	0.00	0.93
1433F	Q04917	0.00	0.00	0.91	0.00	0.00	0.00
1433G	P61981	0.94	0.92	0.92	0.96	0.93	0.92
1433T	P27348	0.94	0.93	0.00	0.00	0.93	0.93
1433Z	P63104	0.92	0.98	0.99	0.99	0.98	0.92
2AAA	P30153	0.99	0.99	0.99	0.00	0.91	0.00
2AAB	P30154	0.98	0.88	0.00	0.00	0.00	0.00
3MG	P29372	0.00	0.00	0.00	0.98	0.99	1.00
A16A1	Q8IZ83	0.00	0.00	0.00	0.91	0.92	0.90
AAAS	Q9NRG9	0.00	0.00	0.00	1.00	0.00	0.98
ABCF1	Q8NE71	0.00	0.00	0.00	1.00	0.00	0.98
ACLY	P53396	1.00	0.98	1.00	1.00	1.00	1.00
ADT4	Q9H0C2	0.00	0.00	0.00	0.00	0.00	0.82
AGO1	Q9UL18	1.00	1.00	1.00	1.00	1.00	1.00
AGO2	Q9UKV8	1.00	1.00	1.00	1.00	1.00	1.00
AGO3	Q9H9G7	1.00	0.99	1.00	1.00	1.00	1.00
AGO4	Q9HCK5	1.00	0.83	1.00	0.99	0.98	0.99
AHR	P35869	0.00	0.00	0.00	0.00	0.87	0.00
AIP	O00170	0.00	0.00	0.00	1.00	1.00	1.00
AL1L2	Q3SY69	0.00	0.00	0.00	0.00	0.00	0.97
AMPM1	P53582	0.00	0.00	0.00	0.00	0.00	0.91
ANKY2	Q8IV38	0.00	0.00	0.00	1.00	1.00	1.00
APBB1	O00213	0.00	0.00	0.00	0.89	0.98	0.99
APC7	Q9UJX3	0.00	0.00	0.00	0.92	0.00	0.93
ARAF	P10398	1.00	1.00	1.00	0.00	0.00	0.00
ASNS	P08243	0.00	0.00	0.00	0.00	0.98	0.00
AT1A1	P05023	0.85	0.00	0.00	0.00	0.00	0.92
ATD3A	Q9NVI7	0.00	0.00	0.85	0.00	0.93	0.00
ATP5H	O75947	0.00	0.00	0.97	0.00	0.00	0.92
ATPO	P48047	0.00	0.97	0.00	0.00	0.00	0.00
AURKB	Q96GD4	1.00	1.00	1.00	1.00	1.00	1.00
AURKC	Q9UQB9	0.93	0.97	0.97	0.00	0.00	0.92
BBS1	Q8NFJ9	0.00	0.00	0.00	0.89	0.00	0.00
BCAS3	Q9H6U6	0.00	0.00	0.00	0.83	0.00	0.00
BOLA2	Q9H3K6	0.93	0.00	0.93	0.00	0.96	0.93

C1TC	P11586	0.91	0.00	0.00	0.90	0.91	0.00
CAF1B	Q13112	0.00	0.00	0.00	0.89	0.00	0.00
CALX	P27824	0.00	0.00	0.90	0.00	0.00	0.00
CAPZB	P47756	0.00	0.92	0.96	0.00	0.00	0.00
CBX1	P83916	0.00	0.00	0.00	0.94	0.00	0.00
CBX3	Q13185	0.00	0.98	0.81	1.00	0.99	1.00
CD11A	Q9UQ88	1.00	1.00	1.00	0.00	0.00	0.00
CD11B	P21127	1.00	1.00	1.00	0.00	0.00	0.00
CDC37	Q16543	1.00	1.00	1.00	0.90	1.00	1.00
CDC7	O00311	0.00	0.00	0.00	0.98	0.97	0.00
CDK1	P06493	1.00	1.00	1.00	1.00	0.98	0.98
CDK18	Q07002	0.00	0.00	0.89	0.00	0.00	0.00
CDK2	P24941	0.00	0.00	0.91	0.00	0.00	0.00
CDK3	Q00526	0.00	0.00	0.92	0.00	0.00	0.00
CDK4	P11802	0.99	0.99	1.00	0.00	0.00	0.00
CDK7	P50613	0.98	0.00	0.00	0.00	0.00	0.00
CDK9	P50750	0.98	1.00	1.00	0.86	0.00	0.00
CH60	P10809	0.00	0.88	0.92	0.00	0.93	0.85
CHIP	Q9UNE7	0.00	0.00	0.00	1.00	1.00	1.00
CHTOP	Q9Y3Y2	0.00	0.00	0.81	0.00	0.00	0.00
CMC2	Q9UJS0	0.00	0.00	0.00	0.00	0.90	0.00
CN080	Q86SX3	0.00	0.00	0.00	0.99	0.88	1.00
CN166	Q9Y224	0.00	0.00	0.00	1.00	1.00	1.00
CN37	P09543	0.00	0.00	0.00	0.00	0.00	0.91
CNOTA	Q9H9A5	0.00	0.00	0.00	0.00	0.98	0.00
CO044	Q96SY0	0.00	0.00	0.00	0.00	0.90	0.00
COPA	P53621	0.99	1.00	1.00	1.00	1.00	1.00
COPB	P53618	0.00	0.98	0.00	0.00	0.92	0.00
COPB2	P35606	0.00	0.00	0.89	0.00	0.00	0.83
COPE	O14579	0.00	0.00	0.00	0.92	0.96	0.00
COPG	Q9Y678	0.00	0.83	0.00	0.00	0.00	0.00
CPSF1	Q10570	0.00	0.00	0.96	0.98	0.99	0.00
CSK21	P68400	1.00	0.00	1.00	0.00	0.00	0.00
CSK2B	P67870	0.96	0.00	0.96	0.00	0.00	0.00
CSTF2	P33240	0.00	0.00	0.90	0.00	0.00	0.00
CSTFT	Q9H0L4	0.00	0.00	0.88	0.00	0.00	0.00
CT004	Q9Y312	0.00	0.00	0.97	0.00	0.00	0.00
CTNA1	P35221	0.00	0.81	0.00	0.00	0.00	0.00
CUL5	Q93034	0.00	0.00	0.00	0.00	0.88	0.00
CX057	Q6NSI4	0.00	0.00	0.96	1.00	1.00	1.00
CYBP	Q9HB71	0.00	1.00	1.00	1.00	1.00	1.00

DCTN2	Q13561	0.00	0.00	0.84	0.00	0.00	0.00
DDB1	Q16531	0.00	0.00	0.00	0.97	0.86	0.00
DDX1	Q92499	0.00	0.00	0.00	1.00	1.00	1.00
DDX21	Q9NR30	0.00	0.90	0.00	0.00	0.00	0.00
DDX5	P17844	0.00	0.00	0.00	0.00	0.00	0.81
DHB4	P51659	0.99	0.00	0.97	0.98	1.00	1.00
DHX34	Q14147	0.00	0.00	0.00	1.00	0.00	0.00
DHX36	Q9H2U1	0.00	0.00	0.00	0.00	0.97	0.98
DHX40	Q8IX18	0.00	0.00	0.00	0.00	0.89	0.00
DJC11	Q9NVH1	0.00	0.00	0.00	0.91	0.00	0.00
DLRB1	Q9NP97	0.00	0.00	0.00	0.00	0.00	0.89
DNA2L	P51530	0.00	0.00	0.96	1.00	0.99	0.99
DNJA1	P31689	0.00	0.95	0.98	1.00	0.99	1.00
DNJB6	O75190	0.00	0.00	0.00	0.91	0.98	0.00
DNJC7	Q99615	0.00	0.00	0.00	0.98	0.00	0.00
DPOD1	P28340	0.89	0.00	0.00	1.00	1.00	1.00
DPOE3	Q9NRF9	0.00	0.00	0.00	0.00	0.00	0.88
DRG1	Q9Y295	0.00	0.00	0.00	0.97	0.97	0.00
DX39A	O00148	0.00	0.91	0.00	0.00	0.00	0.00
DX39B	Q13838	0.00	0.90	0.00	0.00	0.00	0.00
DYHC1	Q14204	0.00	0.00	0.81	0.00	0.00	0.00
ECHA	P40939	0.00	0.99	0.00	0.99	0.97	0.99
EF2	P13639	1.00	1.00	1.00	1.00	1.00	1.00
EGLN1	Q9GZT9	0.00	0.00	0.00	1.00	1.00	1.00
EIF3D	O15371	0.00	0.91	0.00	0.00	0.00	0.00
EIF3G	O75821	0.00	0.92	0.97	0.00	0.00	0.93
EIF3M	Q7L2H7	0.00	0.81	0.82	0.00	0.00	0.00
ELOB	Q15370	0.00	0.00	1.00	0.00	0.97	1.00
ELOC	Q15369	0.00	0.00	1.00	0.00	1.00	1.00
ELP1	O95163	1.00	0.00	0.00	1.00	0.00	1.00
ENOA	P06733	0.00	0.99	0.89	0.00	0.00	0.00
ENOB	P13929	0.00	0.99	0.90	0.00	0.00	0.00
ENPL	P14625	1.00	1.00	1.00	0.99	1.00	0.99
F10A1	P50502	0.00	0.88	0.00	0.91	0.99	0.00
F10A5	Q8NFI4	0.00	0.00	0.00	0.00	0.99	0.00
F115A	Q9Y4C2	0.00	0.00	0.00	1.00	0.00	0.00
F116A	Q8IWF6	0.00	0.00	0.00	0.00	0.91	0.00
F203A	Q9BTY7	0.98	0.00	0.00	0.00	0.00	0.00
F203B	P0CB43	0.98	0.00	0.00	0.00	0.00	0.00
FA98B	Q52LJ0	0.00	0.00	0.00	0.00	0.97	0.91
FAS	P49327	1.00	1.00	1.00	1.00	1.00	1.00

FETUA	P02765	0.00	0.00	0.00	0.00	0.93	0.97
FKBP4	Q02790	0.00	0.00	0.00	1.00	1.00	1.00
FKBP5	Q13451	1.00	1.00	1.00	1.00	1.00	1.00
FKBP8	Q14318	0.00	0.00	0.00	1.00	1.00	1.00
FLII	Q13045	0.88	0.83	0.93	0.98	0.87	0.97
FUBP2	Q92945	0.00	0.98	0.89	0.91	0.00	0.91
FUS	P35637	0.00	0.90	0.00	0.00	0.00	0.84
G3P	P04406	0.92	0.99	0.89	0.99	0.92	0.92
GBLP	P63244	1.00	0.00	1.00	0.00	0.00	0.00
GCR	P04150	0.88	0.00	0.00	1.00	1.00	1.00
GDIB	P50395	0.00	0.00	0.00	0.91	0.00	0.00
GLMN	Q92990	1.00	0.99	0.99	0.00	0.00	0.00
H31	P68431	0.00	0.00	0.00	0.00	0.96	0.00
H31T	Q16695	0.00	0.00	0.00	0.00	0.95	0.00
H32	Q71DI3	0.00	0.00	0.00	0.00	0.96	0.00
H33	P84243	0.00	0.00	0.00	0.00	0.95	0.00
H90B2	Q58FF8	1.00	1.00	1.00	1.00	1.00	1.00
H90B3	Q58FF7	1.00	1.00	1.00	1.00	1.00	1.00
H90B4	Q58FF6	1.00	1.00	1.00	1.00	1.00	1.00
HAT1	O14929	0.00	0.00	0.97	0.92	0.00	0.00
HAUS5	O94927	0.00	0.00	0.00	0.00	0.00	0.97
HCFC1	P51610	0.00	0.00	0.00	0.94	0.00	0.00
HNRCL	O60812	0.00	0.88	0.00	0.00	0.00	0.00
HNRL2	Q1KMD3	0.00	0.00	0.00	0.87	0.00	0.00
HNRPF	P52597	0.94	0.97	0.92	0.97	0.00	0.00
HNRPR	O43390	0.00	0.97	0.90	0.00	0.00	0.92
HPS6	Q86YV9	0.00	0.00	0.00	0.00	0.00	0.90
HS105	Q92598	0.00	0.91	0.91	0.93	0.00	0.93
HS74L	O95757	0.00	0.99	1.00	0.99	0.00	0.00
HS902	Q14568	1.00	1.00	1.00	1.00	1.00	1.00
HS904	Q58FG1	1.00	1.00	1.00	1.00	1.00	1.00
HS905	Q58FG0	1.00	1.00	1.00	1.00	1.00	1.00
HS90A	P07900	0.99	0.98	0.98	0.99	0.99	0.99
HS90B	P08238	0.85	0.80	0.81	0.84	0.90	0.88
HSP74	P34932	0.84	0.96	0.93	0.99	0.97	1.00
I2BP1	Q8IU81	0.00	0.00	0.00	0.96	0.00	0.00
IF2B1	Q9NZI8	0.00	0.00	0.00	0.00	0.00	0.92
IF2G	P41091	0.00	0.00	0.00	0.90	0.00	0.00
IF4A1	P60842	0.93	0.98	0.98	0.98	0.00	0.00
IF4A2	Q14240	0.93	0.98	0.98	0.97	0.00	0.00
IF5A2	Q9GZV4	0.90	0.00	0.00	0.00	0.00	0.00

IKKA	O15111	1.00	0.99	1.00	0.00	0.00	0.00
IKKB	O14920	1.00	0.99	1.00	0.00	0.00	0.00
ILF2	Q12905	0.00	0.00	0.00	0.00	0.98	0.00
ILF3	Q12906	0.00	0.99	0.00	0.98	0.00	0.90
ILK	Q13418	0.00	0.00	0.00	0.00	0.00	0.92
IMA2	P52292	0.00	0.00	0.99	0.92	0.00	0.92
IMB1	Q14974	0.00	0.00	0.88	0.00	0.00	0.00
INO1	Q9NPH2	0.00	0.00	0.00	0.99	0.00	0.98
IPO5	O00410	0.84	0.80	0.99	0.99	0.98	0.98
IRS4	O14654	0.99	0.00	0.88	1.00	1.00	1.00
K1967	Q8N163	0.00	0.84	0.98	0.99	0.89	1.00
K6PF	P08237	0.00	0.00	0.00	1.00	0.95	0.97
K6PL	P17858	0.00	0.00	0.00	0.97	0.00	0.00
K6PP	Q01813	0.00	0.00	0.00	0.86	0.00	0.00
KBP	Q96EK5	0.86	0.96	0.00	1.00	1.00	1.00
KC1A	P48729	0.00	0.00	0.00	0.92	0.00	0.96
KDM1A	O60341	0.00	0.00	0.00	0.90	0.90	0.92
KLH26	Q53HC5	0.00	0.00	0.97	0.00	0.00	0.00
KPRB	O60256	0.00	0.00	0.00	0.00	0.00	0.89
KPYM	P14618	0.97	0.00	0.97	0.99	0.98	0.98
L2GL1	Q15334	0.97	0.95	0.86	0.99	0.99	0.97
LAP2A	P42166	0.00	0.97	0.97	0.00	0.00	0.97
LAP2B	P42167	0.00	0.98	0.97	0.00	0.00	0.98
LDHA	P00338	0.00	0.00	0.00	0.97	0.00	0.00
LIMS1	P48059	0.00	0.00	0.00	0.96	0.00	0.00
LIS1	P43034	0.00	0.00	0.00	0.98	0.00	0.98
LPPRC	P42704	0.00	0.00	0.00	0.00	0.00	0.94
MA7D3	Q8IWC1	0.00	0.00	0.97	0.00	0.00	0.00
MAGD4	Q96JG8	0.00	0.00	0.00	0.00	0.00	0.90
MATK	P42679	0.91	0.00	0.00	0.00	0.00	0.00
MCCB	Q9HCC0	0.00	0.00	0.00	0.00	0.00	0.97
MCM2	P49736	0.00	0.00	0.88	0.99	0.00	0.00
MCM3	P25205	0.00	0.00	0.83	0.00	0.00	0.00
MCM4	P33991	1.00	0.99	1.00	0.00	0.00	1.00
MCM5	P33992	1.00	0.97	0.97	0.99	0.87	0.90
MCM6	Q14566	1.00	1.00	1.00	0.00	0.00	0.00
MCM7	P33993	1.00	1.00	1.00	1.00	0.94	0.99
MCM8	Q9UJA3	0.00	0.00	0.00	0.00	0.00	0.98
MCMBP	Q9BTE3	1.00	1.00	1.00	0.00	0.00	0.00
METH	Q99707	0.00	0.00	0.00	1.00	0.99	1.00
MKS1	Q9NXB0	0.00	0.00	0.00	0.88	0.00	0.00

ML12A	P19105	0.00	0.00	0.00	0.00	0.93	0.00
ML12B	O14950	0.00	0.00	0.00	0.00	0.91	0.00
MON1A	Q86VX9	0.00	0.00	0.00	0.00	0.00	0.90
MOV10	Q9HCE1	0.00	0.00	0.00	0.86	0.00	0.00
MSH6	P52701	0.00	0.00	0.00	1.00	0.99	0.99
MTA2	O94776	0.00	0.94	0.96	0.00	0.00	0.00
MTA3	Q9BTC8	0.00	0.90	0.91	0.00	0.00	0.00
MTDC	P13995	0.00	0.00	0.00	0.00	0.92	0.00
NEIL3	Q8TAT5	0.00	0.00	0.00	0.96	0.00	0.00
NEMO	Q9Y6K9	1.00	1.00	1.00	0.00	0.00	0.00
NOC3L	Q8WTT2	0.00	0.00	0.00	0.86	0.00	0.00
NOP56	O00567	0.00	0.00	0.00	0.00	0.84	0.00
NOP58	Q9Y2X3	0.00	0.90	0.00	0.00	0.00	0.00
NP1L1	P55209	0.00	0.91	0.91	0.00	0.00	0.00
NP1L4	Q99733	0.00	0.00	0.00	0.00	0.81	0.00
NPM	P06748	0.00	0.00	0.00	0.99	0.94	0.80
NSUN2	Q08J23	0.00	0.00	0.00	0.89	0.00	0.00
NSUN5	Q96P11	0.00	0.00	0.00	0.92	0.92	0.00
NUDC	Q9Y266	0.93	0.00	0.92	0.00	0.00	0.00
NUDC3	Q8IVD9	0.99	0.97	0.98	0.00	0.00	0.00
NVL	O15381	0.00	0.00	0.00	0.97	0.00	0.00
OAT	P04181	0.93	0.91	0.98	0.00	0.92	0.00
PDCD2	Q16342	0.98	0.90	0.99	0.98	0.93	0.98
CBFβ	Q13951	0.00	0.00	0.92	0.00	0.00	0.92
PFD2	Q9UHV9	0.00	0.00	0.00	0.00	0.00	0.88
PGRC1	O00264	0.00	0.00	0.00	0.93	0.92	0.00
PHLB3	Q6NSJ2	0.00	0.00	0.00	0.97	0.00	0.00
PIHD1	Q9NWS0	0.00	0.00	0.00	0.98	0.98	0.93
PKN3	Q6P5Z2	0.85	0.00	0.00	0.00	0.00	0.00
PLPL2	Q96AD5	0.99	0.98	0.99	0.97	0.00	0.00
PP2AA	P67775	0.00	0.90	0.00	0.00	0.00	0.00
PPIA	P62937	0.00	0.00	0.00	0.92	0.91	0.00
PPIB	P23284	0.00	0.93	0.92	0.00	0.00	0.00
PPID	Q08752	0.00	0.00	0.00	0.90	0.00	0.00
PPP5	P53041	0.00	0.00	0.00	1.00	1.00	1.00
PR14L	Q5THK1	1.00	0.99	1.00	0.00	0.00	0.88
PRDX1	Q06830	0.00	0.92	0.98	0.00	0.97	0.97
PRDX3	P30048	0.83	0.00	0.00	0.00	0.00	0.00
PRDX6	P30041	0.00	0.00	0.96	0.00	0.00	0.00
PRKDC	P78527	0.00	0.84	0.00	0.00	0.97	0.00
PROF1	P07737	0.00	0.98	0.91	0.00	0.00	0.00

PRP19	Q9UMS4	0.00	0.99	0.00	0.98	0.98	0.91
PRPS3	P21108	0.82	0.00	0.96	0.00	0.00	0.82
PRS10	P62333	0.96	0.96	0.98	0.00	0.95	0.00
PRS6A	P17980	0.89	0.00	0.91	0.00	0.00	0.00
PRS6B	P43686	0.93	0.91	0.92	0.00	0.00	0.96
PSA4	P25789	0.00	0.96	0.97	0.00	0.00	0.00
PSB4	P28070	0.99	0.00	0.00	0.00	0.00	0.00
PSD12	O00232	0.00	0.00	0.88	0.00	0.00	0.00
PSD7	P51665	0.00	0.80	0.00	0.00	0.00	0.00
PSMD1	Q99460	0.96	0.84	0.89	0.00	0.95	0.00
PSMD6	Q15008	0.00	0.00	0.97	0.00	0.00	0.00
PTBP1	P26599	0.00	0.00	0.00	0.99	0.00	0.00
PTOV1	Q86YD1	1.00	1.00	1.00	1.00	1.00	1.00
PUR6	P22234	0.00	0.92	0.00	0.00	0.00	0.93
PYGL	P06737	0.00	0.00	0.00	0.97	0.00	0.00
PYR1	P27708	0.00	0.00	0.00	0.91	0.80	0.81
QCR2	P22695	0.00	0.00	0.00	0.00	0.00	0.91
RAF1	P04049	0.00	0.00	0.97	0.00	0.00	0.00
RBM14	Q96PK6	0.00	0.89	0.00	0.00	0.00	0.00
RBM39	Q14498	0.00	0.92	0.91	0.00	0.00	0.00
RBP56	Q92804	0.00	0.88	0.00	0.00	0.00	0.00
RCC1	P18754	0.00	0.96	0.00	0.00	0.00	0.00
RCC2	Q9P258	0.00	0.00	0.00	0.00	0.97	0.00
RECQ4	O94761	0.00	0.00	0.00	0.00	0.00	0.97
REXON	Q96IC2	0.00	0.00	0.98	0.90	0.92	0.92
RIR1	P23921	0.00	0.00	0.00	0.86	0.00	0.00
RL10	P27635	0.00	0.00	0.00	0.81	0.81	0.00
RL13	P26373	0.00	0.00	0.00	0.89	0.00	0.00
RL35	P42766	0.00	0.00	0.00	0.83	0.00	0.00
RL4	P36578	0.00	0.92	0.00	0.93	0.00	0.00
RLA2	P05387	0.00	0.96	0.92	0.93	0.00	0.94
RMP	O94763	0.00	0.00	0.00	0.00	0.00	0.89
RNZ2	Q9BQ52	0.00	0.00	0.00	0.86	0.00	0.00
ROA3	P51991	0.00	0.00	0.00	0.91	0.00	0.00
RPAP3	Q9H6T3	0.00	0.00	0.00	0.99	0.99	0.97
RPB2	P30876	1.00	0.00	0.84	1.00	1.00	1.00
RPC2	Q9NW08	0.00	0.00	0.00	0.00	0.00	0.83
RPN1	P04843	0.00	0.00	0.00	0.00	0.00	0.91
RRP44	Q9Y2L1	0.00	0.00	0.00	0.82	0.00	0.00
RS15A	P62244	0.00	0.00	0.93	0.92	0.00	0.98
RS20	P60866	0.00	0.00	0.81	0.00	0.00	0.00

RS23	P62266	0.00	0.84	0.00	0.00	0.00	0.00
RS24	P62847	0.00	0.89	0.00	0.00	0.00	0.00
RS29	P62273	0.91	0.92	0.92	0.00	0.00	0.00
RS7	P62081	0.92	0.91	0.99	0.99	0.99	0.99
RT21	P82921	0.00	0.00	0.00	0.00	0.88	0.00
RTCB	Q9Y3I0	0.00	0.00	0.00	1.00	1.00	1.00
RTEL1	Q9NZ71	0.89	0.00	0.00	0.00	0.89	0.98
RUVB1	Q9Y265	0.00	0.00	0.00	0.94	0.87	0.90
RUVB2	Q9Y230	0.00	0.00	0.94	0.99	1.00	0.99
SAMH1	Q9Y3Z3	0.00	0.00	0.00	0.99	0.00	0.00
SC23A	Q15436	0.00	0.00	0.00	0.87	0.00	0.00
SC61B	P60468	0.00	0.00	0.00	0.00	0.00	0.92
SEPT2	Q15019	0.00	0.91	0.00	0.00	0.00	0.00
SKP1	P63208	0.00	0.00	0.00	0.99	0.99	0.99
SMCA5	O60264	0.00	0.00	0.88	0.90	0.91	0.91
SMG8	Q8ND04	0.00	0.00	0.00	0.83	0.00	0.00
SMRC1	Q92922	0.00	0.81	0.00	0.00	0.00	0.00
SND1	Q7KZF4	0.00	0.00	0.96	0.88	0.00	0.00
SNUT2	Q53GS9	0.00	0.89	0.00	0.00	0.00	0.00
SNW1	Q13573	0.98	0.00	0.00	0.92	0.00	0.00
SP16H	Q9Y5B9	0.00	0.00	0.94	0.00	0.82	0.97
SPIN3	Q5JUX0	0.00	0.91	0.00	0.00	0.00	0.00
SRP09	P49458	0.00	0.00	0.00	0.91	0.99	0.98
SRP14	P37108	0.00	0.00	0.00	1.00	0.99	0.99
SRSF1	Q07955	0.00	0.81	0.00	0.00	0.00	0.00
SRSF2	Q01130	0.00	0.92	0.92	0.95	0.00	0.00
SSRD	P51571	0.00	0.00	0.00	0.92	0.00	0.91
ST134	Q8IZP2	0.00	0.91	0.00	0.92	0.92	0.00
STIP1	P31948	0.97	0.90	0.00	0.00	0.00	0.00
STXB3	O00186	0.00	0.00	0.00	0.00	0.90	0.00
SUGT1	Q9Y2Z0	1.00	1.00	1.00	1.00	0.96	0.99
SYFA	Q9Y285	0.00	0.00	0.00	1.00	1.00	1.00
SYTM	Q9BW92	0.00	0.00	0.00	0.00	0.00	0.96
SYVC	P26640	0.99	0.99	0.99	0.83	0.95	0.99
TEBP	Q15185	1.00	1.00	1.00	1.00	1.00	1.00
TF3C4	Q9UKN8	0.00	0.00	0.00	0.00	0.87	0.00
TF3C5	Q9Y5Q8	0.98	0.99	0.97	1.00	1.00	1.00
TFAM	Q00059	0.00	0.00	0.89	0.98	0.98	0.98
TIM13	Q9Y5L4	0.00	0.00	0.00	0.99	0.99	0.00
TKT	P29401	0.00	0.00	0.00	0.87	0.00	0.00
TNR6B	Q9UPQ9	0.00	0.99	0.97	0.00	0.00	0.00

TOM34	Q15785	0.00	0.00	0.00	0.00	0.91	0.00
TOM70	O94826	0.00	0.00	0.00	0.90	0.00	0.00
TOP2A	P11388	1.00	1.00	0.99	1.00	1.00	1.00
TOP2B	Q02880	0.97	0.99	1.00	1.00	1.00	1.00
TPIS	P60174	0.00	0.90	0.00	0.00	0.00	0.00
TRM2A	Q8IZ69	0.98	0.00	0.98	1.00	0.99	0.99
TRM6	Q9UJA5	0.00	0.00	0.00	0.90	0.97	0.00
TTC26	A0AVF1	0.00	0.00	0.00	0.99	0.91	0.99
TTC37	Q6PGP7	0.00	0.00	0.00	0.99	0.87	0.97
TTC4	O95801	1.00	0.00	0.83	1.00	1.00	1.00
TTC9C	Q8N5M4	0.00	0.00	0.00	0.00	0.91	0.00
TTF2	Q9UNY4	0.00	0.00	0.00	0.00	0.83	0.00
U5S1	Q15029	0.82	0.00	0.00	0.94	0.00	0.95
UBA1	P22314	0.00	0.85	0.00	0.97	0.00	0.00
UBQL2	Q9UHD9	0.00	0.00	0.00	0.89	0.00	0.00
UHRF1	Q96T88	0.00	0.00	0.00	0.88	0.00	0.00
UN45A	Q9H3U1	0.80	0.00	0.00	0.99	1.00	1.00
VDAC2	P45880	0.00	0.00	0.00	0.00	0.00	0.98
WDR34	Q96EX3	0.00	0.00	0.00	0.97	0.00	0.00
WDR36	Q8NI36	0.00	0.00	0.00	0.98	0.00	0.00
WDR6	Q9NNW5	0.00	0.00	0.00	1.00	0.99	0.00
WDR61	Q9GZS3	0.00	0.00	0.00	0.96	0.92	0.00
WDR67	Q96DN5	0.00	0.00	0.00	0.84	0.00	0.00
XRCC5	P13010	0.00	0.00	0.98	0.98	0.98	0.99
XRCC6	P12956	0.00	0.00	0.89	0.97	0.00	0.97
XRN2	Q9H0D6	0.00	0.00	0.00	0.83	0.00	0.00
YTDC2	Q9H6S0	0.00	0.00	0.00	0.98	1.00	0.00
ZN326	Q5BKZ1	0.00	0.87	0.00	0.00	0.00	0.00

References

Ackley, C.D., Yamamoto, J.K., Levy, N., Pedersen, N.C., and Cooper, M.D. (1990). Immunologic abnormalities in pathogen-free cats experimentally infected with feline immunodeficiency virus. J. Virol. *64*, 5652–5655.

Ai, Y., Zhu, D., Wang, C., Su, C., Ma, J., Ma, J., and Wang, X. (2014). Core-binding factor subunit beta is not required for non-primate lentiviral Vif mediated APOBEC3 degradation. J. Virol.

Altschul, S.F., Gish, W., Miller, W., Myers, E.W., and Lipman, D.J. (1990). Basic local alignment search tool. J. Mol. Biol. *215*, 403–410.

Ayllon, J., Hale, B.G., and Garcia-Sastre, A. (2012). Strain-Specific Contribution of NS1-Activated Phosphoinositide 3-Kinase Signaling to Influenza A Virus Replication and Virulence. J. Virol. *86*, 5366–5370.

Barré-Sinoussi, F., Chermann, J.C., Rey, F., Nugeyre, M.T., Chamaret, S., Gruest, J., Dauguet, C., Axler-Blin, C., Vézinet-Brun, F., Rouzioux, C., et al. (1983). Isolation of a T-lymphotropic retrovirus from a patient at risk for acquired immune deficiency syndrome (AIDS). Science *220*, 868–871.

Beltrao, P., Cagney, G., and Krogan, N.J. (2010). Quantitative genetic interactions reveal biological modularity. Cell *141*, 739–745.

Berndsen, C.E., and Wolberger, C. (2014). New insights into ubiquitin E3 ligase mechanism. Nat. Struct. Mol. Biol. *21*, 301–307.

Binka, M., Ooms, M., Steward, M., Simon, V., Manuscript, R., Health, T.G., Gustave, O., and Place, L.L. (2012). The activity spectrum of Vif from multiple HIV-1 subtypes against APOBEC3G, APOBEC3F, and APOBEC3H. J. Virol. *86*, 49–59.

Bloom, J., and Pagano, M. (2005). Experimental tests to definitively determine ubiquitylation of a substrate. Methods Enzymol. *399*, 249–266.

Bogerd, H.P., Tallmadge, R.L., Oaks, J.L., Carpenter, S., and Cullen, B.R. (2008). Equine infectious anemia virus resists the antiretroviral activity of equine APOBEC3 proteins through a packaging-independent mechanism. J. Virol. *82*, 11889–11901.

Bosco, D. a, Eisenmesser, E.Z., Clarkson, M.W., Wolf-Watz, M., Labeikovsky, W., Millet, O., and Kern, D. (2010). Dissecting the microscopic steps of the cyclophilin A enzymatic cycle on the biological HIV-1 capsid substrate by NMR. J. Mol. Biol. *403*, 723–738.

Bowen, D.G., and Walker, C.M. (2005). Adaptive immune responses in acute and chronic hepatitis C virus infection. Nature *436*, 946–952.

Braaten, D., and Luban, J. (2001). Cyclophilin A regulates HIV-1 infectivity, as demonstrated by gene targeting in human T cells. EMBO J. *20*, 1300–1309.

Caprera, A., Lazzari, B., Stella, A., Merelli, I., Caetano, A.R., and Mariani, P. (2007). GoSh: a web-based database for goat and sheep EST sequences. Bioinformatics *23*, 1043–1045.

Carbon, S., Ireland, A., Mungall, C.J., Shu, S., Marshall, B., Lewis, S., Lomax, J., Mungall, C., Hitz, B., Balakrishnan, R., et al. (2009). AmiGO: Online access to ontology and annotation data. Bioinformatics *25*, 288–289.

Castresana, J. (2000). Selection of conserved blocks from multiple alignments for their use in phylogenetic analysis. Mol. Biol. Evol. *17*, 540–552.

Chan, E., Towers, G.J., and Qasim, W. (2014). Gene therapy strategies to exploit TRIM derived restriction factors against HIV-1. Viruses *6*, 243–263.

De Chassey, B., Meyniel-Schicklin, L., Vonderscher, J., André, P., and Lotteau, V. (2014). Virus-host interactomics: new insights and opportunities for antiviral drug discovery. Genome Med. *6*, 1–14.

Choi, H., Larsen, B., Lin, Z.-Y., Breitkreutz, A., Mellacheruvu, D., Fermin, D., Qin, Z.S., Tyers, M., Gingras, A.-C., and Nesvizhskii, A.I. (2011). SAINT: probabilistic scoring of affinity purification-mass spectrometry data. Nat. Methods *8*, 70–73.

Choi, M., Chang, C.-Y., Clough, T., Broudy, D., Killeen, T., MacLean, B., and Vitek, O. (2014). MSstats: an R package for statistical analysis of quantitative mass spectrometry-based proteomic experiments. Bioinformatics 1–2.

Clague, M.J., Heride, C., and Urbé, S. (2015). The demographics of the ubiquitin system. Trends Cell Biol. 1–10.

Daugherty, M.D., and Malik, H.S. (2012). Rules of engagement: molecular insights from host-virus arms races. Annu. Rev. Genet. *46*, 677–700.

Davey, N.E., Travé, G., and Gibson, T.J. (2011). How viruses hijack cell regulation. Trends Biochem. Sci. *36*, 159–169.

Davis, Z.H., Verschueren, E., Jang, G.M., Kleffman, K., Johnson, J.R., Park, J., Shales, M., Dollen, J. Von, Maher, M.C., Johnson, T., et al. (2015). Global Mapping of Herpesvirus-Host Protein Complexes Reveals a Transcription Strategy for Late Genes. Mol. Cell *57*, 349–360.

Dereeper, A., Guignon, V., Blanc, G., Audic, S., Buffet, S., Chevenet, F., Dufayard, J.-F., Guindon, S., Lefort, V., Lescot, M., et al. (2008). Phylogeny.fr: robust phylogenetic analysis for the non-specialist. Nucleic Acids Res. *36*, W465–W469.

Derse, D., Hill, S. a, Princler, G., Lloyd, P., and Heidecker, G. (2007). Resistance of human T cell leukemia virus type 1 to APOBEC3G restriction is mediated by elements in nucleocapsid. Proc. Natl. Acad. Sci. U. S. A. *104*, 2915–2920.

Deshaies, R.J., and Joazeiro, C.A.P. (2009). RING Domain E3 Ubiquitin Ligases. Annu. Rev. Biochem. *78*, 399–434.

Doehle, B.P., Schäfer, A., Wiegand, H.L., Bogerd, H.P., and Cullen, B.R. (2005). Differential sensitivity of murine leukemia virus to APOBEC3-mediated inhibition is governed by virion exclusion. J. Virol. *79*, 8201–8207.

Douville, R.N., and Hiscott, J. (2010). The interface between the innate interferon response and expression of host retroviral restriction factors. Cytokine *52*, 108–115.

Dubé, M., Bego, M.G., Paquay, C., and Cohen, É.A. (2010). Modulation of HIV-1-host interaction: role of the Vpu accessory protein. Retrovirology *7*, 114.

Erlejman, A.G., De Leo, S. a, Mazaira, G.I., Molinari, A.M., Camisay, M.F., Fontana, V. a, Cox, M.B., Piwien-Pilipuk, G., and Galigniana, M.D. (2014). NF-κB Transcriptional Activity is Modulated by FK506-binding Proteins FKBP51 and FKBP52: A Role for Peptidyl-prolyl Isomerase Activity. J. Biol. Chem. *289*, 26263–26276.

Etienne, L., Hahn, B.H., Sharp, P.M., Matsen, F. a, and Emerman, M. (2013). Gene loss and adaptation to hominids underlie the ancient origin of HIV-1. Cell Host Microbe *14*, 85–92.

Fischer, G., Bang, H., and Mech, C. (1984). Determination of enzymatic catalysis for the cis-trans-isomerization of peptide binding in proline-containing peptides. Biomed. Biochim. Acta *43*, 1101–1111.

Fischer, G., Wittmann-Liebold, B., Lang, K., Kiefhaber, T., and Schmid, F.X. (1989). Cyclophilin and peptidyl-prolyl cis-trans isomerase are probably identical proteins. Nature *337*, 476–478.

Fletcher, A.J., and Towers, G.J. (2013). Inhibition of retroviral replication by members of the TRIM protein family. Curr. Top. Microbiol. Immunol. *371*, 29–66.

Franke, D., and Svergun, D.I. (2009). DAMMIF , a program for rapid ab-initio shape determination in small-angle scattering. J. Appl. Crystallogr. *42*, 342–346.

Frankel, A.D., and Young, J.A. (1998). HIV-1: fifteen proteins and an RNA. Annu. Rev. Biochem. *67*, 1–25.

Galigniana, N.M., Ballmer, L.T., Toneatto, J., Erlejman, A.G., Lagadari, M., and Galigniana, M.D. (2012). Regulation of the glucocorticoid response to stress-related disorders by the Hsp90-binding immunophilin FKBP51. J. Neurochem. *122*, 4–18.

Gallo, R.C., Sarin, P.S., Gelmann, E.P., Robert-Guroff, M., Richardson, E., Kalyanaraman, V.S., Mann, D., Sidhu, G.D., Stahl, R.E., Zolla-Pazner, S., et al. (1983). Isolation of human T-cell leukemia virus in acquired immune deficiency syndrome (AIDS). Science *220*, 865–867.

Gamble, T.R., Vajdos, F.F., Yoo, S., Worthylake, D.K., Houseweart, M., Sundquist, W.I., and Hill, C.P. (1996). Crystal structure of human cyclophilin A bound to the amino-terminal domain of HIV-1 capsid. Cell *87*, 1285–1294.

Gifford, R.J. (2012). Viral evolution in deep time: lentiviruses and mammals. Trends Genet. *28*, 89–100.

Gifford, R.J., Katzourakis, A., Tristem, M., Pybus, O.G., Winters, M., and Shafer, R.W. (2008). A transitional endogenous lentivirus from the genome of a basal primate and implications for lentivirus evolution. Proc. Natl. Acad. Sci. U. S. A. *105*, 20362–20367.

Gillick, K., Pollpeter, D., Phalora, P., Kim, E.-Y., Wolinsky, S.M., and Malim, M.H. (2013). Suppression of HIV-1 infection by APOBEC3 proteins in primary human CD4(+) T cells is associated with inhibition of processive reverse transcription as well as excessive cytidine deamination. J. Virol. *87*, 1508–1517.

Goldstone, D.C., Ennis-Adeniran, V., Hedden, J.J., Groom, H.C.T., Rice, G.I., Christodoulou, E., Walker, P.A., Kelly, G., Haire, L.F., Yap, M.W., et al. (2011). HIV-1 restriction factor SAMHD1 is a deoxynucleoside triphosphate triphosphohydrolase. Nature *480*, 379–382.

Gould, S.J., and Vrba, E.S. (1982). Exaptation-A Missing Term in the Science of Form. Paleobiology *8*, 4–15.

Greninger, A.L., Knudsen, G.M., Betegon, M., Burlingame, A.L., and Derisi, J.L. (2012). The 3A protein from multiple picornaviruses utilizes the golgi adaptor protein ACBD3 to recruit PI4KIIIβ. J. Virol. *86*, 3605–3616.

Greninger, A.L., Knudsen, G.M., Betegon, M., Burlingame, A.L.B., and DeRisi, J.L. (2013). ACBD3 interaction with TBC1 domain 22 protein is differentially affected by enteroviral and kobuviral 3A protein binding. MBio *4*, e00098–13 – e00098–13.

Gudmundsson, B., Jónsson, S.R., Olafsson, O., Agnarsdóttir, G., Matthíasdóttir, S., Georgsson, G., Torsteinsdóttir, S., Svansson, V., Kristbjornsdóttir, H.B., Franzdóttir, S.R., et al. (2005). Simultaneous mutations in CA and Vif of Maedi-Visna virus cause attenuated replication in macrophages and reduced infectivity in vivo. J. Virol. *79*, 15038–15042.

Guo, Y., Dong, L., Qiu, X., Wang, Y., Zhang, B., Liu, H., Yu, Y., Zang, Y., Yang, M., and Huang, Z. (2014). Structural basis for hijacking CBF-β and CUL5 E3 ligase complex by HIV-1 Vif. Nature *505*, 229–233.

Haché, G., Shindo, K., Albin, J.S., Harris, R.S., Haché, G., and Harris, R.S. (2008). Evolution of HIV-1 isolates that use a novel Vif-independent mechanism to resist restriction by human APOBEC3G. Curr. Biol. *18*, 819–824.

Han, X., Liang, W., Hua, D., Zhou, X., Du, J., Evans, S.L., Gao, Q., Wang, H., Viqueira, R., Wei, W., et al. (2014). Evolutionarily conserved requirement for core binding factor beta in the assembly of the human immunodeficiency virus/simian immunodeficiency virus Vif-cullin 5-RING E3 ubiquitin ligase. J. Virol. *88*, 3320–3328.

Harris, R.S., and Dudley, J.P. (2015). APOBECs and virus restriction. Virology *479-480*, 131–145.

Harris, R.S., Bishop, K.N., Sheehy, A.M., Craig, H.M., Petersen-Mahrt, S.K., Watt, I.N., Neuberger, M.S., and Malim, M.H. (2003). DNA deamination mediates innate immunity to retroviral infection. Cell *113*, 803–809.

Holt, S.E., Aisner, D.L., Baur, J., Tesmer, V.M., Dy, M., Ouellette, M., Trager, J.B., Morin, G.B., Toft, D.O., Shay, J.W., et al. (1999). Functional requirement of p23 and Hsp90 in telomerase complexes. Genes Dev. *13*, 817–826.

De Hoon, M.J.L., Imoto, S., Nolan, J., and Miyano, S. (2004). Open source clustering software. Bioinformatics *20*, 1453–1454.

Howes, R., Barril, X., Dymock, B.W., Grant, K., Northfield, C.J., Robertson, A.G.S., Surgenor, A., Wayne, J., Wright, L., James, K., et al. (2006). A fluorescence polarization assay for inhibitors of Hsp90. Anal. Biochem. *350*, 202–213.

Huang, D.T., Ayrault, O., Hunt, H.W., Taherbhoy, A.M., Duda, D.M., Scott, D.C., Borg, L.A., Neale, G., Murray, P.J., Roussel, M.F., et al. (2009). E2-RING expansion of the NEDD8 cascade confers specificity to cullin modification. Mol. Cell *33*, 483–495.

Huang, G., Shigesada, K., Ito, K., Wee, H.J., Yokomizo, T., and Ito, Y. (2001). Dimerization with PEBP2beta protects RUNX1/AML1 from ubiquitin-proteasome-mediated degradation. EMBO J. *20*, 723–733.

Hultquist, J.F., Lengyel, J.A., Refsland, E.W., LaRue, R.S., Lackey, L., Brown, W.L., Harris, R.S., and Apobecd, R. (2011). Human and rhesus APOBEC3D, APOBEC3F, APOBEC3G, and APOBEC3H demonstrate a conserved capacity to restrict Vif-deficient HIV-1. J. Virol. *85*, 11220–11234.

Hultquist, J.F., Binka, M., LaRue, R.S., Simon, V., and Harris, R.S. (2012). Vif proteins of human and simian immunodeficiency viruses require cellular CBFβ to degrade APOBEC3 restriction factors. J. Virol. *86*, 2874–2877.

Iwatani, Y., Chan, D.S.B., Wang, F., Maynard, K.S., Sugiura, W., Gronenborn, A.M., Rouzina, I., Williams, M.C., Musier-Forsyth, K., and Levin, J.G. (2007). Deaminase-independent inhibition of HIV-1 reverse transcription by APOBEC3G. Nucleic Acids Res. *35*, 7096–7108.

Jäger, S., Gulbahce, N., Cimermancic, P., Kane, J., He, N., Chou, S., D'Orso, I., Fernandes, J., Jang, G., Frankel, A.D., et al. (2011). Purification and characterization of HIV-human protein complexes. Methods *53*, 13–19.

Jäger, S., Cimermancic, P., Gulbahce, N., Johnson, J.R., McGovern, K.E., Clarke, S.C., Shales, M., Mercenne, G., Pache, L., Li, K., et al. (2012a). Global landscape of HIV-human protein complexes. Nature *481*, 365–370.

Jäger, S., Kim, D.Y., Hultquist, J.F., Shindo, K., LaRue, R.S., Kwon, E., Li, M., Anderson, B.D., Yen, L., Stanley, D., et al. (2012b). Vif hijacks CBF-β to degrade APOBEC3G and promote HIV-1 infection. Nature *481*, 371–375.

Jarmuz, A., Chester, A., Bayliss, J., Gisbourne, J., Dunham, I., Scott, J., and Navaratnam, N. (2002). An anthropoid-specific locus of orphan C to U RNA-editing enzymes on chromosome 22. Genomics *79*, 285–296.

Jáuregui, P., Crespo, H., Glaria, I., Luján, L., Contreras, a, Rosati, S., de Andrés, D., Amorena, B., Towers, G.J., and Reina, R. (2012). Ovine TRIM5α can restrict visna/maedi virus. J. Virol. *86*, 9504–9509.

Jaya, N., Garcia, V., and Vierling, E. (2009). Substrate binding site flexibility of the small heat shock protein molecular chaperones. Proc. Natl. Acad. Sci. U. S. A. *106*, 15604–15609.

Johnson, J.L., and Toft, D.O. (1994). A novel chaperone complex for steroid receptors involving heat shock proteins, immunophilins, and p23. J. Biol. Chem. *269*, 24989–24993.

Jónsson, S.R., Haché, G., Stenglein, M.D., Fahrenkrug, S.C., Andrésdóttir, V., and Harris, R.S. (2006). Evolutionarily conserved and non-conserved retrovirus restriction activities of artiodactyl APOBEC3F proteins. Nucleic Acids Res. *34*, 5683–5694.

Kachroo, A.H., Laurent, J.M., Yellman, C.M., Meyer, A.G., Wilke, C.O., and Marcotte, E.M. (2015). Systematic humanization of yeast genes reveals conserved functions and genetic modularity. Science (80-.). *348*, 921–925.

Kamura, T., Maenaka, K., Kotoshiba, S., Matsumoto, M., Kohda, D., Conaway, R.C., Conaway, J.W., and Nakayama, K.I. (2004). VHL-box and SOCS-box domains determine binding specificity for Cul2-Rbx1 and Cul5-Rbx2 modules of ubiquitin ligases. Genes Dev. *18*, 3055–3065.

Karagoz, G.E., Duarte, A.M.S., Ippel, H., Uetrecht, C., Sinnige, T., van Rosmalen, M., Hausmann, J., Heck, A.J.R., Boelens, R., and Rudiger, S.G.D. (2011). N-terminal domain of human Hsp90 triggers binding to the cochaperone p23. Proc. Natl. Acad. Sci. *108*, 580–585.

Katzourakis, A., Tristem, M., Pybus, O.G., and Gifford, R.J. (2007). Discovery and analysis of the first endogenous lentivirus. Proc. Natl. Acad. Sci. U. S. A. *104*, 6261–6265.

Kawai, T., and Akira, S. (2006). Innate immune recognition of viral infection. Nat. Immunol. *7*, 131–137.

Kawakami, T., Sherman, L., Dahlberg, J., Gazit, A., Yaniv, A., Tronick, S.R., and Aaronson, S.A. (1987). Nucleotide sequence analysis of equine infectious anemia virus proviral DNA. Virology *158*, 300–312.

Kim, D.Y., Kwon, E., Hartley, P.D., Crosby, D.C., Mann, S., Krogan, N.J., and Gross, J.D. (2013). CBFβ stabilizes HIV Vif to counteract APOBEC3 at the expense of RUNX1 target gene expression. Mol. Cell *49*, 632–644.

Kingston, R.E., Chen, C.A., and Okayama, H. (2003). Calcium phosphate transfection. Curr. Protoc. Cell Biol. *Chapter 20*, Unit 20.3.

Klase, Z., Yedavalli, V.S.R.K., Houzet, L., Perkins, M., Maldarelli, F., Brenchley, J., Strebel, K., Liu, P., and Jeang, K.-T. (2014). Activation of HIV-1 from latent infection via synergy of RUNX1 inhibitor Ro5-3335 and SAHA. PLoS Pathog. *10*, e1003997.

Knoblauch, R., and Garabedian, M.J. (1999). Role for Hsp90-associated cochaperone p23 in estrogen receptor signal transduction. Mol. Cell. Biol. *19*, 3748–3759.

Konarev, P. V., Petoukhov, M. V., Volkov, V. V., and Svergun, D.I. (2006). ATSAS 2.1, a program package for small-angle scattering data analysis. J. Appl. Crystallogr. *39*, 277–286.

Koning, F.A., Newman, E.N.C., Kim, E.-Y., Kunstman, K.J., Wolinsky, S.M., and Malim, M.H. (2009). Defining APOBEC3 Expression Patterns in Human Tissues and Hematopoietic Cell Subsets. J. Virol. *83*, 9474–9485.

Laguette, N., Sobhian, B., Casartelli, N., Ringeard, M., Chable-Bessia, C., Ségéral, E., Yatim, A., Emiliani, S., Schwartz, O., and Benkirane, M. (2011). SAMHD1 is the dendritic- and myeloid-cell-specific HIV-1 restriction factor counteracted by Vpx. Nature *474*, 654–657.

LaRue, R.S., Jónsson, S.R., Silverstein, K.A.T., Lajoie, M., Bertrand, D., El-Mabrouk, N., Hötzel, I., Andrésdóttir, V., Smith, T.P.L., and Harris, R.S. (2008). The artiodactyl APOBEC3 innate immune repertoire shows evidence for a multi-functional domain organization that existed in the ancestor of placental mammals. BMC Mol. Biol. *9*, 104.

LaRue, R.S., Andresdottir, V., Blanchard, Y., Conticello, S.G., Derse, D., Emerman, M., Greene, W.C., Jonsson, S.R., Landau, N.R., Lochelt, M., et al. (2009). Guidelines for Naming Nonprimate APOBEC3 Genes and Proteins. J. Virol. *83*, 494–497.

LaRue, R.S., Lengyel, J., Jónsson, S.R., Andrésdóttir, V., and Harris, R.S. (2010). Lentiviral Vif degrades the APOBEC3Z3/APOBEC3H protein of its mammalian host and is capable of cross-species activity. J. Virol. *84*, 8193–8201.

Lee, K. a., Hammerle, L.P., Andrews, P.S., Stokes, M.P., Mustelin, T., Silva, J.C., Black, R. a., and Doedens, J.R. (2011). Ubiquitin ligase substrate identification through quantitative proteomics at both the protein and peptide levels. J. Biol. Chem. *286*, 41530–41538.

Letvin, N.L., Daniel, M.D., Sehgal, P.K., Desrosiers, R.C., Hunt, R.D., Waldron, L.M., MacKey, J.J., Schmidt, D.K., Chalifoux, L. V, and King, N.W. (1985). Induction of AIDS-like disease in macaque monkeys with T-cell tropic retrovirus STLV-III. Science *230*, 71–73.

Li, M., Shandilya, S.M.D., Carpenter, M.A., Rathore, A., Brown, W.L., Perkins, A.L., Harki, D.A., Solberg, J., Hook, D.J., Pandey, K.K., et al. (2012). First-in-class small molecule inhibitors of the single-strand DNA cytosine deaminase APOBEC3G. ACS Chem. Biol. *7*, 506–517.

Löchelt, M., Romen, F., Bastone, P., Muckenfuss, H., Kirchner, N., Kim, Y.-B., Truyen, U., Rösler, U., Battenberg, M., Saib, A., et al. (2005). The antiretroviral activity of APOBEC3 is inhibited by the foamy virus accessory Bet protein. Proc. Natl. Acad. Sci. U. S. A. *102*, 7982–7987.

Luban, J., Bossolt, K.L., Franke, E.K., Kalpana, G. V, and Goff, S.P. (1993). Human immunodeficiency virus type 1 Gag protein binds to cyclophilins A and B. Cell *73*, 1067–1078.

Luo, K., Xiao, Z., Ehrlich, E., Yu, Y., Liu, B., Zheng, S., and Yu, X.-F. (2005). Primate lentiviral virion infectivity factors are substrate receptors that assemble with cullin 5-E3 ligase through a HCCH motif to suppress APOBEC3G. Proc. Natl. Acad. Sci. U. S. A. *102*, 11444–11449.

Mahon, C., Krogan, N., Craik, C., and Pick, E. (2014). Cullin E3 Ligases and Their Rewiring by Viral Factors. Biomolecules *4*, 897–930.

Mahrour, N., Redwine, W.B., Florens, L., Swanson, S.K., Martin-Brown, S., Bradford, W.D., Staehling-Hampton, K., Washburn, M.P., Conaway, R.C., and Conaway, J.W. (2008). Characterization of Cullin-box sequences that direct recruitment of Cul2-Rbx1 and Cul5-Rbx2 modules to Elongin BC-based ubiquitin ligases. J. Biol. Chem. *283*, 8005–8013.

Malim, M.H., and Emerman, M. (2008). HIV-1 accessory proteins--ensuring viral survival in a hostile environment. Cell Host Microbe *3*, 388–398.

Mangeat, B., Turelli, P., Caron, G., Friedli, M., Perrin, L., and Trono, D. (2003). Broad antiretroviral defence by human APOBEC3G through lethal editing of nascent reverse transcripts. Nature *424*, 99–103.

Mansur, D.S., Maluquer de Motes, C., Unterholzner, L., Sumner, R.P., Ferguson, B.J., Ren, H., Strnadova, P., Bowie, A.G., and Smith, G.L. (2013). Poxvirus Targeting of E3 Ligase β-TrCP by Molecular Mimicry: A Mechanism to Inhibit NF-κB Activation and Promote Immune Evasion and Virulence. PLoS Pathog. *9*.

Mark, K.G., Simonetta, M., Maiolica, A., Seller, C. a, and Toczyski, D.P. (2014). Ubiquitin Ligase Trapping Identifies an SCF(Saf1) Pathway Targeting Unprocessed Vacuolar/Lysosomal Proteins. Mol. Cell *53*, 148–161.

Marks, A.R. (1996). Cellular functions of immunophilins. Physiol. Rev. *76*, 631–649.

McLaughlin, S.H., Sobott, F., Yao, Z., Zhang, W., Nielsen, P.R., Grossmann, J.G., Laue, E.D., Robinson, C. V., and Jackson, S.E. (2006). The Co-chaperone p23 Arrests the Hsp90 ATPase Cycle to Trap Client Proteins. J. Mol. Biol. *356*, 746–758.

McMichael, A.J., Borrow, P., Tomaras, G.D., Goonetilleke, N., and Haynes, B.F. (2010). The immune response during acute HIV-1 infection: clues for vaccine development. Nat. Rev. Immunol. *10*, 11–23.

McNab, F., Mayer-Barber, K., Sher, A., Wack, A., and O'Garra, A. (2015). Type I interferons in infectious disease. Nat. Rev. Immunol. *15*, 87–103.

Mehle, A., Strack, B., Ancuta, P., Zhang, C., McPike, M., and Gabuzda, D. (2004). Vif overcomes the innate antiviral activity of APOBEC3G by promoting its degradation in the ubiquitin-proteasome pathway. J. Biol. Chem. *279*, 7792–7798.

Miyagi, E., Kao, S., Yedavalli, V., and Strebel, K. (2014). CBFβ enhances de novo protein biosynthesis of its binding partners HIV-1 Vif and RUNX1 and potentiates the Vif-induced degradation of APOBEC3G. J. Virol. *88*, 4839–4852.

Münk, C., Beck, T., Zielonka, J., Hotz-Wagenblatt, A., Chareza, S., Battenberg, M., Thielebein, J., Cichutek, K., Bravo, I.G., O'Brien, S.J., et al. (2008). Functions, structure, and read-through alternative splicing of feline APOBEC3 genes. Genome Biol. *9*, R48.

Neil, S.J.D., Zang, T., and Bieniasz, P.D. (2008). Tetherin inhibits retrovirus release and is antagonized by HIV-1 Vpu. Nature *451*, 425–430.

Nguyen, P.M., Wang, D., Wang, Y., Li, Y., Uchizono, J.A., and Chan, W.K. (2012). P23 co-chaperone protects the aryl hydrocarbon receptor from degradation in mouse and human cell lines. Biochem. Pharmacol. *84*, 838–850.

Ni, L., Yang, C.-S., Gioeli, D., Frierson, H., Toft, D.O., and Paschal, B.M. (2010). FKBP51 Promotes Assembly of the Hsp90 Chaperone Complex and Regulates Androgen Receptor Signaling in Prostate Cancer Cells. Mol. Cell. Biol. *30*, 1243–1253.

Nisole, S., Lynch, C., Stoye, J.P., and Yap, M.W. (2004). A Trim5-cyclophilin A fusion protein found in owl monkey kidney cells can restrict HIV-1. Proc. Natl. Acad. Sci. U. S. A. *101*, 13324–13328.

Notredame, C., Higgins, D.G., and Heringa, J. (2000). T-Coffee: A novel method for fast and accurate multiple sequence alignment. J. Mol. Biol. *302*, 205–217.

Nowarski, R., Britan-Rosich, E., Shiloach, T., and Kotler, M. (2008). Hypermutation by intersegmental transfer of APOBEC3G cytidine deaminase. Nat. Struct. Mol. Biol. *15*, 1059–1066.

Ooms, M., Brayton, B., Letko, M., Maio, S.M., Pilcher, C.D., Hecht, F.M., Barbour, J.D., and Simon, V. (2013). HIV-1 Vif Adaptation to Human APOBEC3H Haplotypes. Cell Host Microbe *14*, 411–421.

Oxelmark, E., Roth, J.M., Brooks, P.C., Braunstein, S.E., Schneider, R.J., and Garabedian, M.J. (2006). The cochaperone p23 differentially regulates estrogen receptor target genes and promotes tumor cell adhesion and invasion. Mol. Cell. Biol. *26*, 5205–5213.

Pare, J.M., LaPointe, P., and Hobman, T.C. (2013). Hsp90 cochaperones p23 and FKBP4 physically interact with hAgo2 and activate RNA interference-mediated silencing in mammalian cells. Mol. Biol. Cell *24*, 2303–2310.

Peluso, R., Haase, A., Stowring, L., Edwards, M., and Ventura, P. (1985). A Trojan Horse mechanism for the spread of visna virus in monocytes. Virology *147*, 231–236.

Pettersen, E.F., Goddard, T.D., Huang, C.C., Couch, G.S., Greenblatt, D.M., Meng, E.C., and Ferrin, T.E. (2004). UCSF Chimera--a visualization system for exploratory research and analysis. J. Comput. Chem. *25*, 1605–1612.

Petursson, G. (1994). Experience with visna virus in Iceland. In Annals of the New York Academy of Sciences, pp. 43–49.

R Core Team (2014). R: A Language and Environment for Statistical Computing.

Rahman, M.M., and McFadden, G. (2011). Modulation of NF-κB signalling by microbial pathogens. Nat. Rev. Microbiol. *9*, 291–306.

Ramage, H.R., Kumar, G.R., Verschueren, E., Johnson, J.R., Von Dollen, J., Johnson, T., Newton, B., Shah, P., Horner, J., Krogan, N.J., et al. (2015). A Combined Proteomics/Genomics Approach Links Hepatitis C Virus Infection with Nonsense-Mediated mRNA Decay. Mol. Cell *57*, 329–340.

Rasaiyaah, J., Tan, C.P., Fletcher, A.J., Price, A.J., Blondeau, C., Hilditch, L., Jacques, D. a, Selwood, D.L., James, L.C., Noursadeghi, M., et al. (2013). HIV-1 evades innate immune recognition through specific cofactor recruitment. Nature *503*, 402–405.

Rasband, W.S. (2007). ImageJ.

Rice, P., Longden, I., and Bleasby, A. (2000). EMBOSS: the European Molecular Biology Open Software Suite. Trends Genet. *16*, 276–277.

Roguev, A., Bandyopadhyay, S., Zofall, M., Zhang, K., Fischer, T., Collins, S.R., Qu, H., Shales, M., Park, H., Hayles, J., et al. (2008). Conservation and rewiring of functional modules revealed by an epistasis map in fission yeast. Science *322*, 405–410.

Ryan, C.J., Roguev, A., Patrick, K., Xu, J., Jahari, H., Tong, Z., Beltrao, P., Shales, M., Qu, H., Collins, S.R., et al. (2012). Hierarchical modularity and the evolution of genetic interactomes across species. Mol. Cell *46*, 691–704.

Saldanha, A.J. (2004). Java Treeview--extensible visualization of microarray data. Bioinformatics *20*, 3246–3248.

Sali, A., and Blundell, T.L. (1993). Comparative protein modelling by satisfaction of spatial restraints. J. Mol. Biol. *234*, 779–815.

Sarikas, A., Hartmann, T., and Pan, Z.-Q. (2011). The cullin protein family. Genome Biol. *12*, 220.

Sauter, D. (2014). Counteraction of the multifunctional restriction factor tetherin. Front. Microbiol. *5*, 163.

Sauter, D., Hotter, D., Van Driessche, B., Stürzel, C.M., Kluge, S.F., Wildum, S., Yu, H., Baumann, B., Wirth, T., Plantier, J.-C., et al. (2015). Differential regulation of NF-κB-mediated proviral and antiviral host gene expression by primate lentiviral Nef and Vpu proteins. Cell Rep. *10*, 586–599.

Sayah, D.M., Sokolskaja, E., Berthoux, L., and Luban, J. (2004). Cyclophilin A retrotransposition into TRIM5 explains owl monkey resistance to HIV-1. Nature *430*, 569–573.

Schneidman-Duhovny, D., Hammel, M., and Sali, A. (2010). FoXS: a web server for rapid computation and fitting of SAXS profiles. Nucleic Acids Res. *38*, W540–W544.

Schwartz, D.C., and Hochstrasser, M. (2003). A superfamily of protein tags: Ubiquitin, SUMO and related modifiers. Trends Biochem. Sci. *28*, 321–328.

Schwefel, D., Groom, H.C.T., Boucherit, V.C., Christodoulou, E., Walker, P.A., Stoye, J.P., Bishop, K.N., and Taylor, I.A. (2014). Structural basis of lentiviral subversion of a cellular protein degradation pathway. Nature *505*, 234–238.

Schwefel, D., Boucherit, V.C., Christodoulou, E., Walker, P.A., Stoye, J.P., Bishop, K.N., and Taylor, I.A. (2015). Molecular Determinants for Recognition of Divergent SAMHD1 Proteins by the Lentiviral Accessory Protein Vpx. Cell Host Microbe *17*, 489–499.

Sharp, P.M., and Hahn, B.H. (2011). Origins of HIV and the AIDS pandemic. Cold Spring Harb. Perspect. Med. *1*, a006841.

Sheehy, A.M., Gaddis, N.C., Choi, J.D., and Malim, M.H. (2002). Isolation of a human gene that inhibits HIV-1 infection and is suppressed by the viral Vif protein. Nature *418*, 646–650.

Sheehy, A.M., Gaddis, N.C., and Malim, M.H. (2003). The antiretroviral enzyme APOBEC3G is degraded by the proteasome in response to HIV-1 Vif. Nat. Med. *9*, 1404–1407.

Sokolskaja, E., and Luban, J. (2006). Cyclophilin, TRIM5, and innate immunity to HIV-1. Curr. Opin. Microbiol. *9*, 404–408.

Sowa, M.E., Bennett, E.J., Gygi, S.P., Harper, J.W., and Results, I.S. (2009). Defining the human deubiquitinating enzyme interaction landscape. Cell *138*, 389–403.

Spiess, C., Miller, E.J., McClellan, A.J., and Frydman, J. (2006). Identification of the TRiC/CCT substrate binding sites uncovers the function of subunit diversity in eukaryotic chaperonins. Mol. Cell *24*, 25–37.

St-Louis, M.-C., Cojocariu, M., and Archambault, D. (2004). The molecular biology of bovine immunodeficiency virus: a comparison with other lentiviruses. Anim. Health Res. Rev. *5*, 125–143.

Stamatakis, A., Hoover, P., and Rougemont, J. (2008). A rapid bootstrap algorithm for the RAxML Web servers. Syst. Biol. *57*, 758–771.

Stanley, B.J., Ehrlich, E.S., Short, L., Yu, Y., Xiao, Z., Yu, X.-F., and Xiong, Y. (2008). Structural insight into the human immunodeficiency virus Vif SOCS box and its role in human E3 ubiquitin ligase assembly. J. Virol. *82*, 8656–8663.

Stanley, D.J., Bartholomeeusen, K., Crosby, D.C., Kim, D.Y., Kwon, E., Yen, L., Cartozo, N.C., Li, M., Jäger, S., Mason-Herr, J., et al. (2012). Inhibition of a NEDD8 Cascade Restores Restriction of HIV by APOBEC3G. PLoS Pathog. *8*, e1003085.

Stenglein, M.D., and Harris, R.S. (2006). APOBEC3B and APOBEC3F Inhibit L1 Retrotransposition by a DNA Deamination-independent Mechanism. J. Biol. Chem. *281*, 16837–16841.

Stenglein, M.D., Burns, M.B., Li, M., Lengyel, J., and Harris, R.S. (2010). APOBEC3 proteins mediate the clearance of foreign DNA from human cells. Nat. Struct. Mol. Biol. *17*, 222–229.

Stremlau, M., Owens, C.M., Perron, M.J., Kiessling, M., Autissier, P., and Sodroski, J. (2004). The cytoplasmic body component TRIM5alpha restricts HIV-1 infection in Old World monkeys. Nature *427*, 848–853.

Svergun, D.I. (1999). Restoring low resolution structure of biological macromolecules from solution scattering using simulated annealing. Biophys. J. *76*, 2879–2886.

Swaney, D.L., Wenger, C.D., and Coon, J.J. (2010). The value of using multiple proteases for large scale mass spectrometry based proteomics. Digestion *9*, 1323–1329.

Szabo, S.J., Kim, S.T., Costa, G.L., Zhang, X., Fathman, C.G., and Glimcher, L.H. (2000). A novel transcription factor, T-bet, directs Th1 lineage commitment. Cell *100*, 655–669.

Szczepankiewicz, A., Leszczyńska-Rodziewicz, A., Pawlak, J., Narozna, B., Rajewska-Rager, A., Wilkosc, M., Zaremba, D., Maciukiewicz, M., and Twarowska-Hauser, J. (2014). FKBP5 polymorphism is associated with major depression but not with bipolar disorder. J. Affect. Disord. *164*, 33–37.

Tahirov, T.H., Inoue-Bungo, T., Morii, H., Fujikawa, A., Sasaki, M., Kimura, K., Shiina, M., Sato, K., Kumasaka, T., Yamamoto, M., et al. (2001). Structural analyses of DNA recognition by the AML1/Runx-1 Runt domain and its allosteric control by CBFbeta. Cell *104*, 755–767.

Takahashi, N., Hayano, T., and Suzuki, M. (1989). Peptidyl-prolyl cis-trans isomerase is the cyclosporin A-binding protein cyclophilin. Nature *337*, 473–475.

Tammsalu, T., Matic, I., Jaffray, E.G., Ibrahim, A.F.M., Tatham, M.H., and Hay, R.T. (2015). Proteome-wide identification of SUMO modification sites by mass spectrometry. Nat. Protoc. *10*, 1374–1388.

Tanioka, T., Nakatani, Y., Semmyo, N., Murakami, M., and Kudo, I. (2000). Molecular Identification of Cytosolic Prostaglandin E2 Synthase That Is Functionally Coupled with Cyclooxygenase-1 in Immediate Prostaglandin E2Biosynthesis. J. Biol. Chem. *275*, 32775–32782.

Tatro, E.T., Everall, I.P., Kaul, M., and Achim, C.L. (2009). Modulation of glucocorticoid receptor nuclear translocation in neurons by immunophilins FKBP51 and FKBP52: Implications for major depressive disorder. Brain Res. *1286*, 1–12.

Thali, M., Bukovsky, A., Kondo, E., Rosenwirth, B., Walsh, C.T., Sodroski, J., and Göttlinger, H.G. (1994). Functional association of cyclophilin A with HIV-1 virions. Nature *372*, 363–365.

Thériault, Y., Logan, T.M., Meadows, R., Yu, L., Olejniczak, E.T., Holzman, T.F., Simmer, R.L., and Fesik, S.W. (1993). Solution structure of the cyclosporin A/cyclophilin complex by NMR. Nature *361*, 88–91.

Thormar, H. (2005). Maedi-visna virus and its relationship to human immunodeficiency virus. AIDS Rev. *7*, 233–245.

Torsteinsdottir, S., Andresdottir, V., Arnarson, H., and Petursson, G. (2007). Immune response to maedi-visna virus. Front. Biosci. *12*, 1532–1543.

Towers, G.J., Hatziioannou, T., Cowan, S., Goff, S.P., Luban, J., and Bieniasz, P.D. (2003). Cyclophilin A modulates the sensitivity of HIV-1 to host restriction factors. Nat. Med. *9*, 1138–1143.

Volkov, V. V., and Svergun, D.I. (2003). Uniqueness of ab initio shape determination in small-angle scattering. J. Appl. Crystallogr. *36*, 860–864.

Vranken, W.F., Boucher, W., Stevens, T.J., Fogh, R.H., Pajon, A., Llinas, M., Ulrich, E.L., Markley, J.L., Ionides, J., and Laue, E.D. (2005). The CCPN data model for NMR spectroscopy: development of a software pipeline. Proteins *59*, 687–696.

Wang, P., and Heitman, J. (2005). The cyclophilins. Genome Biol. *6*, 226.

Waterhouse, A.M., Procter, J.B., Martin, D.M. a, Clamp, M., and Barton, G.J. (2009). Jalview Version 2--a multiple sequence alignment editor and analysis workbench. Bioinformatics *25*, 1189–1191.

Weinkam, P., Pons, J., and Sali, A. (2012). Structure-based model of allostery predicts coupling between distant sites. Proc. Natl. Acad. Sci. U. S. A. *109*, 4875–4880.

White, E. a, Walther, J., Javanbakht, H., and Howley, P.M. (2014). Genus Beta HPV E6 Proteins Vary in their Effects on the Transactivation of p53 Target Genes. J. Virol. *88*, 8201–8212.

White, E.A., Sowa, M.E., Jie, M., Tan, A., Jeudy, S., Hayes, S.D., Santha, S., Münger, K., Harper, J.W., Howley, P.M., et al. (2012). Systematic identification of interactions between host cell proteins and E7 oncoproteins from diverse human papillomaviruses. Proc. Natl. Acad. Sci. U. S. A. *109*, E260–E267.

Xu, H., Svarovskaia, E.S., Barr, R., Zhang, Y., Khan, M.A., Strebel, K., and Pathak, V.K. (2004). A single amino acid substitution in human APOBEC3G antiretroviral enzyme confers resistance to HIV-1 virion infectivity factor-induced depletion. Proc. Natl. Acad. Sci. U. S. A. *101*, 5652–5657.

Xu, P., Duong, D.M., Seyfried, N.T., Cheng, D., Xie, Y., Robert, J., Rush, J., Hochstrasser, M., Finley, D., and Peng, J. (2009). Quantitative Proteomics Reveals the Function of Unconventional Ubiquitin Chains in Proteasomal Degradation. Cell *137*, 133–145.

Ye, Y., and Rape, M. (2009). Building ubiquitin chains: E2 enzymes at work. Nat. Rev. Mol. Cell Biol. *10*, 755–764.

Yen, H.-C.S., and Elledge, S.J. (2008). Identification of SCF ubiquitin ligase substrates by global protein stability profiling. Science *322*, 923–929.

Yu, X.X.-F., Yu, Y., Liu, B., Luo, K., Kong, W., and Mao, P. (2003). Induction of APOBEC3G ubiquitination and degradation by an HIV-1 Vif-Cul5-SCF complex. Science *302*, 1056–1060.

Yu, Y., Xiao, Z., Ehrlich, E.S., and Yu, X.X.-F. (2004). Selective assembly of HIV-1 Vif-Cul5-ElonginB-ElonginC E3 ubiquitin ligase complex through a novel SOCS box and upstream cysteines. Genes Dev. *18*, 2867–2872.

Zhang, H., Yang, B., Pomerantz, R.J., Zhang, C., Arunachalam, S.C., and Gao, L. (2003). The cytidine deaminase CEM15 induces hypermutation in newly synthesized HIV-1 DNA. Nature *424*, 94–98.

Zhang, J., Wu, J., Wang, W., Wu, H., Yu, B., Wang, J., Lv, M., Wang, X., Zhang, H., Kong, W., et al. (2014a). Role of cullin-elonginB-elonginC E3 complex in bovine immunodeficiency virus and maedi-visna virus Vif-mediated degradation of host A3Z2-Z3 proteins. Retrovirology *11*, 77.

Zhang, W., Du, J., Evans, S.L., Yu, Y., and Yu, X.-F. (2012). T-cell differentiation factor CBF-β regulates HIV-1 Vif-mediated evasion of host restriction. Nature *481*, 376–379.

Zhang, W., Wang, H., Li, Z., Liu, X., Liu, G., Harris, R.S., and Yu, X.-F. (2014b). Cellular Requirements for BIV Vif-Mediated Inactivation of Bovine APOBEC3 Proteins. J. Virol.

Zhang, Y., Gao, J., Chung, K.K., Huang, H., Dawson, V.L., and Dawson, T.M. (2000). Parkin functions as an E2-dependent ubiquitin- protein ligase and promotes the degradation of the synaptic vesicle-associated protein, CDCrel-1. Proc. Natl. Acad. Sci. U. S. A. *97*, 13354–13359.

Publishing Agreement

It is the policy of the University to encourage the distribution of all theses, dissertations, and manuscripts. Copies of all UCSF theses, dissertations, and manuscripts will be routed to the library via the Graduate Division. The library will make all theses, dissertations, and manuscripts accessible to the public and will preserve these to the best of their abilities, in perpetuity.

I hereby grant permission to the Graduate Division of the University of California, San Francisco to release copies of my thesis, dissertation, or manuscript to the Campus Library to provide access and preservation, in whole or in part, in perpetuity.

Author Signature

04 September 2015

Date